# Bench Scale Demonstration of Redox Flow Battery based on Fungal Quinone Phoenicin as Negolyte

*Reproducibility of phoenicin used in a bench-scaled RFB to store the energy produced by the solar panel*

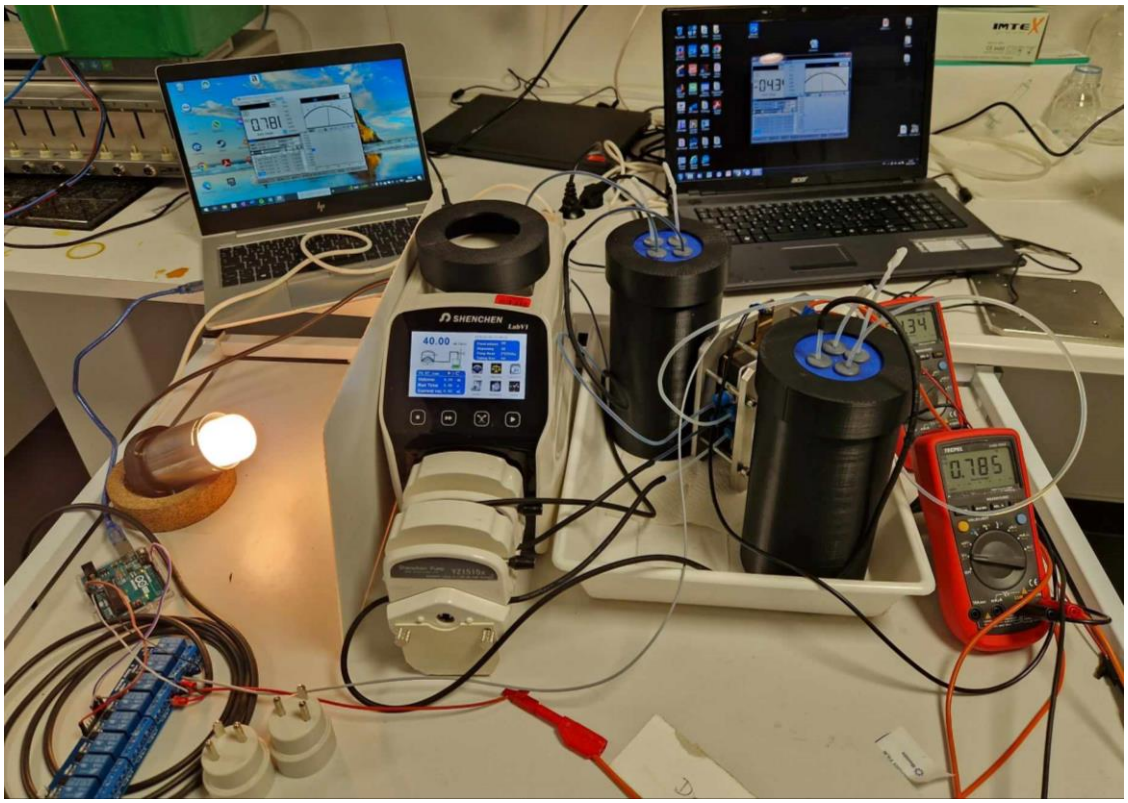


Elise Paula Madvig Jørgensen Reetz

AALBORG UNIVERSITY
STUDENT REPORT

Title: Bench Scale Demonstration of Redox Flow Battery based on Fungal Quinone Phoenicin as Negolyte

Theme: Fungal-based Redox Flow Battery

Project Period: Long Master thesis

Project Group: CE4-5-F24

Supervisor(s): Jens Muff and Jens Laurids Sørensen

Copies: 1

Page Numbers: 128

Date of Completion: 03-06-24

Participant(s):

Elise P.M.J. Reetz 

# Abstract

There is a growing need for renewable energy utilization, where the redox flow battery (RFB) is an alternative greener option in the sector of battery technologies used for energy storage. This thesis focuses on the bench scaling of the already-proven working redox flow battery containing the fungal-sourced compound. The bench scaling is led by the connection of a solar panel to the RFB to investigate if the battery can store the solar panel's produced energy.

The battery properties being judged upon in this thesis are the capacity of the battery compared to the energy produced by the solar panel, the three efficiencies: coulombic (CE), voltage (VE), and energy (EE), and the capacity loss per cycle and hour.

The results show that the principle of an RFB operating on phoenicin can store energy produced by the PV panel with some adjustments based on the previously conducted quality check RFBs in this project.

It can be concluded that, based on the RFB, it is a viable option to store energy produced by a renewable energy source.

# Preface

This Master thesis project was written by Elise P.M.J. Reetz, enrolled at Aalborg University Esbjerg in Chemical Engineering for the 9th and 10th semesters 2023/2024. All experiments were conducted on campus at the Aalborg University laboratory property from 01.09.2023 to 10.06.2024 during the Master thesis project period. This thesis was supervised by Jens Muff and Jens Laurids Sørensen and consulted by Charlotte Overgaard Wilhelmsen. The project is associated with the further research concerning the phoenicin redox flow battery development and the project conducted by DTU. The research is funded by the Danish Research Council and the Novo Nordisk Foundation.

Aalborg University, May 10, 2024

# Table of Contents

# 1. Introduction

Renewable and green energy sources are becoming more popular as the energy demand is rising yearly, as shown in Figure 1.1. [1], [2], [3] In the year 2022, global energy consumption had a slight decrease of +2.1%/year compared to the previous year with +4.9%/year, but it still remains higher than the average from 2010-2019 with +1.4%/year. [1]

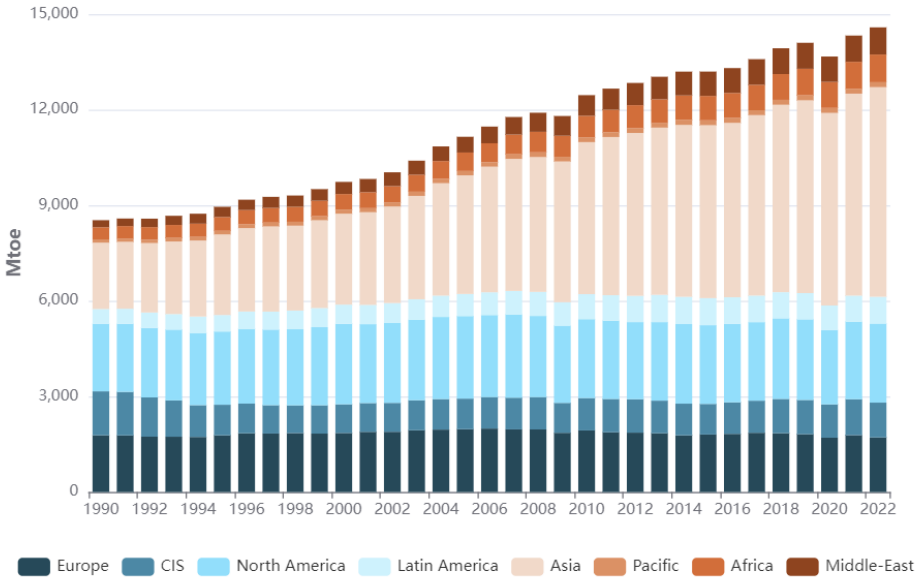


*Figure 1.1: Energy consumption from 1990-2022 [1]*

In the current situation, renewable energies are only producing a small part of the world´s energy, which can be seen in Figure 1.2, and the most significant portion is still produced by the unsustainable way of using fossil fuels in the case of oil and coal produce energy. [4], [5] What also can be seen from this figure is that in the last 5-10 years, there has been an increase in energy created by wind and solar, as indicated by the growing yellow and dark green sections. [4]

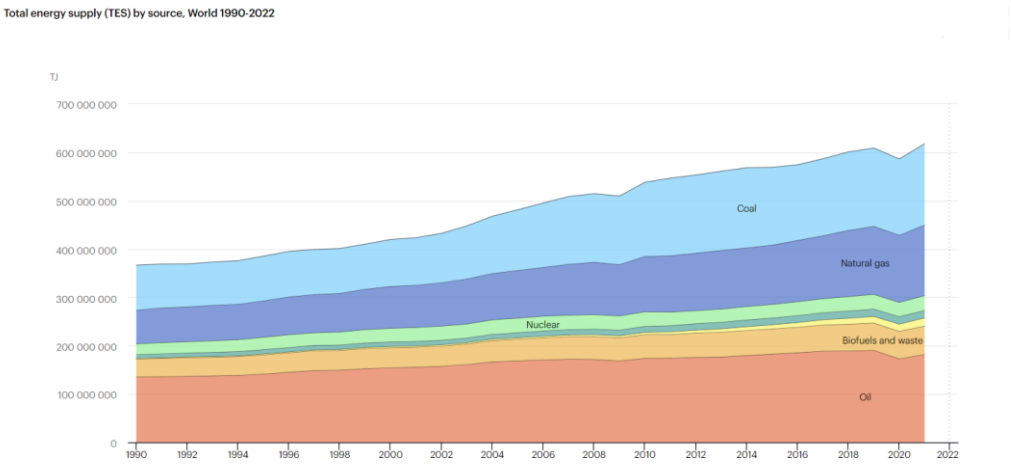


*Figure 1.2: Energy supply distribution from 1990-2022 [4]*

Renewable energy sources, usually solar and wind energy, are free, but their availability varies with the time periods when the power source, either sun or wind, is accessible. To overcome this unpredictable behaviour of these energy sources, a cheap and scalable

storage technology needs to be developed to guarantee a stable and sustainable energy supply. [6], [7], [8]

A solution for this problem is the energy storage solution (ESS), which could follow energy generation and storage if needed. An example of this ESS is energy storage batteries, which could be used for wind turbines and solar panels. The batteries would be charged on windy days and stored and discharged on days with insufficient wind to produce energy. The same concept can also be used for solar panels. There are two different types of energy storage batteries. [9]

One is the most common type, the solid-state battery, which consists of a metal electrolyte and a chemical solution. The most viable and well-known example of this type is the Li-ion battery. [10]

The second type of ESS battery is the redox flow battery (RFB), which uses the redox reaction of its liquid electrolytes to generate electric current. The advantage of these liquid electrolytes is the easy scaling of the battery depending on the operation needed, as it only depends on the tank volume of the electrolytes. The most well-known example of an RFB is the vanadium redox flow battery (VRFB). The disadvantages of the VRFB are the toxicity of the electrolyte, the mining cost, and the cost of vanadium. RFBs have overall disadvantages compared to Li-ion batteries in terms of low energy densities and lower efficiencies. The current research is looking into finding alternative renewable and "clean" compounds to be used in an RFB. Non-metal compounds are being considered to protect the environment and keep the cost as low as possible while testing possible scale-up production solutions in order to keep up with the increasing demand for ESS. [10], [10], [11], [12], [13]

A study by Wilhelmsen et al. investigated the quinone known as phoenicin as a possible negolyte in a redox flow battery. This showed that phoenicin participates in a two-electron redox reaction, resulting in a single-cell battery test operating on phoenicin as the negative electrolyte running for 14 days and a capacity loss of 50%. [6]

To improve the use of the phoenicin-operated RFB in the green development of the ESS sector to increase further the renewable energy sector usage by possible storage of the not used energy and less the usage of the fossil fuels, the following initial question for this thesis is constructed:

*"What requirements are needed to scale up a phoenicin-operated RFB from lab to bench/pilot scale?"*

To answer this question, this thesis presents organic redox flow batteries, the compound phoenicin, and possible renewable energy sources usable for connecting to an RFB.

# 2. Redox Flow Battery

A redox flow battery (RFB) is an electrochemical device which consists of two half-cells. The potential differences between the redox couples, also known as the electrolytes, used in the half-cells are utilized to interconvert chemical and electrical energy through the reduction and oxidation of the respective electrolytes. The negative electrolyte is called the negolyte (anolyte), and the positive electrolyte is called the posolyte (catholyte). [12], [14], [15]

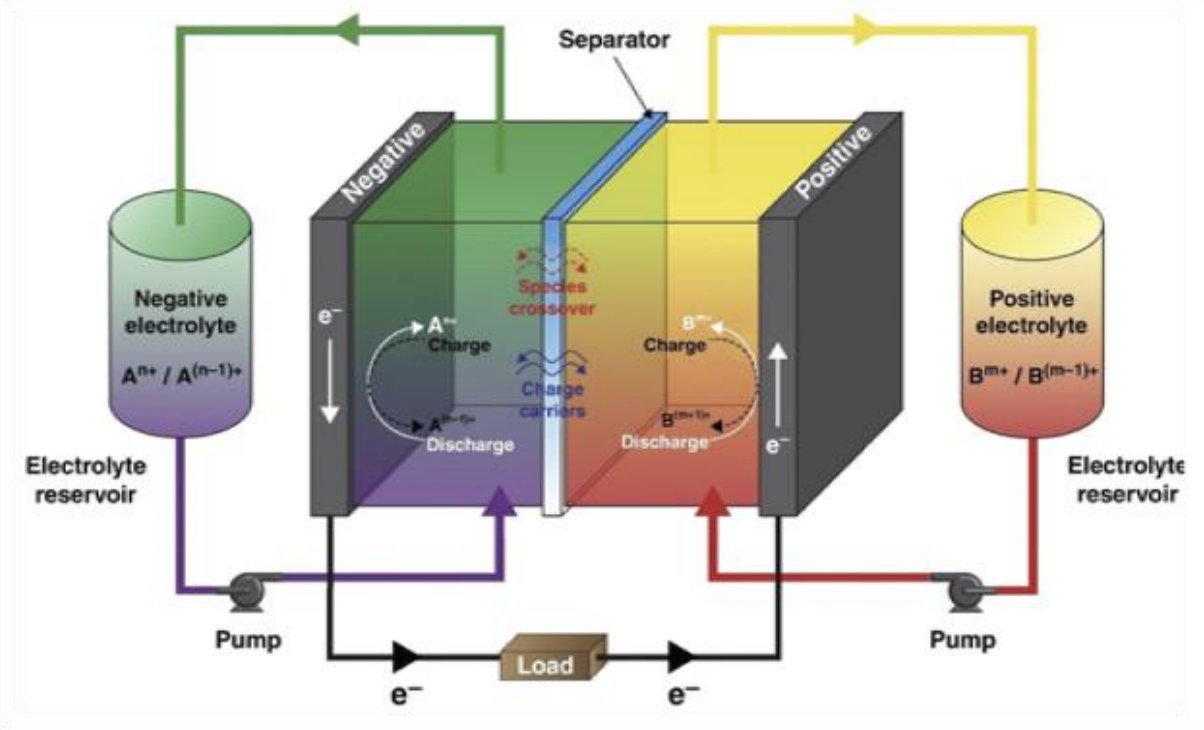


*Figure 2.1: RFB setup [16]*

Figure 2.1 shows the setup of the RFB, from which it can be seen that half cells are separated by an ion-exchange membrane through which the protons are diffused, and the electrons are transported through the circuit from the oxidized electrolyte to the reduced electrolyte. The electrons are transported from the posolyte to the negolyte in the battery's charging process. The electrons are transported from the negolyte to the posolyte for the discharge process. [9], [14], [17], [18] The redox reaction for the discharge process of the used RFB operating on phoenicin as an negolyte can be seen in Equation 1 below.

*Equation 1: Redox discharge reactions inside the battery cell*

$$Negolyte\colon\ \mathrm{C_{14}H_8O_6^{-4}} \rightleftharpoons \mathrm{C_{14}H_{10}O_6^{-2}} + 2e^-$$

$$Posolyte\colon\ 2\mathrm{Fe(CN)_6^{-3}} + 2e^- \rightleftharpoons 2\mathrm{Fe(CN)_6^{-4}}$$

An advantage of the RFB is that it is independently scalable compared to conventional batteries in power and capacity by separating the sizing of the tank volumes and reaction cells. [12], [15], [19]

A type of RFB is the organic redox flow batteries (ORFB), which use organic active molecules as electroactive materials in at least one of the electrolytes. Using organic materials is a way to avoid using more metals for energy storage, resulting in more green energy storage as the organic materials can also be reproduced and are not limited. [13], [20], [21], [22] The organic materials are dissolved in aqueous or non-aqueous solution

where the aqueous solution has the advantage of ionic conductivity, high solubility and costs. The disadvantages of these batteries are that the cell voltage simultaneously for the aqueous systems are still a challenge, and the reversibility of the compound may be compromised, resulting in a possible need for a catalyst. Another advantage of the RFBs compared to Li-ion batteries is that they store the charge in the recirculating electrolyte and not just within the cell. [20], [23]

## 2.1. Battery properties and parameters

For the RFB, there are three essential efficiencies through which the performance can be judged: coulombic efficiency (CE), voltage efficiency (VE) and energy efficiency (EE). [19]

The CE is also known as current efficiency, and it expresses the relationship between the applied charge in the charging process and the retained charge of the discharge process in the same charge/discharge cycle. A crossover of the redox-active material into the opposite half-cell through the membrane or irreversible side reactions of the redox material in the electrolytes can be indicated through a CE value below 99%. [19] Another cause of a CE below 50% % can be the compound's degradation throughout the testing. The possibility of side reactions might cause a CE value above 100% suggesting these are taking place. A reduction of the coulombic efficiency is most commonly due to a secondary reaction, for example, the electrolysis of water or other undesired reactions in the battery. [24], [25] The CE of a flooded lead-acid battery lies between 71% to 95% [26], and for a lithium-ion battery is 99% or above. [27] This efficiency is one of the most significant parameters when comparing different batteries with each other, and its equation can be seen in Equation 2.

*Equation 2: Coulombic efficiency equation [19]*

$$CE = \frac{discharge\ capacity}{charge\ capacity} * 100\%$$

The VE, as seen in Equation 3, is defined as the ratio between mean discharging and charging voltage at a constant current. [19] This efficiency is established by a cycle test at a constant current density, which describes the different sources of overvoltage, i.e., kinetics, ohmic, and mass transport losses. These sources will negatively affect the VE, causing it to decrease. It also reflects on the resistance of the electrode and membrane, the internal resistance, which can be represented by a capacity fade. [6], [19]

*Equation 3: Voltage efficiency equation [19]*

$$VE = \frac{average\ discharge\ voltage}{average\ charge\ voltage} * 100\%$$

The last efficiency is the EE, which is the product of coulombic and voltage and is stated as the ratio of energy discharged to charged, as shown in Equation 4. Typically, the EE value lies between 50% and 90%, depending on both CE and VE. [19], [28]

*Equation 4: Energy efficiency equation [19]*

$$EE = CE * VE$$

The averaged efficiencies determined in the different studies from Wilhelmsen et al. can be seen in Table 2.1 below for the specific phoenicin single-cell cycling battery test. These values will later be used to compare the efficiencies achieved by this project. [6]

*Table 2.1: Table of previous study efficiencies [6]*

| Averaged Efficiencies [%] | Paper 1 [29] | Paper 2 [30] |
|---|---|---|
| CE | 98.5 | 95 |
| VE | 37.5 | 79 |
| EE | 36.9 | 77 |

A battery parameter is the volumetric capacity indicating the amount of charge which can be stored in the electrolyte. It is also called the theoretical specific capacity. It depends both on the amount of redox-active material and the number of reacting electrons, as seen in Equation 5, where z or n is the number of electrons transferred, M is the molar mass, m is the mass of the material, F is the Faraday´s constant, and V is the volume of the tank. [26]

*Equation 5*: *Theoretical volumetric capacity equation [26]*

$$C = \frac{z * F}{3600 * MW} \; or \; C = \frac{m * n * F}{3600 * MW * V}$$

Phoenicin is expected to have a two-electron transfer, resulting in a theoretical maximum capacity of 53.5 mAh for a volume of 20 mL and a concentration of 50 mM used for one part of this project. For the battery connected to the solar panel, the theoretical maximum capacity was calculated based on the solar panel's power; the calculations are seen further on, and it was found to be 16 mAh.

Energy density is defined as the amount of energy that can be stored in an RFB. The given unit is either Wh/kg for gravimetric energy density or Wh/L for volumetric energy density. It is determined by the flow battery voltage or by the electron transfer number of the redox reaction. An increase in battery voltage will lead to an increase in energy density, resulting in a lighter battery compared to a lower energy density battery with similar capacity. The voltage can be increased by using redox species with a broader equilibrium potential difference. This would require widening the electrochemical window of the electrolytes, which is generally limited by the water electrolysis or by tuning the electrolytes' pH. [10], [24], [31]

# 3. Phoenicin

The compound used as an electrolyte for the RFB in this thesis is the naturally in fungus as of the genus Penicillium and Talaromyces occurring compound phoenicin ($C_{14}H_{10}O_6$). When found in crystal form, it is yellow-brownish and turns red-violet if dissolved in a basic solute. [32], [33]

Phoenicin belongs to the class of naphthoquinones, a subgroup of the quinone family known for their carbonyl groups. This categorization of phoenicin is because it has two aromatic rings in its chemical structure, as seen in Figure 3.1. [32]

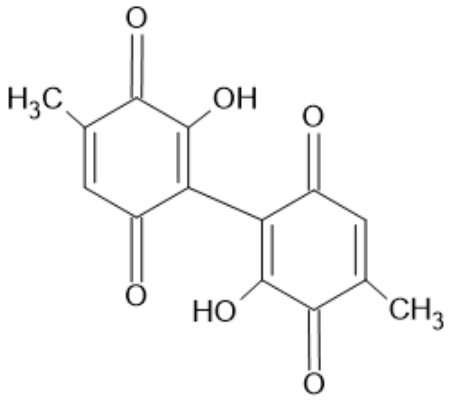


*Figure 3.1: Chemical structure of phoenicin*

The disadvantages of quinones are their low solubility, especially at neutral pH, but also in general stability issues, and their operation on low voltages. The stability issue can be counteracted by adding either a base or acid; however, the compound could possibly undergo unwanted chemical reactions, resulting in compromising the stability.[34]

The functional groups can be seen from the chemical structure mentioned above. Seen from Figure 3.1 is that phoenicin has four electron-withdrawing groups, the ketone groups, and four electron-donation groups, the two alcohol and methyl groups. The electron-donating groups allow for a four-electron transfer, but commonly, only two electrons are transferred. In the case of a four-electron transfer, the capacity would double, resulting in a higher capacity to store more energy. Below in Figure 3.2 and Figure 3.3 are shown both the two-electron and the four-electron transfer. [34], [35], [36], [37]

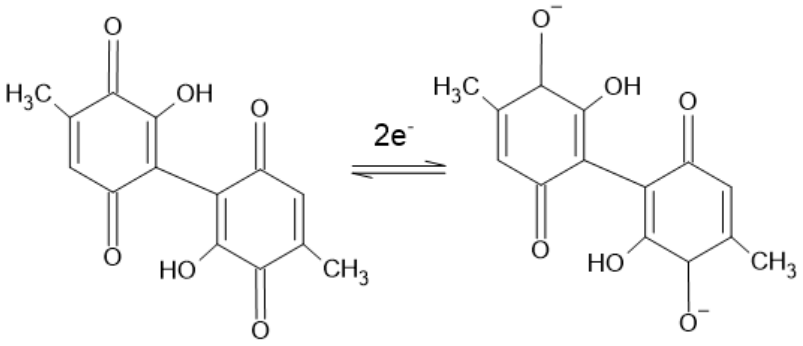


*Figure 3.2: Phoenicin two-electron transfer*

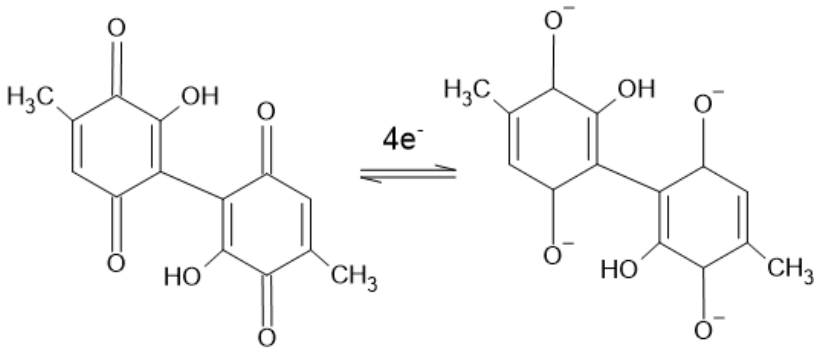


*Figure 3.3: Phoenicin four-electron transfer*

In the previously mentioned study by Wilhelmsen et al., 95% pure phoenicin was used in a similar setup of a single-cell battery test. In these tests, phoenicin was used as a negolyte with a tank volume of 20 mL, resulting in a theoretical capacity of 214.4 mAh for a two-electron transfer, but it only achieved 139.4 mAh. In another study conducted by Wilhelmsen et al., a mix of different phoenicin in the negolyte tank of 10 mL was used, corresponding to a theoretical capacity of 16.41 mAh for a four-electron transfer, but it was assumed that there would only be a two-electron transfer with a capacity of 8.21 mAh. But in the first charging cycle, 15.79 mAh was achieved, implying a four-electron transfer. The capacity drops to 3.91 mAh at the end of the test. [6], [29]

Some chemical side reactions, such as gem-diol formation and Michael addition, can reduce the capacity, both shown in Figure 3.4 and Figure 3.5. The gem-diol formation is a reversible reaction involving the reaction of water with the quinones carbonyl groups, resulting in a hydrate. In the Michael addition of hydroxide ions onto the unsubstituted carbon atoms, which is likely to occur, as shown in the research of Wilhelmsen et al., causing the capacity to fade because of the irreversible reaction causing the loss of electron to donate. [6], [10], [38], [39]

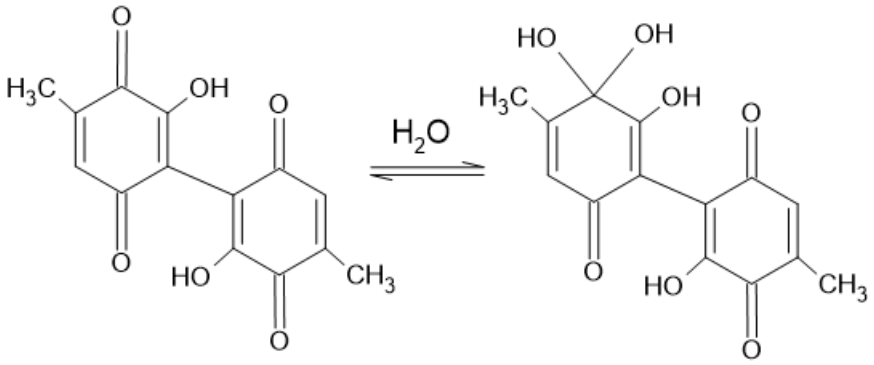


*Figure 3.4: Possible gem-diol formation of phoenicin*

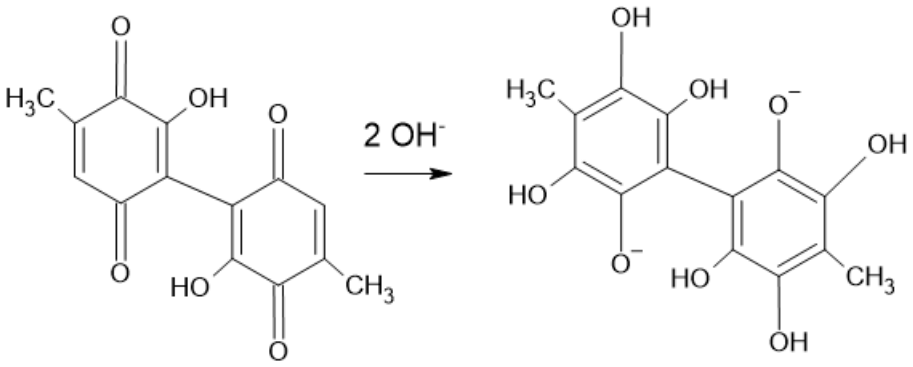


*Figure 3.5: Michael addition of phoenicin*

In the study by Wilhelmsen et al., a mix of different self-produced phoenicin was used to operate an RFB, and the dimer structure of phoenicin was also found in this mix, which structure is visually represented below in Figure 3.6 [6], [40]

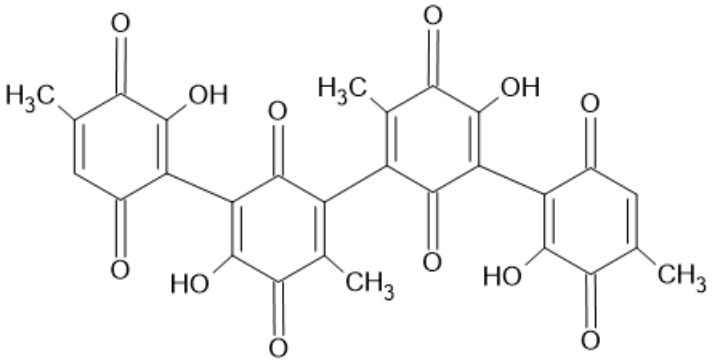


*Figure 3.6: Chemical structure of phoenicin dimer*

The dimer formation causes impurity of the produced phoenicin batches if produced in the phoenicin extraction process. If the dimer occurs in the batch, it will cause a loss of capacity and lower the cell voltage due to the double molecular weight while maintaining the same number of possible electrons to react. It was found in the previously mentioned study that the dimer can also be an advantage to have in the mix in terms of avoiding the Michael addition on the unsubstituted carbon positions. This showed that the phoenicin is utilized to its full potential, reaching its full capacity and causing an increase in CE. [6], [41], [42]

Cyclic voltammetry (CV) is used to study the charge transport/transfer in the electrolyte to validate the phoenicin batches for the cycling battery tests. Wilhelmsen et al. conducted some CV analysis of phoenicin, as seen in Figure 3.7, which will be used to compare the CV done in this project with all the produced batches. The initial investigation by the CV showed that phoenicin had a half-wave potential of -0.37 vs SHE, and coupling it with ferrocyanide in a battery would provide a theoretical operating voltage of 0.86 V. [6], [43], [44]

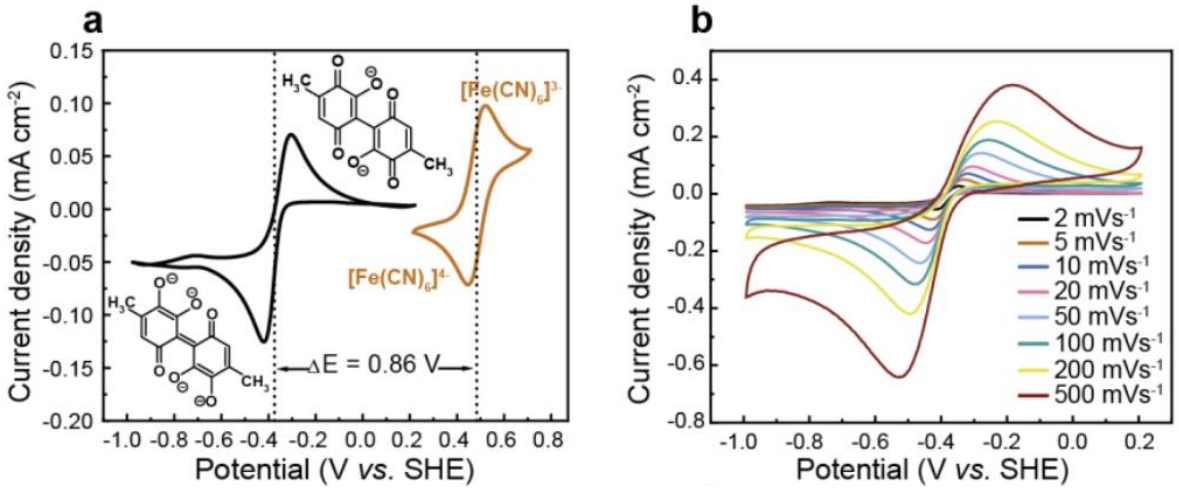


*Figure 3.7: CV from Wilhelmsen et al. studies [6]*

# 4. Solar Panel

One renewable energy source is solar energy. The energy with solar power is produced by converting sun energy into power useable for energy consumption in different sectors. The two possible forms of energy produced by solar power are electricity and heat, and solar panels produce both. [45] Solar energy has the issue of intermittency, leading to periods with either high or low energy production during the day. As the energy demand and consumption do not match, storage technologies for this energy are needed to work with the variability of the available energy from this renewable energy source. The energy storage technologies in the grid infrastructure must balance the energy demand and renewable power generation at peak load time, which requires a fast response time to sudden fluctuations. [6]

The world's largest producer of electricity from solar power in the year 2022 was China, closely followed by the US. The energy generated by solar PV in 2022 reached a record of 270 TWh, surpassing wind energy in absolute generation growth, as seen in Figure 4.1. Also represented in the figure is that solar PV energy will exceed the coal-produced energy by 2027. [46] This indicates the growing importance of solar energy, even above wind energy in the energy generation for the next 3 years. Compared to the wind turbines needing wind, which is not sufficient in the whole world, does the solar panel only need light that is coming through clouds to produce energy. Another factor for the solar panel is that it requires less space compared to the wind turbines, even if a wind turbine can produce ca. five times the energy with a strong wind compared to the PV panel.[47]

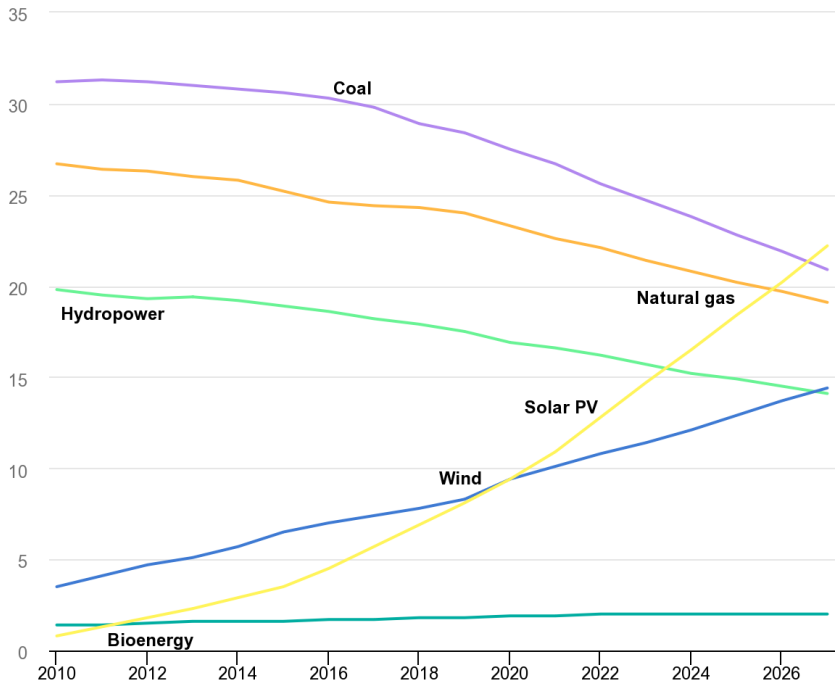


*Figure 4.1: Absolute energy generation [46]*

Solar panels are commonly made from silicon or another semiconductor material installed into a metal panel frame with a glass casing. If this material structure is exposed to photons from the sunlight, it will release electrons, producing an electric charge known as the photovoltaic (PV) effect. The wiring in the panels then captures the created electric current from the previous produced PV charge. With an inverter, the created DC is converted to AC, which is the standard electric current used for normal wall sockets. [45] These panels are

known as solar PV panels, and the panels for heat generation are called solar thermal panels. The solar thermal panels heat the water in a cylinder, providing hot water and heat.

From Figure 4.2, the setup of solar PV technology can be seen. The solar panels produce DC electricity, which runs through a charge controller to monitor and adjust the charge for the following apparatus in this setup. The following figure shows batteries in the set-up, as solar panels can not produce energy without the sun for the photovoltaic effect. The batteries are helpful for storing the energy produced on sunny days and discharge this energy at night or on days without sun. The currently operating batteries are lead-acid or Li-ion batteries, but to improve and make it more "clean", a redox flow battery could also be installed instead of the common solid-state batteries. After the batteries, the DC electricity will be converted to AC electricity through the inverter for useable energy for the household. [48]

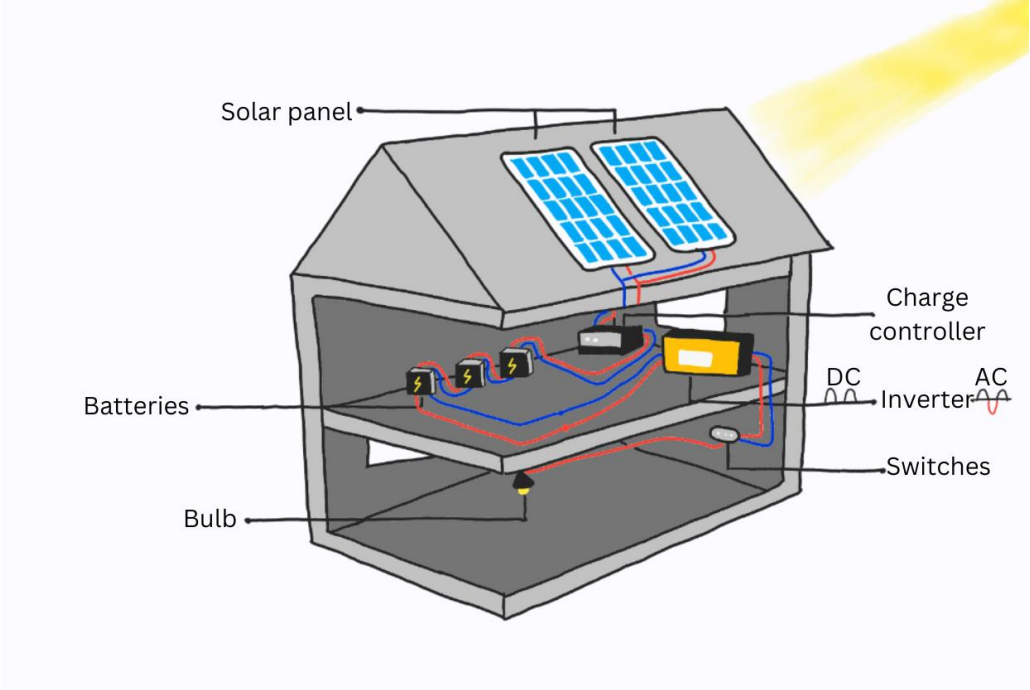


*Figure 4.2: Solar panel setup [48]*

The 10 Wh PV panel used in this project is from the university, and UV light simulates the sun. For the single-cell cycling battery test, the panel's power needs to be converted to capacity for further calculations, and Equation 6 shows the calculation, where mAh is the capacity, Wh is the power and V is the used voltage.

*Equation 6: Phoenicin capacity equation*

$$mAh = Wh * V$$

For the redox flow battery used in the cycling tests, the PV panel is connected to a circuit board connected to multimeters controlling the voltage and current used, as this is a test running with constant current and varying voltage. The electronic setup can be seen in Figure 4.3.

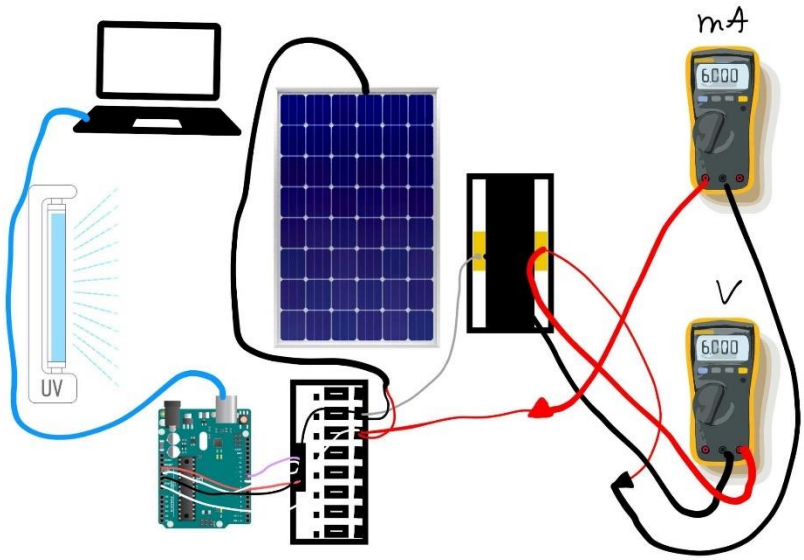


*Figure 4.3: Bench-scale battery test electronics setup*

Utility-scale solar farms commonly consist of hundreds of thousands of PV panels and can produce between 1 MW to 2000 MW. For approximately 25 acres of land, 5 MW can be produced, which is energy for around 10000 homes and businesses. A community solar farm can produce from 100 kW up to 5 MW for local communities. [49] Lithium-ion batteries are the most common form of energy storage for solar farms because of their high energy density, lightweight, high efficiencies and low maintenance needed. [49], [50]

If capturing all the generated energy throughout the day is desirable, a battery should be double the kilowatt peak (kWp) of the used solar array. [51] If the battery is smaller, there will only be spare electricity to use, and if it is bigger, it will cause issues for the system to charge the battery fully. The depth of discharge (DoD) is the ratio of electricity that can be safely discharged before it should be recharged. Lithium-ion solar batteries have a DoD of 95%, and lithium-ion batteries have a DoD closer to 50%. [51]

# 5. TRL of organic RFB

The term technology readiness level (TRL) has many different meanings and definitions, but overall, it is understood as a method for assessing a technology's maturity level. The TRL includes a scale with nine levels representing how mature the technology is. The different levels can be seen in Table 5.1. [52] As ORFB is still a growing research field, it can be beneficial to look at the current TRL of ORFB as well as where this project stands on the table compared to other research.

*Table 5.1: Table of TRL [52]*

| | Level Number | Description |
|---|---|---|
| Deployment | 9 | Actual system proven in operational environment |
| Deployment | 8 | System complete and qualified |
| Deployment | 7 | System prototype demonstration in operational environment |
| Development | 6 | Technology demonstrated in relevant environment |
| Development | 5 | Technology validated in relevant environment |
| Development | 4 | Technology validated in lab |
| Research | 3 | Experimental proof of concept |
| Research | 2 | Technology concept formulated |
| Research | 1 | Basic principles observed |

The TRL allows the technology to evolve from conception to research, development and deployment, where universities focus on TRL 1-4, and the private sector focuses on TRL 7-9. [52]

This project could be placed in either TRL 4 or TRL 5 because the studies of Wilhelmsen et al. proved the concept of phoenicin being able to be used as a negolyte in an RFB, which is TRL 3. This experiment integrates the RFB with a PV panel. Depending on the stability/repeatability of this RFB, it can be either placed in TRL 4 or TRL 5.

Research has been conducted on organic RFB in use as energy storage, further investigating how far this technology is on the TRL scale overall. Mansha et al. conducted a study in 2024 on the current development statutes of aqueous organic redox flow batteries where they revealed that, except for some RFBs, the majority of the RFBs are still in the research phase due to the obstacles in energy densities, cyclability, electrolyte lifespan and cross-over of redox-active species through the membranes. Having discussed the different ORFB types, they concluded that the AORFBs are the most valuable technology as an electrochemical ESS based on their low cost, safety, excellent conductivity, stability, and high voltages. In this study, the levelized cost of storage (LCOS) was introduced, which researchers use to assess the technology potential for commercialisation as it explains the lifetime costs normalised by the cumulative delivered electricity. In the study conducted by Darling et al., the AORFBs received high LCOS due to the costs of the membranes and redox molecules, making it not a viable alternative for the lithium-ion battery currently. [20], [53]

Two companies, CMBlu and Kemiwatt, have employed organic redox flow batteries in their technology catalogues. This means that both companies' technologies are TRL 9.

The CMBlu battery, which operates on carbon-base compounds as electrolytes, is the first of its kind to be commercialised. The carbon material is a fully recyclable organic material, but the electrolytes are not fully liquid. This ORFB is a solid-flow battery that has active solid and

liquid material as electrolytes. CMBlu specifies that this ORFB has an efficiency above 90% and has a battery capacity of up to GWh range. [54]

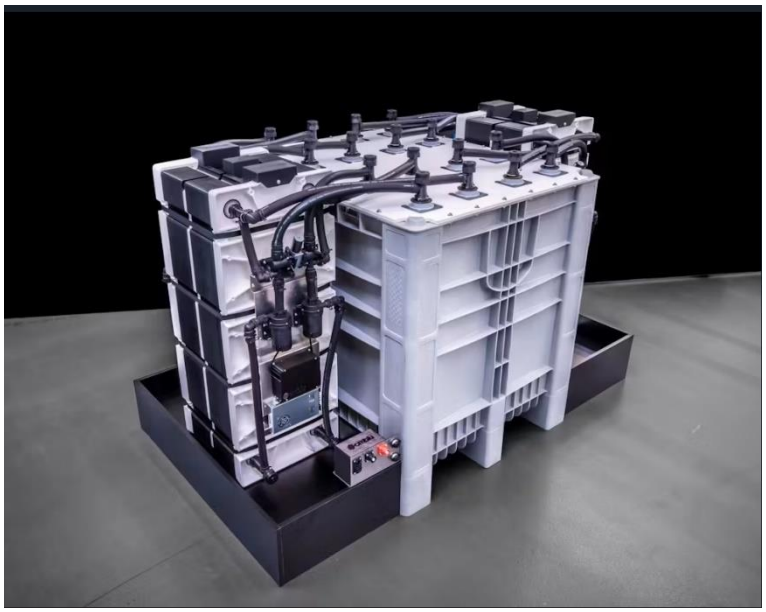

*Figure 5.1: CMBlu RFB*

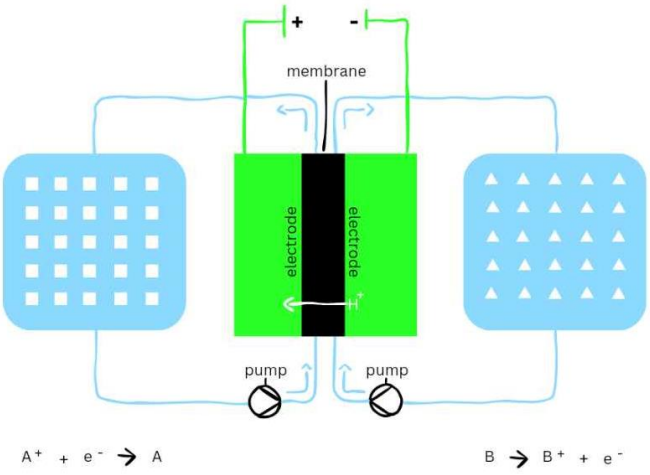


*Figure 5.2: Setup of CMBlu organic SolidFlow battery*

Kemiwatt was the first to create the first AORFB prototype and the first industrial demonstrator. This battery operated with potassium ferrocyanide as posolyte and an anthraquinone derivative as negolyte. The efficiencies achieved for these electrolytes were over 70%. The prototype had a power of 10 kW, and the following demonstration AORFB had a power of 20 kW. [55], [56]

*Figure 5.3: Kemiwatt 10 kW prototype*

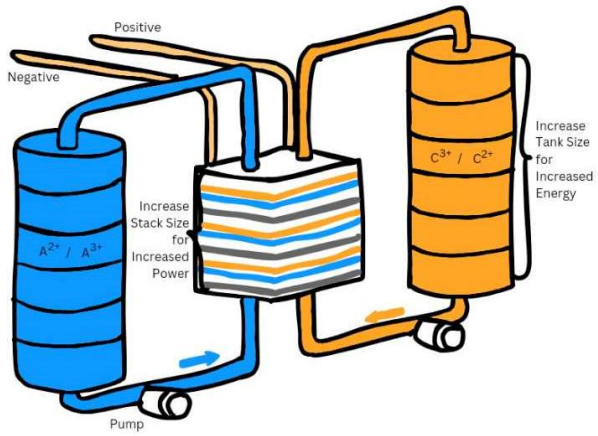


*Figure 5.4: Setup for Kemiwatt RFB*

# 6. Problem Formulation

Based on the problem analysis of which energy source requirement could be used with a phoenicin battery, the solar panel has been chosen as a potential energy source for bench/pilot scaling the phoenicin operating RFB. The following problem formulation was made:

*“How well is a bench-scaled redox flow battery operating with phoenicin as a negolyte reproducible to be used to store a solar panel's energy?"*

To answer this question, single-cell tests of the redox flow battery will be bench-scaled compared to the previously shown redox flow battery and attached to a solar panel. The battery test will be running on different self-produced phoenicin compounds to investigate the possibility of reproducibility. The efficiency of the redox flow battery operating with phoenicin will be evaluated based on efficiencies (CE, VE, and EE), capacity capability, and loss. All batteries will be looked into individually, and then, for the question above, they will be compared to answer the question based on the previously mentioned criteria.

# 7. Project Delineation

To answer the problem formulation, the redox flow battery will be bench-scaled to accompany the energy capacity of the attached solar panel, which is 10 Wh. The solar panel will be connected to investigate if a bench-scaled battery can be used for a more conventional use outside the lab. The experiments will consist of multiple single-cell battery tests of the RFB on different produced phoenicin batches to validate the possible use of a phoenicin-operating battery to store energy from a solar panel.

The phoenicin used in this experiment was self-produced in-house within the scope of this thesis Wilhelmsens et al. paper will be used to guide the production of the phoenicin. The in-house production of the phoenicin will give a high chance of change in the purity of the phoenicin as this is not the focus of this thesis, but also, being an organic compound, it will result in inconsistencies. The process of phoenicin production is described later in Chapter 8, but throughout the whole thesis, 14.71 g of phoenicin was produced.

Because of the limited amount of phoenicin possible to produce in one cycle while working on the battery simultaneously, it was concluded to first do some quality testing by using single-cell tests with a small quantity of the produced phoenicin to make sure that the phoenicin would be able to be used in a bench-scaled battery. The phoenicin concentration for these smaller scale tests was fixed to a value of 50 mM with a total volume of 20 mL. These values were taken from past experiments and to account for the limited production of phoenicin.

The catholyte is potassium ferrocyanide, $K_4Fe(CN)_6$, the same as in the previous experiments but also in the paper from Wilhelmsen et al.. Both anolyte and catholyte were dissolved in a KOH solution with different concentrations based on the ionic strength, which was accounted for to equalize the pressure across the membrane to be sure that in case of a failure the membrane would not fracture and cause transfer of the electrolytes but instead that the cause would be the phoenicin side meaning that electrolyte has run dry. The anolyte was kept as the limiting side throughout all single-cell battery tests, resulting in the catholyte, potassium ferrocyanide, being in an excess amount of a volume of 100 mL and 30 mL. The reason for also choosing the catholyte to be in excess amount is due to the stoichiometric coefficient for the discharge/charge reaction.

After quality testing, feasible phoenicin batches will be used in the bench-scale single-cell battery tests running with the power produced by the attached PV panel. The amount of phoenicin needed to store the produced energy from the PV panel is connected with the possible power produced by the panel, which in this study was 10 Wh. First, it was believed a 280 Wh PV panel would be used for this project, also resulting in the production of multiple phoenicin batches to have enough amount of phoenicin needed but after consulting, it was decided not to use this PV panel but instead go with the 10 Wh panel. The first step was to convert the power from Wh into mAh. The Wh needs to be multiplied by the voltage, which was taken to be the highest voltage used for the cycling tests, being 1.6 V, and this calculation is shown in Equation 7.

*Equation 7: Capacity equation*

$$mAh = Wh * V \rightarrow 10\,Wh * 1.6\,V = 16\,mAh$$

From this possible maximum capacity produced by the PV panel, the amount of phoenicin needed to have that capacity was calculated, which can be seen in Equation 8 below.

*Equation 8: Phoenicin mass equation*

$$mAh = \frac{n * F * m}{3600 * MW} \rightarrow m = \frac{0.016\ mAh * 3600 * 274.23\ mol/g}{2 * 96485.33\ Ah/mol} = 0.082\ g$$

Because of the results gathered from the quality, it was decided to go with almost double the amount of phoenicin, which was 0.153 g. After fixing the amount of phoenicin needed together with the calculated number of moles and molarity, the electrolyte's volume was calculated, resulting in a tank volume of 11 mL.

From there, these values were used together with the knowledge that the catholyte should use KOH of 1M. The concentration of the anolyte KOH solution and the volume of the catholyte tank were determined, as seen in Figure 7.1. The SOC difference should be as close as possible to zero to have equalized pressure across the membrane to not cause fracture of it. The volume of the catholyte tank was set to 30 mL with 0.553 g potassium ferrocyanide with a 1M KOH solution, and the acolyte tank has a volume of 11 mL with 0.153 g phoenicin with a 2.8M KOH solution.

| | Nmol/L | | | | | |
|---|---|---|---|---|---|---|
| Supportive electrolyte | 1 | | | | | |
| Catholyte | 5,00E-01 | | | | | |
| Volume (L) | 3,00E-02 | pH | 13 | | | |
| Species | Nmol | Concentration(mol/L) | Charge | IS_Part | OS_eq1 | OS_eq2 |
| OH- | 0,03 | 1,00 | 1 | 1 | 24,30207 | |
| K+ | 0,08500 | 2,8333 | 1 | 2,833333 | 68,85586 | |
| FeCN6 4- | 0,01000 | 0,33333 | 4 | 5,33E+00 | 8,10E+00 | |
| FeCN6 3- | 0,00500 | 0,17 | 3 | 1,50E+00 | 4,05E+00 | |
| | | | | | | |
| Gas constant | 0,08206 | | | | | |
| Temperature | 296,15 | | | | | |
| | | | | | | |
| IS_POS_Catholyte | | | | 5,333333 | | |
| | | | | | | |
| Eq1= C*R*T*i | | | | | | |
| OS_eq1__POS_Catholyte | | | | 105,309 | | |

| SOC - χ | 0,5 |
|---|---|
| mlim (mol) | 5,00E-03 |
| Stoechio coef | 2,00E+00 |
| | |
| Difference SOC | -0,03333 |
| Must be = 0 | |
| | |
| Difference OS | 42,93366 |
| Must be = 0 | |

| | mol/L | | | | | |
|---|---|---|---|---|---|---|
| Supportive electrolyte | 2,8 | | | | | |
| Anolyte | 5,00E-01 | | | | | |
| Volume (L) | 1,00E-02 | pH | 13 | | | |
| Species | Nmol | Concentration (mol/L) | Charge | IS_Part | OS_eq1 | OS_eq2 |
| OH- | 0,0230 | 2,30000 | 1 | 2,3 | 55,8948 | |
| K+ | 0,0330 | 3,30000 | 1 | 3,3 | 80,1968 | |
| phendischarged | 0,0025 | 0,25000 | 2 | 1 | 6,07552 | |
| phencharged | 0,0025 | 0,25000 | 4 | 4 | 6,07552 | |
| | | | | | | |
| IS_POS_Anolyte | | | | 5,3 | | |
| | | | | | | |
| OS_eq1_POS_Anolyte | | | | 148,243 | | |

*Figure 7.1: Ionic strength calculations for bench-scale battery with 10 Wh PV panel*

The stoichiometric coefficient is determined by the oxidation state of charge of phoenicin and ferrocyanide in their reduced and oxidized states, respectively. Phoenicin occurs as phoenicin$^{-2}$ in the electrolyte and can either accept two or four electrons. It will be reduced to either phoenicin$^{-4}$ or phoenicin$^{-6}$. For ferrocyanide, it occurs as $[Fe(CN)_6]^{-4}$ in the electrolyte and will be $[Fe(CN)_6]^{-3}$ in the oxidized state. These two reactions can be seen in Equation 9. This redox reaction results in a stoichiometric coefficient of 2, and the corresponding ionic strength of this reaction is calculated from the movements of all ions in the electrolyte solutions.

*Equation 9: Redox reaction of the RFB*

$$C_{14}H_8O_6^{-2} + 2e^- + 2Fe(CN)_6^{-4} \rightleftharpoons C_{14}H_{10}O_6^{-4} + 2Fe(CN)_6^{-3} + 2e^-$$

The pump's flow rate was first set to 40 mL/min as a higher flow rate would take a longer time per cycle and rejected due to the time constraint, but it has also shown better efficiencies in previous studies. The slower flow rate has shown less capacity loss per day, similar to the higher one compared to the 40 mL/min.

# 8. Methods and Materials

In this project, two main methods were conducted: the cultivation and production of the compound phoenicin and the single-cell test of the redox flow battery.

## 8.1. Fungal cultivation for phoenicin production

The fungal strain used for the production of phoenicin was *penicillium mangini*, which is also known as *penicillium atrosanguineum,* which was used in the PhD study from Wilhelmsen et al. The study is used as a guide for the cultivation and extraction of phoenicin and later for comparison of the battery test results. For cultivation, the fungus was transferred onto plates and was cultivated for 12 days at a temperature of ca. 28°C, which is a discrepancy from the study's setup, where the fungus was cultivated at 25°C.

After the fungi were cultivated on the plate, a spore suspension was made, which was used together with broth grow media in flasks to produce a phoenicin-broth solution. These flasks were incubated for 14 days at a temperature of around 28°C, where the incubator was changed halfway through the batches because of equipment changes. Following the cultivation and production of the phoenicin-broth solution, phoenicin is extracted from that solution for later use in the RFB.

### 8.1.1. Experimental setup

The equipment used for this method included plates, 50 mL centrifuge tubes, ten 1 L flasks, and 5 mL and 300 µL pipettes. Other materials used for the cultivation were the fungal strain *penicillium mangini*, Potato Detox (Agar), MERCK, yeast extract, Czapek Dox broth, sucrose, $CuSO_4*5H_2O$, $FeSO_4*7H_2O$, $ZnSO_4*7H_2O$, $MnSO_4*2H_2O$, $Na_2B_4O_7*10H_2O$ and $Na_2MoO_4*2H_2O$.

As already mentioned, the fungal strain used in this project is the penicillium mangini, which was already given on two plates and used later to remake more plates for cultivation. For the cultivation, 35 plates of 39 g/L Potato Dextrose Agar were made, 5 per cultivation cycle. The strain was cultivated on the prepared plates for 5-10 days in an incubator set at around 28°C in darkness. The fungal strain was transferred from the original two plates, see Figure 8.1 for the first cultivation, and from there on, these plates were used for further transfer of the strain onto the used plates for the cultivation. These changes from the study were made either because of the state of the operating systems or because of time constraints due to limited time.

*Figure 8.1: Original plates*

*Figure 8.2: Plates after use for suspension*

After the plate incubation, a spore suspension, also called preinoculum, was prepared see Figure 8.3 and Figure 8.4. This suspension was prepared from one plate of the five or more prepared where three 1x1 cm, see Figure 8.2 pieces were suspended in 10 mL of PDA made from 39 g/L of Potato Dextrose Agar (liquid) and 1 mL/L trace metal solution of 10 g/L MERCK and 5 g/L $CuSO_4*5H_2O$. This suspension was let to rest for between max. 24 to min. 12 hours in an incubator at 30°C and a rotation of 200 rpm before the next step. Different plates were used for the different batches of phoenicin, but batches 6 and 7 were from the same plate.

*Figure 8.3: All three suspensions for one batch*

*Figure 8.4: A single suspension*

Next is transferring the suspension to the ten Ehrlenmeyer flasks used for growing the fungus and producing the phoenicin in the liquid. The ten flasks were filled with 100 mL of a

modified Czapek-yeast-broth growth media containing 5 g/L yeast extract, 35 g/L Czapek Dox broth, 60 g/L sucrose and 20 mL of a mineral mix. The mineral mix is made out of 0.4 g/L $CuSO_4*5H_2O$, 0.8 g/L $FeSO_4*/H_2O$, 8.0 g/L $ZnSO_4*7H_2O$, 0.8 g/L $MnSO_4*2H_2O$, 0.04 g/L $Na_2B_4O_7*10H_2O$ and 0.8 g/L $Na_2MoO_4*2H_2O$. The growth media was prepared one day before being transferred into the flasks and autoclaved. Afterwards, it was filled first with 20 mL of the mineral mix and second with 1 L of autoclaved mineral water. It was only used 10%, aka. 100 mL of the produced growth media in the 1 L flasks to achieve the best possible surface area for the fungi to grow. There were limited amounts of Ehrlenmeyer flasks in the labs; some of the incubations were conducted with a mix of normal 1L flasks and Ehrlenmeyer flasks. From the suspension 300 µL are added to each of the ten flasks already containing the growth media. To transfer the suspension, the pipette tip mustn't touch the fungal piece inside the tube. After adding all the liquids, the flasks are tightened loosely to have still oxygen coming into the flasks for the fungi to grow. The flasks were incubated for min. 14 days in darkness at around 26°C, which can be seen in Figure 8.5 on the right side where the liquid is yellow from the broth.

*Figure 8.5: Fungi growing in the flasks*

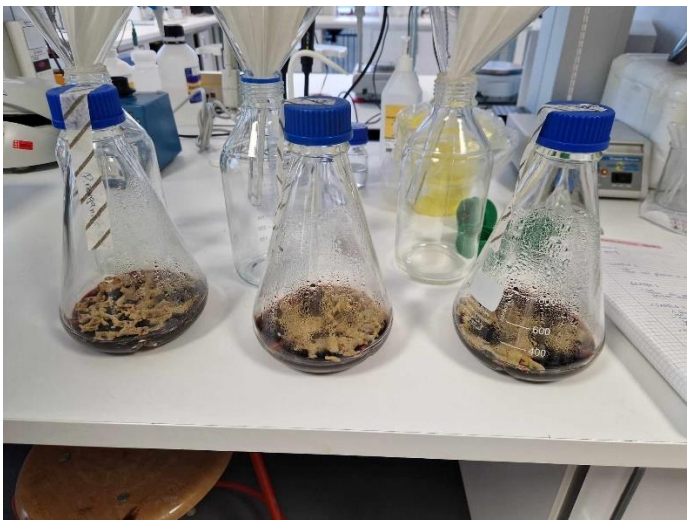

*Figure 8.6: Fungi grown after three weeks of incubation*

## 8.2. Extraction

After the fungi grew inside the flask with the growth media producing phoenicin, the phoenicin was extracted. The extraction method included the separation of the inorganic and organic phase, which contains the phoenicin. Following is the different drying process of the phoenicin to have it in powder form for the use for the RFB.

### 8.2.1. Experimental setup

The equipment used to extract the phoenicin from the broth included three funnels, six 1 L laboratory bottles, a coffee filter, a 1 L separation funnel, a rotary evaporator, three round flasks, 15 mL centrifuge tubes, a nitrogen evaporator, and a freeze dryer. The only chemical used in this method was ethyl acetate.

The fungi have grown on top of the growth media, and the liquids have turned dark red/violet during the incubation, indicating the production of phoenicin, which can be seen in Figure 8.5 on the left side and in Figure 8.6. The liquid was filtered through an ordinary coffee filter, and 10-15 mL of 1M hydrochloric acid was added per 300 mL of phoenicin liquid. This resulted in three batches of phoenicin liquid for extraction, ideally containing twice 300 mL and once 400 mL, as shown in Figure 8.7, if all ten flasks could be used. For batch 5, there were once 200 mL and twice 300 mL due to contamination in the flasks, and for batch 4, it was three times 300 mL. The specific achieved volumes for each batch can be found in Table 8.1 at the end of this chapter. The hydrochloric acid was added to acidify the solution to a pH of 2.

*Figure 8.7: Filter process*

After that, the extraction process is conducted in three steps: liquid partitioning, nitrogen evaporation and dry freezing.

For the first step, the liquid partitioning to the filtered phoenicin liquid, an equal volume of ethyl acetate was added first to the flasks seen in Figure 8.8. This addition results in a separation of inorganic (bottom) and organic (top) phases, with the organic phase containing the phoenicin being the important one.


*Figure 8.8: Separation in a flask*

The phoenicin liquid and ethyl acetate mixture is added to a separation funnel, where it will sit for at least 10 minutes to ensure the phases have been separated, as shown in Figure 8.9. The inorganic phases will be reused using the same steps as before, which include adding ethyl acetate and separating the phases.

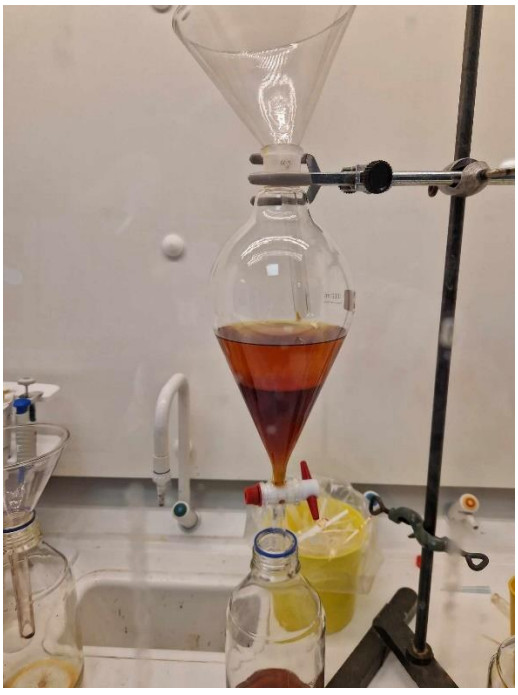

*Figure 8.9: Separation funnel with inorganic and organic phase*

The separation results in three flasks containing double the amount of organic phase liquid compared to before the extraction seen in Figure 8.11, and in Figure 8.10, for one single flask, the combined organic phase liquid can be seen. Comparing these two pictures, it can be seen that every batch has a slight colour difference.

*Figure 8.10: Combined organic phase of a single flask*

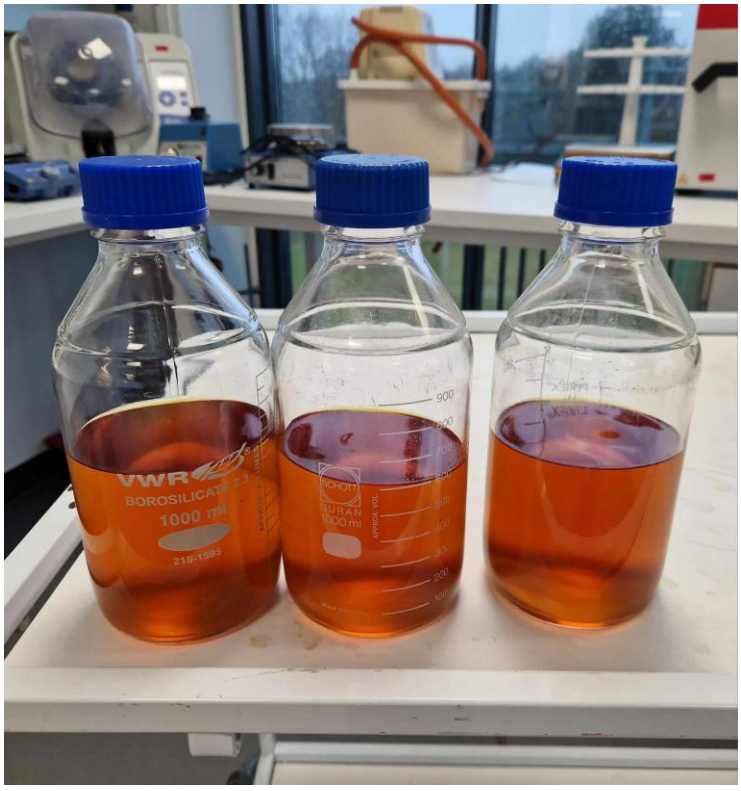


*Figure 8.11: All three flasks for one batch with combined organic phase liquid*

After obtaining the flasks with the organic phases, these are transferred to a rotary evaporator to evaporate the still-remaining ethyl acetate and acquire dry matter, phoenicin. The evaporator was operated with the water bath set to a temperature of 40°C, which is ca. 30°C below the boiling point of ethyl acetate and the rotation of the flask was set to 80 rpm. The evaporation was done in either three or four steps/pours as the amount of liquid added into the flasks was advised not to be above 200 mL in each pour because of the angle of the flask while rotating. The setup is shown in Figure 8.12.

*Figure 8.12: Rotary evaporator setup*

After evaporating the entire flask of organic matter, the dry phoenicin mass was re-dissolved in 12 mL of ethyl acetate and transferred into a 15 mL centrifuge tube. Because we had three flasks with the organic phase, we also had three 15 mL centrifuge tubes. Each batch has its own rotary evaporator flask due to the dry matter not being able to be re-dissolved entirely in a small amount of ethyl acetate used and to ensure as much compound was re-dissolved as possible with this small amount.

Following this, the solution was nitrogen evaporated, see Figure 8.13, to again evaporate the ethyl acetate and to receive just the dry phoenicin. The nitrogen evaporator was set to a temperature of 65°C ca. 10°C below the boiling point of ethyl acetate. This evaporation also resulted in completely dry phoenicin, but it was still too viscous to be sure of how much actually would be used for the battery because of this state.

*Figure 8.13: Nitrogen evaporation setup*

The last step of the phoenicin extraction was the freeze-drying of the viscous phoenicin from the previous step. For this, the freeze dryer ran for between 16 and 24 hours with the tubes

inside. Halfway through the experiment, the freeze dryer was changed; Figure 8.14 shows the old freeze dryer used for batches 1-4, and Figure 8.15 shows the new freeze dryer used for batches 5-7.

*Figure 8.14: Old freezer dryer*


*Figure 8.15: New freezer dryer*

After the extraction, the dried phoenicin was scraped inside the tubes to obtain powdered phoenicin. Each tube was weighed to calculate the amount of phoenicin acquired for this process, as shown in Table 8.1.

*Table 8.1: Table of phoenicin amounts in g from each tube and all tubes added*

| Sample | 1. [g] | 2. [g] | 3. [g] | Total Weighed [g] | Broth Volume [mL] |
|---|---|---|---|---|---|
| 1 | 0.73 | 0.25 | 0.83 | - | 2*300 and 1*400 |
| 2 | 0.87 | 1.38 | 1.27 | 2.68 | 2*300 and 1*350 |
| 3 | 0.97 | 1.43 | 1.14 | 2.68 | 2*300 and 1*350 |
| 4 | 0.38 | 0.56 | 0.56 | 1.2 | 3*300 |
| 5 | 0.65 | 0.68 | 0.45 | 1.54 | 2*300 and 1*200 |
| 6 | 0.94 | 0.94 | 0.88 | 2.17 | 3*300 |
| 7 | 0.9 | 1.05 | 1.02 | 2.63 | 3*300 |

Before the phoenicin was used in the battery, each tube of each batch was run through the cyclic voltammetry (CV) to measure the passing current from the applied potential. This is done to see if the phoenicin produced has reversible electrochemical properties matching pure phoenicin, which can be seen by the graph produced where the peaks identify the possible electron transfer. After each tube has been tested, the powder of all tubes from the same batch are combined into one tube and tested again. The combined phoenicin samples are used for the battery test. This experiment's main reason was to ensure that the self-produced phoenicin would perform the same behaviour as the phoenicin from Wilhelmsen et al. studies. The reduction and oxidation peaks should appear and grow with increasing scan rates. Sharper peaks can indicate faster oxidation or reduction, and smaller peak separation indicates faster redox processes. [6]

## 8.3. Single-cell test of RFB

The main focus of this thesis is the battery test with phoenicin as the anolyte. This part of the method has been divided into different test setups, which included the test with previous small concentrations of phoenicin and the test with the battery coupled with the solar panel. The first tests were conducted to investigate the capacity capabilities of the self-produced phoenicin and whether it could be used for a bench-scaled battery coupled with the solar panel.

### 8.3.1. Experimental setup

The chemicals used for this part of the method are phoenicin, potassium ferrocyanide and KOH solution with 1M, 2.8M and 3.1M concentrations. The equipment utilized was a Redox flow battery test cell from redox-flow.com, PTFE tubes, Masterflex tubes, cation exchange membrane, Sigradet GDL 39 AA, Freudenberg H23, DOW CORNING high vacuum grease, Telefon tape, Parafilm, Shenchen peristaltic pump YZ1515x, Neware battery testing system BTS4000 (CT-4008-5V6A-S1), two 1 L laboratory bottles and two 100 mL laboratory bottles.

This part of the thesis starts with making the two electrolyte solutions, the anolyte with phoenicin and the catholyte with potassium ferrocyanide.

The first tests were to ensure that the phoenicin produced had electron-chemical properties and would be functional in the bench-scaled battery. For these, the catholyte contained 100 mL of KOH, in which 2.112 g of potassium ferrocyanide was dissolved, and the anolyte contained 0.274 g of phoenicin dissolved in 20 mL of 3.1M KOH. Both solutions had a concentration of 50mM, which was calculated based on the adjustment of the phoenicin side being the limited side. These values were taken from experiments that had previously been done. Both solutions were stirred with a magnetic stirrer to ensure the complete dissolvement

of the powders in KOH. The second type of test contained 0.553 g of potassium ferrocyanide in 30 mL of KOH for the catholyte, and for the anolyte, 0.153 g of phoenicin was dissolved in 11 mL of KOH.

Both electrolyte solution tanks were thereafter submerged in water, see Figure 8.16, tanks with self-made dark covers. The submerging was done to reduce the chances of oxygen being brought into the system, and the covers were added because the electrolyte could potentially be photosensitive.

*Figure 8.16: Submerged 100 mL bottle in 1 L bottle*

After that, the solutions underwent nitrogen purging after each other because of equipment problems for ca. 20 minutes, shown in Figure 8.17, where phoenicin was already purged and ferrocyanide was being purged.


*Figure 8.17: Nitrogen purging of one bottle*

While the first one is being purged, the other one is assembled, including the submerging and having it ready for the purge. The nitrogen purge was done to reduce the oxygen content in the solution because the reduced products of the solution could possibly react with the

oxygen. Before the purge, the connection tubes for the battery were sealed with Parafilm, and after the purge, the last two tubes were sealed off. The tube connections at the top of the tanks are fastened by hand and afterwards with tools, and to reduce the oxygen further, these connections sometimes have to be taped with Parafilm if the connection leaks oxygen while submerging.

While the electrolyte tanks are nitrogen purged, the battery cell is constructed, which is the same for both tests. The components are assembled from the bottom to the top or from the right to the left side; see Figure 8.18:

- Metal plate (bottom)
- Rubber square plate
- Current collector
- Graphite block with flow field towards (B block)
- 2 rubber gaskets
- Carbon paper electrodes
- Rubber gaskets with membrane downwards + the other rubber gasket
- Carbon paper electrodes
- Graphite block with flow field downwards (A block)
- Current collector

*Figure 8.18: Battery cell assembled*

The membrane used in the thesis is the cation exchange membrane named Fumasep E630K, which is different from most commonly used membrane, Nafion 117, which was also used in previous studies. The carbon paper has to be made hydrophilic to ensure that the electrolytes will be adsorbed and can react with each other. This is done by baking the paper at 400°C for at least 24 hours. The carbon paper was switched from Sigract GDL 39AA to Freudenberg H23 for the battery tests with the PV panel. For each battery test, six carbon papers are used, which are all wetted before being stacked onto each other in two stacks of three carbon papers per stack for both sides of the membrane. Both the carbon papers and the membrane have an active area of 6.125 $cm^2$, but the membrane is cut out a bit bigger to

fit over the hole with the dimension of the active area. After each piece of the battery is assembled, the battery will be screwed together with 5 mm screws and fastened with a Newton meter at 5N.

Each graphite block has two tube connections, one for the flow into the battery (bottom) and one for the flow out of the battery (top). The tubes from the tanks are connected to the battery after both tanks are purged to avoid the introduction of too much oxygen into the system/battery cell and inserted into the pump.

The flow rate of the connected pump is 40 mL/min, and the battery is running for a short time to make sure there is no leakage of the compound from the graphite tube connections or some other problems present. After that, the two clamps are attached to the current collector plates, which are connected to the battery tester, which starts the single-cell tests. Figure 8.19 shows the battery test set-up after running for 100 charge/discharge cycles, which can be indicated through the yellowish ferrocyanide, which shows that the ferrocyanide has reacted.

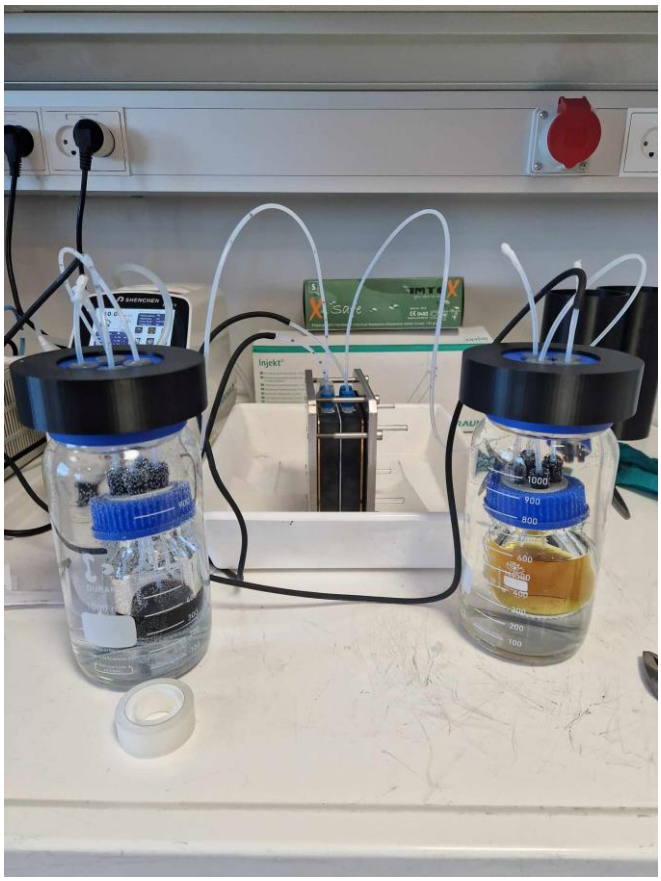

*Figure 8.19: Battery cell setup with electrolyte tanks*

The battery set-up for the bench-scale test had these additions to the small battery tests, which included two multimeters, a 10 Wh PV panel, an Arduino circuit board, a single channel DC 5 V Relay Modul and a 10 ohm resistance.

The PV panel is the power source imitating the sun instead of the battery tester in the small battery cell tests. Arduino is used to change from charge to discharge and sets the limits of 1.6 V and 0.6 V for the respective cycle. While fine-tuning the settings, it was discovered that the battery's current was so low a 10 ohm resistance was added to get the current at one decimal point mA. The data recorded on the multimeters instead of over the battery tester were transferred via a USB connection to a laptop for voltage and current, respectively and saved on the laptops.

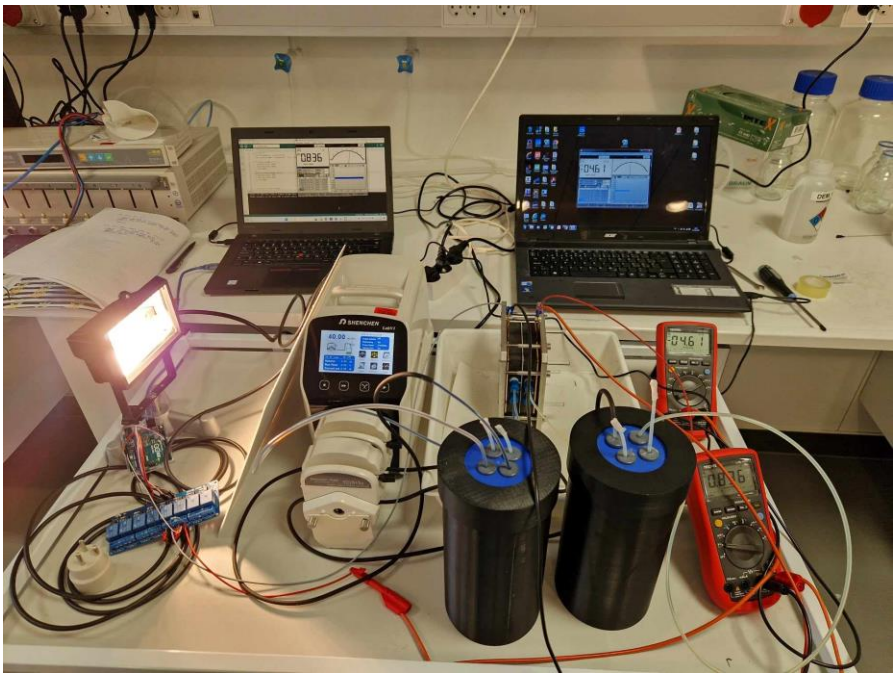

*Figure 8.20: Bench-scale battery cell setup*

Because of some issues saving the data from the multimeters to the laptop, it was decided to stop the sun and the data recording from 21 o´clock to 5:30 o´clock the next day to save the date from the day without any issues.

#### 8.3.1.1. Battery test for 90 Wh PV panel

Before the decision on a 10 Wh PV panel was made, there were some discussions about using a 90 Wh panel first. For this case, a battery with bigger electrolyte tanks compared to the tanks used for the quality testing was conducted, which will be further referenced as the big battery and is a result based on the assumption of using a 90 Wh PV panel. The used chemicals and equipment were 0.737 g phoenicin in 54 mL of 2.8M KOH, 2.763 g potassium ferrocyanide in 150 mL of 1M KOH, and two 250 mL laboratory bottles and two 10 L buckets, respectively.

These values of phoenicin and ferrocyanide are based on calculations using 90 Wh as the base solar panel power, resulting in 144 mAh and the ionic strength between the two electrolytes.

Because of the larger amount of electrolytes, the tanks needed to change from 100 mL bottles in 1 L bottles to 250 mL in 10 L buckets, as shown in Figure 8.21. This picture shows the complete setup for this big battery.

*Figure 8.21: Big battery cell setup with electrolyte tanks*

Because the tanks are closed containers without the option to look into them, it was impossible to check if the small bottles were correctly submerged in the water; some were pre-submerged. As seen in Figure 8.22 and Figure 8.23, the small bottles were submerged in a 1 L beaker to check if the bottles were not leaking.

*Figure 8.22. Pre-submerged phoenicin*

*Figure 8.23: Pre-submerged ferrocyanide*

After it was found that the bottles were not leaking, they were submerged in the buckets, as shown in Figure 8.24. After checking, the buckets were sealed and opened again after the battery was done.

*Figure 8.24: Electrolyte tanks*

The rest of the procedure was the same as the batteries conducted for the quality check testing regarding the nitrogen purging and assembling from the large battery. Because the PV panel could not be used and the rest of the electronic equipment was not ready yet, the battery test was still conducted with the battery tester as the power source.

Table 8.2 shows all the battery tests conducted in this project.

*Table 8.2: Table of battery tests conducted throughout the project*

| Battery Tests | Phoenicin Amount [g] | Applied Voltage [V] | Current [mA] | Cycles |
|---|---|---|---|---|
| Quality batch 2 | 0.275 | 0.6-1.6 | 62.5 and 31.3 | 100 |
| Quality batch 3 | 0.276 | 0.6-1.6 | 62.5 and 31.3 | 100 |
| Quality batch 4 | 0.275 | 0.6-1.6 | 62.5 and 31.3 | 100 |
| Quality batch 5 | 0.274 | 0.6-1.6 | 62.5 and 31.3 | 100 |
| Quality batch 6 | 0.277 | 0.6-1.6 | 62.5 and 31.3 | 100 |
| Quality batch 7 | 0.275 | 0.6-1.6 | 62.5 and 31.3 | 100 |
| Big battery | 0.738 | 0.6-1.6 | 62.5 and 31.3 | 100 |
| Bench batch 2 | 0.154 | 0.6-1.7 | 62.5 and 3.31 | 100 |
| Bench batch 3 | 0.154 | 0.6-1.7 | 62.5 and 3.31 | 100 |
| Bench batch 4 | 0.154 | 0.6-1.7 | 62.5 and 3.31 | 100 |
| Bench batch 5 | 0.153 | 0.6-1.7 | 10 and 3.31 | 28 |
| Bench batch 6 | 0.156 | 0.6-1.7 | 10 and 3.31 | 28 |
| Bench batch 7 | 0.154 | 0.6-1.7 | 10 and 3.31 | 16 |

# 9. Results and Discussion

The phoenicin production resulted in seven phoenicin batches, each used in a respective battery test. There were differences in each phoenicin batch, which included three of the batches that had bacteria contamination, resulting in the discarding of between one to three flasks of the fungi. The most significant difference was the plate culture used for the suspension.

The study from Wilhelmsen et al. was used both as guidance and as a comparison for the battery test results. However, in this study, different from that study, all the battery tests were conducted to run for 100 cycles constantly to have a reference and to thoroughly compare all tests with each other regardless of whether the battery reached 0 mAh or not. This decision had to be changed for batteries later on because of time constraints.

As mentioned, before any battery test was set up, the phoenicin samples underwent cyclic voltammetry (CV) to indicate if the sample had electrochemical properties. If it does have electrochemical properties, it would be shown by how the peaks look; it also could indicate if there is a possible four-electron transfer instead of the expected two-electron transfer, which would indicate double the possible capacity achievable based on Equation 5. Another reason why CV was used was to have a first indication of any difference in the phoenicin batches before using them in the battery. The voltammograms of batches 1, 3, and 4 are shown below in Figure 9.1, Figure 9.2, and Figure 9.3, respectively. The rest of the CV curves can be seen in the appendix in Chapter 13. The CV curve for batch 1 also shows no oxidation peaks and one slight peak for the reduction, indicating that this phoenicin seems not to have reversible electrochemical properties and no electron transfer, which is further proven by the unsuccessful battery test. For the other two figures, two CV graphs from two different scan rates are shown to represent that for these batches, as well as for batches 2, 5, 6 and 7, and the peaks are indeed increasing with increasing scan rate, which follows the observation made in studies of Wilhelmsen et al. The peaks of batch 3 are sharper, which indicates faster oxidation or reduction on the electrode surface. [6]

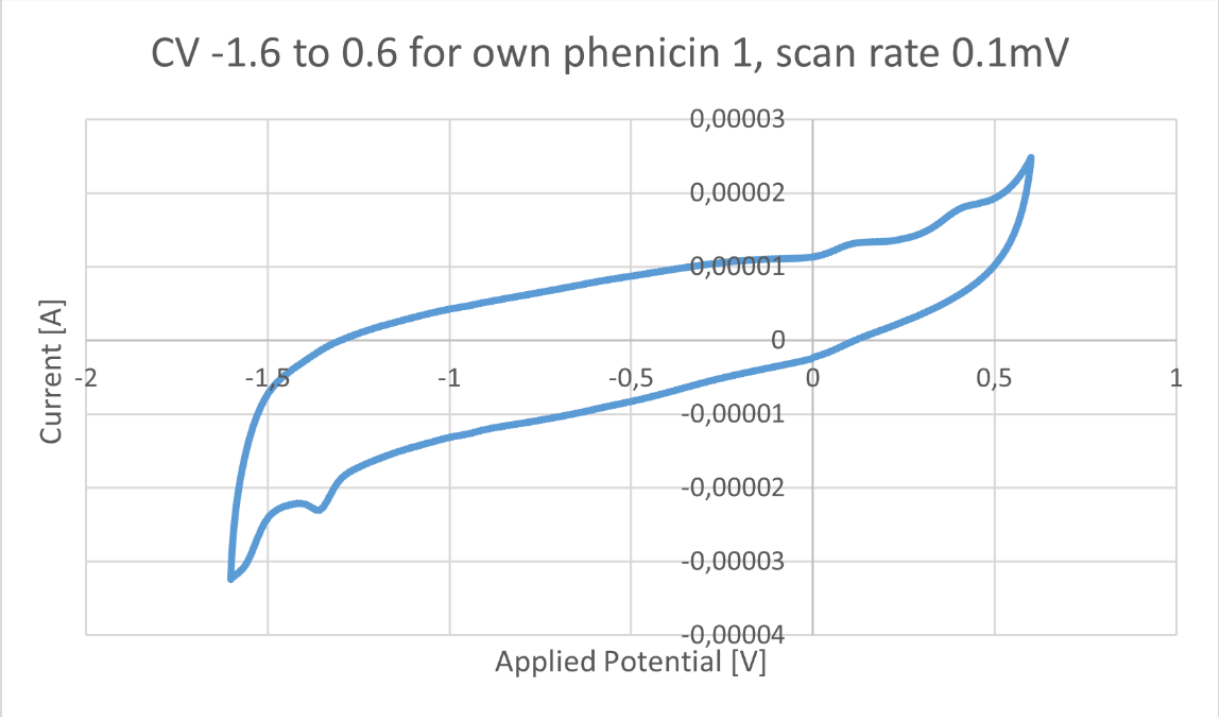


*Figure 9.1: CV curve of batch 1 all tubes together at scan rate 100 mV/s*

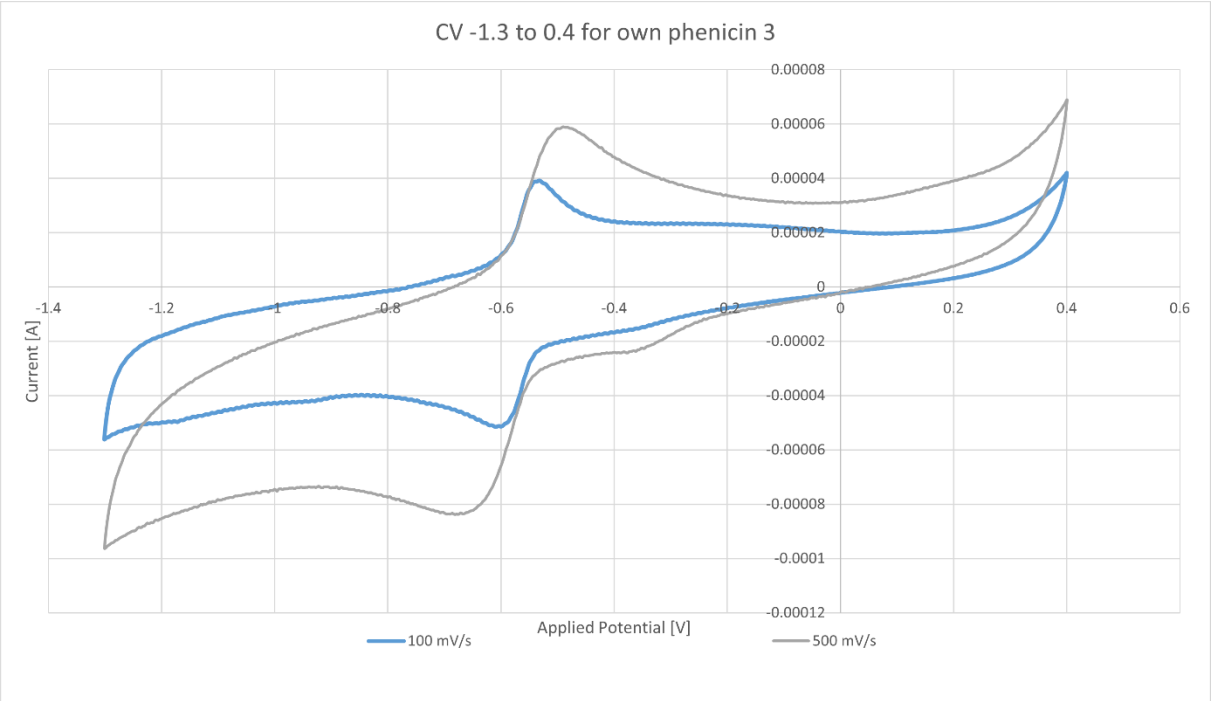


*Figure 9.2: CV of batch 3 with scan rates 500 and 100 mV/s*

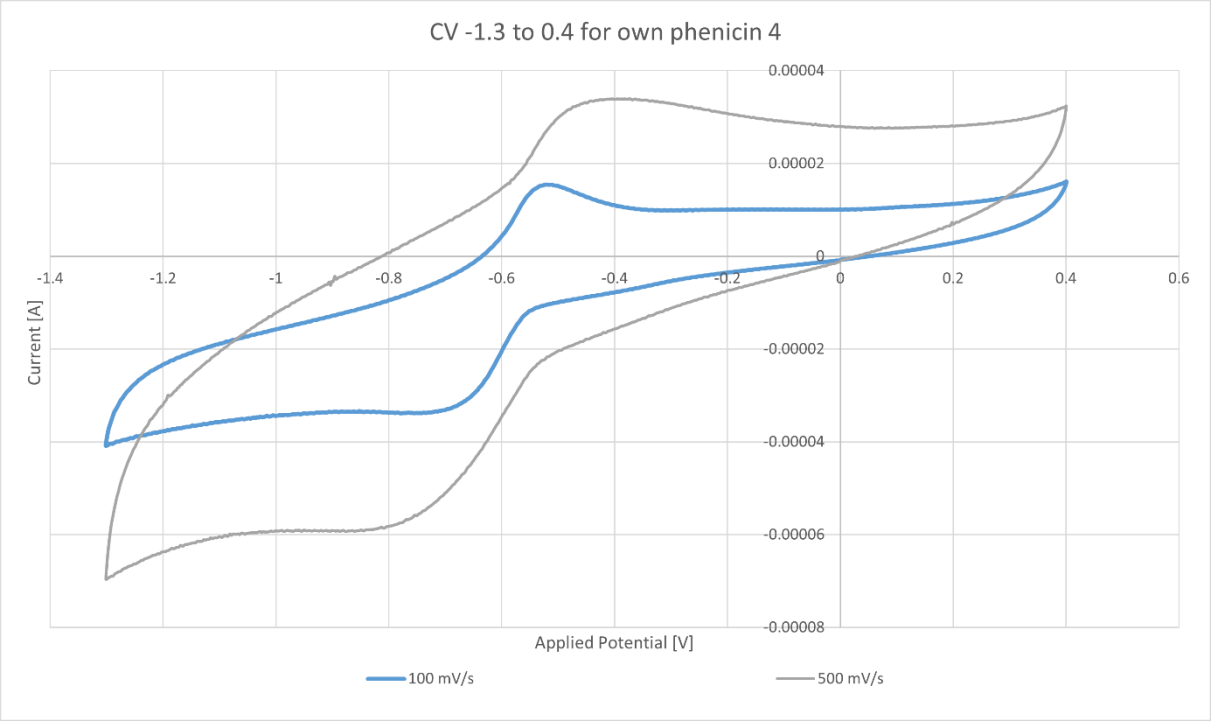


*Figure 9.3: CV of batch 4 with scan rates 500 and 100 mV/s*

An HPLC analysis on the six combined phoenicin batches was done after having conducted all the necessary single-cell cycling battery tests, quality checks, and bench-scaled. This was decided to be done late in the process because it was more important to ensure that there would be enough phoenicin for all the experiments. However, it also affected the outcome of the analysis because the majority of the compounds had already been used. Calculating the purity usually involves measuring the areas of the peaks and calculating the ratio between the areas of the main peak and the impurities. But because these values or the values of the

peak high were not given, a modified version was used where if there were any larger unidentified peaks other than the phoenicin peak, it was assumed to be less pure. The concentrations of the different batches measured from the HPLC can be seen in Table 9.1, and the chromatograms for each batch are in Chapter 16. Based on these and the modified methods, it can be assumed that the phoenicin batches are relatively pure as no larger unidentified peak expected the phoenicin peak can be seen.

*Table 9.1: Concentration of phoenicin in the different batches from the HPLC*

| Batch | Concentration [mg/L] |
|---|---|
| 2 | 335.02 |
| 3 | 664.63 |
| 4 | 337.46 |
| 5 | 278.23 |
| 6 | 635.79 |
| 7 | 271.67 |

## 9.1. Single-cell tests of RFB in small-scale

The results of the small-scale battery tests are used to control the quality of the produced phoenicin and see if it would work in the bench-scaled battery. The requirements are that the batteries run and can run for 100 charge/discharge cycles and have reasonable efficiencies. These battery tests were also performed to understand how all the batches would perform in terms of achievable capacity. All battery tests were conducted once without any replicates because of time restrictions. Further results of all individual battery tests can be seen in Chapter 14, but the focus of this part is a brief showing of the voltage vs time graphs of all graphs followed by a comparison of all conducted batteries.

#### 9.1.1.1. Battery running on batch 1

The 1$^{st}$ batch of produced phoenicin was used in the small-scale battery test, but it ran for just about 40 minutes, see Figure 9.4 and reached a capacity of less than 1 mAh, so it was disregarded from further use and data handling. This batch also did not have the signature phoenicin red color compared to the other batches, indicating why the battery did not run as predicted. This could be due to earlier mixing up of the mineral mix and the PDA plus metal mix in the phoenicin production process.

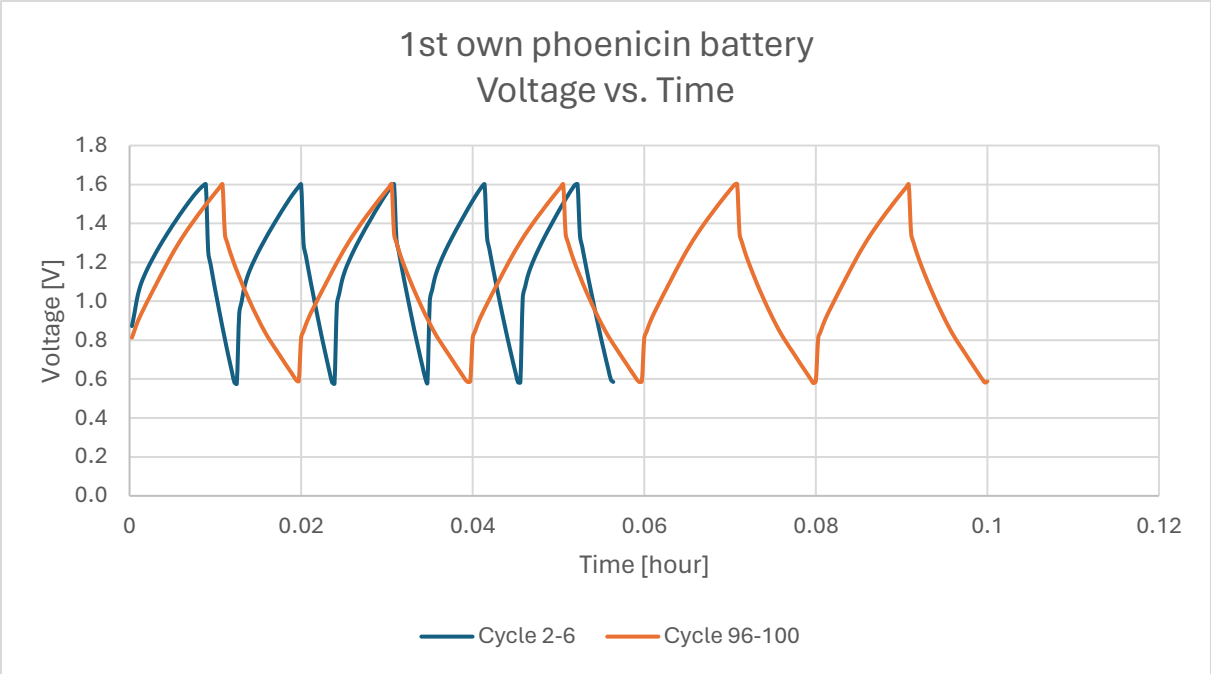


*Figure 9.4: Charge and discharge cycle rate for the 2-6 and 96-100 cycles for the battery running on the 1st own phoenicin*

### 9.1.1.2. Battery running on batch 2

The battery test had some complications for the 2nd batch of phoenicin produced. From cycle 49, there was a weird rapid decrease in capacity, and after cycle 54, the capacity decreased to below 1 mAh. Another thing that happened twice was that from cycles 64 to 65 and from cycles 95 to 96, the discharge capacity was high, and the charge was also for the following cycle, but then the capacity decreased to below 1 mAh again for the discharge of cycles 65 and 95. This unusual behaviour can be seen in Figure 9.5.

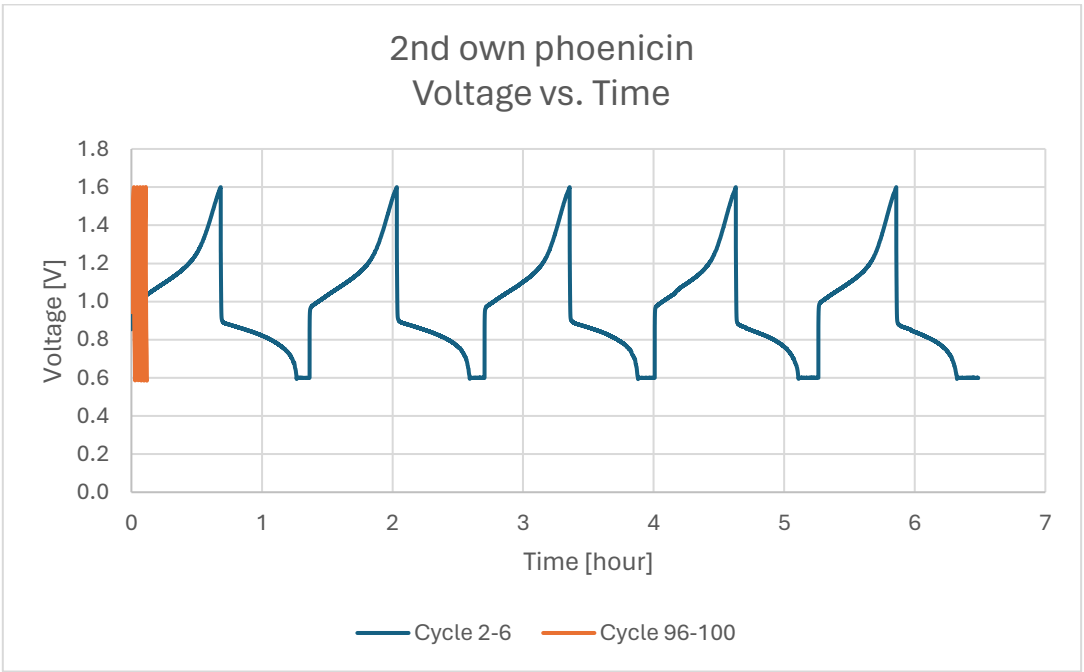


*Figure 9.5: Charge and discharge cycle rate for the 2-6 and 96-100 cycles for the battery running on the 2nd own phoenicin*

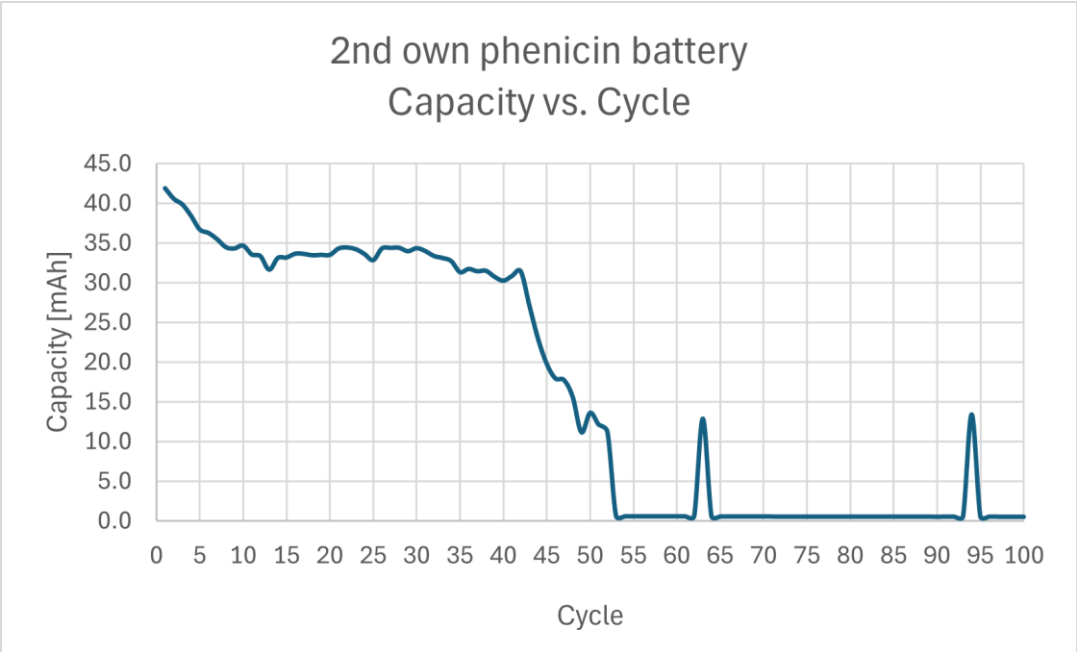


*Figure 9.6: 2nd battery unusual behaviour with discharge capacity for all 100 cycles*

#### 9.1.1.3. Battery running on batch 3

The batch 3 battery did run without any complications.

#### 9.1.1.4. Battery running on batch 4

Similar to batch 3, the battery running on batch 4 was conducted without any issues.

#### 9.1.1.5. Battery running on batch 5

The battery running with the 5th phoenicin batch was generally running with a constant decrease of capacity, but then it charged itself around cycles 49-50, as seen in Figure 9.8. The only issue was that after the first 54 cycles, the battery was stopped, but with a delay of 20 min, the battery was restored, adding up both runs to 100 charge/discharge cycles.

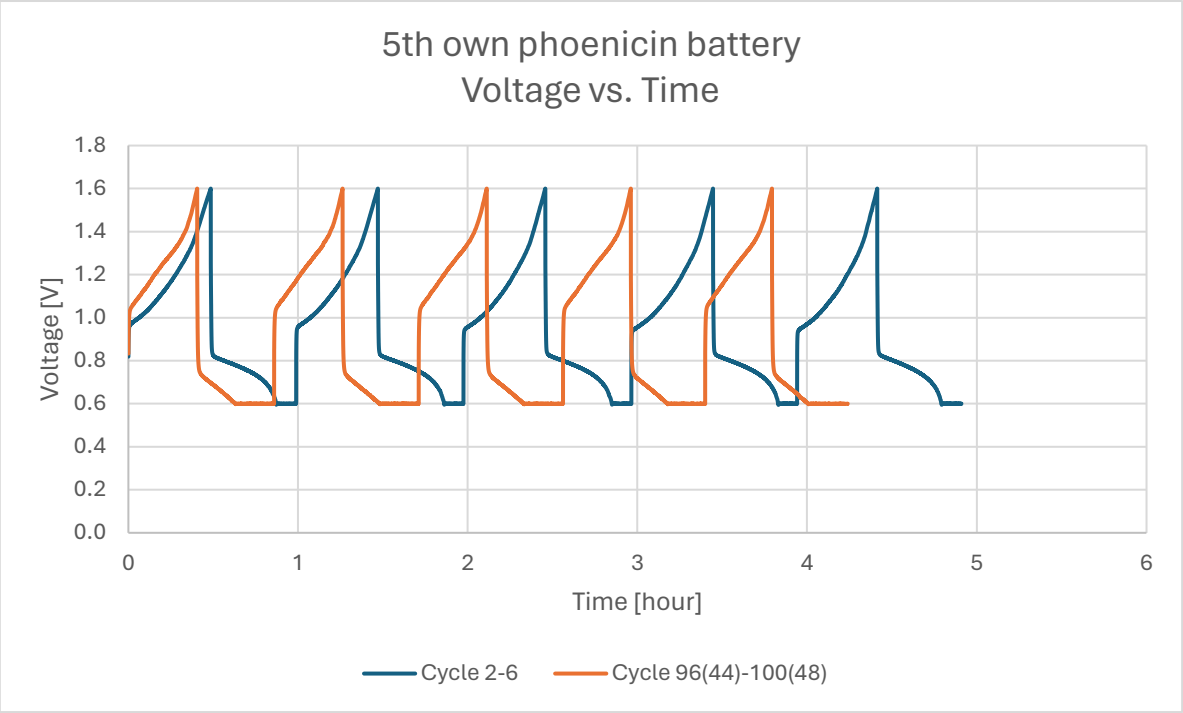


*Figure 9.7: Charge and discharge cycle rate for the 2-6 and 96-100 cycles for the battery running on the 5th own phoenicin*

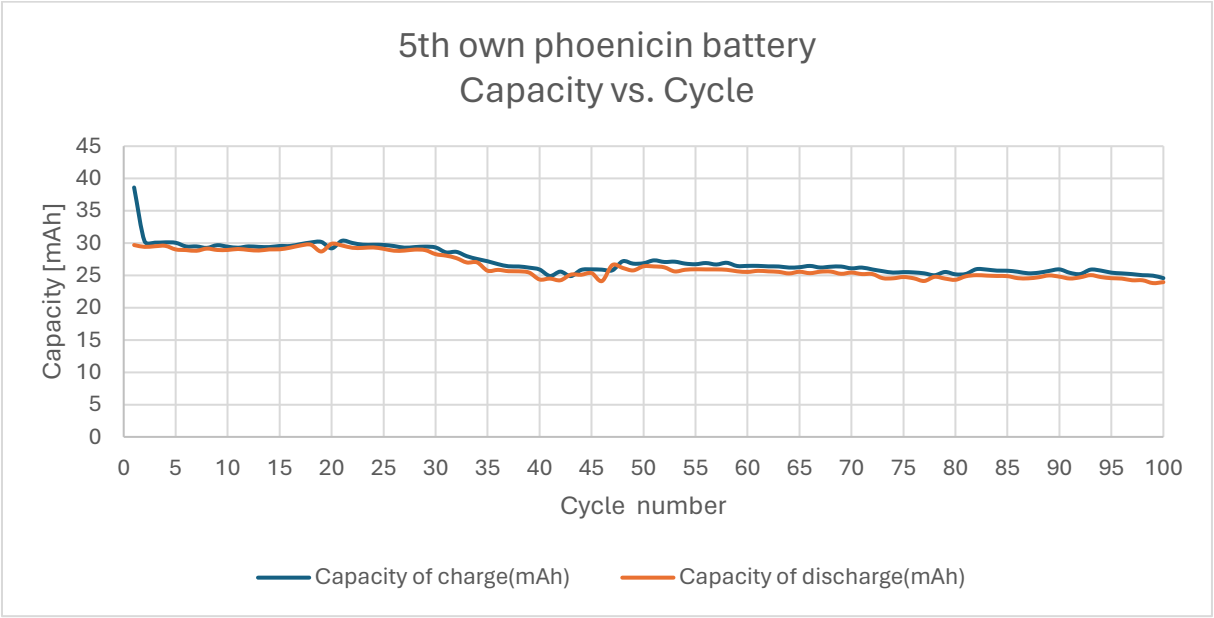


*Figure 9.8: 5th battery charge and discharge capacity for all 100 cycles*

### 9.1.1.6. Battery running on batch 6

For the 6th phoenicin batch conducted battery, the capacity was decreased for the first 10 cycles and then increased for ca. 30 cycles until decreasing again, as shown in Figure 9.10.

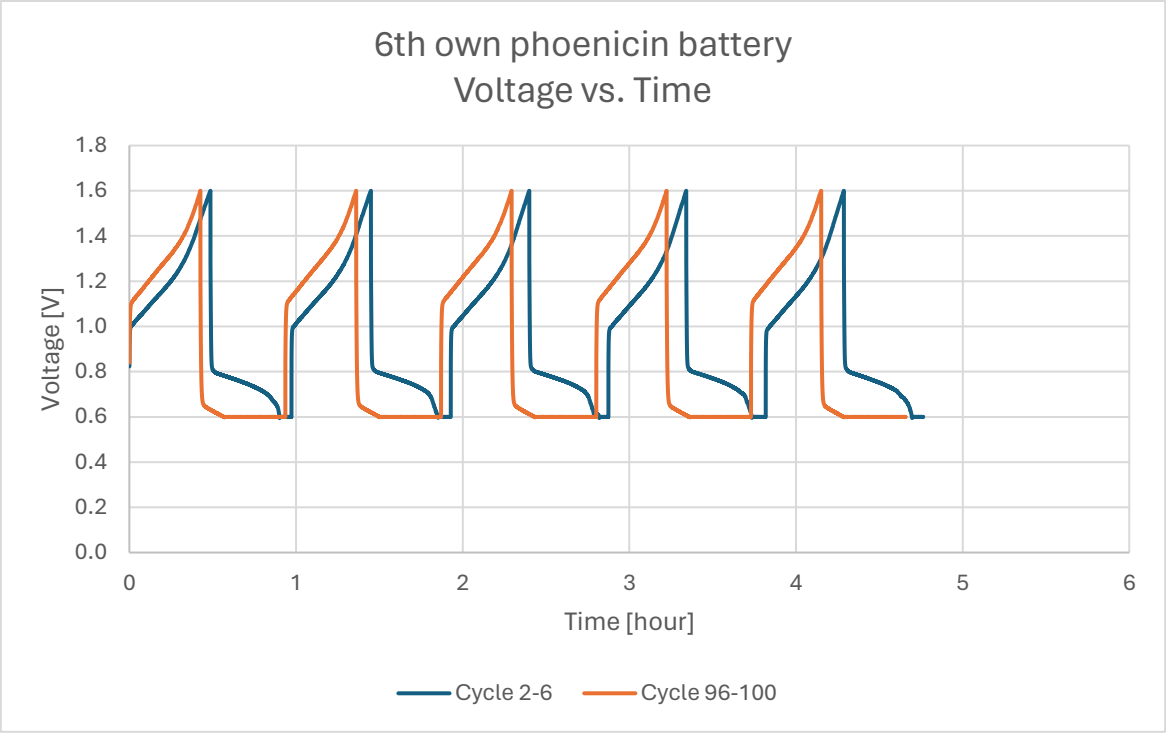


*Figure 9.9: Charge and discharge cycle rate for the 2-6 and 96-100 cycles for the battery running on the 6th own phoenicin*

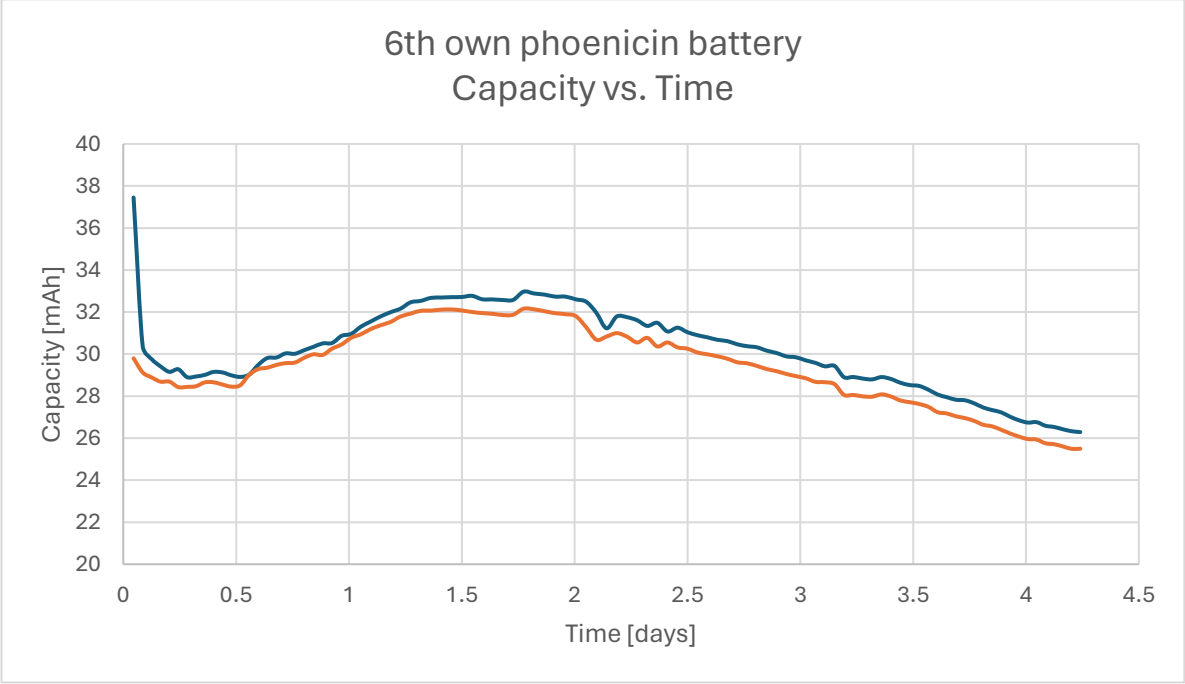


*Figure 9.10: 6th battery charge and discharge capacity for all 100 cycles*

### 9.1.1.7. Battery running on batch 7

The mineral mix from the 7th batch was changed and used in the broth for the incubation. As seen from Figure 9.10, this battery had the longest initial five cycles.

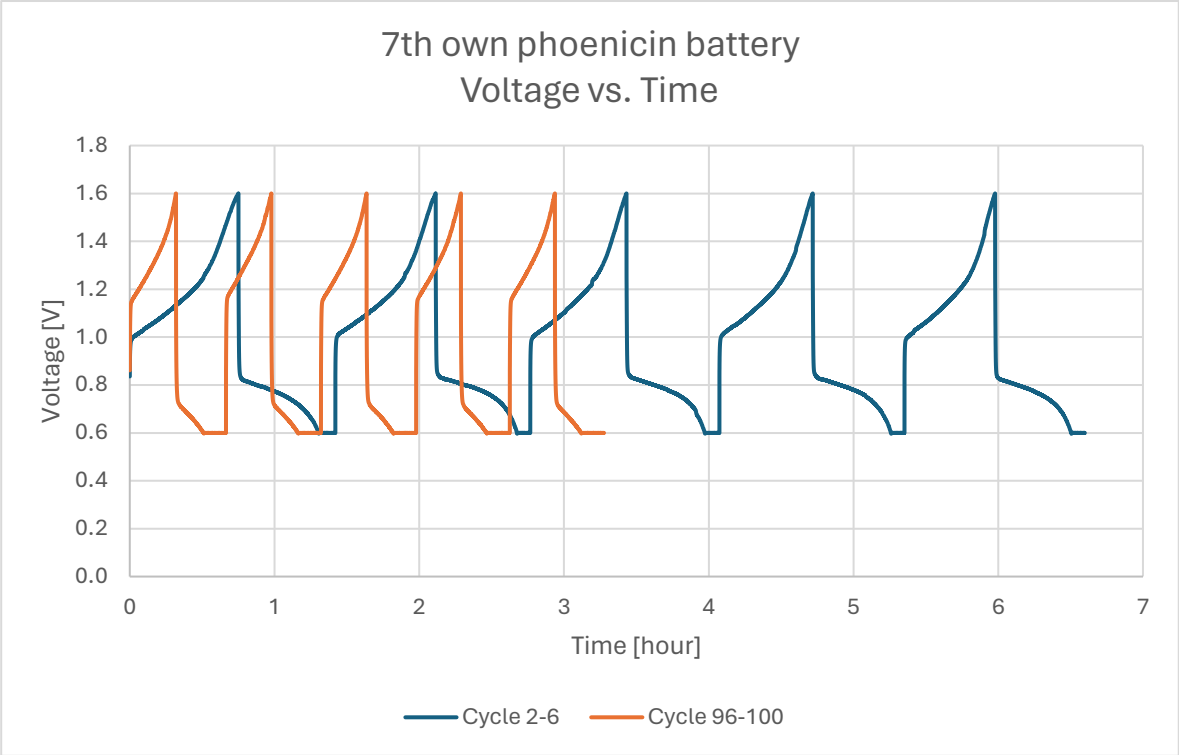


*Figure 9.11: Charge and discharge cycle for the 2-6 and 96-100 cycles for the battery running on the 7th own phoenicin*

### 9.1.2. Comparison of all quality check battery tests

After having a short look at the individual quality check batteries, this part of the project will investigate the difference between the conducted tests.

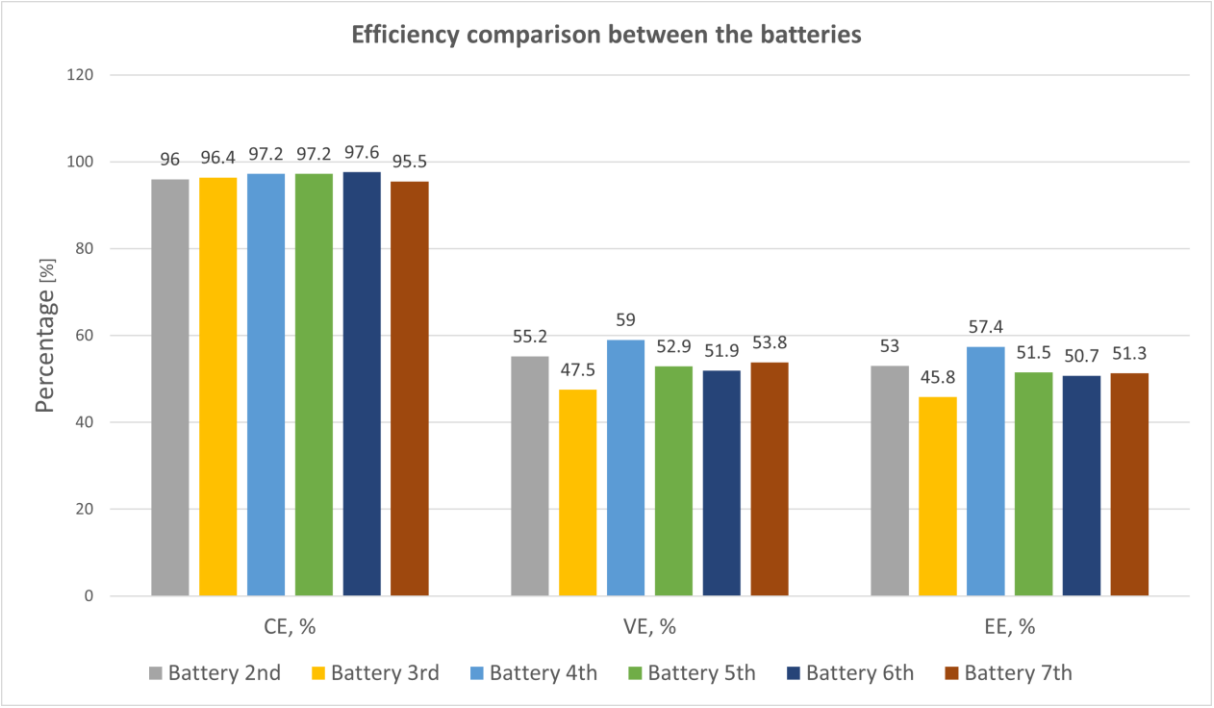


*Figure 9.12: Efficiency comparison between the quality check batteries*

The efficiencies for all batteries are visually represented in Figure 9.12. The CE for all batteries lies under the typical 99%, the highest being 97.6%, indicating that there might have occurred some mixing of phoenicin and ferrocyanide through the membrane, which is a high possibility because for every battery; the membrane showed some rupture. Another reason for the CE below 99% is the possible chemically irreversible side reactions of phoenicin. Also shown in Figure 9.12 are the VE for all the conducted batteries, and this efficiency has a more distinct difference between the batteries. Regarding the VE, a high value can indicate a low resistance, and a low value indicates the opposite. The low VE can result from either a rupture membrane, which is the case in all of these batteries see Figure 9.13 resulting in cross-over causing pressure problems and resistance, or it could have been caused by the electrodes, which may not be hydrophilic enough to allow fast electron transfer.

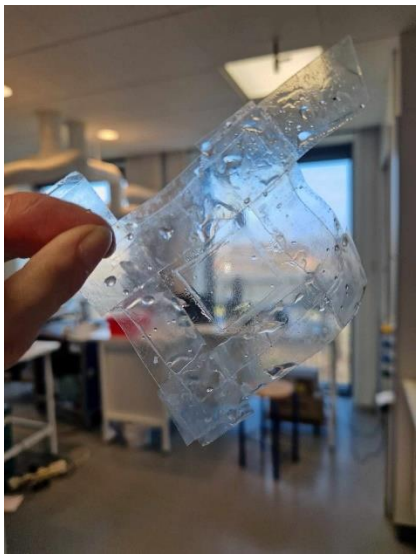

*Figure 9.13: Example of fractured membrane*

Based on this, it can be concluded that regarding resistance, the least resistance was achieved in the battery running with the 4$^{th}$ phoenicin batch, and the highest resistance was achieved with the 3$^{rd}$ batch. However, all batteries have a VE of around 50%, indicating that the battery test had a high resistance, which increased over time with decreased VE values. This can be seen for each battery respectively in Chapter 14, where a figure shows the CE, VE and EE for each cycle of the batteries. Since CE are quite similar, the variations in VE provide similar patterns in EE.

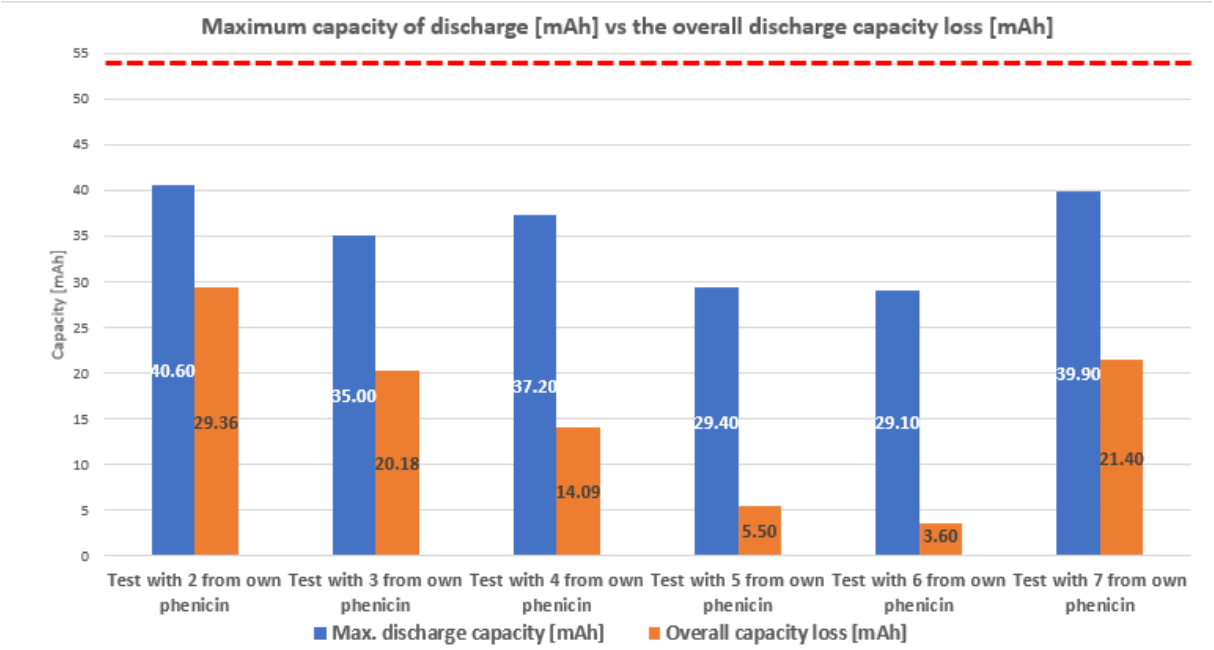


*Figure 9.14: Comparison of maximum capacities and capacity loss between the batteries; red dotted line indicating the max theoretical capacity*

The calculated maximum theoretical capacity of the small batteries was 53.5 mAh, and Figure 9.14 shows the maximum capacity of each battery and the respective overall capacity loss throughout the 100 charge/discharge cycles, where the red dotted line indicates the 53.5 mAh. As the figure shows, none of the batteries reached the maximum theoretical capacity but ranged between 40 and 30 mAh. This difference in maximum capacity could be due to possible impurities in the produced phoenicin, as the theoretical capacity is calculated with the assumption of pure phoenicin. This is most likely not the case for this self-produced phoenicin, as each sample is mixed from three different extraction run samples, which are different in electrochemical properties, as seen in Chapter 13, from one phoenicin production batch. Samples 4 and 5 had some bacteria contact with bacteria contamination, which could explain the difference in capacity achieved. Another assumption was that the battery would not experience any resistance or disturbances.

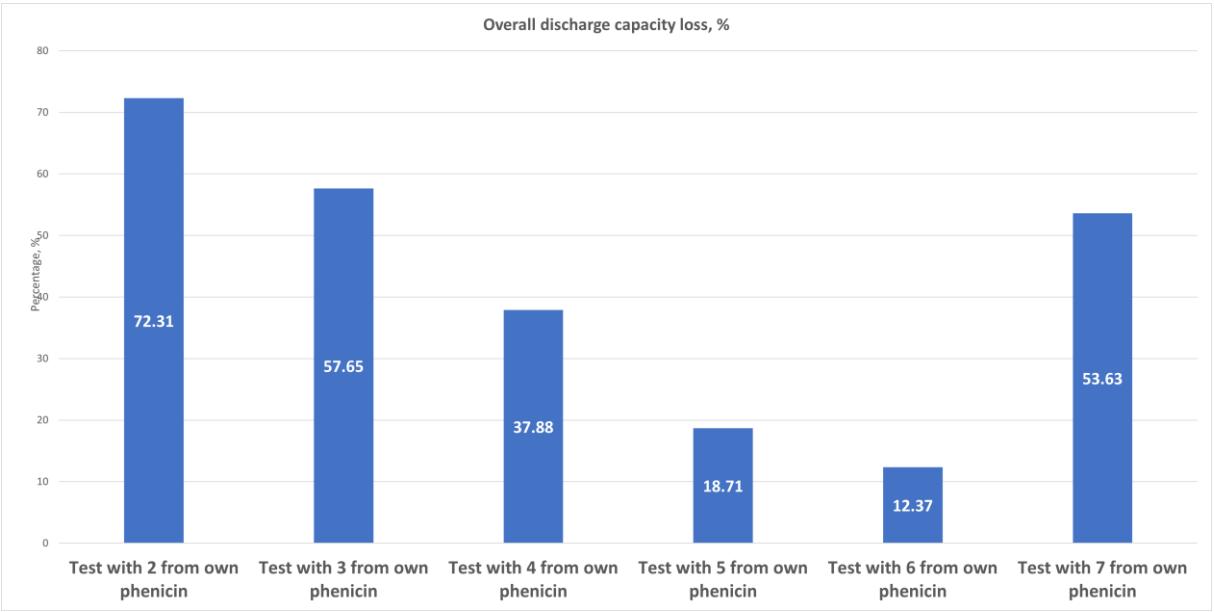


*Figure 9.15: Comparison of overall discharge capacity loss between the batteries*

The overall capacity loss from the batteries operating on batches 5 and 6 had a loss of less than 20%. The battery running on batch 2, which had the highest capacity, also had the highest capacity loss of over 70%, which can be seen in Figure 9.15 showing a comparison of all batteries overall discharge capacity loss. Table 9.2 also shows these values but also at which cycle 50% of the maximum capacity was lost for each battery of the respective phoenicin batch. The table shows that three out of the six batteries did not reach 50% of the maximum overall capacity in 100 charge/discharge cycles. This indicates a relatively stable battery test, and those two's overall discharge capacity loss is relatively low. In contrast, the battery running with the second phoenicin reached 50% of the max capacity at cycle 45 and had the highest discharge capacity loss, indicating an unstable battery.

*Table 9.2: Overall discharge capacity loss and cycle where 50% of discharge capacity is lost for every battery*

| Battery Tests | Discharge Capacity Loss [%] | Cycle Of 50% Capacity Loss |
|---|---|---|
| 2 | 72.3 | 45 |
| 3 | 57.7 | 77 |
| 4 | 37.9 | - |
| 5 | 18.7 | - |
| 6 | 12.4 | - |
| 7 | 56.6 | 90 |

Regarding the discharge capacity loss per cycle and hour, some differences exist between the batteries shown in Figure 9.16. As in the other factors, the battery running on the 2nd batch of phoenicin had the highest percentage loss per cycle and hour, being 1.92%, almost double the others. The capacity loss per cycle for the other five batteries is similar, around 1% loss per cycle, but the fifth battery had the best, with 0.91% loss per cycle. The percentage loss of the capacity per hour ranges from 1.73% to the lowest of 0.12%. Similar to the previous figure, the batteries running on the phoenicin batches 5 and 6 were the lowest, indicating a relatively stable battery with a low capacity loss.

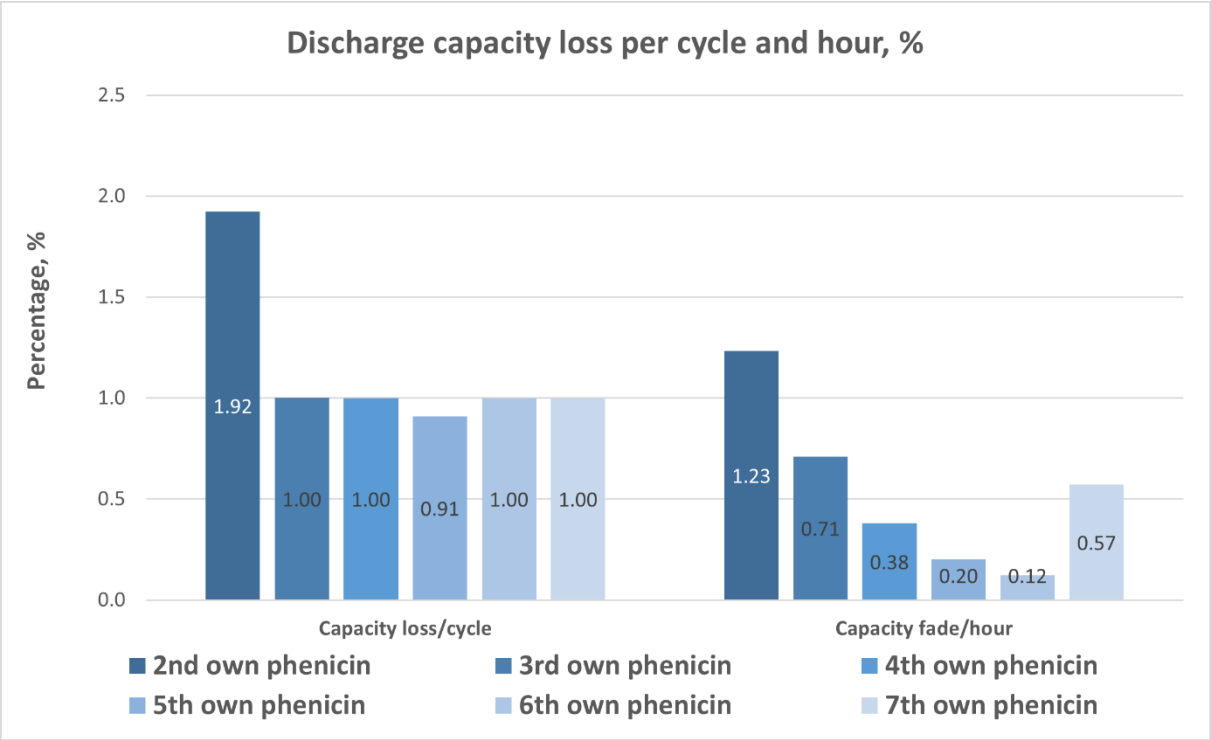


*Figure 9.16: Comparison of capacity loss per cycle and hour between the batteries*

Through this quality control, it can be concluded that batches 5 and 6 are the most stable regarding capacity loss, but their disadvantage is the over 20 mAh difference from the theoretical maximum capacity, indicating an impure but more stable product. The 2nd batch of phoenicin has shown the worst data from all six batches with the highest capacity loss, indicating that this batch could not run in a large-scale battery test. Batches 3 and 7 are relatively similar in max capacity, capacity loss, and other factors. They are also the other two batteries that reach 50% of their max capacity while running for 100 cycles. The battery running on the 4$^{th}$ batch is in the middle between the 5 and 6 and 3 and 7 batches concerning capacity loss, but it is also the third battery not reaching 50% of its max capacity. Overall, the best batch for the bench-scale battery testing would be samples 4, 5 and 6 because of their low capacity loss, implying a stable electrochemical phoenicin, and these also do not reach 50% of their maximum overall capacity in these battery tests.

The averaged efficiencies determined in the different studies from Wilhelmsen et al. can be seen in Table 9.3 below for the specific phoenicin single-cell cycling battery test. [6] As already mentioned, the 95% pure phoenicin (Paper 1) had a theoretical capacity of 214.4 mAh for a two-electron transfer but only achieved 139.4 mAh.

*Table 9.3: Table of previous study efficiencies [6]*

| Averaged Efficiencies [%] | Paper 1 [29] | Paper 2 [30] |
|---|---|---|
| CE | 98.5 | 95 |
| VE | 37.5 | 79 |
| EE | 36.9 | 77 |

Comparing the values from the table to the efficiencies from these quality control batteries, the apparent difference is that the batteries conducted in this thesis have better VE compared to the ones from the study of Wilhelmsen et al. This indicates that the quality control batteries have lower internal resistances compared to the batteries from the study.

Because of the lower VE value, the EE value of the study is also lower than all of the quality control batteries conducted. For the CE, the study has a slightly higher value, but also this one is below the typical 99%, indicating side reactions or degradation. In terms of efficiencies, the quality control batteries are on the same level as the batteries conducted by Wilhelmsen et al.

A look at the achieved capacity shows that the study has a much higher capacity compared to the ones achieved in this project. The average capacity achieved for these batteries tests was 42.24 mAh, which is 30.3% of the achieved 139.4 mAh of the study. This massive difference is on the basis of the use of different battery test settings, which included running on a combination of constant current with varying voltage and constant voltage with varying current, and for this thesis, the battery was running with constant current and varying voltage. Also, the used mass of 1.2 g in the study is higher than the phoenicin amount, increasing the theoretical capacity as well.

## 9.2. Big quality check battery test

As discussed earlier, before it was decided to use a 10 Wh PV panel, a 90 Wh PV panel was considered as a power source for the battery.

For this experiment, it was calculated that the battery would have a capacity of 144 mAh based on the 90 Wh PV panel, resulting in needing 0.737 g, so almost 1 g of phoenicin to achieve this capacity. Based on this calculation, it was decided to use phoenicin batch 3 because it was one of the batches with the biggest produced amount, but results from the previously conducted battery test showed that batch 3 was a more stable product compared to batch 2, which also a had a big phoenicin production.

Because the setup for the attachment of the single-cell and the PV panel was not ready on time for this experiment, it was decided to run this test with the battery tester as a power source and measuring device instead of the PV and multimeters, respectively.

The visual represented in Figure 9.17 is the difference between the charge-discharge cycle rate from the initial five cycles (blue) to the final five cycles (orange). Other than for the other tests, the 100th cycle was not used in this test because, for this cycle, some testing of the setup with a PV panel was done, resulting in the cycle stopping abruptly. The rate increase corresponds to a decrease in capacity throughout the cycling period, as initially, to reach a capacity of 80 mAh, it took a cycle ca. 78 min, and towards the end, to reach 44 mAh, it took a cycle 37 min. Showing that halving the capacity correlates with halving the time needed for a cycle to achieve this capacity.

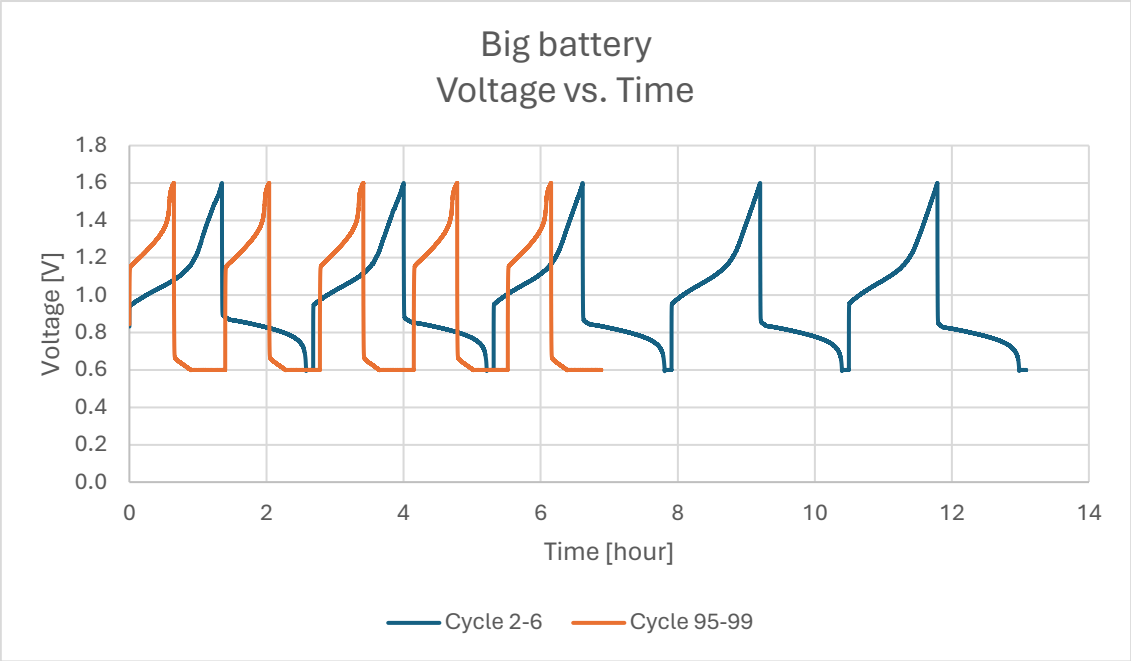


*Figure 9.17: Change and discharge cycle rate for the 2-6 and 95-99 cycle for the big battery*

As already mentioned, the first charge cycle did not reach the highest capacity, but it was actually the lowest capacity with 25 mAh, which can be seen in Figure 9.18 showing the average capacity for all charge-discharge cycles excluding the 100$^{th}$ cycle. The represented trend of decreased capacity after the 25$^{th}$ cycle over time correlates with Figure 9.19 and Figure 9.17 that around cycle 25, the battery reached the highest capacity over 100 mAh and an increase in cycle rate as time progressed, respectively. As Wilhelmsen et al. reported in their study, the overall decrease in capacity indicates that phoenicin undergoes some chemical degradation over the cycling period and is no longer available for reduction. If the charge and discharge capacity would perfectly overlap this would imply that the phoenicin sites available for reduction are fully utilized.

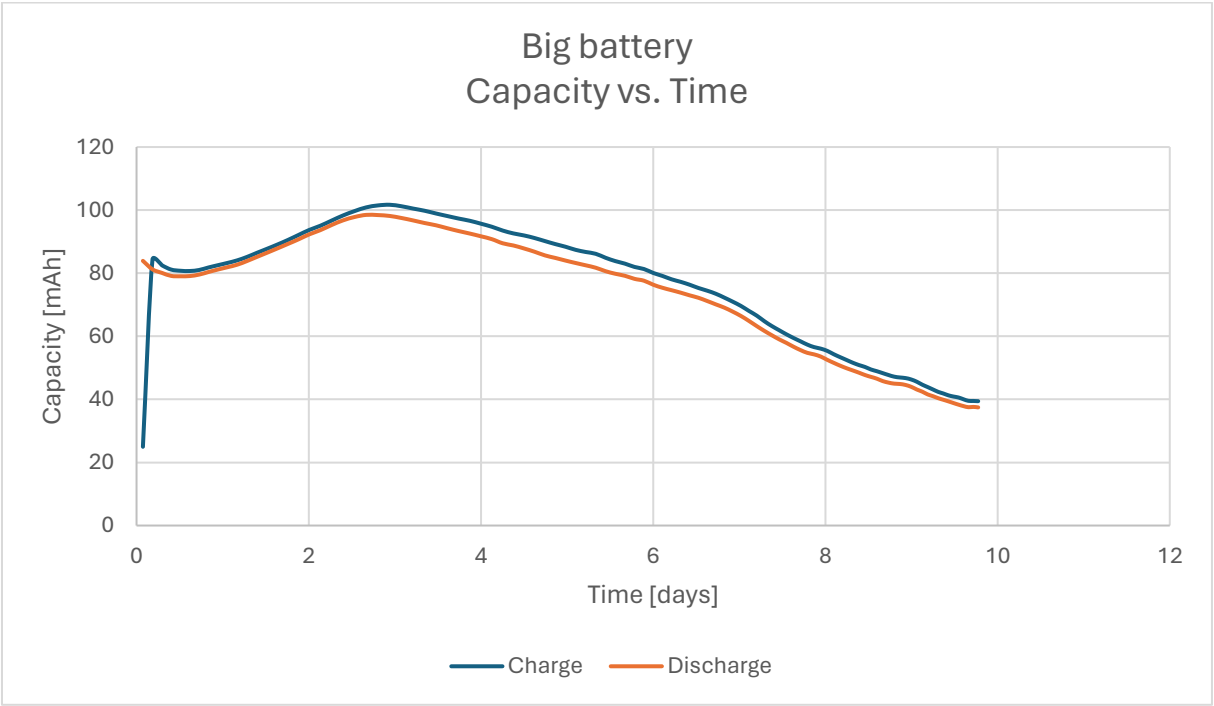


*Figure 9.18: Average capacity per cycle for the big battery*

Figure 9.19 shows the capacity over applied voltage for various charge and discharge cycles. Generally, for these figures, the charge of the first cycle would be the highest, so the furthest right, but for this battery, it is the opposite. The capacity for this cycle was the lowest at 25 mAh of all 100 cycles.

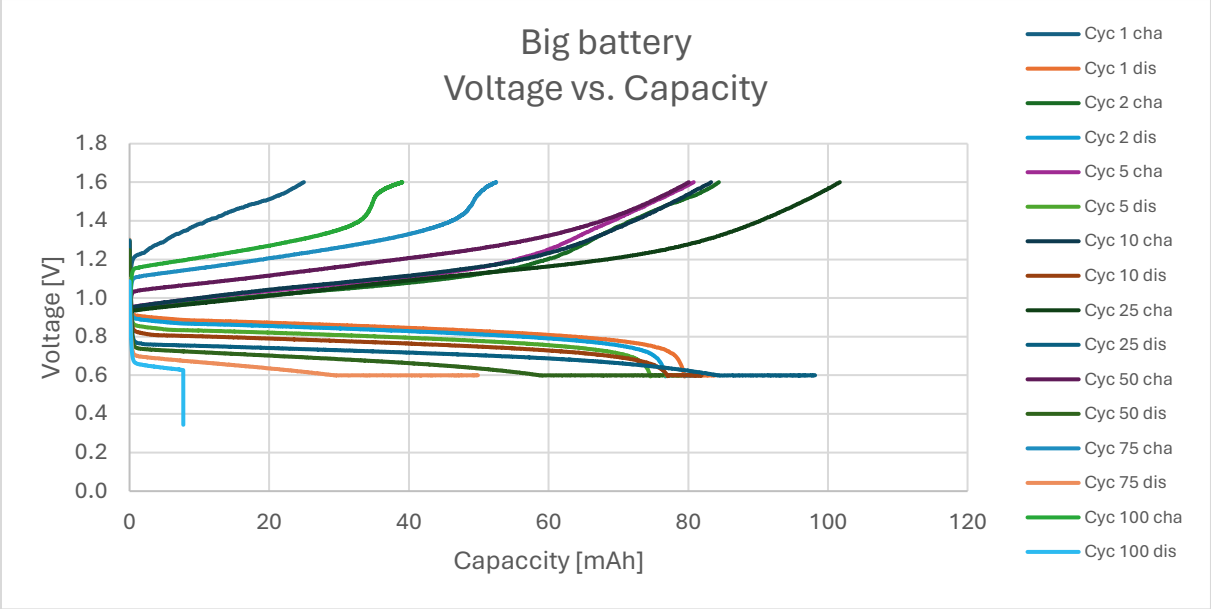


*Figure 9.19: The relation between applied voltage and capacity of the charge and discharge for different cycles for the big battery*

Figure 9.20 shows the average CE, VE, and EE progress over the cycle period for this battery constructed. The graphs show the same tendency from cycle 23 to 24, where there is a slightly more significant decrease in all three efficiencies. Otherwise, the CE graph remains steady at 95%, and the VE and EE graphs steadily decrease from 69/67% to 47/44%.

The slight jump in the CE can be directly related to where the difference in charge and discharge capacities start to increase in Figure 9.18. This is an unfavourable case because it would be preferred to see that the same amount of capacity can be discharged from the charged battery.

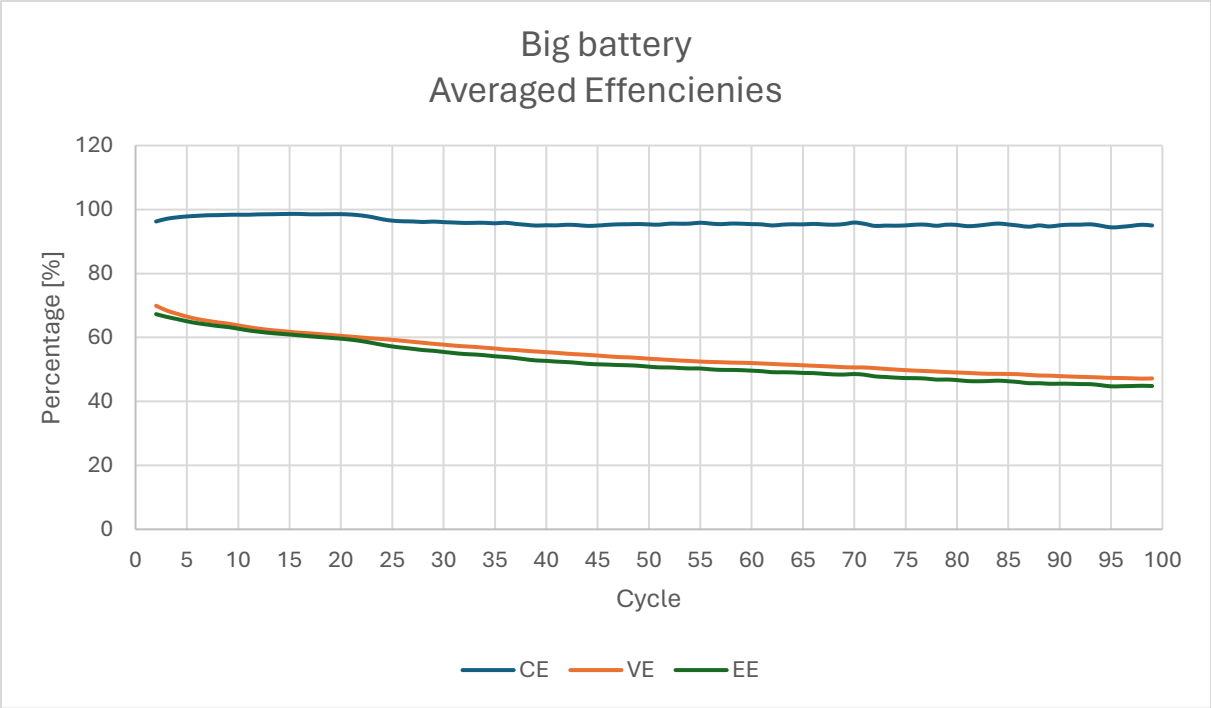


*Figure 9.20: Average CE, VE and EE for the big battery*

Similar to the previous battery test, the VE of this battery decreased, indicating high resistance, which increased, causing the VE to decrease. The increased resistance was most probably caused by a crossover of the phoenicin from the permeation through the membrane, shown in Figure 9.21 and Figure 9.22, showing the anolyte and the used membrane.

*Figure 9.21: Posolyte of the big battery*

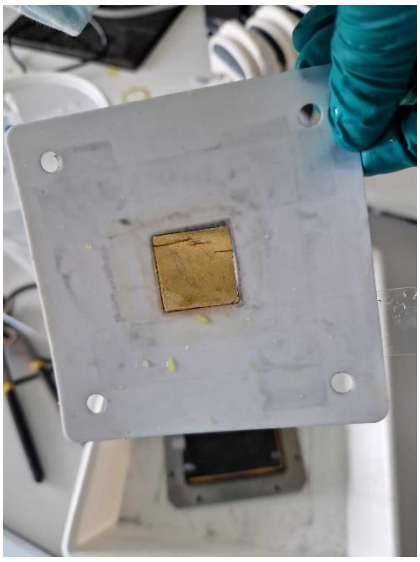

*Figure 9.22: Membrane of big battery*

The EE is again below the VE graph, as the VE is the lower one. This affects the EE more than the CE graph, even though both should have the same effect on EE.

Comparing all three efficiencies of this battery to the efficiencies from Wilhelmsen et al. papers, these big battery efficiencies are close to those of paper one, being CE = 98.5%, VE = 37.5%, and EE = 36.9%. However, this one has slightly better VE and corresponding EE. The efficiencies of paper two are still better, with values of CE = 95%, VE = 79%, and EE = 77%.

Table 9.4 compares the big battery with the quality check battery running on the same batch.

*Table 9.4: Comparison between small and big battery running on batch 3*

| | Small Battery | Big Battery |
|---|---|---|
| Capacity Loss Per Cycle [mAh] | 0.202 | 0.442 |
| Capacity Loss Per Cycle [%] | 1.00 | 1.01 |
| Overall Capacity Loss [%] | 57.65 | 53.94 |
| Capacity Loss Per Hour [%] | 0.71 | 0.23 |
| CE [%] | 96.4 | 96 |
| VE [%] | 47.5 | 54.7 |
| EE [%] | 45.8 | 52.5 |

The big battery is more stable regarding the overall capacity loss in percentage and capacity loss per hour in percentage. For the stability per cycle, the small battery is more stable but only a bit if we look at the percentage of 0.01%, so there is no significant difference. For the efficiencies, the small battery is slightly better with the ratio of capacity released during discharge to capacity released during charge, but both values are below 99%, indicating possible electrolyte crossover and unwanted side reactions. The other two efficiencies are significantly better for the big battery. Overall, the big battery was running more stable than the small one based on the observations above.

## 9.3. Single-cell tests of RFB in bench-scale with a 10 Wh PV panel

Based on the quality check battery tests, all six used batches are functional for a bench-scaled single-cell cycling battery test.

An observation made from the quality check batteries was that usually, the phoenicin from each batch would only reach 50% of the maximum theoretical capacity. Because of that observation and the fact that the to-reach capacity for these batteries is relatively small, the amount of phoenicin was roughly doubled to account for the capacity fade of 50%. The calculations are shown in Chapter 7 for 16 mAh, for which 0.082 g is needed, but because of the previously mentioned observation, it was chosen to use 0.153 g. With the new mass of the maximum theoretical capacity would be 29.9 mAh, as seen in the Equation 10 below:

*Equation 10: Phoenicin mass equation*

$$mAh = \frac{n * F * m}{3600 * MW} \rightarrow mAh = \frac{2 * 96485.33\ Ah/mol * 0.153g}{3600 * 274.23\ mol/g} = 0.0299\ Ah = 29.9\ mAh$$

However, the comparison will only be examined if the battery achieves the needed 16 mAh, as it is expected to reach only 50% of the calculated theoretical capacity.

The bench-scaled batteries were run in the same sequence as the quality-check batteries, starting from batch 2 and ending in batch 7. The data from the bench-scaled battery running on batch 2 was not usable because of problems with the data recording and safety from the multimeters. Based on that, it was decided to use the batch 2 battery as a test to see if the setup works and what adjustments are needed for better operation for future batteries. Because of time constraints, this battery running on batch 2 was not redone. This resulted in only five bench-scaled battery tests being conducted.

All of these five battery tests were running with the new electrode, Freudenberg H23, which differs from the one used in the quality check batteries. The new electrode was treated the same as the previous one, with backing in for 24 hours at 400°C to make it hydrophilic, but compared to the other one, this one was thinner and more movable. Throughout all the bench-scaled battery tests running with this new electrode, it could be observed that the electrolyte did leak out of the battery cell. Still, another possible reason for that happening was that the screws started to get stuck in the metal plate holes resulting in not tightening the battery enough up to the 5N.

Regarding the current for the battery, it was attempted to keep the charge current constant at 62.5 mAh, the same as for the quality control tests with the battery tester. For the discharge, it was also attempted to have the stop current at 31.3 mAh. The discharge current was a tricky situation because it would not reach above 10 mAh and decrease until it reached 3.31 mAh, but first, after adding a 10 ohm resistance to the plating to achieve these high numbers because, without the resistance, the current was very small, below 1 mAh, result of the small power produced from the battery.

### 9.3.1. Individual bench-scale battery tests

Before comparing all the bench-scaled batteries, each individual battery test will be looked at to see more specific details about each to better asses the best battery and also the reproducibility of a phoenicin operating RFB to store the energy from the PV panel.

#### 9.3.1.1. Battery running on batch 3

Starting with the battery running on batch 3, Figure 9.23 visually represents the charge-discharge curves from the initial five cycles (2-6, blue) and the final five cycles (96-100, orange). These curves indicate the cycle rate on how was fast the cycle reaches the specific voltage for charge and discharge, respectively. The rate increases over time, resulting in cycles towards the end taking 20 min compared to the initial taking ca. 75 minutes, so there is a 73% decrease in time for a complete charge-discharge cycle. This cycle rate increase also suggests a reduction in capacity throughout the cycling period. The graphs also display that the discharge process takes longer than the charging process, which can be seen by that after reaching 1.6 V and decreasing to 0.6 V, it takes longer, and after reaching 0.88, it has almost an exponential decay. Comparing this Voltage vs. Time graph with the one from the quality check, it can be seen that both require similar time for the first five initial cycles.

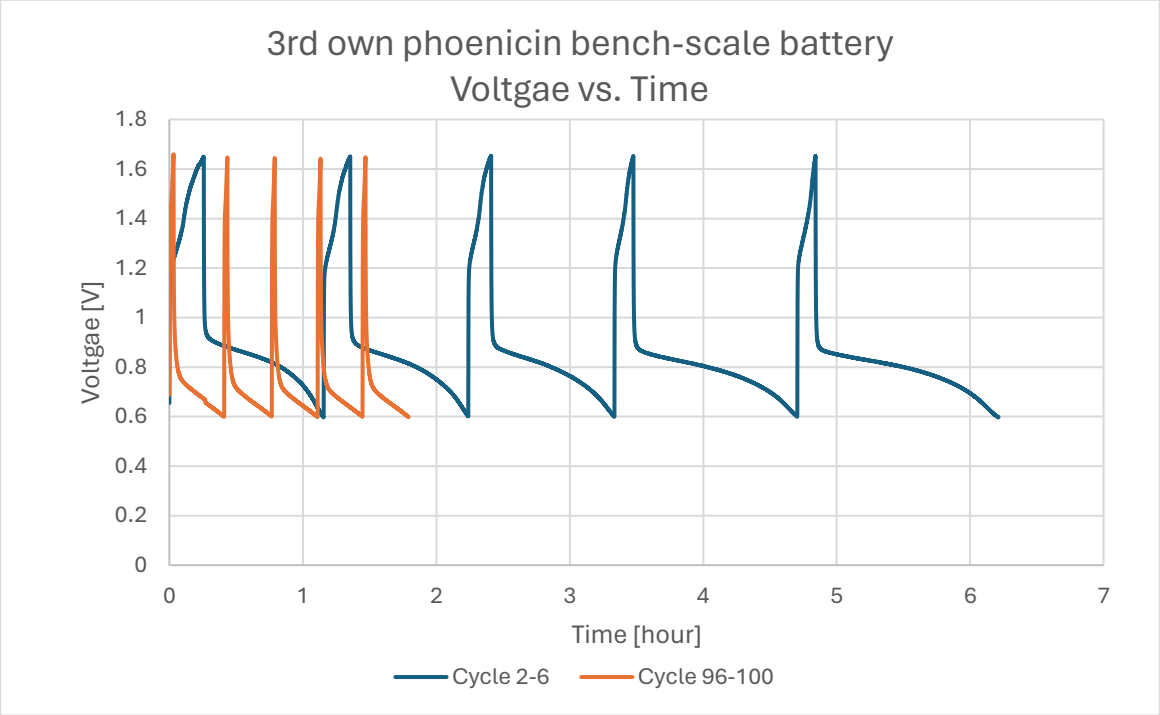


*Figure 9.23: Charge and discharge cycle rate of the 2-6 and 96-100 cycles for the bench-scale battery running on phoenicin batch 3*

Figure 9.24 visually represents the average capacity over the cycling period, and at first glance, it can be seen that the capacity is decaying over the cycling period. For the first cycle, the capacity was 44.9 mAh, 66% higher than the maximum theoretical capacity of 29.9 mAh for this amount of phoenicin. With the knowledge of a possible four-electron transfer, the maximum theoretical capacity for that case would be 59.8 mAh, which is only 33% higher than the achieved capacity of 44.9 mAh, indicating the high possibility for four-electron transfers for the first charging cycle.

Viewing the second charging cycle, the one that is typically referred to as the actual first cycle, the capacity achieved was 15.9 mAh, which is 47% of the theoretical capacity calculated. This supports the observation already made in the quality check battery tests, where only 50% of the maximum theoretical capacity was usually achieved. This is why the amount of phoenicin was almost doubled to even be able to achieve the needed 16 mAh for the power of 10 Wh.

The peaks seen in this graph are usually the first cycle of the battery after it has been resting overnight, and the following cycle shows the correct trend of the capacity decreasing. As

already mentioned for the Capacity vs. Time, the charge capacity is higher than the discharge capacity, indicating that the CE is below 100% as not all the total charge stored during charging is released during discharging. This implied that the phoenicin is degraded steadily or crosses over throughout the cycling period, causing the capacity to decrease.

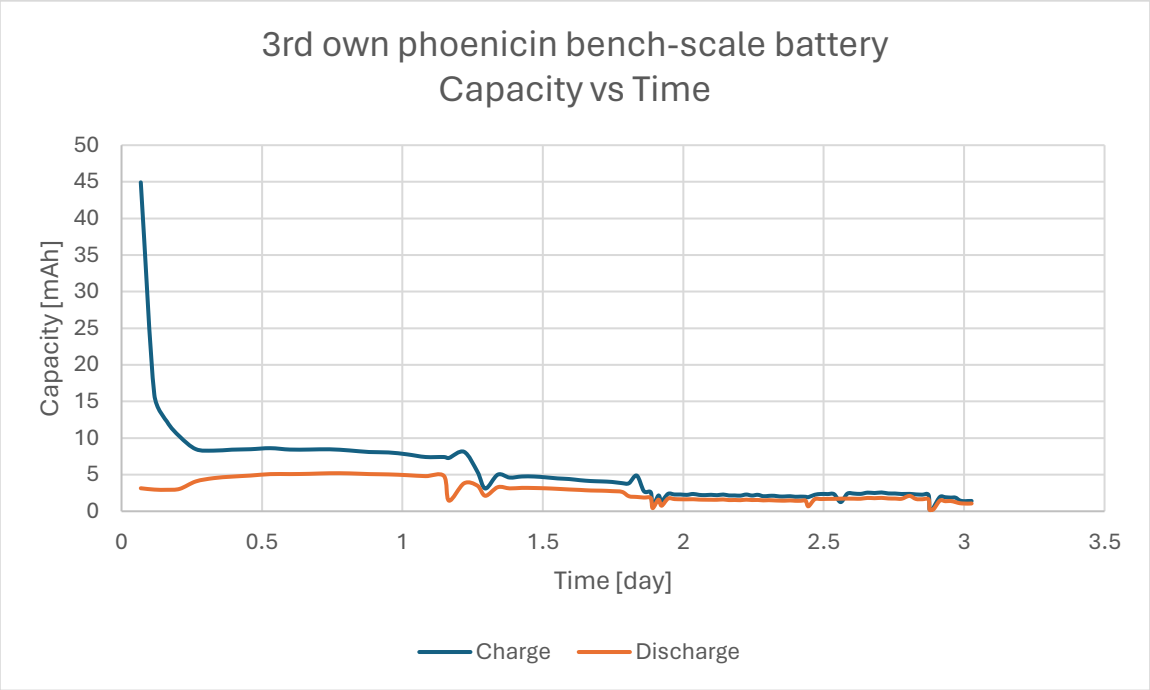


*Figure 9.24:Average capacity per cycle for the bench-scale battery running on phoenicin batch 3*

Figure 9.24 shows the average efficiencies, CE, VE, and EE, for all 99 cycles from the cycle to the 100th cycle. The CE graph displays an unsteady behaviour caused by stopping the battery when the discharge cycles have not been completed, as represented by the drip in the graph.

Unlike the quality check batteries, the VE graph for this bench-scaled battery is steady compared to the quality check batteries, where the CE was steady, and the VE decreased over time. The steadiness of the VE for this bench-scaled battery is the same reason the CE is so unsteady because of ending the battery before the discharge cycle was done, and the VE seems not to be affected by it that much as the CE. The steadiness of the VE indicates that the various resistances in the battery are stable, not increasing or decreasing, which would cause the VE either to decrease or increase, respectively, with the resistance.

Because the CE is an unstable efficiency, the EE follows its tendency except after cycle 95, when the CE was slightly stable and the VE dipped.

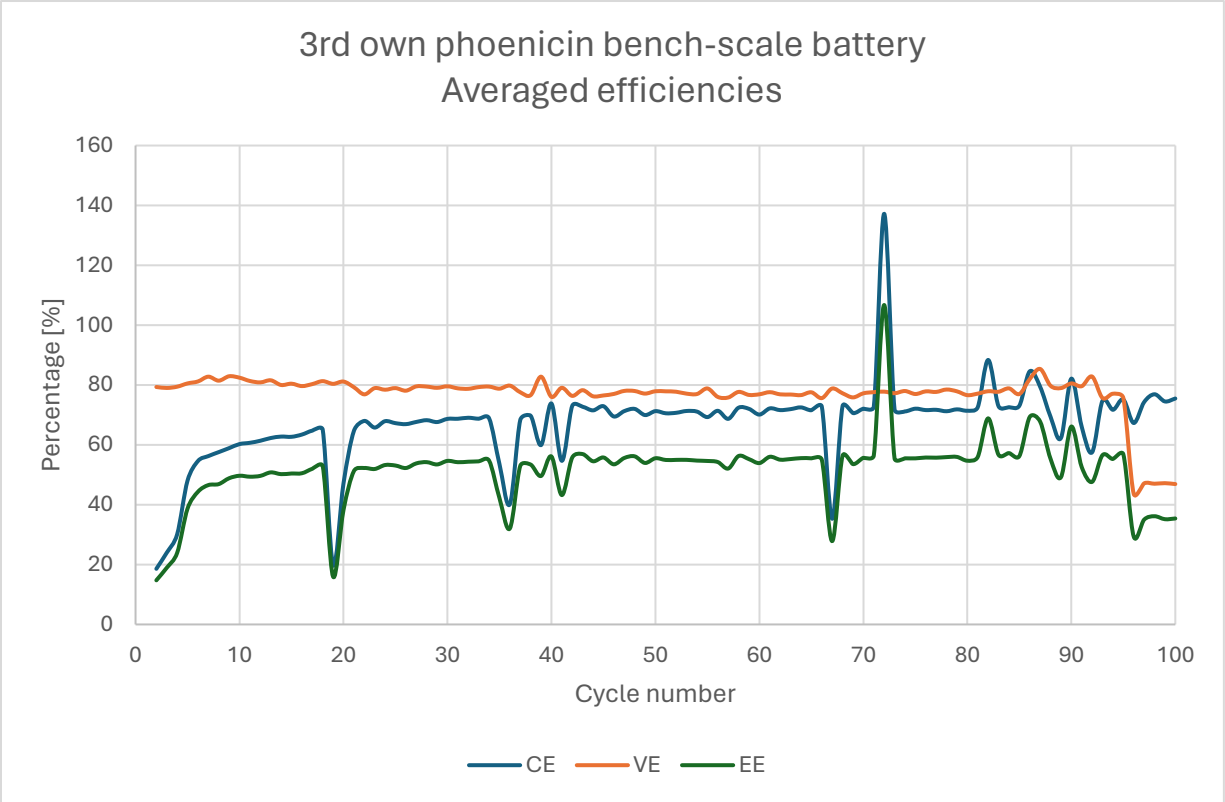


*Figure 9.25: Average CE, VE and EE for the bench-scale battery running on phoenicin batch 3*

Overall, the averaged efficiencies are slightly better in regards to the VE and EE compared to the quality check battery running on batch 3. Still, the CE of the bench-scaled battery was worse than the quality check one, as seen in Table 9.5 below. For this batch there can also be made the comparison between the bench-scaled, quality check and the big battery tests. The table shows that the quality check battery is the best for CE but the worst for the other two efficiencies. The bench-scaled battery is the worst for the CE because of the above mentioned reason, middle for the EE and best regarding the VE. The big battery is the best for the EE out of all three battery tests, and the middle for the other two efficiencies.

*Table 9.5: Comparison between small, big and bench-scale battery running on batch 3*

| | Small Battery | Bench-scale Battery | Big Battery |
|---|---|---|---|
| CE [%] | 96.4 | 67 | 96 |
| VE [%] | 47.5 | 77 | 54.7 |
| EE [%] | 45.8 | 51.6 | 52.5 |

#### 9.3.1.2. Battery running on batch 4

In the second bench-scaled battery operating on the 4$^{th}$ batch, the first considerable leakage of the battery appeared, which can be seen in Figure 9.26, and the problem with the screws also started with this battery.

*Figure 9.26: Leakage of bench-scale batch 4 battery*

Like the battery running on batch 3, the initial five cycles (2-6, blue) are longer than the final five cycles (96-100, orange), as shown in Figure 9.27. These curves indicate again that the cycle rate increases over the cycling period, suggesting that the capacity decreases over time. Unlike the previous battery, the final five cycles barely run for over one minute. This could be due to the leakage of the phoenicin or because the sunlight and the lab light have been shining on the PV panel together with the UV lamp, increasing the power production and resulting in a faster generation. Also seen in the graphs is that in cycle 5, there is a second peak reached above 1.6 V while being in the discharge cycle. A possible reason for that is that the lights in the labs have been turned on, the PV panel was affected, and the voltage increased by the extra light, but the current stayed the same throughout that abnormality.

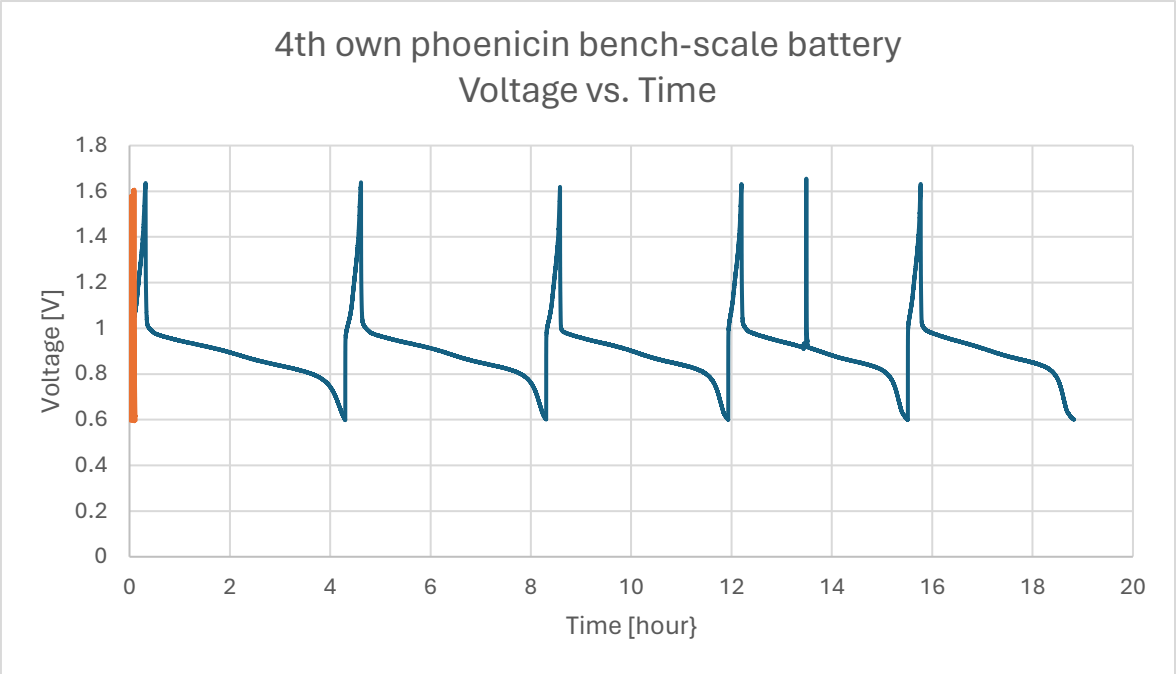


*Figure 9.27: Charge and discharge cycle rate for the 2-6 and 96-100 cycles for the bench-scale battery running on phoenicin batch 4*

Figure 9.28 presents the averaged capacity over the cycling period for charge and discharge for the batch 4 battery, showing a decaying capacity over the time period. The capacity for the first cycle was 24.8 mAh, 17% lower than the maximum theoretical capacity of 29.9 mAh. Compared to the battery run on batch 3, this batch can be said to be considered a two-electron transfer instead of the previous one being a four-electron transfer.

For the second charge cycle, the achieved capacity was 23 mAh, which is 77% of the theoretical capacity and 31% higher than the second cycle capacity of the batch 3 battery. Again, this batch also fulfils the needed 16 mAh for this PV panel.

Similar to the previous battery, the drops and peaks are caused by stopping and restarting the battery. The charge is higher than the discharge capacity curve, indicating again that the CE will be below 100% and that the phoenicin is either degraded steadily or the electrolyte crosses over through the membrane.

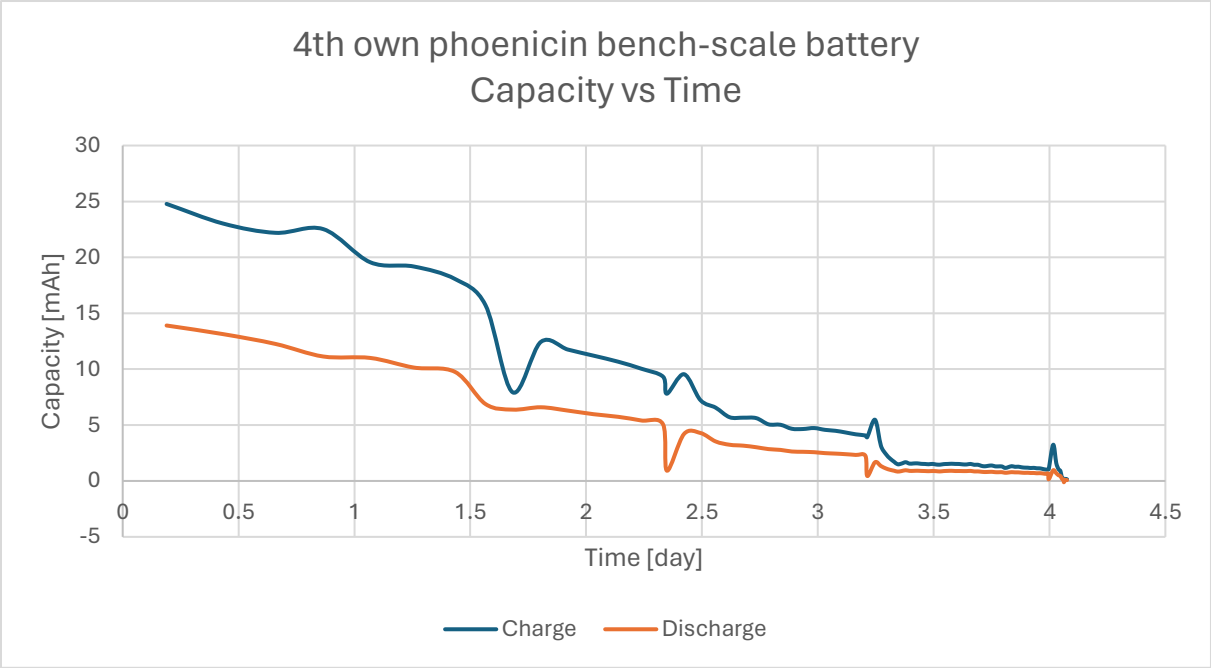


*Figure 9.28: Average capacity per cycle for the bench-scale battery running on phoenicin batch 4*

Figure 9.29 represents the average efficiencies, CE, VE and EE, for all 100 cycles. All three efficiencies curves show some unsteady behaviour caused, as already mentioned, by stopping and then restarting the battery.

Similar to the previous battery, the CE is more affected by the breaks in the cycling tests, resulting in high peaks and drops. From cycle 40 to cycle 80, the CE increases slightly, followed by some unstable peaks and dips.

The VE graph is also in this bench-scaled battery test above the CE for the majority of the cycling test, but where the CE increases, the VE decreases until after cycle 80 but increases again, similar to the CE from there on. The time period of the decreases in the VE can be because of the internal resistance increasing, possibly caused by the already mentioned leakage of the battery resulting from issues of the electrode and a cross-over of electrolytes through the membrane.

The trend of all the efficiencies graphs is the same as the previous bench-scale battery in that the VE is higher than the CE. The EE follows mostly the trend of the CE except between cycles 40 and 80, which is consistent because the CE and VE counterbalance each other. But from cycle 90, the EE follows more the VE than the CE.

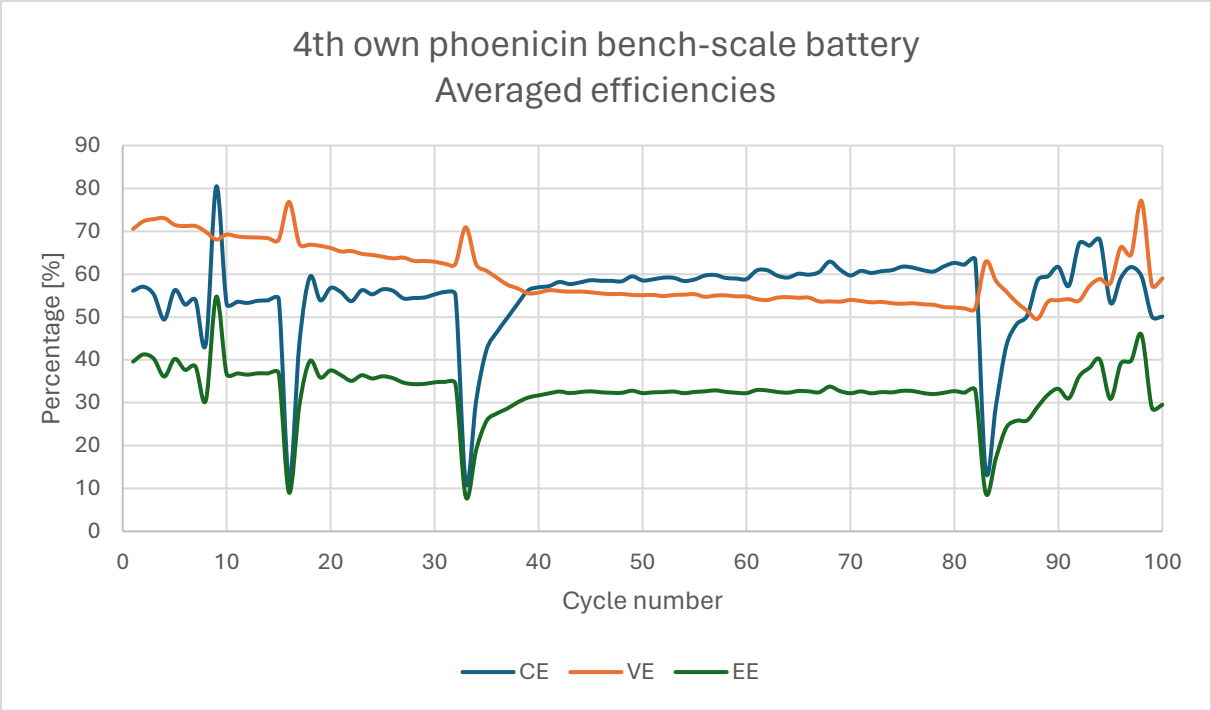


*Figure 9.29: Average CE, VE and EE for the bench-scale battery running on phoenicin batch 4*

Table 9.6 shows the averaged efficiencies for both the quality check and bench-scale battery running on batch 4. Overall, the bench-scaled battery's efficiencies are worse than the quality check battery except for the VE, which is slightly better than the small battery. The most probable cause is the leakage observed, resulting in not the same amount of discharge capacity being released as charge capacity has been produced, causing a decrease in CE, the internal resistances increasing, causing a VE decrease, and the EE is significantly affected by the low CE resulting in a low EE value.

*Table 9.6: Comparison between small and bench-scale battery on batch 4*

| | Small Battery | Bench-scale Battery |
|---|---|---|
| CE [%] | 97.2 | 55.4 |
| VE [%] | 59 | 59.7 |
| EE [%] | 57.4 | 33 |

#### 9.3.1.3. Battery running on batch 5

Throughout the bench-scale battery cycling test experiments, the UV lamp broke after battery 4, causing it to change to a less powerful lamp for the rest of the experiments. This change of lamps was decided to represent different suns in Europa; the first lamp should represent the Mediterranean sun, and the second lamp, the less powerful, should represent the central-northern European sun. This change of power source for the PV panel has resulted in some difference in the produced current compared to the more powerful lamp which results will be discussed later on in this project. Another effect of this change is that the batteries would run longer compared to the previous ones, but because of time constraints again, it was decided not to let the battery run for 100 cycles but instead let it run for a week and see how close the battery has reached to the set 100 cycles.

Because of the lamp change mentioned and its effects, Figure 9.30 shows that the initial five cycles (2-6, blue) took around 32 hours to finish, and the final five cycles (23-27, orange) took a bit over 15 hours. This is double the amount of battery 3 for the initial five cycles and just slightly less time than the initial five cycles of battery 4.

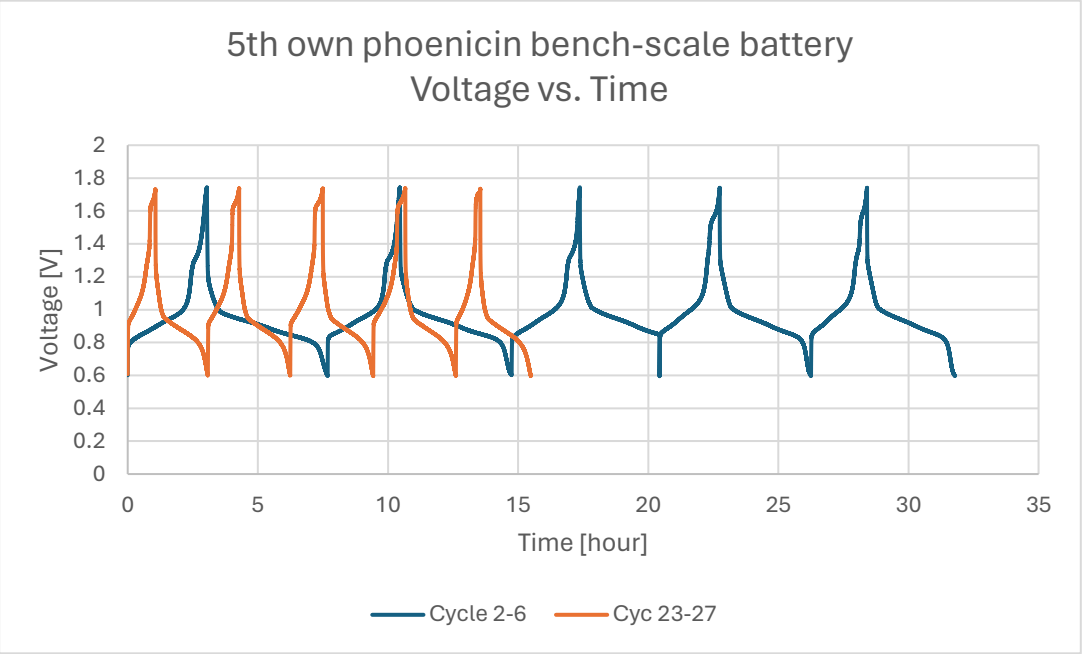


*Figure 9.30: Charge and discharge cycle rate for the 5-6 and 23-27 cycles for the bench-scale battery running on phoenicin batch 5*

Figure 9.31 presents the averaged capacity over the cycling period for charge and discharge for the bench-scaled battery running on batch 5. Displayed in this figure is that the capacity is decaying over the cycling period, losing over 50% of the initial capacity by the end of cycle 28, after 6.5 days. The first cycle reaches a capacity of 29.4 mAh, 1.7% lower than the maximum theoretical capacity of 29.9 mAh, being the second battery to be considered a two-electron transfer, the same as the previous batch 4 battery.

The achieved capacity for the second charge cycle was 28.9 mAh, which is 96.6% of the theoretical capacity, just losing 0.5 mAh from the first to the second charge cycle. This resulted in it being 31% higher than the second cycle capacity of the batch 4 battery and 45% higher than for the batch 3 battery. Again, this batch also fulfils the needed 16 mAh for this PV panel.

Similar to the previous battery, the drops and peaks are caused by stopping and restarting the battery. The charge is higher than the discharge capacity curve, indicating again that the CE will be below 100% and that the phoenicin is either degraded steadily or there is a cross-over of the electrolyte through the membrane. For this battery, the leakage started to increase because of an issue with the screws not being able to get screwed fast enough due to a human error causing more electrolyte to leak as the battery was not under enough pressure resulting in openings for the liquid to leak. This is also the cause why the difference between charge and discharge is that significant, resulting in not all the capacity from the charge being used in the discharge process, causing a smaller discharge capacity value. This is not an ideal case, but comparing the discharge values with the one from the previous batteries around the same time (day), the batterie has more capacity left compared to the ones running on batches 3 and 4, which reach below 5 mAh at 1.5 and around 2.25 days respectively but this one reaches 5 mAh first after 6 days.

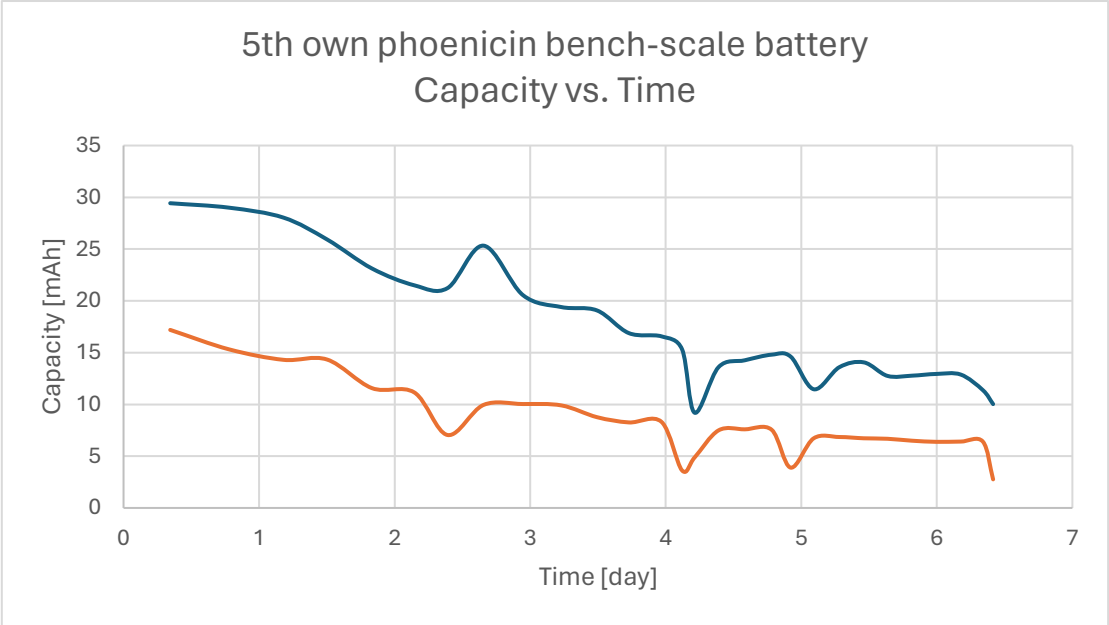


*Figure 9.31: Average capacity per cycle for the bench-scale battery running on phoenicin batch 5*

Figure 9.32 shows the average efficiencies, CE, VE, and EE, for all 28 cycles. All three efficiency curves show some unsteady behaviour caused, as already mentioned, by stopping and then restarting the battery.

Similar to the previous battery, the CE is more affected by the breaks in the cycling tests, resulting in high peaks and drops. Without the drops, the CE would decrease slightly, as shown by the little part of the graph without drops.

The VE graph is also in this bench-scaled battery test above the CE for the majority of the cycling test, but it can be seen that it is decreasing over the time period. The decrease in VE can be due to the increasing internal resistance, possibly caused by the already mentioned battery leakage.

The trend of all the efficiencies graphs is the same as the previous bench-scale batteries in that the VE is higher compared to the CE. The EE follows the trend of the CE closely different from the two previous batteries, where the EE follows the VE in the last five cycles caused by the intersection of the CE and VE.

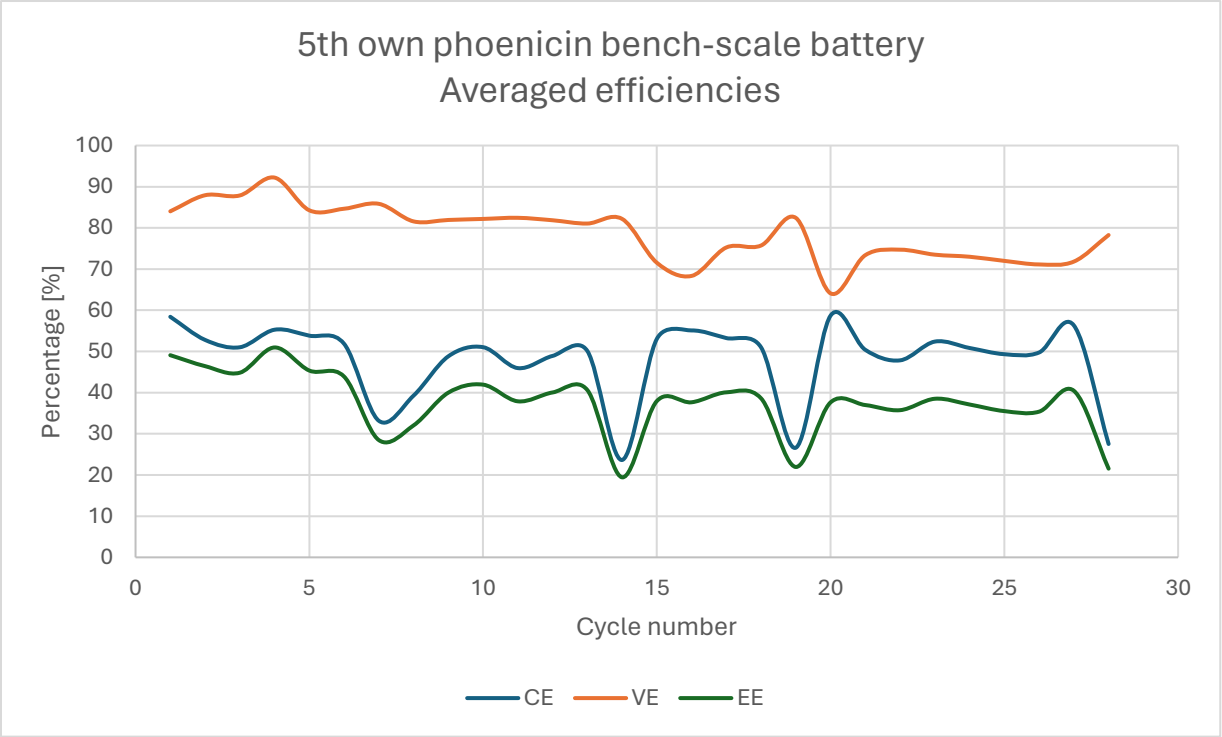


*Figure 9.32: Average CE, VE and EE for the bench-scale battery running on phoenicin batch 5*

Table 9.7 illustrates the averaged efficiencies for batch 5 for quality check and bench-scale batteries. Similar to the two previously shown tables, the bench-scaled battery is worse than the quality check battery except for the VE. The leakage observed presumably resulted in not the same amount of discharge capacity being released as charge capacity produced, causing a decrease in CE.

*Table 9.7: Comparison between small and bench-scale battery running on batch 5*

| | Small Battery | Bench-scale Battery |
|---|---|---|
| CE [%] | 97.2 | 47.7 |
| VE [%] | 52.9 | 78.8 |
| EE [%] | 51.5 | 37.6 |

#### 9.3.1.4. Battery running on batch 6

Similar to the previous battery, this battery running on batch 6 did experience leakage of the electrolytes out of the battery cell, which resulted in the electrolytes running dry. Because of that, after having been running for 4 days and emptying tanks, it was decided to refill the tanks with fresh electrolytes since the capacity fade was not caused by the phoenicin's failure but because of outside impacts. The fresh electrolytes were prepared the same as every electrolyte with the same amount of compound and nitrogen purging of 20 min. Before the electrolytes were changed the battery was running for 20 with some water to flush out the remains of the old electrolytes. Throughout these changes, the battery cell was not altered and was supported through a clam, trying to create more pressure inside the battery cell to minimize the leakage.

Figure 9.33 shows the initial five cycles (2-6, blue) and the final five cycles (23 27, orange) for the bench-scaled battery running on batch 6. Similar to the batch 5 battery, the initial five cycles needed a bit over 30 hours to be finished. The final five cycles also took around 30 hours because of the refill after the fourth day, which resulted in the final five cycles of the

battery before stopping it after a week of cycling. Interestingly, the first final cycle required around 9 hours as it is the first cycle after refill. Comparing the two second cycles for the initial five cycles, the first cycle is the second overall cycle, which took around 7 hours, and for the final five cycles, the second cycle took around 6 hours, showing that even with the new refill, the second cycle is comparable with that one of the original electrolytes which can also be seen in the achieved capacity of those cycles discussed further below.

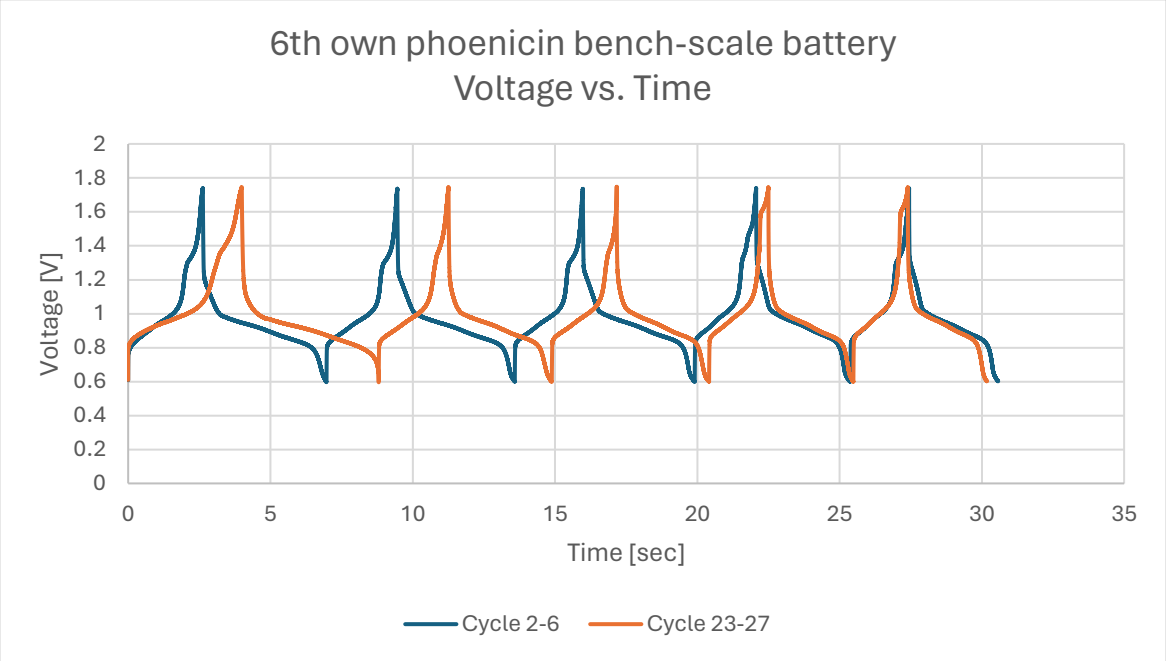


*Figure 9.33: Charge and discharge cycle rate for the 2-6 and 23-27 cycles for the bench-scale battery running on phoenicin batch 6*

Figure 9.36 displays the averaged capacity over the cycling period for charge and discharge for the batch 6 battery. The capacity decay from the first to the fourth day is 80%, caused by the significant leakage of the battery cell represented by Figure 9.34 and Figure 9.35, which show the empty electrolyte tanks and the leakage spill.

*Figure 9.34: Empty tanks, just rest from tubes*

*Figure 9.35: Leakage spill*

The first cycle reaches a capacity of 29.0 mAh, 3.1% lower than the maximum theoretical capacity of 29.9 mAh. This is the third battery to just be considered a two-electron transfer, the same as the previous batch 4 battery. It is also the second battery to be above 95% of the theoretical capacity.

For the second charge cycle, the achieved capacity was 27.9 mAh, which is 93.3% of the theoretical capacity. Although this battery is 3.3% lower than the previous battery running on batch 5, these two batteries seem to perform more stable compared to the first two batteries running on batches 3 and 4. This batch also fulfils the needed 16 mAh for this PV panel.

The prominent peak after 4.25 days is the electrolyte refill, which results in a capacity increase up to 42.3 mAh, which is 70.7% of the maximum theoretical capacity for a four-electron transfer. This is similar to the first cycle of the bench-scaled battery running on batch 3. The following cycle, the second of the refill, did achieve a capacity of 24.5 mAh, which is 3.4 mAh lower than the overall first second cycle of the battery.

The charge is higher than the discharge capacity curve, indicating again that the CE will be below 100% and that the phoenicin is either steadily degraded or the electrolyte is crossing over the membrane. The most significant cause of the difference between charge and discharge is most probably the considerable leakage of the electrolyte.

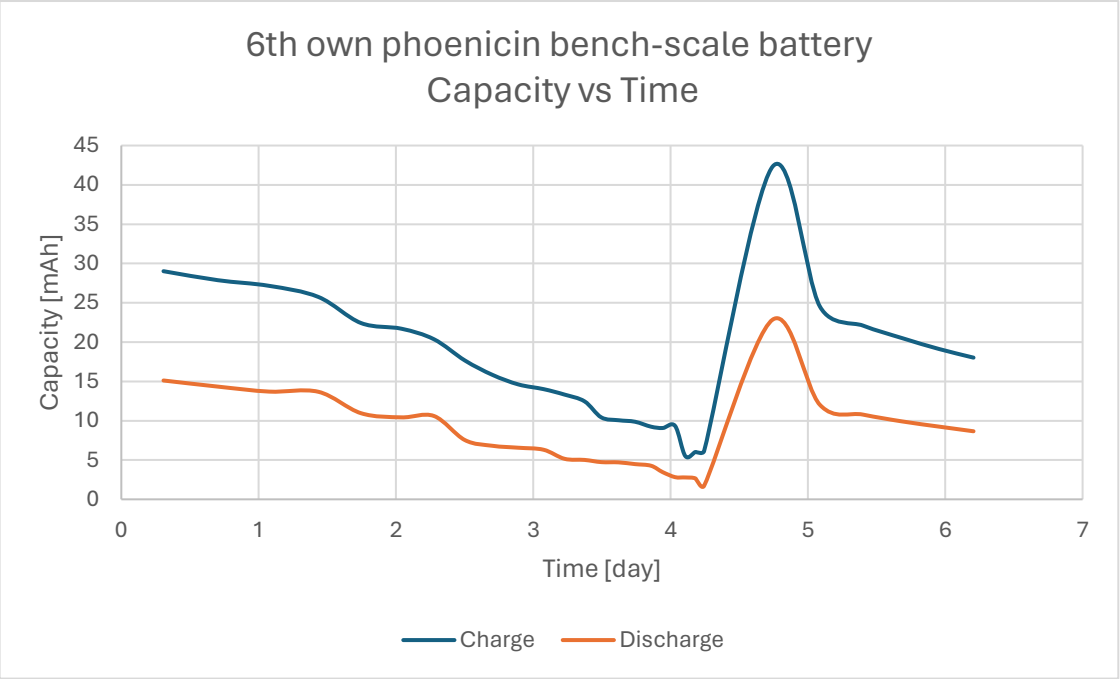


*Figure 9.36: Average capacity per cycle for the bench-scale battery running on phoenicin batch 6*

Figure 9.37 displays the average efficiencies, CE, VE, and EE, for all 28 cycles. As already mentioned, the three efficiency curves show some unsteady behaviour caused by stopping and then restarting the battery and the electrolyte refill.

Again, the CE is more affected by the changes caused by the cycling test and refill breaks, which result in significant drops. If not for the drops, the CE could be interpreted to be decreasing slightly, as shown by the little part of the graph without drops. But after the refill, cycle 23, the CE seems relatively stable around 48%.

The VE graph is also in this bench-scaled battery test above the CE for the cycling test, but it can be seen that it decreases over the time period until the refill, when it increases by over 10%. The decrease in VE can be due to the increasing internal resistance, possibly caused by the already mentioned battery leakage.

The trend of all the efficiencies graphs is the same as the previous bench-scale batteries in that the VE is higher compared to the CE. The EE follows the trend of the CE closely.

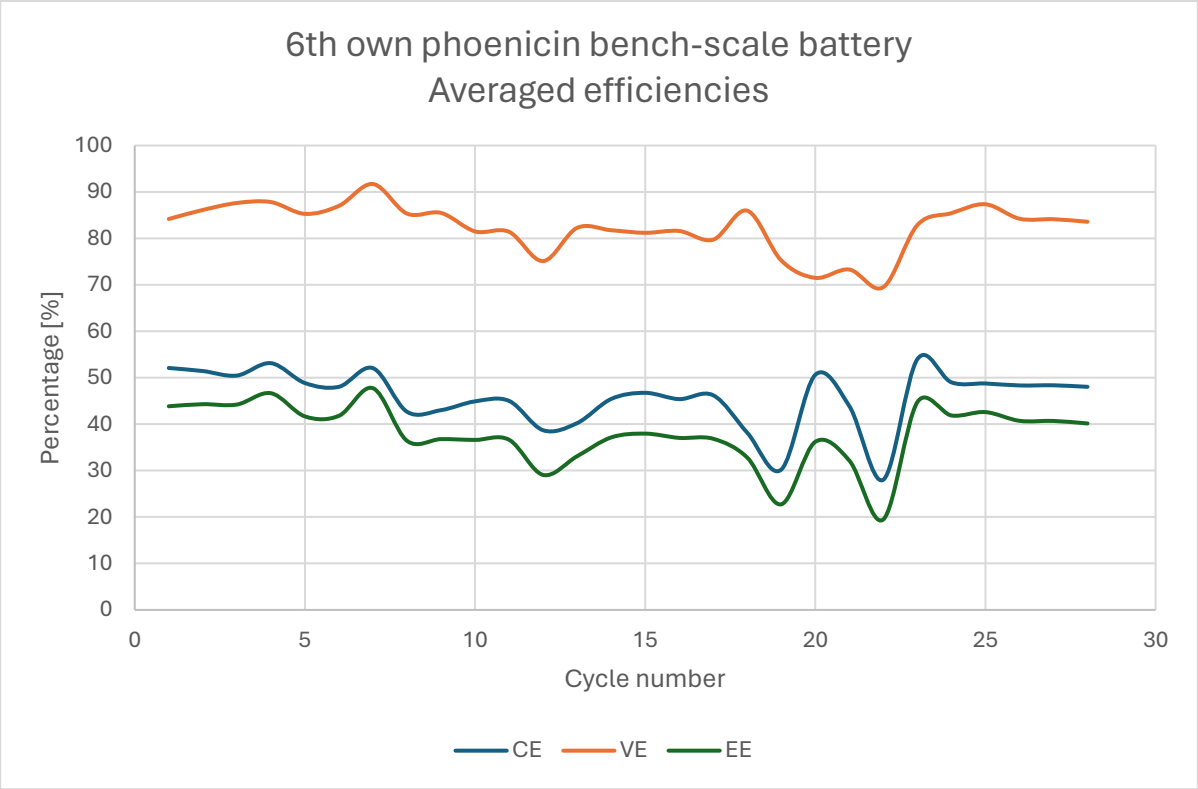


*Figure 9.37: Average CE, VE and EE for the bench-scale battery running on phoenicin batch 6*

Table 9.8 shows the averaged efficiencies for the quality check and bench-scale batteries running on batch 6. The decrease in the CE is presumed to be caused by the leakage observed.

*Table 9.8: Comparison between small and bench-scale battery running on batch 6*

| | Small Battery | Bench-scale Battery |
|---|---|---|
| CE [%] | 97.6 | 45.6 |
| VE [%] | 51.9 | 82.5 |
| EE [%] | 50.7 | 37.6 |

### 9.3.1.5. Battery running on batch 7

The last conducted bench-scaled battery test was for batch 7, for which old metal plates were used because the previously used metal plates could not be used as the screws got stuck entirely in the metals resulting in not being able to disassemble and assemble the battery again after the batch 6 battery was done. A clamp was used to increase the pressure used for the battery cell to be held together just as a precaution against possible leakage of the electrolyte tanks. The use of this setup with the old plates was assembled after having run the battery with the destroyed plates, but after less than 12 hours, the electrolytes were empty because of insufficient pressure in the battery cell, allowing the electrolytes to leak. Because of this almost immediate leakage, it was decided to run the battery with the old metal plates in hopes of no or less leakage compared to the leakage resulting from the new plates. This resulted in the battery only running for a bit over 5 days instead of close to a week.

The initial five cycles (2-6, blue) and the final five cycles (12-16, orange) for batch 7 battery are shown in Figure 9.38. For the initial five cycles, they took the longest time of all the five conducted batteries, needing over 38 hours. It would have been possible that the batch 5 and 6 batteries could have achieved the same time without the leakage, but this is uncertain. The final five cycles needed a bit over half the time of the initial five cycles.

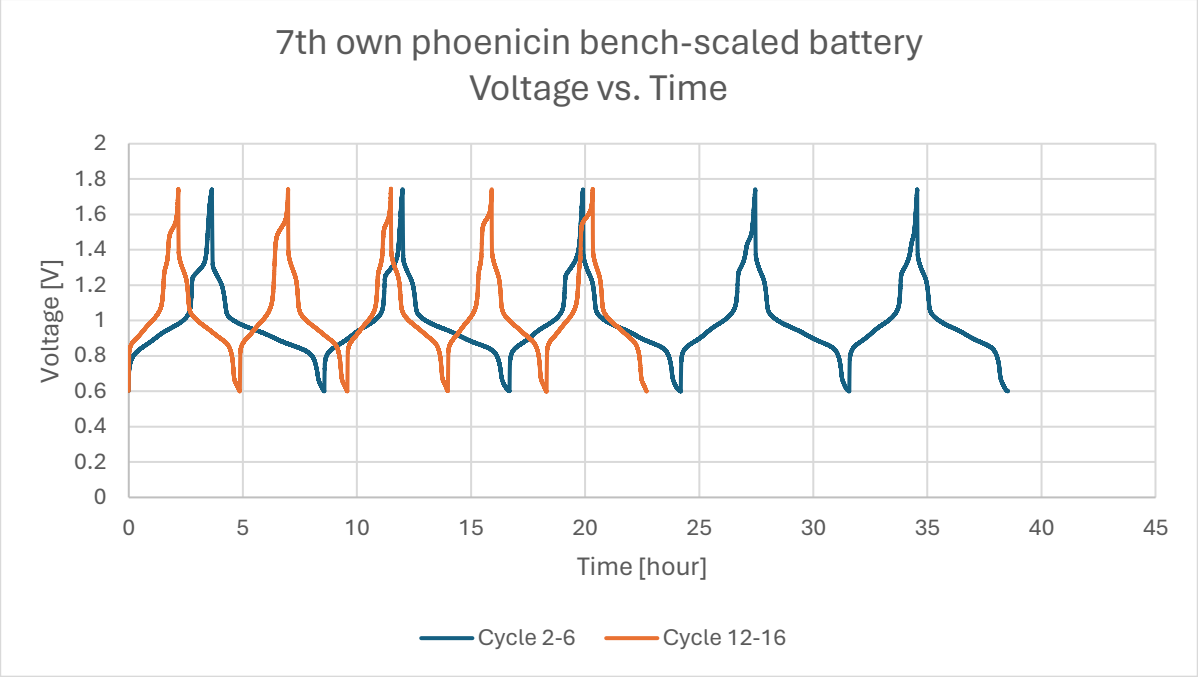


*Figure 9.38: Charge and discharge cycle rate for the 2-6 and 12-16 cycles for the bench-scale battery running on phoenicin batch 7*

Figure 9.39 shows the averaged capacity over the cycling period for charge and discharge of the battery running on batch 7. See that the capacity decreases steadily over the time period where after cycle 16, it lost over 50% of its initial capacity for the first cycle of 37.5 mAh. The stop and restart of the battery causes a small peak slightly before day 3 in the discharge curve. As mentioned, the first cycle achieved a capacity of 37.5 mAh, 25% larger than the maximum theoretical capacity of a two-electron transfer of 29.9 mAh.

The second cycle achieved a charge capacity of 34.3 mAh, 14.7% above the theoretical capacity of 29.9 mAh. These values of the first and second cycles are closer to the two-electron transfer theoretical capacity than the capacity of the four-electron transfer of 59.8 mAh, so it is more likely that this is a two-electron transfer and not a four-electron transfer. As with all the batteries before, this battery fulfils the needed 16 mAh for the PV panel at the beginning of the test. The difference between the charge capacity and discharge capacity is significant, with over 10 mAh difference causing the CE, the ratio of capacity from the charge and used capacity in the discharge, to be below 100%.

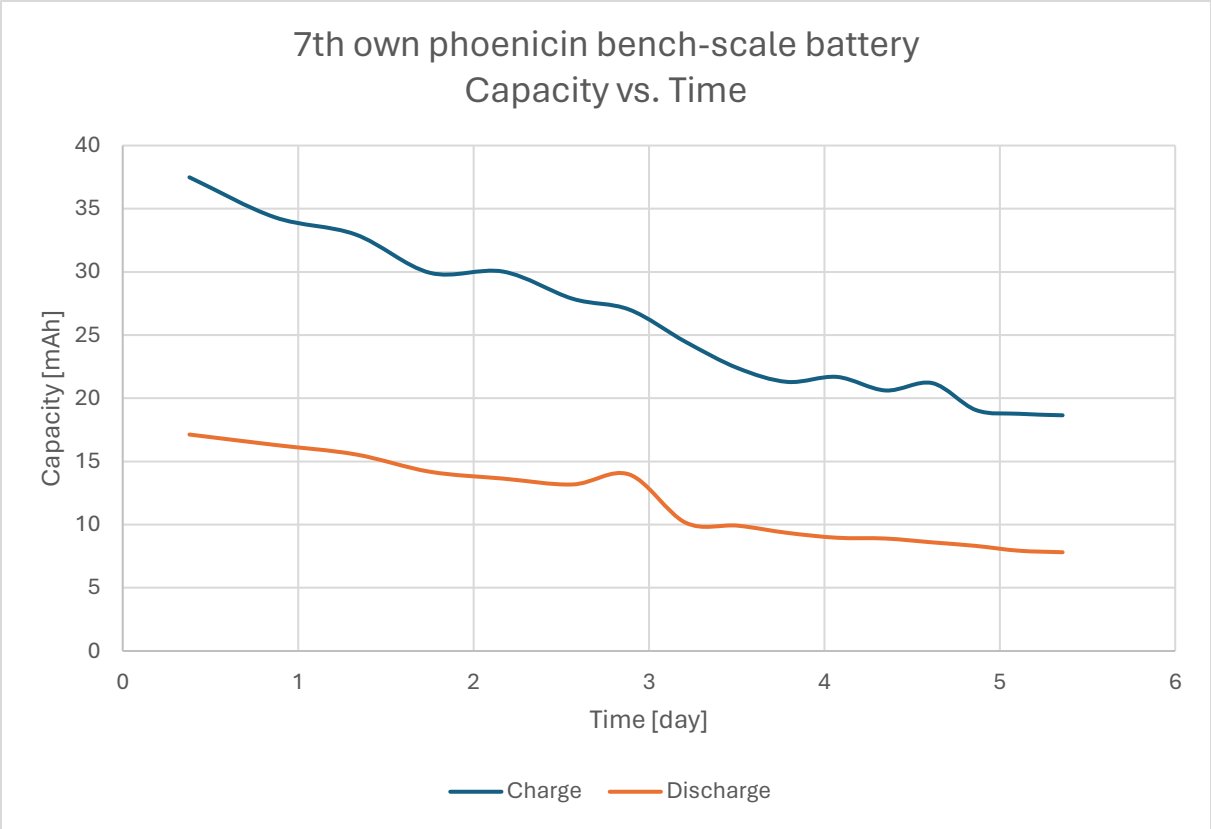


*Figure 9.39: Average capacity per cycle for the bench-scale battery running on phoenicin batch 7*

Figure 9.40 shows the average efficiencies, CE, VE, and EE, for all 16 cycles of the batch 7 battery. All three efficiency curves show some unsteady behaviour caused, as already mentioned, by stopping and then restarting the battery, which happened only once in this battery test.

Similar to the previous battery, the CE is slightly more affected by the breaks in the cycling tests, resulting in a slightly high peak. The CE is overall more affected by the small peaks after the prominent peak resulting from the battery's stop and restart. This figure shows more clearly that the CE would be decreasing slightly, because only one prominent peak would disturb the graph.

The VE graph is also in this bench-scaled battery test above the CE, but it can be seen that it is decreasing slightly over the period, similar to the CE. The decrease of VE can be because the internal resistance is increasing.

The trend of all the efficiencies graphs is the same as the previous bench-scale batteries in that the VE is higher compared to the CE. The EE follows the trend of the CE closely, as in most of the six previous battery tests.

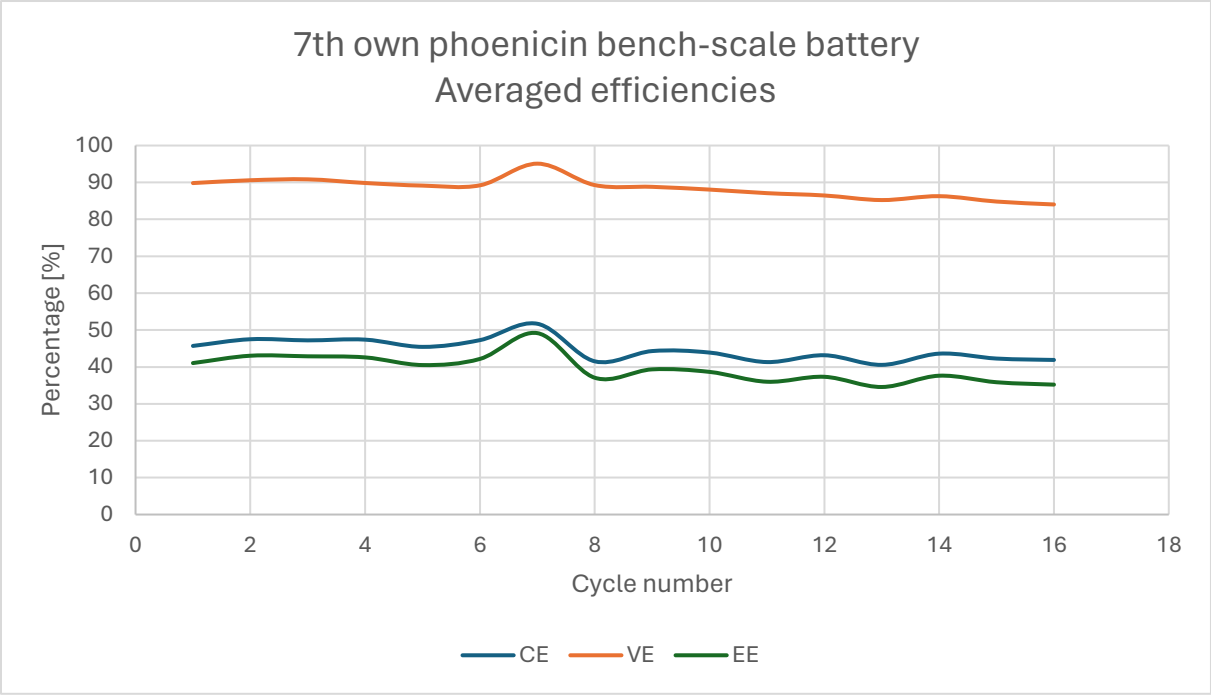


*Figure 9.40: Average CE, VE and EE for the bench-scale battery running on phoenicin batch 7*

Table 9.9 illustrates the averaged efficiencies for batch 5 for quality check and bench-scale batteries. Similar to the two previously shown tables, the bench-scaled battery is worse than the quality check battery except for the VE.

*Table 9.9: Comparison between small and bench-scale battery running on batch 7*

| | Small Battery | Bench-scale Battery |
|---|---|---|
| CE [%] | 95.5 | 44.6 |
| VE [%] | 53.8 | 88.2 |
| EE [%] | 51.3 | 37.6 |

### 9.3.2. Comparison of all battery tests conducted

In this part of the project, after investigating all bench-scaled batteries individually, they will be compared against each other and examined to see if the observations from the quality check batteries can be found or if there are some exceptional observations.

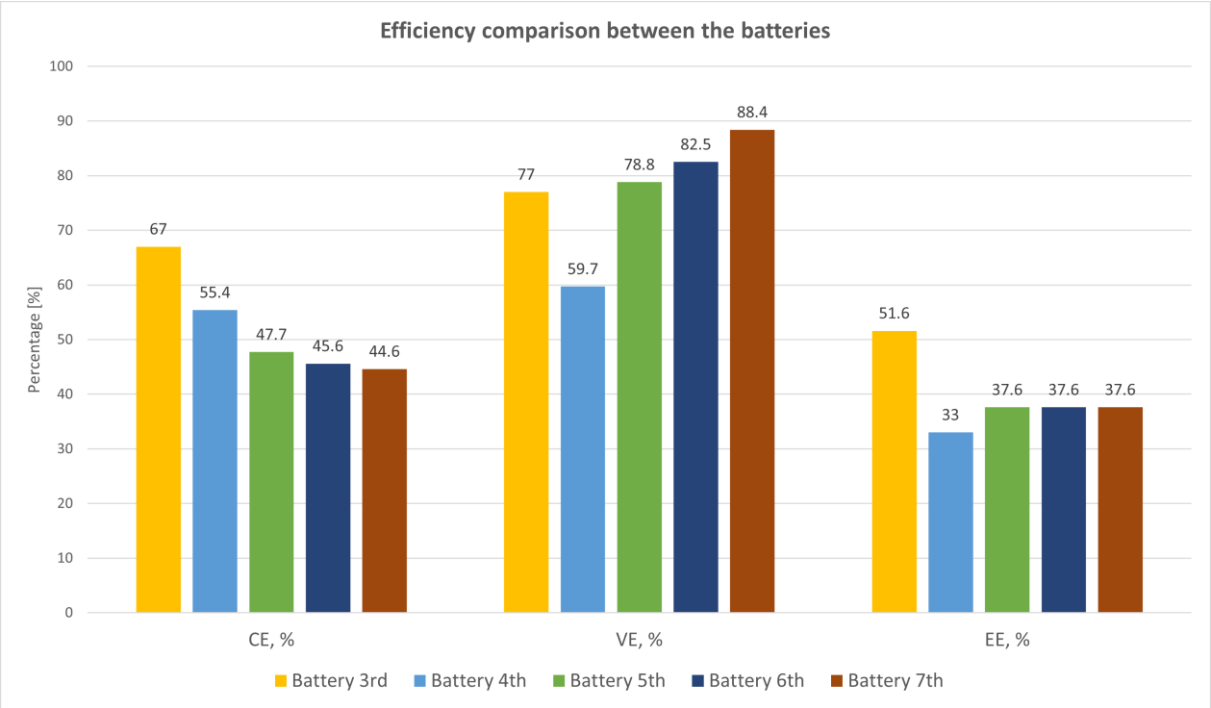


*Figure 9.41: Efficiency comparison between bench-scale batteries*

Similar to the quality check battery tests Figure 9.41 represented visually the efficiencies for all the bench-scaled batteries.

All the CE values for all five conducted batteries lie under the typical 99%, with the highest being 67% from the batch 3 battery. These low values can indicate the mixing of the electrolytes through the membrane. Still, also, for batches 5 and 6, the leakage of the electrolytes is the most probable cause of why the discharge does not fully use the capacity of the charge. Another reason for the CE below 99% is the possible chemically irreversible side reactions of phoenicin. As Wilhelmsen et al. reported in their study, the overall decrease in capacity indicates that phoenicin undergoes some chemical degradation over the cycling period and is no longer available for reduction. If the charge and discharge capacity would perfectly overlap this would imply that the phoenicin sites available for reduction are fully utilized.

The VE is higher compared to the CE values, which is quite unusual and different from the quality check battery tests. As already mentioned, a high VE value can indicate a low resistance, while a low value indicates the opposite. The low VE can result from either a rupture membrane, resulting in cross-over causing pressure problems and resistance, or it could have been caused by the electrodes, which may not be hydrophilic enough to allow fast electron transfer. Interestingly, even if batches 5 and 6 had significant leakages, the VE is relatively high, indicating that the leakage did not cause any high resistance. A possible cause for the higher value in batches 5, 6 and 7 is the change of sun used, lowering the internal resistance compared to the lamp used in batches 3 and 4. Based on this, it can be concluded that in regard to resistance, the least resistance was achieved in the battery running with the 7th phoenicin batch, and the highest resistance was achieved with the 4th batch. This is a different result to the quality check batteries where batch 4 had the lowest resistance of all six conducted batteries and batch had the highest.

Variations in CE and VE have equal influence on the EE and balance each other out. For example, batch 4's low value results in a low EE. For batches 5, 6, and 7, the same EE value results from that in the CE; their values decrease from left to right, and for the VE, their values increase from left to right, resulting in balancing each other out.

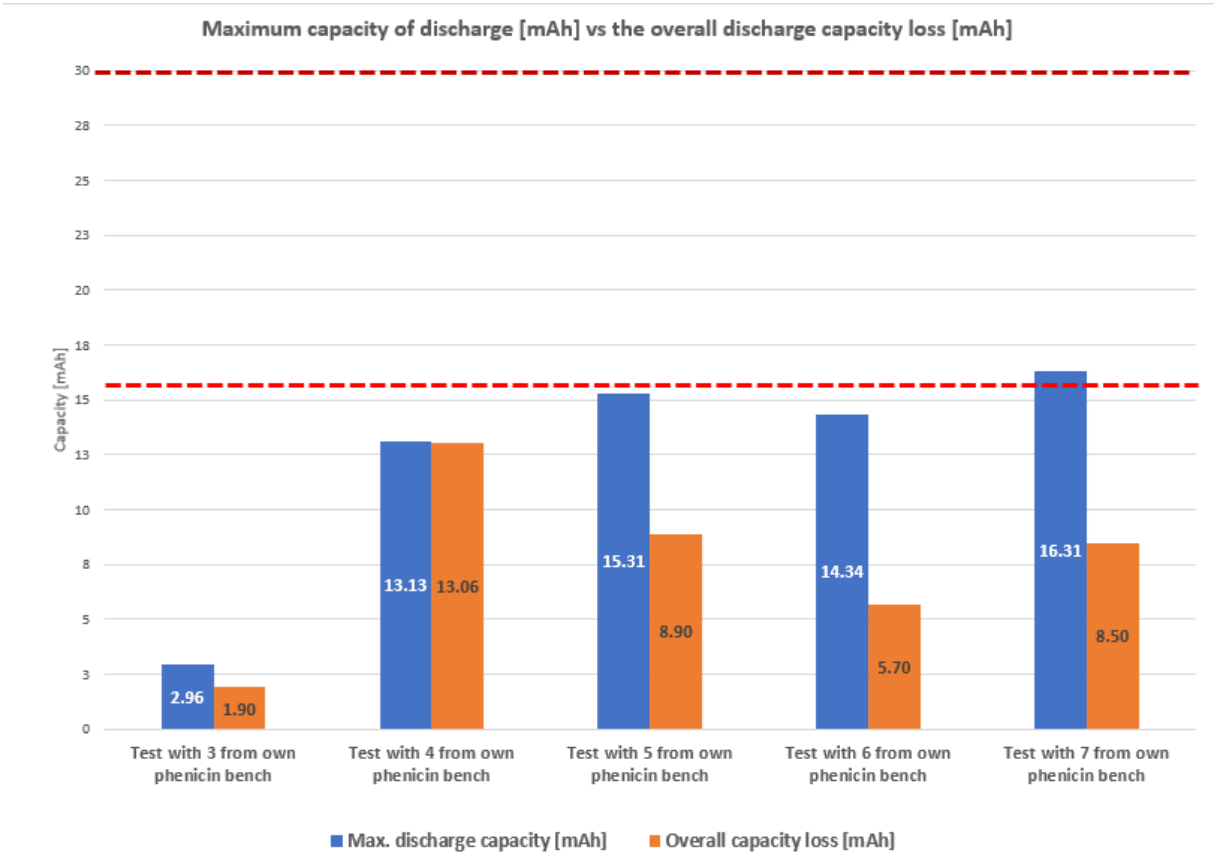


*Figure 9.42: Comparison of maximum capacities and capacity loss between the bench-scale batteries; light red dotted line = needed 16 mAh, dark red dotted line = max theoretical capacity*

The calculated maximum theoretical capacity for a two-electron transfer was 29.9 mAh, and Figure 9.42 shows the maximum capacity of each battery and the respective overall capacity loss throughout the charge/discharge cycles. The light red dotted line indicates the needed 16 mAh for the PV panel, and the dark red dotted line indicates the theoretical capacity.

As seen from the figure, none of the batteries reached the maximum theoretical capacity, and only one, batch 7, reached the needed 16 mAh. As already seen in the quality check batteries, the impurities in the phoenicin cause it only to be able to reach 50% of the maximum theoretical capacity based on the pure phoenicin assumption. The batch 3 battery did not even come close to the 16 mAh, which is not completely clear why the most possible reason is the cross-over of phoenicin into the potassium ferrocyanide side or still figuring the setup out completely.

It has to be remembered that a different, much smaller lamp was used for batches 5, 6, and 7, which influences the maximum discharge capacity. These three seem relatively close to 16 mAh, with batch 7 also achieving it. The smaller power could be causing a better mass flow rate, making it easier for the electrons to transfer. These batteries also ran longer compared to batches 3 and 4, most probably because the smaller lamp provided less power.

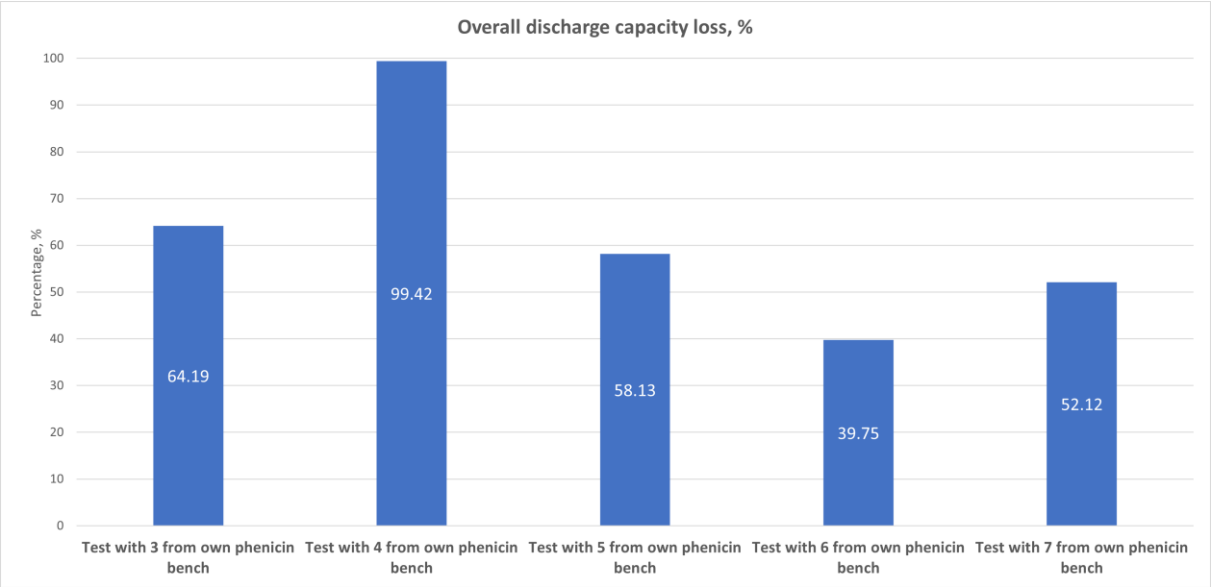


*Figure 9.43: Comparison of overall discharge capacity loss between the bench-scale batteries*

Figure 9.43 visually compares all bench-scaled batteries' overall discharge capacity loss in percentage for the cycling period. The most capacity loss is the one from batch 4, which is almost 100%, which is different compared to the quality check batteries, where batch 4 was in the middle regarding the capacity loss percentage. A possible explanation is the leakage, but another reason could be that the lights in the lab were on the entire time of the battery test, which did not affect the capacity as the charge/discharge process would proceed faster, resulting in lower capacity achieved. The batteries running on the small batteries have similar losses above 50% except for batch 6, which is due to the refill halfway; otherwise, it can be predicted that the capacity loss percentage would be similar to that of batches 5 and 7.

Table 9.10 also shows these values and at which cycle 50% of the maximum capacity was lost for each battery of the respective phoenicin batch. From the table, it can be seen that all batteries reached 50% of the maximum overall capacity quite early from 100 charge/discharge cycles. This indicates an unstable battery test, but it has to be noticed that for batches 5, 6, and 7, the cycles run were 28, 28, and 16, respectively.

*Table 9.10: Overall discharge capacity loss and capacity and cycle where 50% of discharge capacity is lost for every battery*

| Battery Test | Discharge Capacity Loss [%] | Cycle Of 50% Capacity Loss |
|---|---|---|
| 3 | 64.2 | Hard to tell |
| 4 | 99.4 | 11 |
| 5 | 58.1 | 17 |
| 6 | 39.8 | 9 |
| 7 | 52.1 | 15 |

Some differences exist between the batteries shown in Figure 9.44 regarding the discharge capacity loss per cycle and hour.

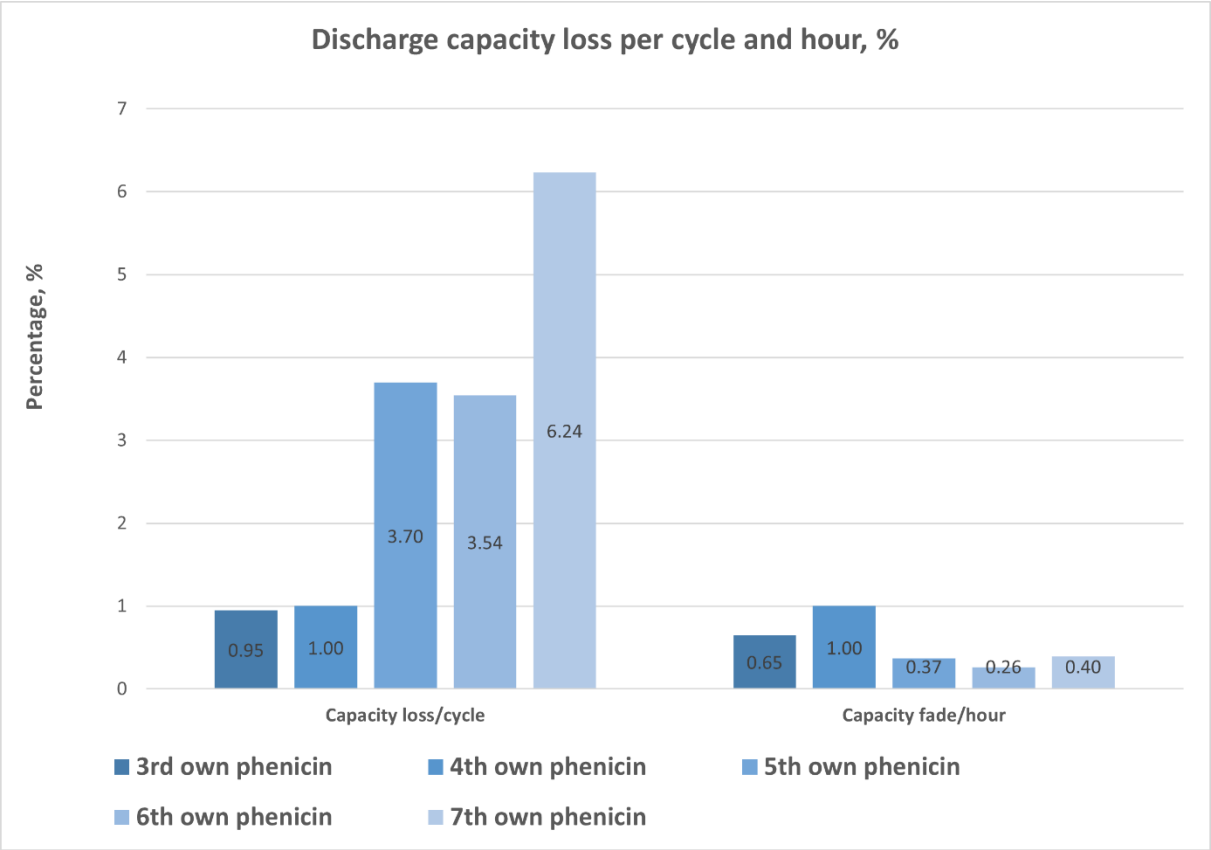


*Figure 9.44: Comparison of capacity loss per cycle and hour between the bench-scale batteries*

For the batches running for fewer cycles, these capacity losses per cycle are evidently higher compared to the batches running for 100 cycles, which causes some complications in comparing these values. For batches 3 and 4, which ran for 100 cycles, the values are the same as those of the quality check batteries, being 1% or lower. The percentage loss of the capacity per hour ranges from 1% to the lowest of 0.26%. Similar to the previous figure, the batteries running on the phoenicin batches 5, 6 and 7 ran for fewer cycles, but these cycles had a longer duration, and the capacity loss per hour was lower compared to batches 3 and 4.

The bench-scaled battery tests have shown that phoenicin can be used to store the energy produced by a PV panel. Throughout the different obstacles that did occur, i.e., the change of lamp, which was decided to simulate different suns, showed that a less powerful sun could cause lower capacity losses either overall or per hour as well as increase the cycling time of the charge/discharge cycles resulting more stable batteries. As already seen in the quality check batteries, it has to be assumed that only 50% of the maximum theoretical capacity will be produced. Still, there were also instances where not only the standard two-electron transfer occurred but also the possible four-electron transfer, resulting in a higher possible capacity. Overall, after investigating the five batches used for the bench-scale cycling battery test, it can be assumed that batches 5, 6, and 7 are more stable than batches 3 and 4 based on the previously mentioned reasons for the capacity loss and maximum capacity achieved.

The CE of the last three batches is below 50%, and the first two are above 50%, but all five values are below 99%, indicating that the phoenicin's redox-active sites are not fully utilized. This can be due to electrolyte cross-over throughout the membrane, which is most probably the case as the membrane fractured in every battery test conducted. The sizeable overall capacity loss also indicates that the phoenicin is steadily undergoing degradation.

The VE is one of the most notable differences between the bench-scaled bat and the quality check batteries, as the values are all above 50%, usually above 75%. This high value indicates low internal resistance, possibly because of the new electrode used compared to quality check batteries. Regarding EE, the values are lower than the quality control batteries due to the low CE values. Overall, in terms of efficiencies, the battery running on batch 3 was the best-performing battery and worse was the batch 4 battery.

In another study (Paper 2) conducted by Wilhelmsen et al., a mixing of different phoenicin in the negolyte tank of 10 mL was used, corresponding to a theoretical capacity of 16.41 mAh for a four-electron transfer, but it was assumed that there would only be a two-electron transfer with a capacity of 8.21 mAh. But in the first charging cycle, 15.79 mAh was achieved, implying a four-electron transfer. The capacity drops to 3.91 mAh at the end of the test.

The averaged efficiencies determined in the different studies from Wilhelmsen et al. can be seen in Table 9.11 below for the specific phoenicin single-cell cycling battery test. [6] As already mentioned, the phoenicin mix (Paper 2) had a theoretical capacity of 16.4 mAh for a four-electron transfer and 8.24 mAh for a two-electron transfer.

*Table 9.11: Table of previous study efficiencies [6]*

| Averaged Efficiencies [%] | Paper 1 [29] | Paper 2 [30] |
|---|---|---|
| CE | 98.5 | 95 |
| VE | 37.5 | 79 |
| EE | 36.9 | 77 |

Comparing the efficiencies of the bench-scale batteries with the ones from the study of Wilhelmsen et al., it can be seen that the CE is the apparent difference between these two. The CE values of all the conducted bench-scale batteries lie, on average, around 52%, which is over 40% less than the CE achieved in the study. As already mentioned, the cause for this low CE is either side reactions or cross-over of the electrolyte but the most probable cause for these is the leakage which occurs while running the battery tests. Because of this, the EE values of the batteries are also lower compared to the EE of the study.

Because of the double amount of used phoenicin in the thesis, the theoretical capacity was 29.9 mAh, which is almost double that of the study, but as already mentioned, it was done to ensure that the needed 16 mAh is reached; otherwise, the capacity would be the same as for the battery conducted in the study from Wilhelmsen et al.

Based on the experiments conducted, an example of a case study of an RFB using phoenicin as a negolyte to store energy from renewable energy sources can be assumed. As already mentioned in Chapter 4, the battery should be double the kWh as the kWp of the solar panel. The average produced energy of a solar panel is 5 MW resulting in 5000 kWp. This means that the battery for this solar farm would need to be 10000 kWh. Based on the equation from Chapter 4, with an operating voltage of 1.6 V, it would come out to 16000000 mAh. The needed phoenicin amount is calculated, seen in Equation 11 below and results in 82 kg.

*Equation 11: Phoenicin mass equation*

$$mAh = \frac{n * F * m}{3600 * MW} \rightarrow m = \frac{16000\ Ah * 3600 * 274.23\ mol/g}{2 * 96485.33\ Ah/mol} = 81855\ g = 82\ kg$$

Based on the observations from the bench-scaled batteries and the quality check batteries, it should be assumed that the calculated amount for the 16000 Ah will only achieve half of that capacity. Therefore, the used phoenicin amount should be doubled to 164 kg to ensure that the capacity does reach 16000 Ah.

The self-production of phoenicin produced an average of around 2 g per 1 L phoenicin broth, which means that for 164 kg, over 82000 L of phoenicin broth should be produced. As seen in Chapter 8, for the phoenicin extraction, the same amount of ethyl acetate as phoenicin broth is needed, which means over 82000 L with a price of 4 € per kg, resulting in 328000 € for this extraction. This amount of phoenicin would result in an electrolyte tank volume of 11939.6 L, around 12000 L for the negolyte with a KOH concentration of 2.7M. The posolyte would need a volume of 30000 L, a KOH of 1M, and a potassium ferrocyanide of 55.3 kg, which is 27.45 € per 250 g, resulting in 6071.94 €. Potassium hydroxide is 42.5€ per kg for both electrolytes, which would result in 148835€ in costs. The total expenses for the things above are ca. 482907€, which do not include equipment or electricity costs, which will vary based on location and delivery possibilities.

From the comparison between the quality check and the big battery, it can be assumed that the RFB will be more stable with a higher phoenicin concentration, which would make the operation in this scale seemingly feasible. However, to be sure, some try-runs should be conducted before. From the bench-scale battery tests, it can be assumed that refilling the electrolytes after some time would be beneficial to keep the capacity fade more stable.

If it is decided to use the phoenicin operating RFB for energy storage, the same calculations above can be used for a wind turbine operating on 5 MW.

# 10. Conclusion

The initial question for this report is:

*"How are the requirements needed to scale up a phoenicin-operated RFB from lab to bench/pilot scale?"*

The focus of the possible renewable energy source attached to be RFB running on phoenicin was the 10 Wh solar panel to simulate the storage of the fluctuating energy from that PV panel. The research problem analysis created the following problem formulation: ´

*"How well is a bench-scaled redox flow battery operating with phoenicin as a negolyte reproducible to be used to store a solar panel's energy?"*

Different phoenicin batches were produced to investigate the reproducibility of an RFB operating on phoenicin as a negolyte used to store the energy produced by the 10 Wh solar panel.

Based on the PV panel of 10 Wh used in this bench-scaled cycling battery test, the different phoenicin batches must achieve 16 mAh of capacity to store the panel's energy. From the previously done batteries, it was found that the phoenicin compounds have an average of 42% capacity loss, which means that the amount of phoenicin should be almost doubled to ensure that the 16 mAh is achieved. This amount of phoenicin would have a maximum theoretical capacity of 29.9 mAh, but for the investigation, it was only first and foremost to make sure that the 16 mAh is reached. Other requirements for reasonable batches are the efficiencies and the capacity losses. Out of the six reasonable phoenicin found batches only five batches results could be used because of some equipment complications.

In terms of efficiencies, the battery running on batch 3 was the best-performing battery and worse was the batch 4 battery. As for overall capacity loss in %, the best was the battery running on batch 6 below 50%, which is a result of the refill of the electrolyte, but if we account for that, batch 5 and batch 7 should be considered to have the lowest overall capacity loss being the best. As for the worse, it was battery of batch 4, in which almost 100% of the capacity was left after the 100 cycles.

As for the needed 16 mAh of capacity, only batch 7 did reach it, but batteries running on batch 5 and 6 were close to that value. Doubling the amount based on the observation of the quality control batteries was the correct decision, as all batteries did not reach the 29.9 mAh maximum theoretical capacity but only around 50% or less. Batches 5, 6 and 7 can be seen as the best batteries conducted tests based on the observations mentioned above, which imply that the conditions for these batches should be followed to achieve these results or similar ones.

Overall, the data from these experiments show that an RFB operating on phoenicin can store the energy produced by a solar panel and is also reproducible in the grand scheme of things if no outside influences occur. The bench-scale batteries running on the five different batches show similar values in regard to efficiency and achieved capacity, underlining the assumption that the setup is reproducible.

# 11. Further Work

To expand on this thesis further, it could be interesting to repeat the experiments in a glove box to improve the performance, as the oxygen contamination is more controllable and minimized.

Other parameters could be explored to further optimize the phoenicin operating RFB. These parameters could be different flow rates and SOC levels. The different flow rates could be invested to see if they affect the battery's capacity, stability, and other properties. The investigation of SOC levels would be informative in finding the optimal battery lifetime to save electrolytes and minimize the possible electrolyte crossover through the membrane.

Another interesting topic to be investigated is symmetric cell cycling for capacity stability. This setup is used to analyze the overall influence of molecular capacity loss mechanisms in AORFBs.

In general, repetitions of the cycling battery tests for each batch should be conducted. This will help analyze whether the phoenicin operating battery is reproducible. Furthermore, more phoenicin batches should be produced, either duplicates for each plate or one plate per batch, which would be too wasteful. Another interesting thing would be to produce phoenicin from different fungi, as was done in one study by Wilhelmsen et al. to identify the best fungi for the phoenicin production.

The project showed that batteries can be used to store energy produced by one renewable energy source. Still, other sources, such as wind energy, should also be investigated to see if the technology is just limited to PV panels or has more operation areas.

# 12. References


[1] ‘World Energy Consumption Statistics | Enerdata’. Accessed: May 24, 2024. [Online]. Available: https://yearbook.enerdata.net/total-energy/world-consumption-statistics.html

[2] I. Sorrenti, T. B. Harild Rasmussen, S. You, and Q. Wu, ‘The role of power-to-X in hybrid renewable energy systems: A comprehensive review’, *Renewable and Sustainable Energy Reviews*, vol. 165, no. 112380, Sep. 2022, doi: 10.1016/j.rser.2022.112380.

[3] J. Mitali, S. Dhinakaran, and A. A. Mohamad, ‘Energy storage systems: a review’, *Energy Storage and Saving*, vol. 1, no. 3, pp. 166–216, Sep. 2022, doi: 10.1016/j.enss.2022.07.002.

[4] ‘Energy Statistics Data Browser – Data Tools’, IEA. Accessed: Jan. 24, 2024. [Online]. Available: https://www.iea.org/data-and-statistics/data-tools/energy-statistics-data-browser

[5] M. J. B. Kabeyi and O. A. Olanrewaju, ‘Sustainable Energy Transition for Renewable and Low Carbon Grid Electricity Generation and Supply’, *Front. Energy Res.*, vol. 9, Mar. 2022, doi: 10.3389/fenrg.2021.743114.

[6] Aalborg University and C. O. Wilhelmsen, ‘Investigating fungal-produced phoenicin as a possible electrolyte candidate for a redox flow battery’, Ph.d, Aalborg University, 2022. doi: 10.54337/aau527275062.

[7] M. Kiehbadroudinezhad, A. Merabet, and H. Hosseinzadeh-Bandbafha, ‘Review of Latest Advances and Prospects of Energy Storage Systems: Considering Economic, Reliability, Sizing, and Environmental Impacts Approach’, *Clean Technologies*, vol. 4, no. 2, Art. no. 2, Jun. 2022, doi: 10.3390/cleantechnol4020029.

[8] A. Riaz, M. R. Sarker, M. H. M. Saad, and R. Mohamed, ‘Review on Comparison of Different Energy Storage Technologies Used in Micro-Energy Harvesting, WSNs, Low-Cost Microelectronic Devices: Challenges and Recommendations’, *Sensors*, vol. 21, no. 15, Art. no. 15, Jan. 2021, doi: 10.3390/s21155041.

[9] T. M. Gür, ‘Review of electrical energy storage technologies, materials and systems: challenges and prospects for large-scale grid storage’, *Energy Environ. Sci.*, vol. 11, no. 10, pp. 2696–2767, Oct. 2018, doi: 10.1039/C8EE01419A.

[10] ‘Alkaline Quinone Flow Battery with Long Lifetime at pH 12 - ScienceDirect’. Accessed: May 30, 2024. [Online]. Available: https://www.sciencedirect.com/science/article/pii/S2542435118302915

[11] ‘The best redox flow battery tech – pv magazine International’. Accessed: May 24, 2024. [Online]. Available: https://www.pv-magazine.com/2021/01/20/the-best-redox-flow-battery-tech/

[12] ‘Electrolyte Lifetime in Aqueous Organic Redox Flow Batteries: A Critical Review | Chemical Reviews’. Accessed: May 30, 2024. [Online]. Available: https://pubs.acs.org/doi/10.1021/acs.chemrev.9b00599

[13] M. O. Bamgbopa, A. Fetyan, M. Vagin, and A. A. Adelodun, ‘Towards eco-friendly redox flow batteries with all bio-sourced cell components’, *Journal of Energy Storage*, vol. 50, p. 104352, Jun. 2022, doi: 10.1016/j.est.2022.104352.

[14] R. Chen, S. Kim, and Z. Chang, ‘Redox Flow Batteries: Fundamentals and Applications’, in *Redox - Principles and Advanced Applications*, M. A. A. Khalid, Ed., InTech, 2017. doi: 10.5772/intechopen.68752.

[15] R. Potash, J. Mckone, S. Conte, and H. Abruña, ‘On the Benefits of a Symmetric Redox Flow Battery’, *Journal of The Electrochemical Society*, vol. 163, pp. A338–A344, Dec. 2015, doi: 10.1149/2.0971602jes.

[16] J. Schumacher, G. Mourouga, and J. Wiodarczyk, ‘Redox Flow Battery Campus’, ZHAW Zürcher Hochschule für Angewandte Wissenschaften. Accessed: May 25, 2024. [Online]. Available: https://www.zhaw.ch/de/forschung/forschungsdatenbank/projektdetail/projektid/2432/

[17] ‘Redox flow batteries: a review | Journal of Applied Electrochemistry’. Accessed: May 30, 2024. [Online]. Available: https://link.springer.com/article/10.1007/s10800-011-0348-2
[18] ‘The Chemistry of Redox-Flow Batteries - Noack - 2015 - Angewandte Chemie International Edition - Wiley Online Library’. Accessed: May 30, 2024. [Online]. Available: https://onlinelibrary.wiley.com/doi/abs/10.1002/anie.201410823
[19] J. Winsberg, T. Hagemann, T. Janoschka, M. D. Hager, and U. S. Schubert, ‘Redox-Flow Batteries: From Metals to Organic Redox-Active Materials’, *Angewandte Chemie International Edition*, vol. 56, no. 3, pp. 686–711, 2017, doi: 10.1002/anie.201604925.
[20] M. Mansha *et al.*, ‘Recent Development of Electrolytes for Aqueous Organic Redox Flow Batteries (Aorfbs): Current Status, Challenges, and Prospects’, *The Chemical Record*, vol. 24, no. 1, p. e202300284, 2024, doi: 10.1002/tcr.202300284.
[21] J. Moutet, D. Mills, M. M. Hossain, and T. L. Gianetti, ‘Increased performance of an all-organic redox flow battery model via nitration of the [4]helicenium DMQA ion electrolyte’, *Mater. Adv.*, vol. 3, no. 1, pp. 216–223, Jan. 2022, doi: 10.1039/D1MA00914A.
[22] L. Tong *et al.*, ‘Molecular Engineering of an Alkaline Naphthoquinone Flow Battery’, *ACS Energy Letters*, vol. 4, no. 8, pp. 1880–1887, 2019.
[23] P. Leung *et al.*, ‘Recent developments in organic redox flow batteries: A critical review’, *Journal of Power Sources*, vol. 360, pp. 243–283, Aug. 2017, doi: 10.1016/j.jpowsour.2017.05.057.
[24] S. Bowden and C. Honsberg, ‘Battery Efficiency | PVEducation’, PVEducation. Accessed: May 25, 2024. [Online]. Available: https://www.pveducation.org/pvcdrom/battery-characteristics/battery-efficiency
[25] T. Hagemann *et al.*, ‘A bipolar nitronyl nitroxide small molecule for an all-organic symmetric redox-flow battery’, *NPG Asia Materials*, vol. 9, p. e340, Jan. 2017, doi: 10.1038/am.2016.195.
[26] H. Wenzl, ‘BATTERIES AND FUEL CELLS | Lifetime’, in *Encyclopedia of Electrochemical Power Sources*, 2009, pp. 552–558. doi: 10.1016/B978-044452745-5.00048-4.
[27] ‘Top 5 Factors That Affect Industrial Battery Efficiency’, Flux Power. Accessed: May 26, 2024. [Online]. Available: https://www.fluxpower.com/blog/top-5-factors-that-affect-industrial-battery-efficiency
[28] J. D. Hofmann and D. Schröder, ‘Which Parameter is Governing for Aqueous Redox Flow Batteries with Organic Active Material?’, *Chemie Ingenieur Technik*, vol. 91, no. 6, pp. 786–794, 2019, doi: 10.1002/cite.201800162.
[29] C. O. Wilhelmsen *et al.*, ‘Demonstrating the Use of a Fungal Synthesized Quinone in a Redox Flow Battery’, *Batteries and Supercaps*, vol. 6, no. 1, 2023, doi: 10.1002/batt.202200365.
[30] C. O. Wilhelmsen *et al.*, ‘On the Capacity and Stability of a Biosynthesized Bis-quinone Flow Battery Negolyte’, *ACS Sustainable Chem. Eng.*, vol. 11, no. 24, pp. 9206–9215, Jun. 2023, doi: 10.1021/acssuschemeng.3c02136.
[31] J. Zhang *et al.*, ‘An all-aqueous redox flow battery with unprecedented energy density’, *Energy Environ. Sci.*, vol. 11, no. 8, pp. 2010–2015, 2018, doi: 10.1039/C8EE00686E.
[32] T. P. Curtin and J. Reilly, ‘Sclerotiorine, C20H20O5Cl, a chlorine-containing metabolic product of *Penicillium sclerotiorum* van Beyma’, *Biochemical Journal*, vol. 34, no. 10–11, p. 1418.1-1421, Nov. 1940, doi: 10.1042/bj0341418.
[33] M. Christensen, J. C. Frisvad, and D. Tuthill, ‘Taxonomy of the *Penicillium miczynskii* group based on morphology and secondary metabolites’, *Mycological Research*, vol. 103, no. 5, pp. 527–541, May 1999, doi: 10.1017/S0953756298007515.
[34] ‘Phenicin’. Accessed: May 27, 2024. [Online]. Available: https://www.drugfuture.com/chemdata/Phenicin.html
[35] C. Highlight, ‘Capacity of Cathode/Anode’. Accessed: May 25, 2024. [Online]. Available: https://www.batteryshortcut.com/2020/01/capacity-of-cathodeanode.html

[36] Y. Liu *et al.*, 'Degradation of electrochemical active compounds in aqueous organic redox flow batteries', *Current Opinion in Electrochemistry*, vol. 32, p. 100895, Apr. 2022, doi: 10.1016/j.coelec.2021.100895.
[37] '(PDF) The Synthesis of Diquinone and Dihydroquinone Derivatives of Calix[4]arene and Electrochemical Characterization on Au(111) surface'. Accessed: May 30, 2024. [Online]. Available: https://www.researchgate.net/publication/308469177_The_Synthesis_of_Diquinone_and_Dihydroquinone_Derivatives_of_Calix4arene_and_Electrochemical_Characterization_on_Au111_surface
[38] D. P. Tabor, R. Gómez-Bombarelli, L. Tong, R. G. Gordon, M. J. Aziz, and A. Aspuru-Guzik, 'Mapping the frontiers of quinone stability in aqueous media: implications for organic aqueous redox flow batteries', *J. Mater. Chem. A*, vol. 7, no. 20, pp. 12833–12841, May 2019, doi: 10.1039/C9TA03219C.
[39] J. Sivanadanam, R. Murugan, H. Khan, I. S. Aidhen, and K. Ramanujam, 'Investigation of Alkyl Amine Substituted Quinone Derivatives for the Redox Flow Battery Applications in Acidic Medium', *J. Electrochem. Soc.*, vol. 169, no. 2, p. 020533, Feb. 2022, doi: 10.1149/1945-7111/ac505f.
[40] 'Concentration-Dependent Dimerization of Anthraquinone Disulfonic Acid and Its Impact on Charge Storage | Chemistry of Materials'. Accessed: May 27, 2024. [Online]. Available: https://pubs.acs.org/doi/10.1021/acs.chemmater.7b00616
[41] 'Dimerization of 9,10-anthraquinone-2,7-Disulfonic acid (AQDS) | Request PDF'. Accessed: May 30, 2024. [Online]. Available: https://www.researchgate.net/publication/333528741_Dimerization_of_910-anthraquinone-27-Disulfonic_acid_AQDS
[42] M.-A. Goulet *et al.*, 'Extending the Lifetime of Organic Flow Batteries via Redox State Management', *J. Am. Chem. Soc.*, vol. 141, no. 20, pp. 8014–8019, May 2019, doi: 10.1021/jacs.8b13295.
[43] J. D. Milshtein *et al.*, 'High current density, long duration cycling of soluble organic active species for non-aqueous redox flow batteries', *Energy Environ. Sci.*, vol. 9, no. 11, pp. 3531–3543, Nov. 2016, doi: 10.1039/C6EE02027E.
[44] J. Heinze, 'Cyclic Voltammetry—"Electrochemical Spectroscopy". New Analytical Methods (25)', *Angewandte Chemie International Edition in English*, vol. 23, no. 11, pp. 831–847, 1984, doi: 10.1002/anie.198408313.
[45] 'How does solar power work? | Solar energy explained | National Grid Group', nationalgrid. Accessed: Jan. 24, 2024. [Online]. Available: https://www.nationalgrid.com/stories/energy-explained/how-does-solar-power-work
[46] 'Renewables 2023 – Analysis', IEA. Accessed: May 27, 2024. [Online]. Available: https://www.iea.org/reports/renewables-2023
[47] admin, 'Photovoltaik (PV) oder Windkraft? Was eignet sich für Ihre Freifläche?', FlächenMakler. Accessed: Jun. 01, 2024. [Online]. Available: https://www.flaechenmakler.de/photovoltaik-oder-windkraft/
[48] Alycia Gordan, 'Step by step guide on how to set up solar power at home', EcoIdeaz. Accessed: Jan. 24, 2024. [Online]. Available: https://www.ecoideaz.com/expert-corner/step-by-step-guide-on-how-to-set-up-solar-power-at-home
[49] 'What Is A Solar Farm? Costs, Land Needs & More'. Accessed: May 22, 2024. [Online]. Available: https://www.solarreviews.com/blog/what-is-a-solar-farm-do-i-need-one
[50] R. Cathcart, 'Solar Farms: Everything You Need To Know', Solar Fast. Accessed: May 27, 2024. [Online]. Available: https://solarfast.co.uk/blog/solar-farms/
[51] 'Explaining Battery Storage for Solar Panels', Eco Quote Today. Accessed: May 22, 2024. [Online]. Available: https://ecoquotetoday.co.uk/solar-panels/battery-storage-for-solar-panels
[52] 'What are Technology Readiness Levels (TRL)?' Accessed: May 27, 2024. [Online]. Available: https://www.twi-global.com/technical-knowledge/faqs/technology-readiness-levels.aspx

[53] R. M. Darling, ‘Techno-economic analyses of several redox flow batteries using levelized cost of energy storage’, *Current Opinion in Chemical Engineering*, vol. 37, p. 100855, Sep. 2022, doi: 10.1016/j.coche.2022.100855.
[54] ‘Organic SolidFlow Battery Technology | CMBlu Energy AG’. Accessed: May 22, 2024. [Online]. Available: https://www.cmblu.com/en/technology/
[55] AdminCometPublishing, ‘Kemiwatt’s Aqueous Organic RedOx Flow Battery (AORFB)’, Hybris. Accessed: May 22, 2024. [Online]. Available: https://hybris-project.eu/kemiwatts-aqueous-organic-redox-flow-battery-aorfb/
[56] ‘Discover Our History - KEMIWATT | Your Energy Bank’, Kemiwatt. Accessed: May 22, 2024. [Online]. Available: https://kemiwatt.com/history/

# 13. Appendix A – CV data

This is the first appendix, including all the CV data curves from all seven phoenicin batches.

## 13.1. 1st own produced phoenicin

The first batch was run using previous experiments applied potential window of -1.6 to 0.6.

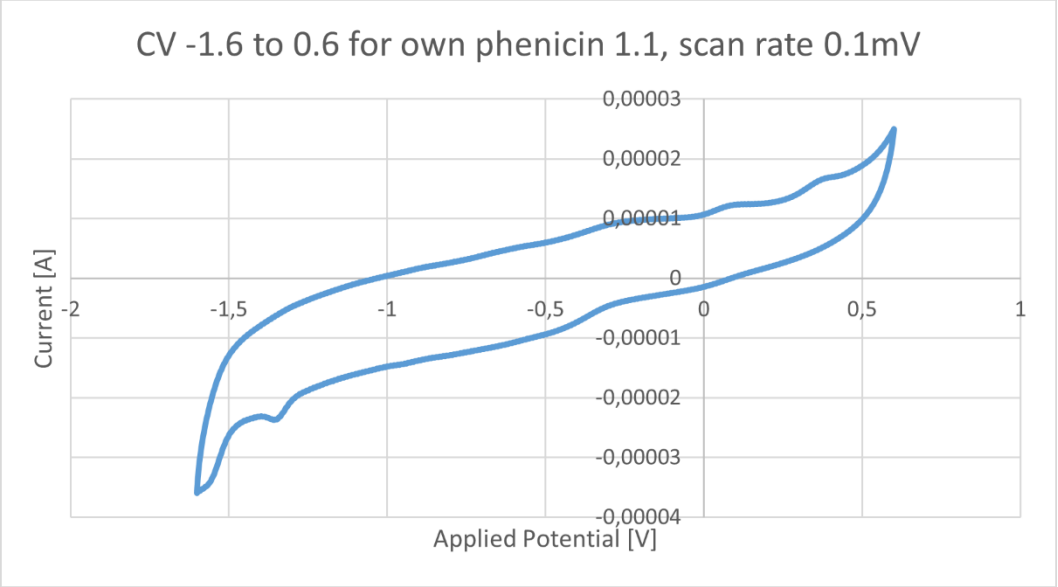


*Figure 13.1: CV curve for batch 1 first tube*

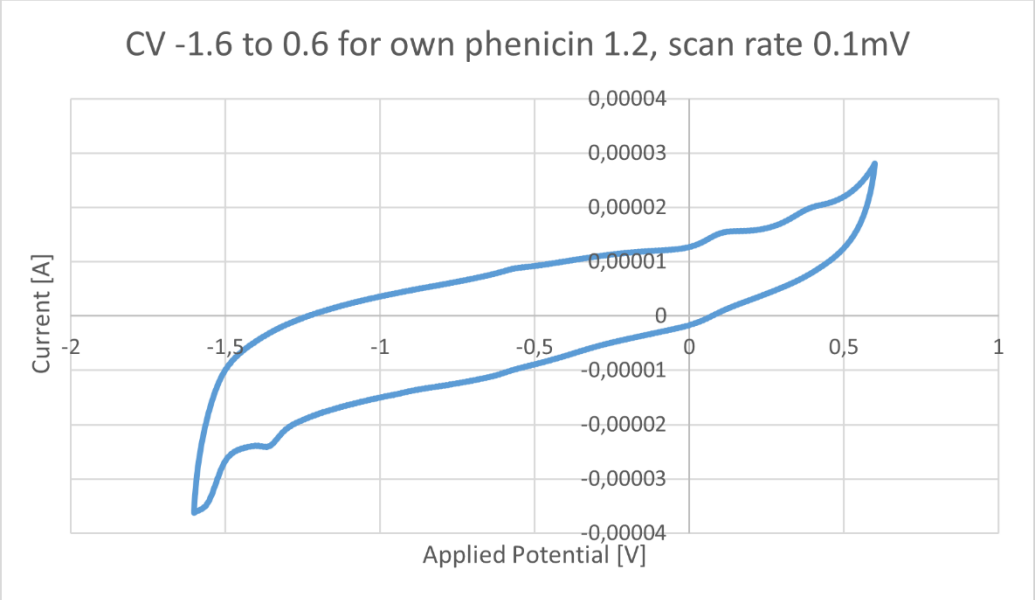


*Figure 13.2: CV curve for batch 1 second tube*

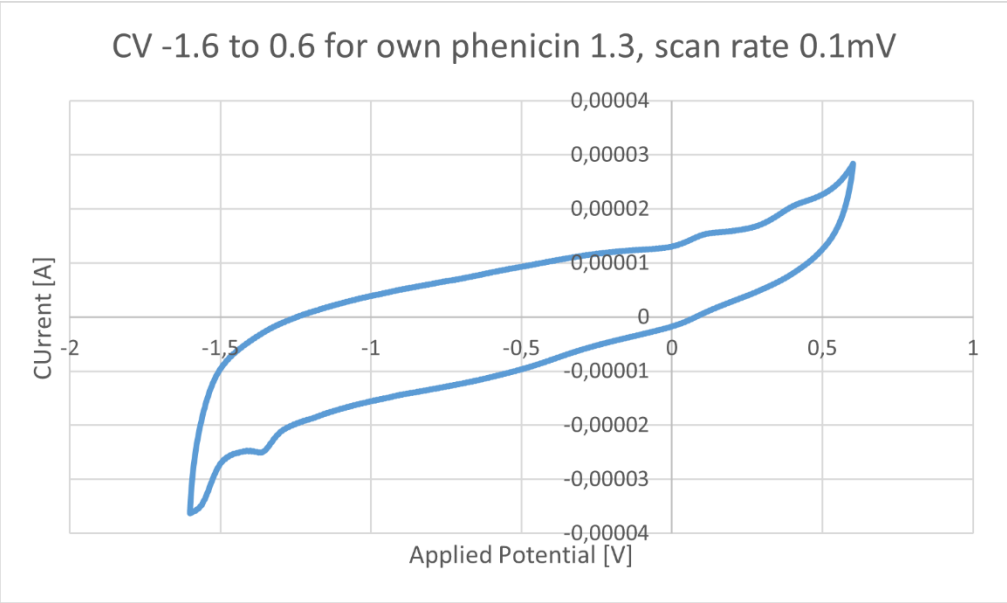


*Figure 13.3: CV curve for batch 1 third tube*

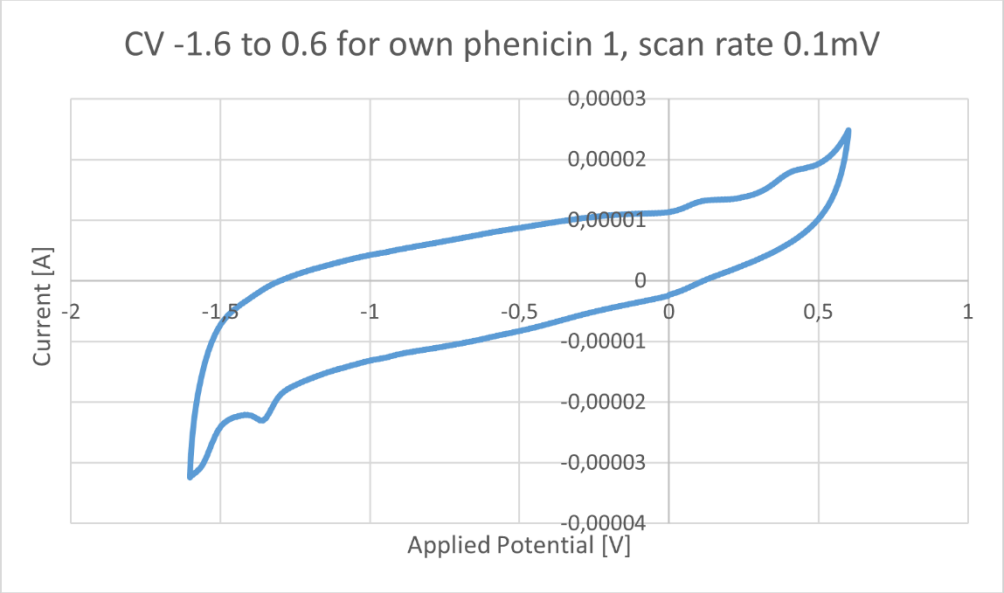


*Figure 13.4: CV curve for batch 1 all tubes together*

## 13.2. 2nd own produced phoenicin

From the 2nd batch, the potential window was shortened from -1.6 to -1.3 and from 0.6 to 0.4 to see the peak more distinct, which can be seen when comparing Figure 13.6 to Figure 13.7, where the first one had the window -1.6 to 0.6 and the second -1.3 to 0.4.

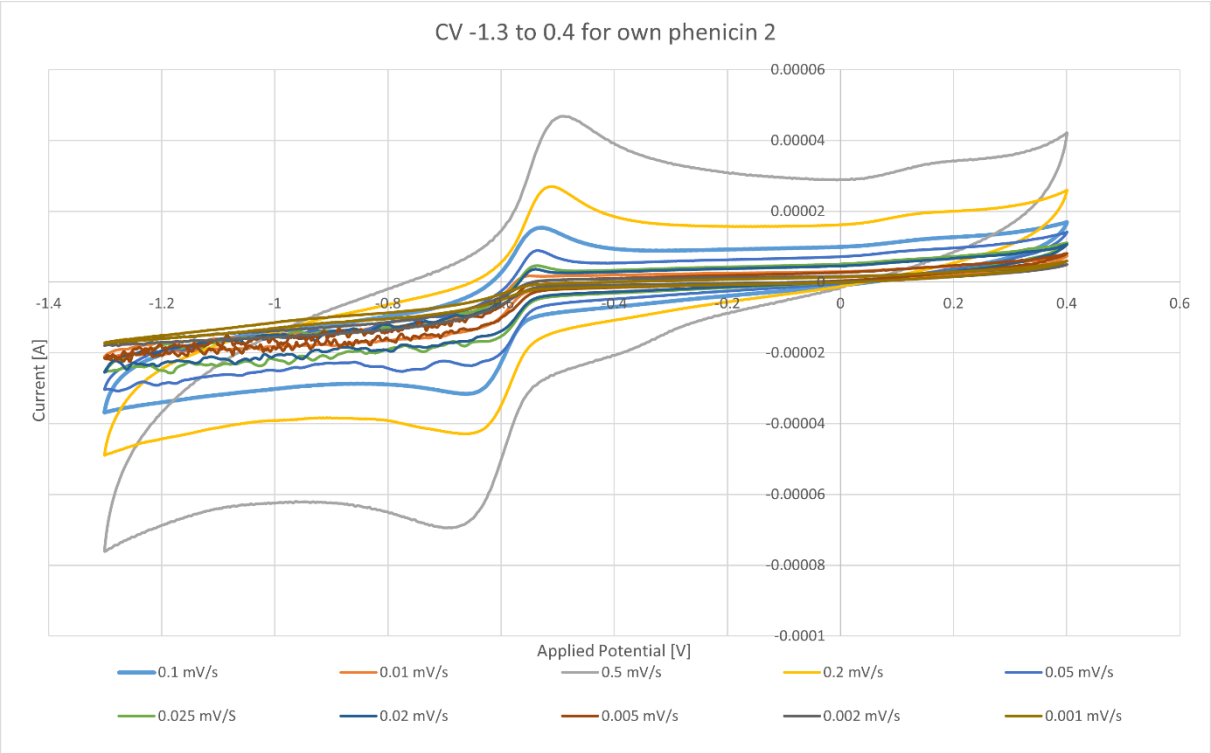


*Figure 13.5: CV curves for batch 2 with all 10 scan rates with the potential window of -1.3 to 0.4*

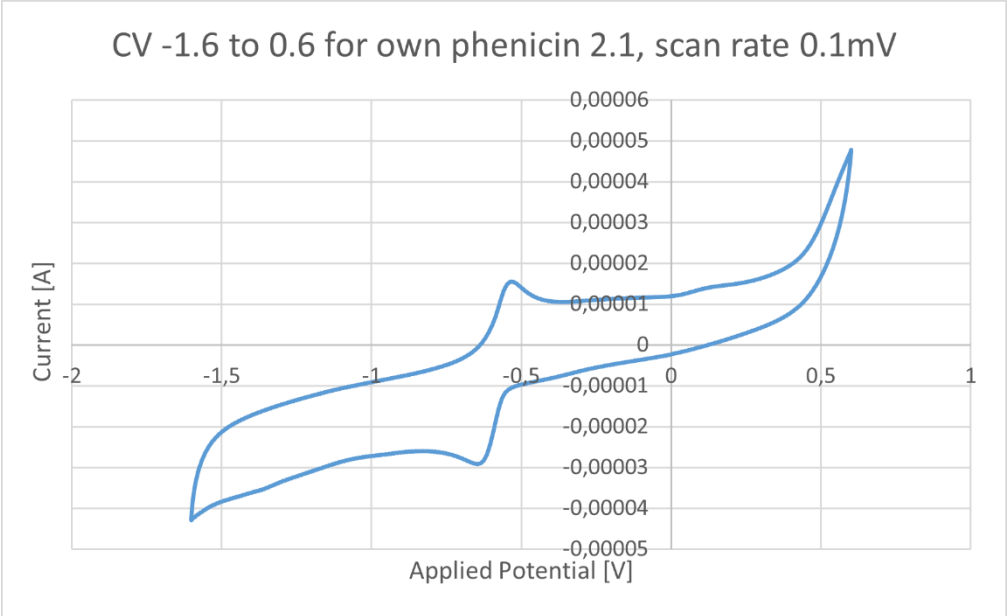


*Figure 13.6: CV curve for batch 2 first tube with the potential window of -1.6 to 0.6*

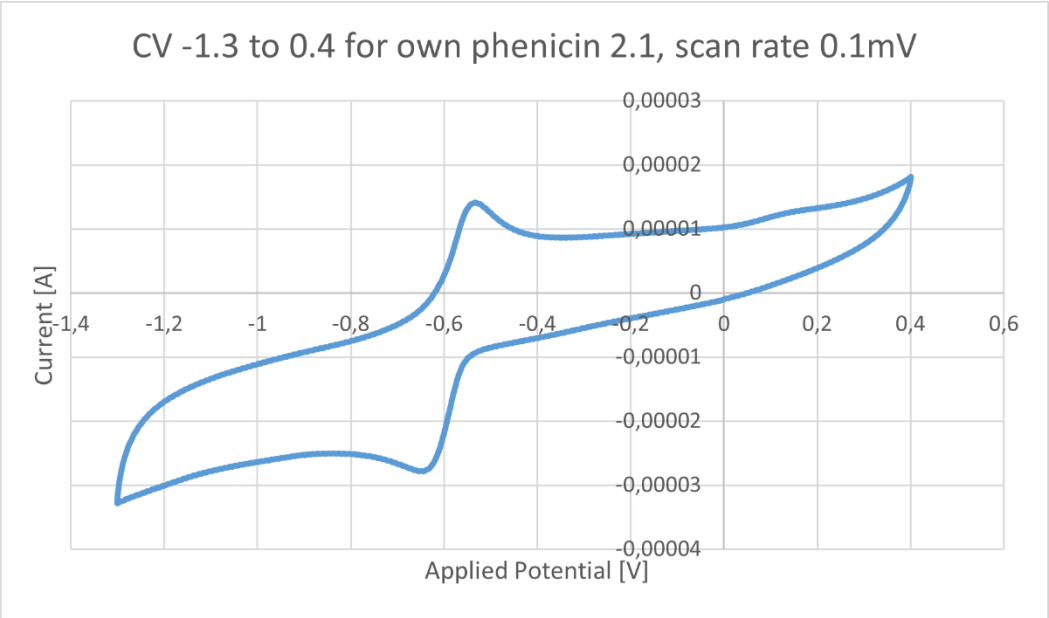


*Figure 13.7: CV curve for batch 2 first tube with the potential window of -1.3 to 0.4*

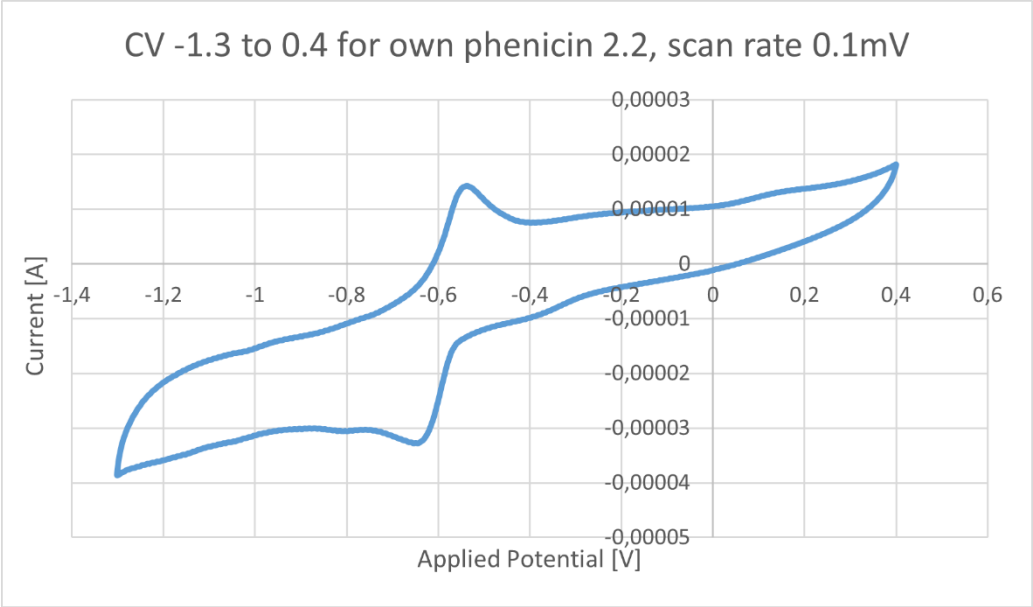


*Figure 13.8: CV curve for batch 2 second tube*

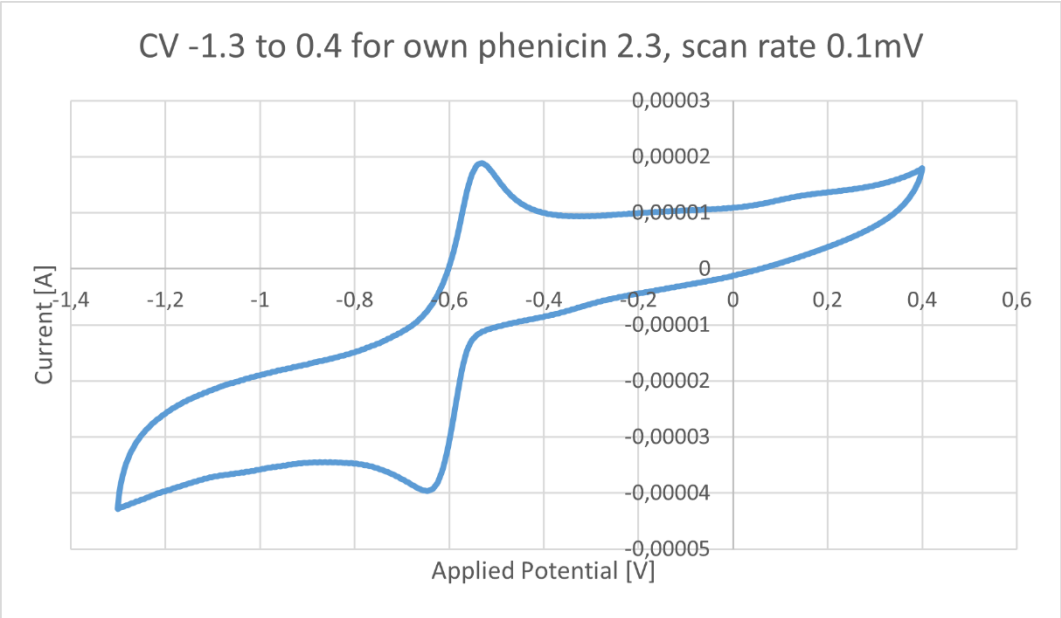


*Figure 13.9: CV curve for batch 2 third tube*

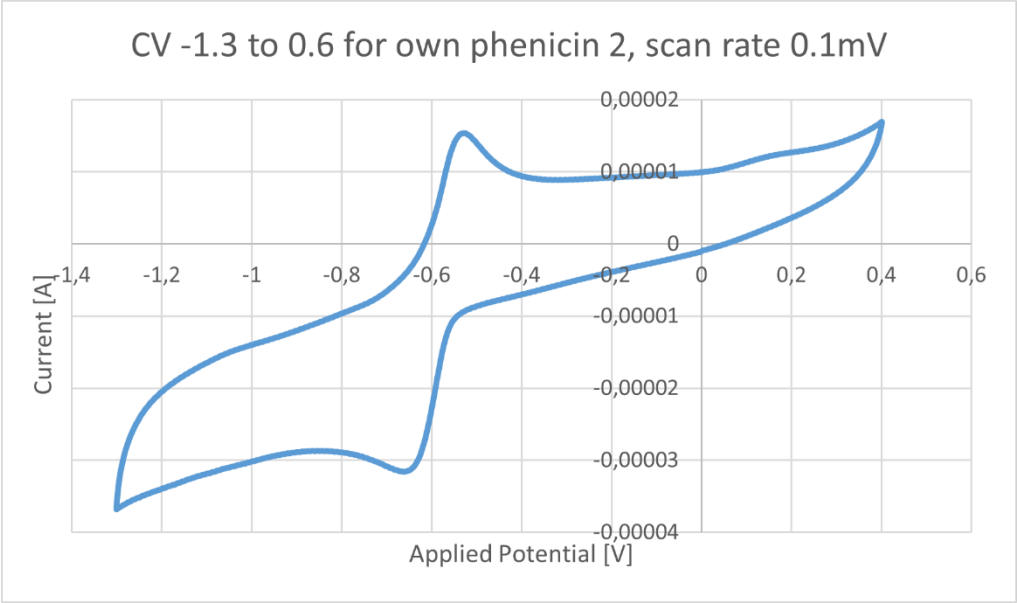


*Figure 13.10: CV curve for batch 2 all tubes together*

## 13.3. 3rd own-produced phoenicin

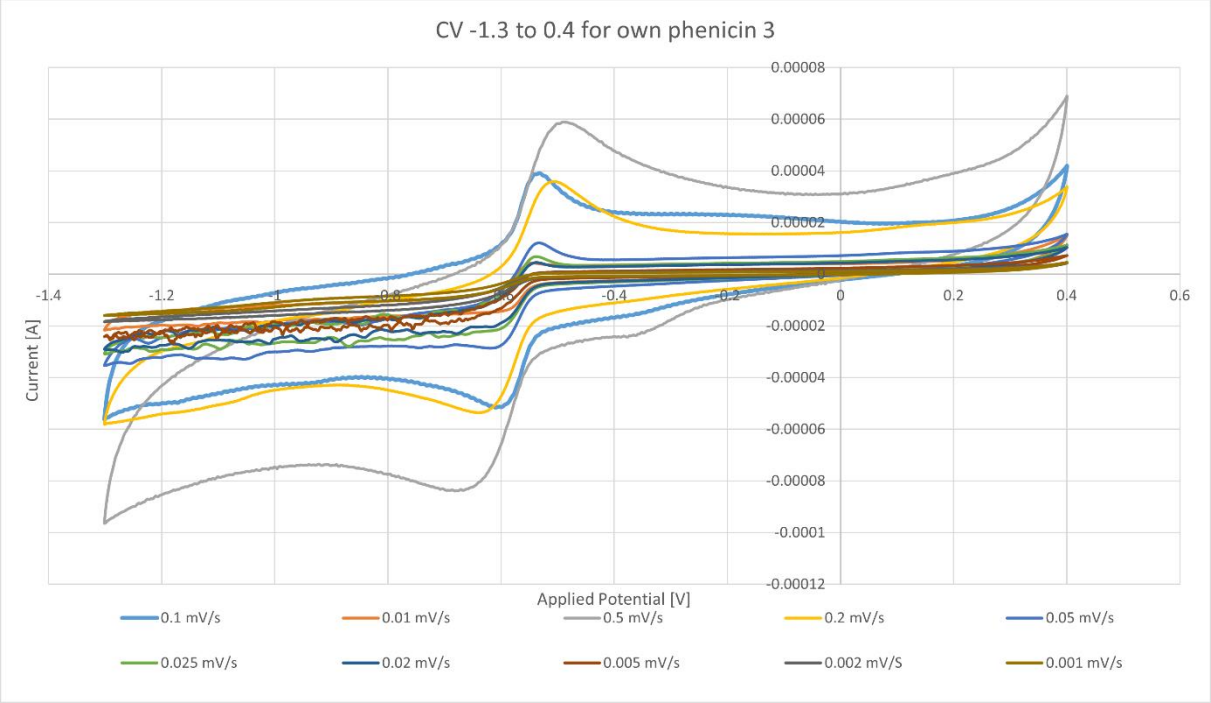


*Figure 13.11: CV curves for batch 3 with all 10 scan rates with the potential window of -1.3 to 0.4*

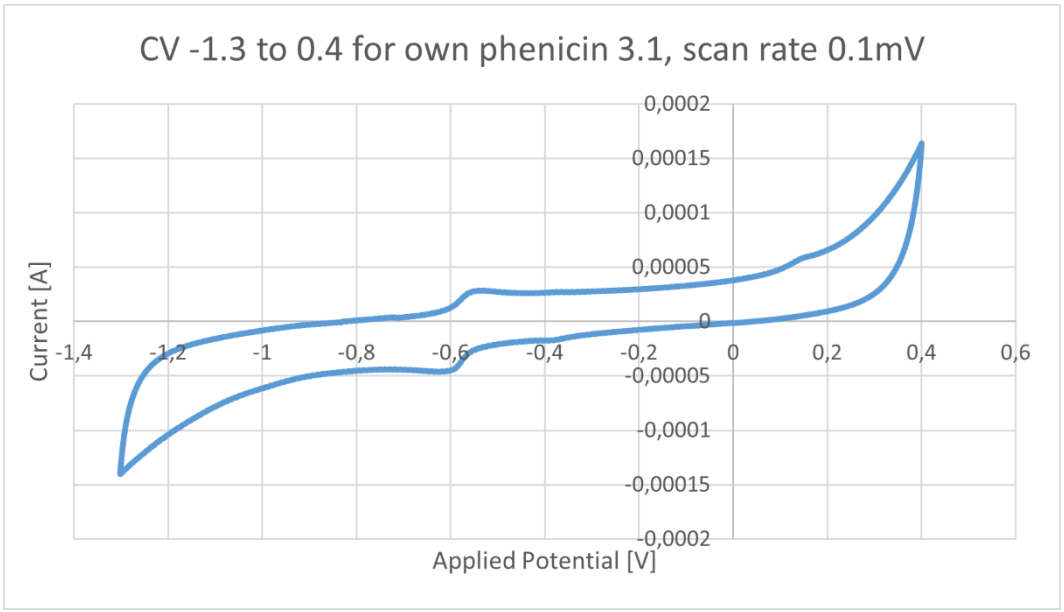


*Figure 13.12: CV curve for batch 3 first tube*

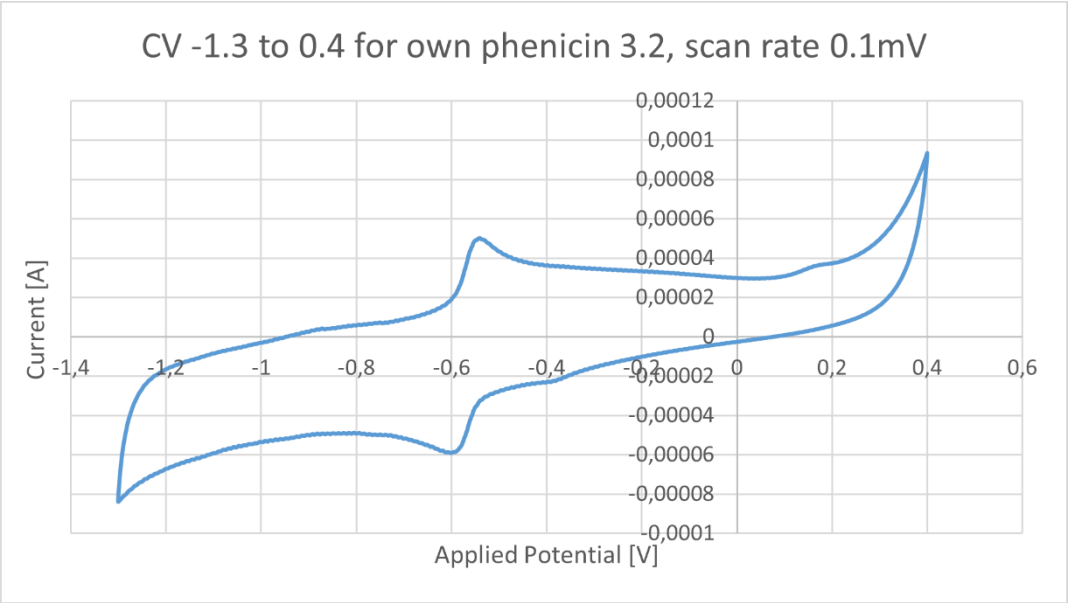


*Figure 13.13: CV curve for batch 3 second tube*

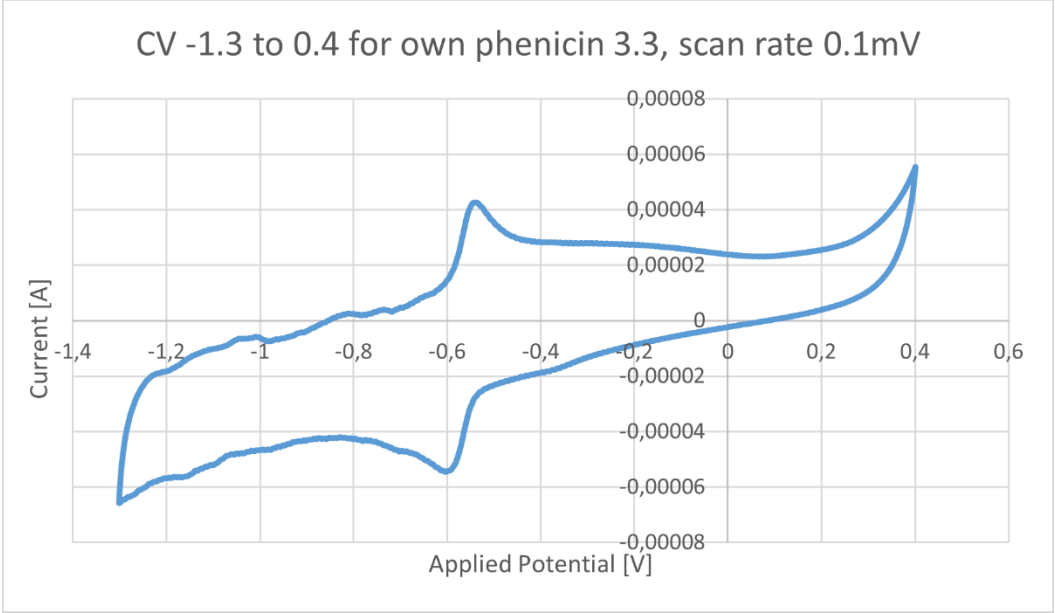


*Figure 13.14: CV curve for batch 3 third tube*

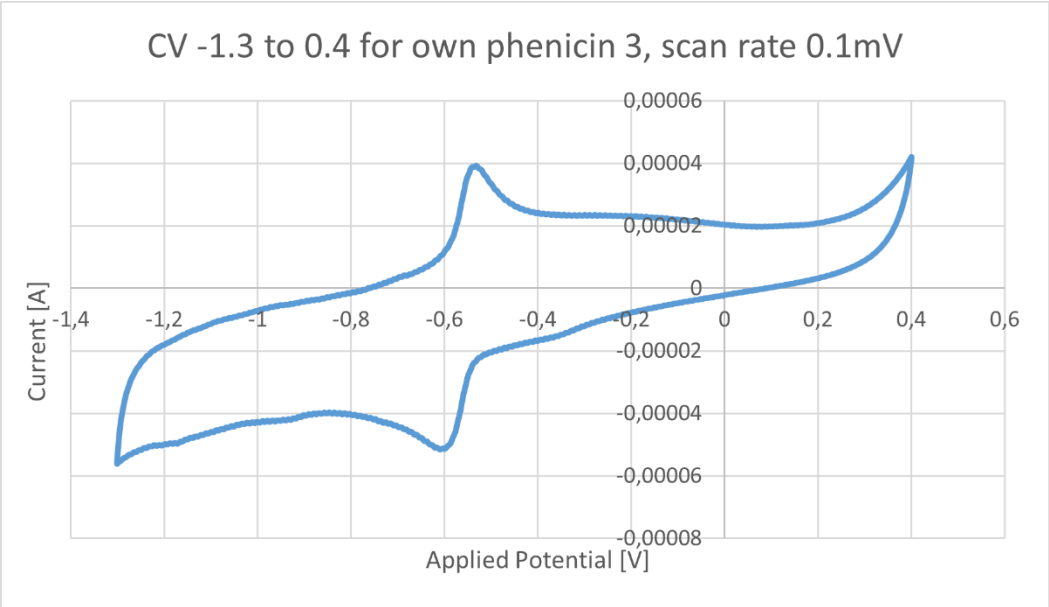


*Figure 13.15: CV curve for batch 3 all tubes together*

## 13.4. 4th own-produced phoenicin

In the third tube, this batch had some indication of possible further reduction peaks after the first initial prominent peak.

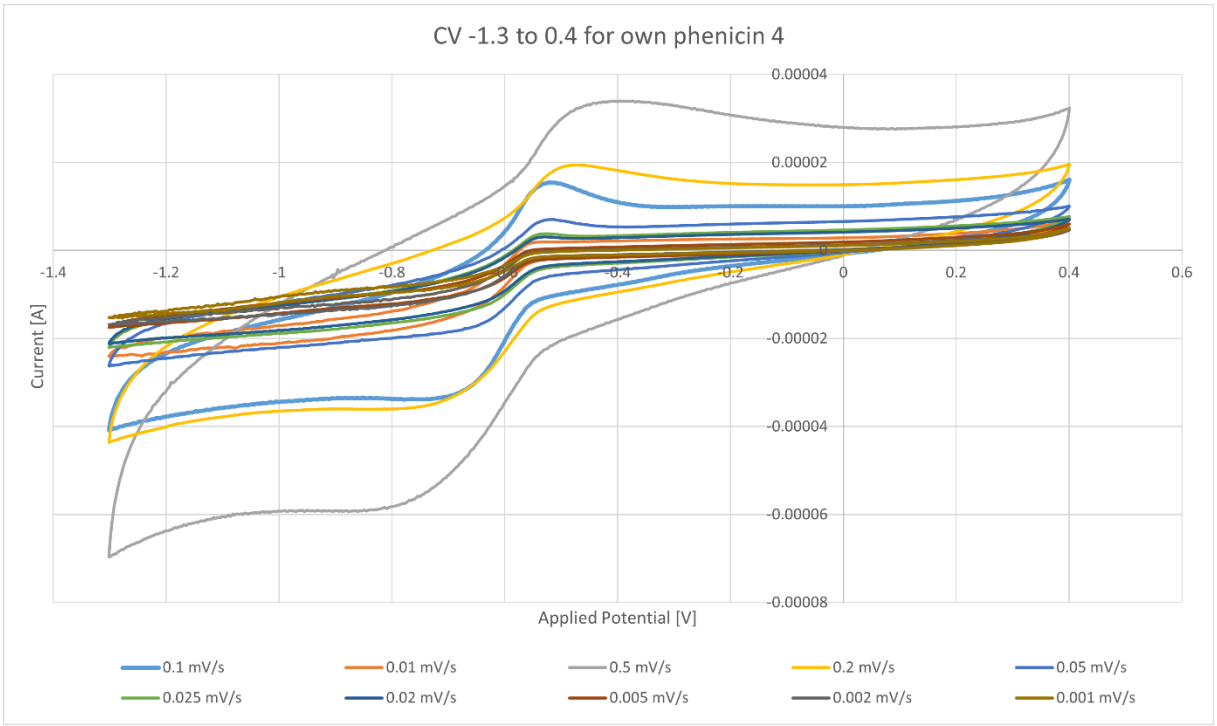


*Figure 13.16: CV curve for batch 4 with all 10 scan rates with the potential window of -1.3 to 0.4*

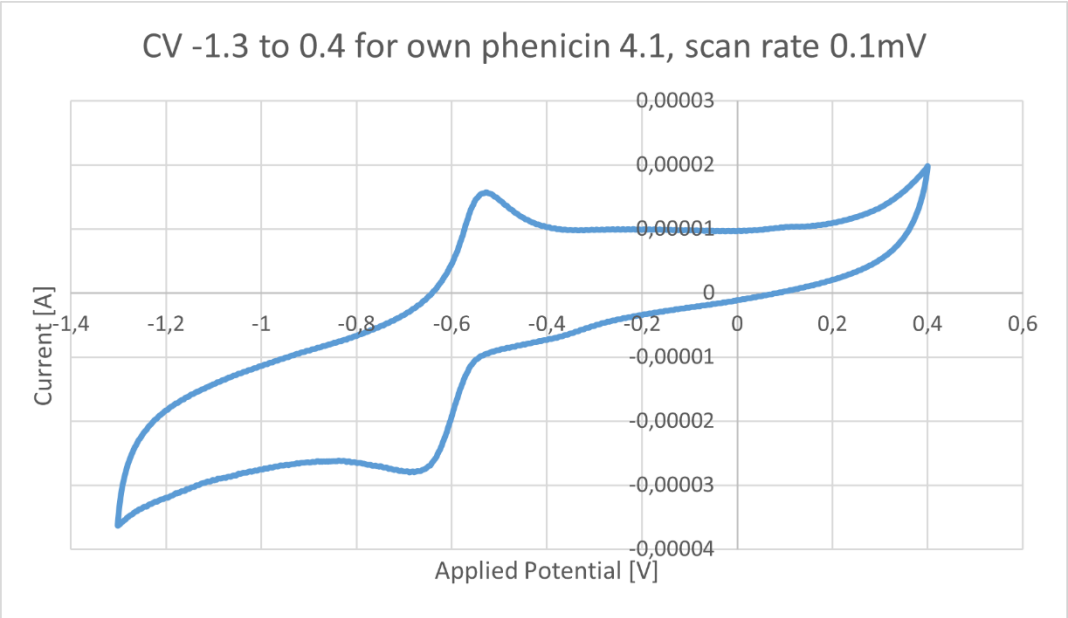


*Figure 13.17: CV curve for batch 4 first tube*

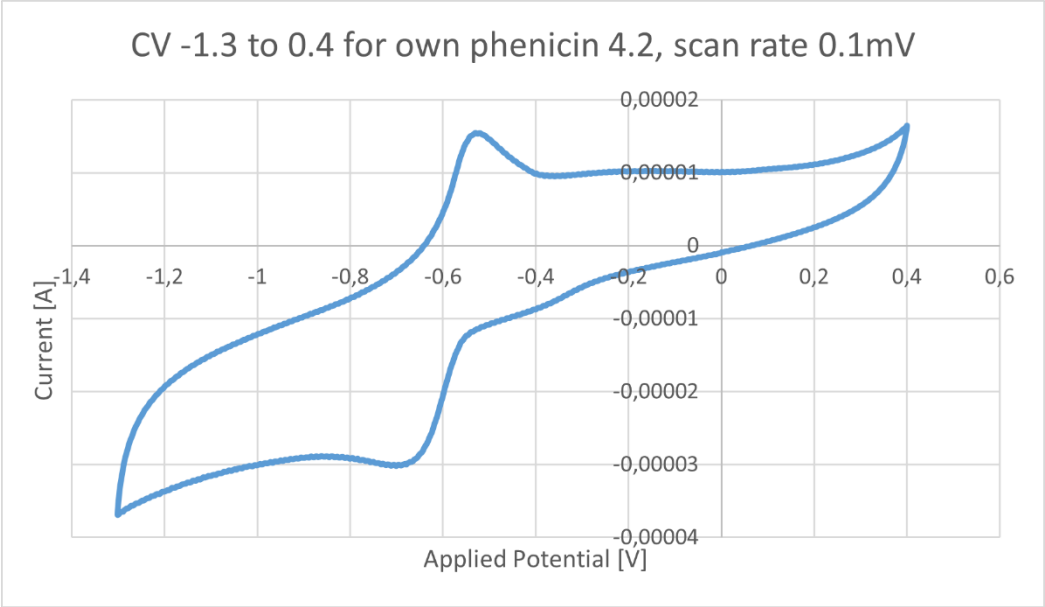


*Figure 13.18: CV curve for batch 4 second tube*

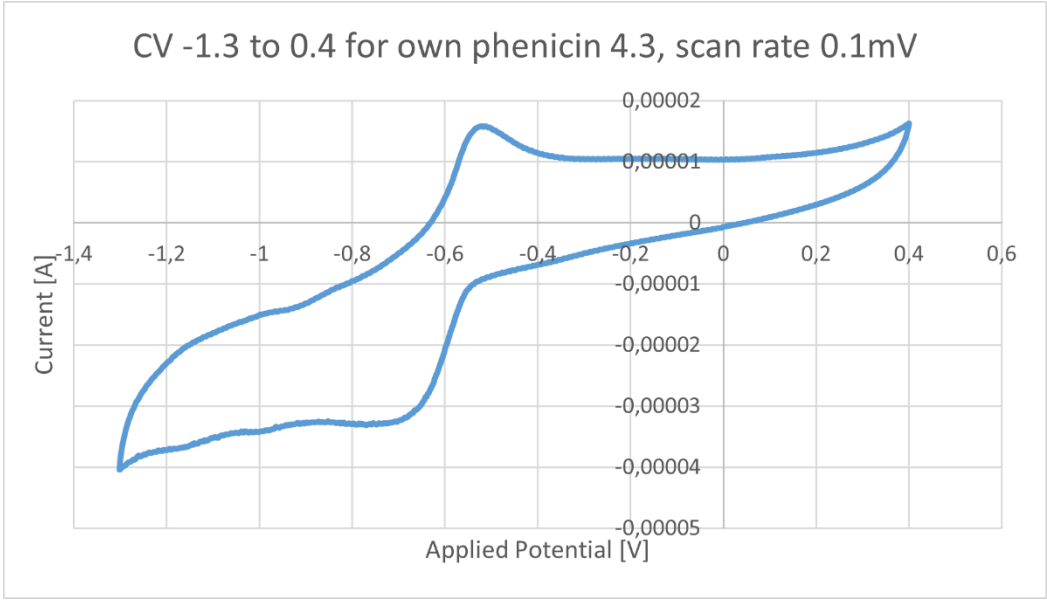


*Figure 13.19: CV curve for batch 4 third tube*

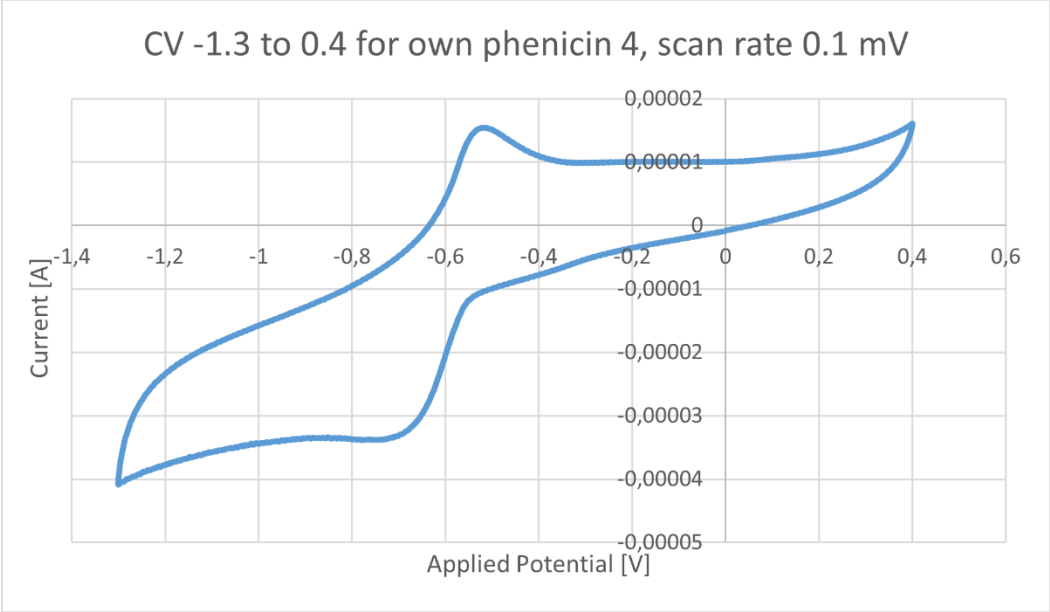


*Figure 13.20: CV curve for batch 4 all tubes together*

## 13.5. 5th own-produced phoenicin

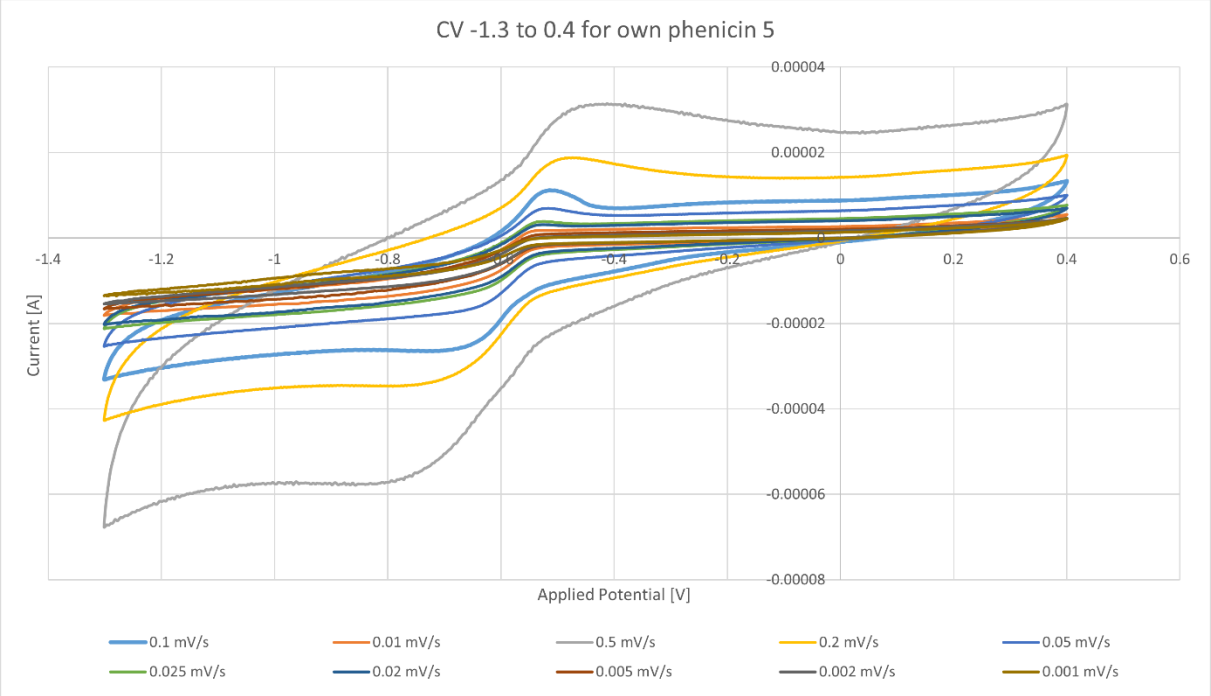


*Figure 13.21: CV curves for batch 5 with all 10 scan rates with the potential window of -1.3 to 0.4*

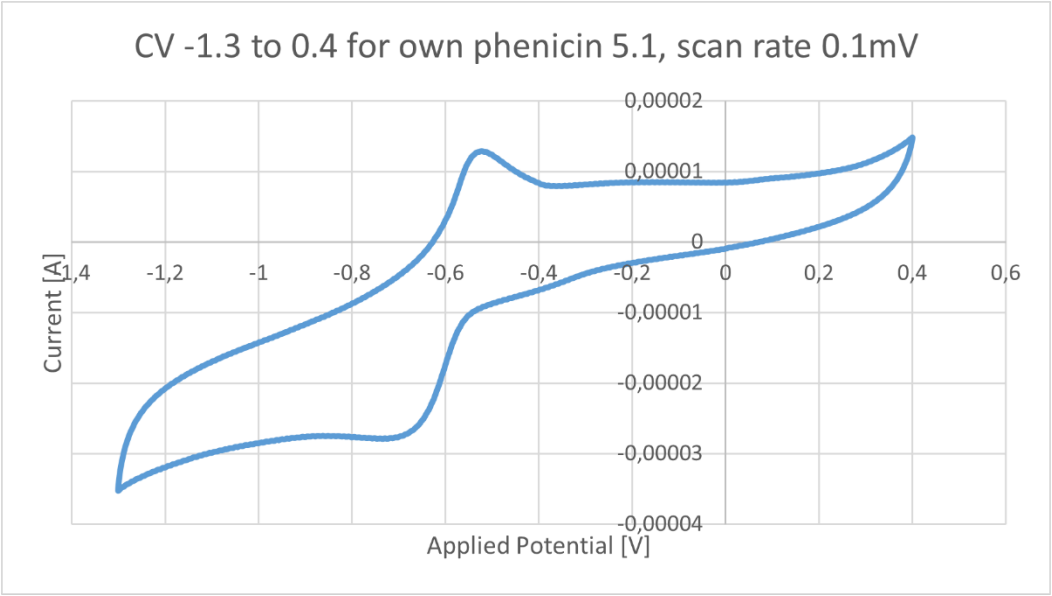


*Figure 13.22: CV curve for batch 5 first tube*

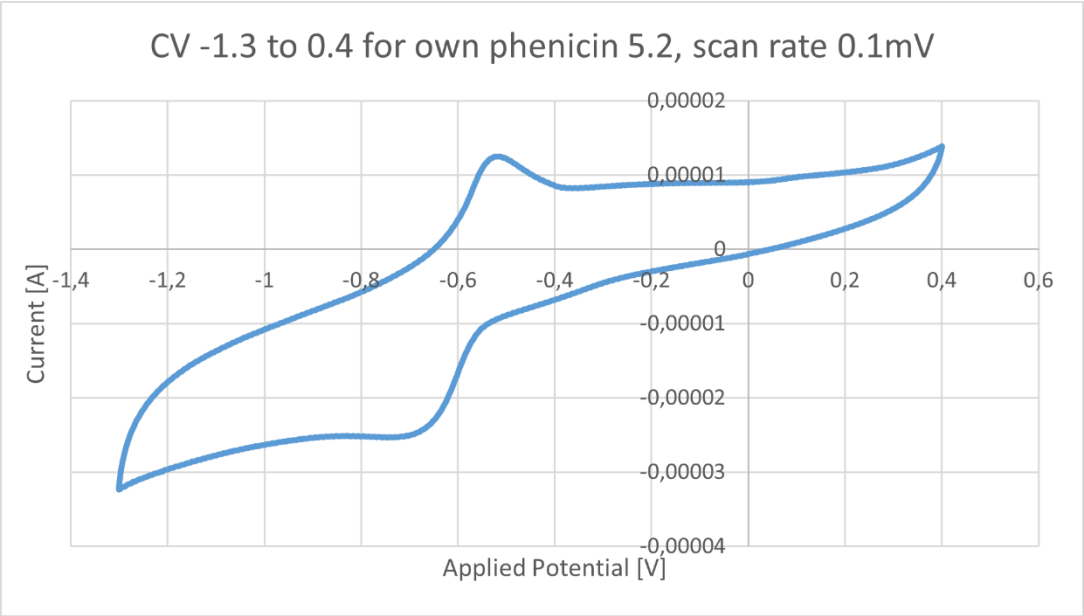


*Figure 13.23: CV curve for batch 5 second tube*

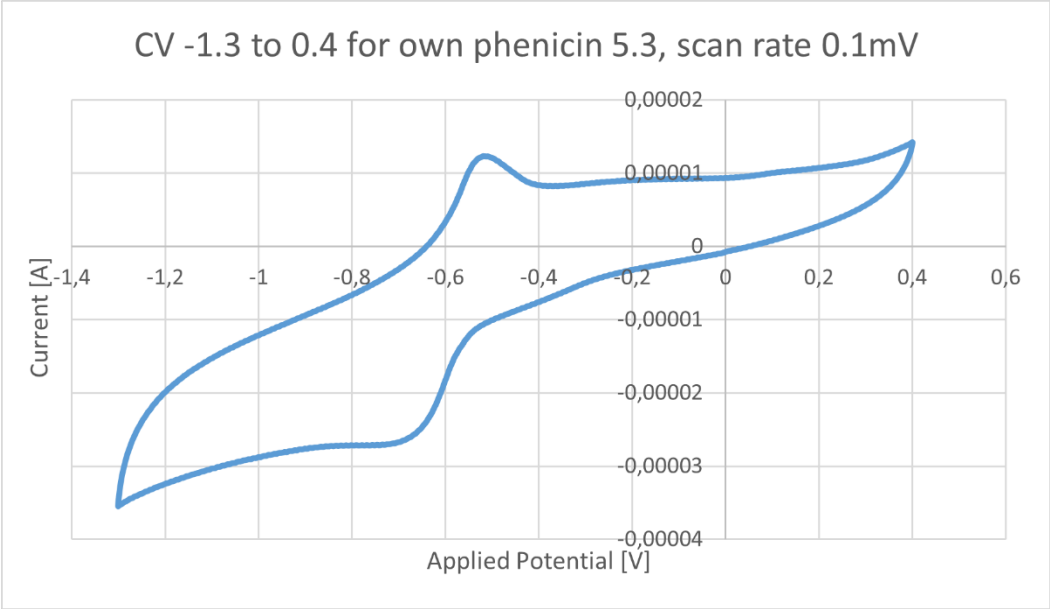


*Figure 13.24: CV curve for batch 5 third tube*

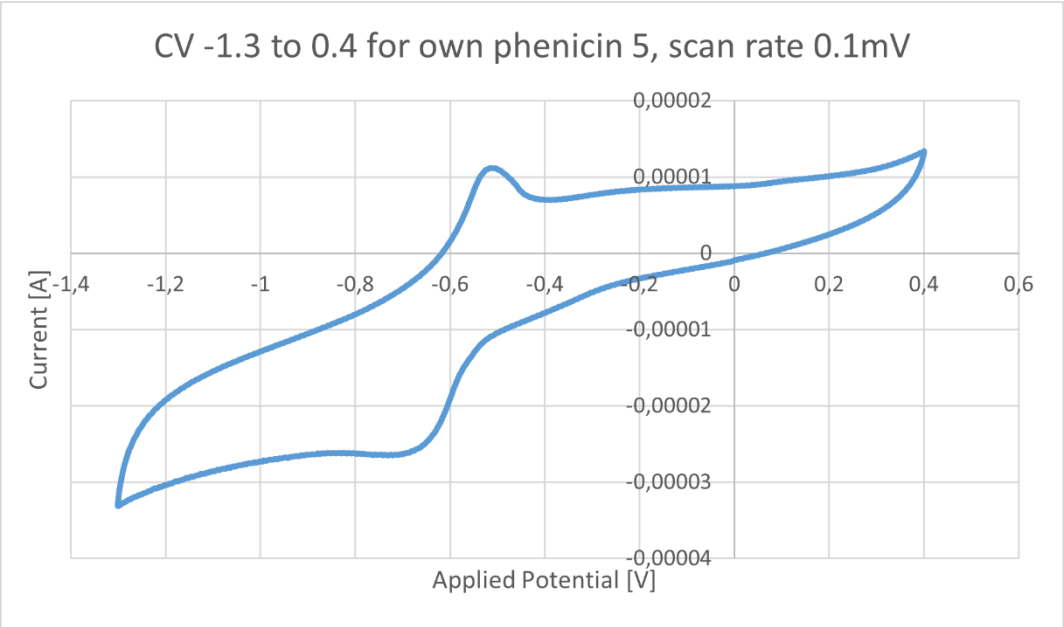


*Figure 13.25: CV curve batch 5 all tubes together*

## 13.6. 6th own-produced phoenicin

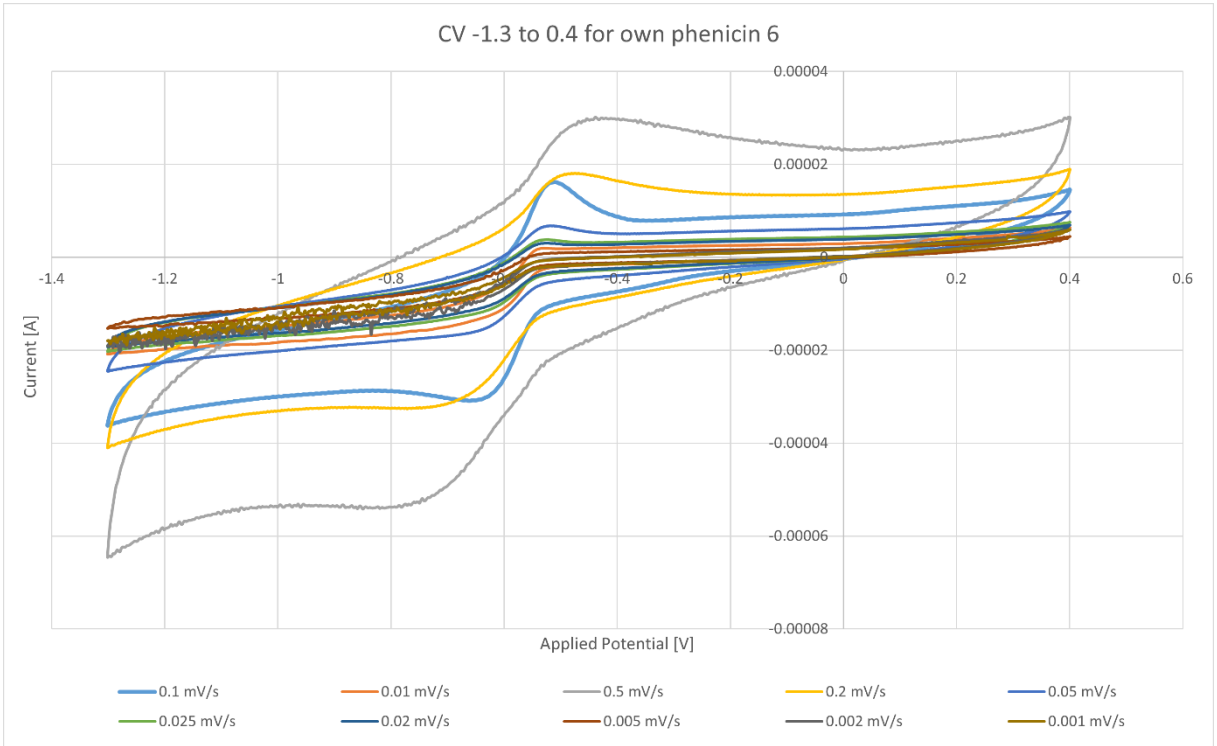


*Figure 13.26: CV curve for batch 6 with all 10 scan rates with the potential window of -1.3 to 0.4*

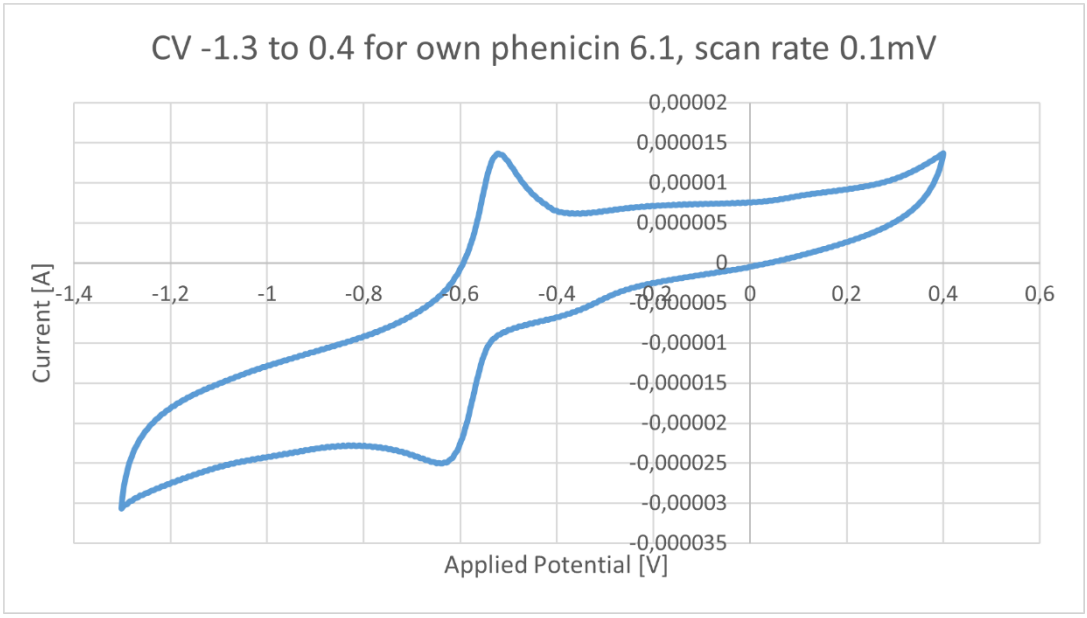


*Figure 13.27. CV curve for batch 6 first tube*

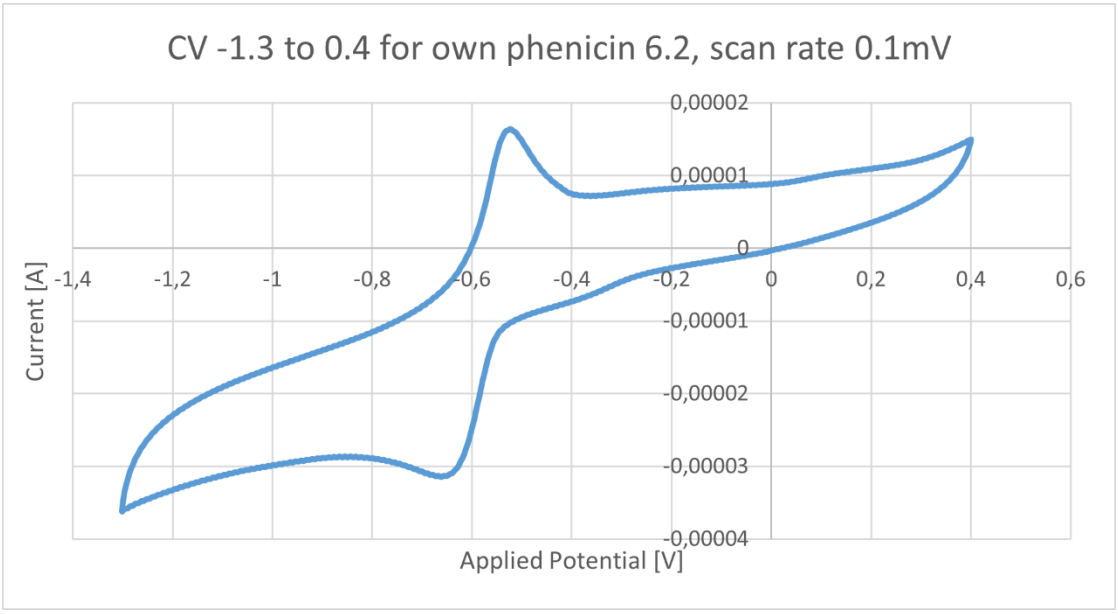


*Figure 13.28: CV curve for batch 6 second tube*

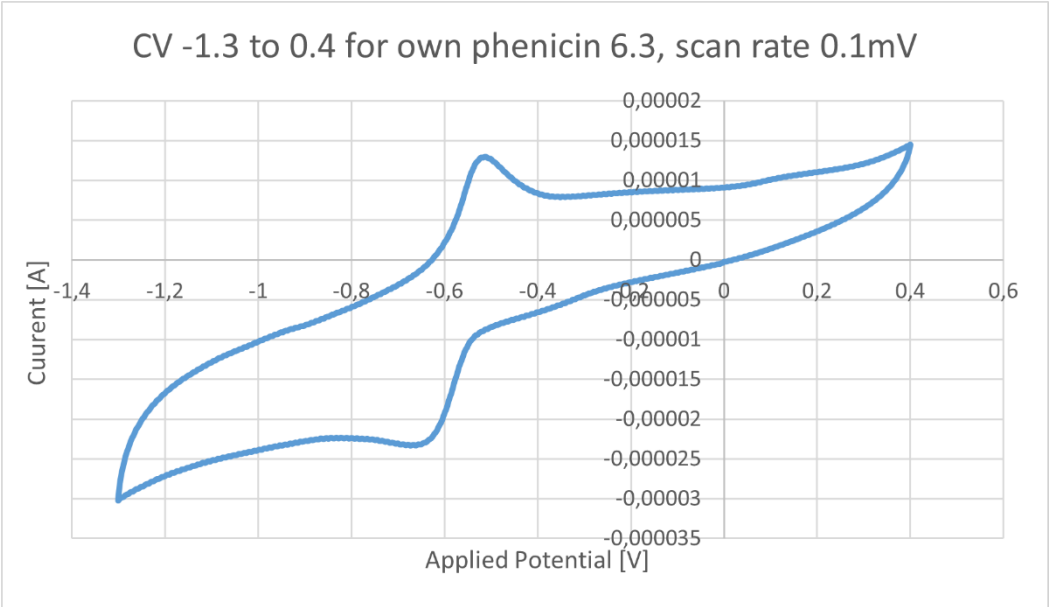


*Figure 13.29: CV curve for batch 6 third tube*

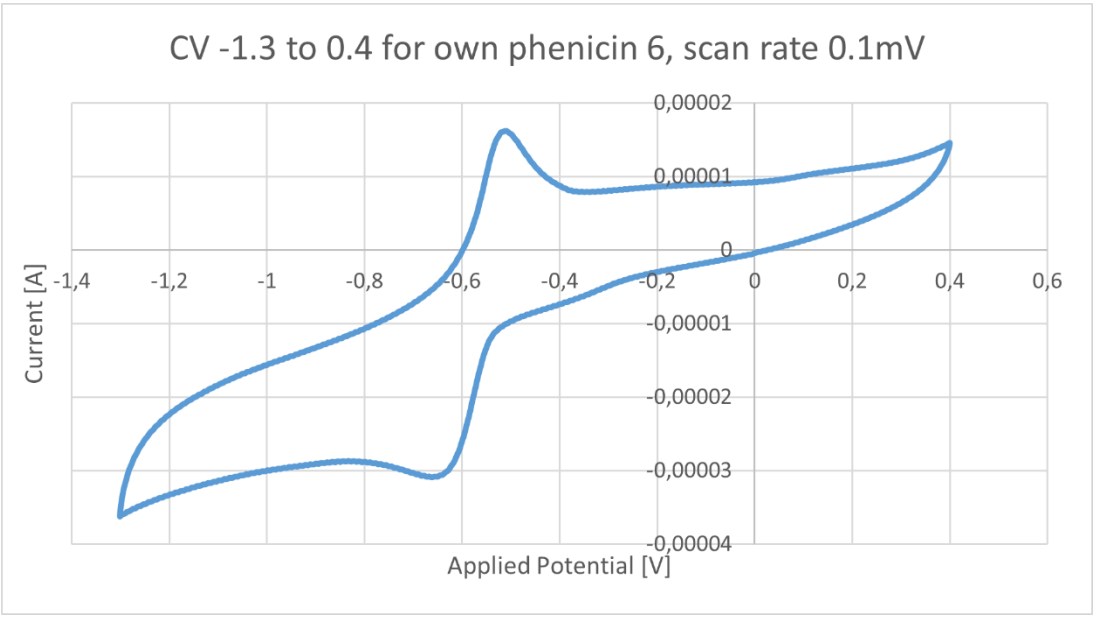


*Figure 13.30: CV curve for batch 6 all tubes together*

## 13.7. 7th own produced phoenicin

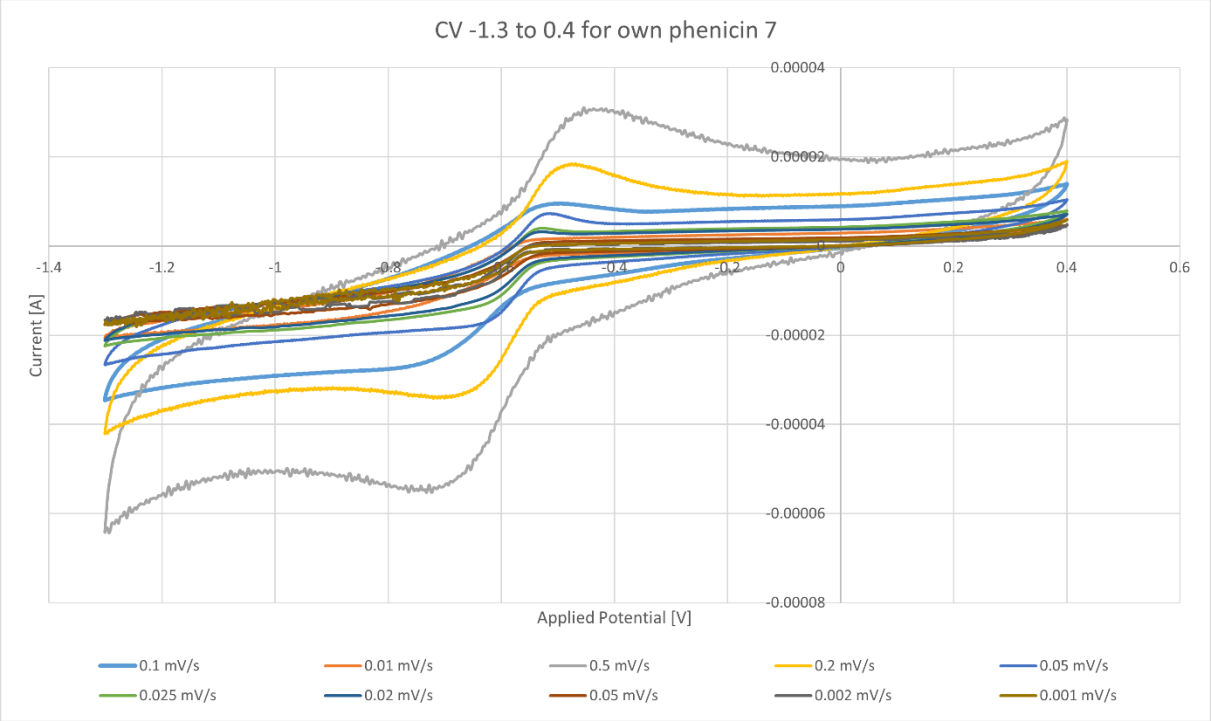


*Figure 13.31: CV curves for batch 7 with all 10 scan rates with the potential window of -1.3 to 0.4*

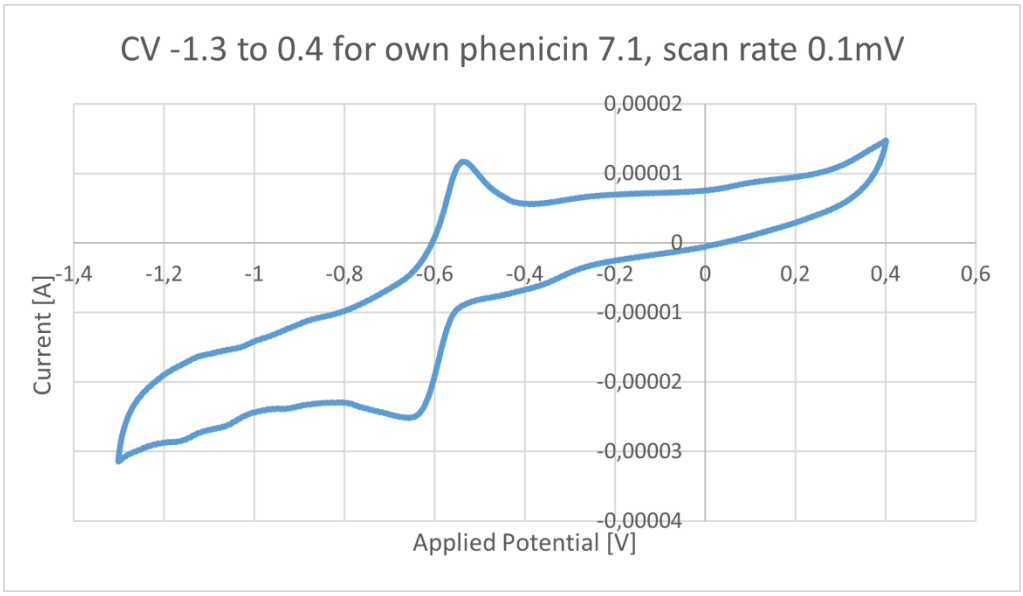


*Figure 13.32. CV curve for batch 7 first tube*

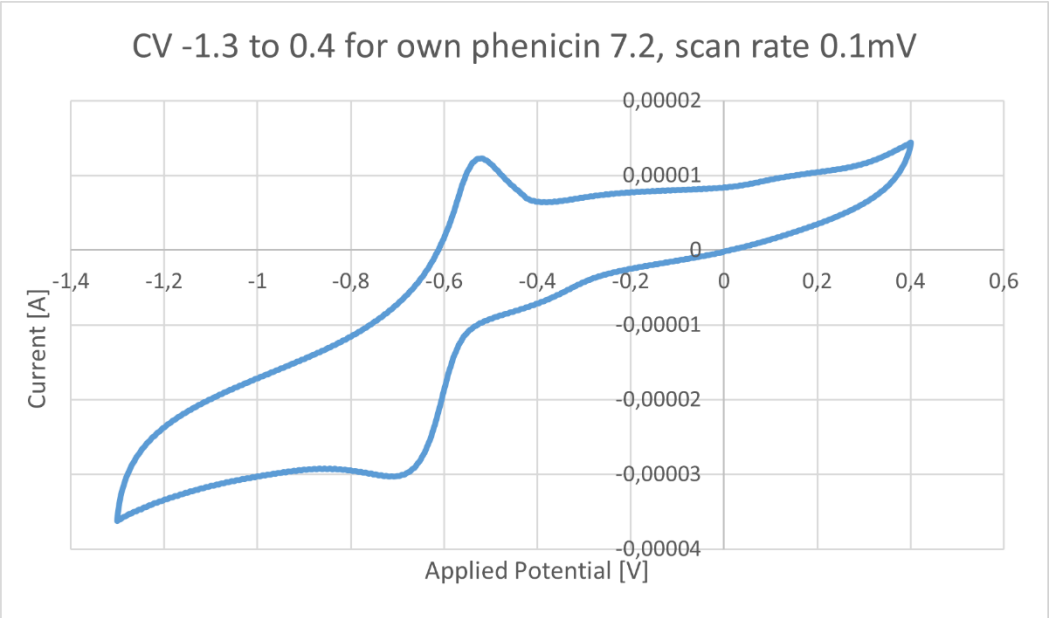


*Figure 13.33: CV curve for batch 7 second tube*

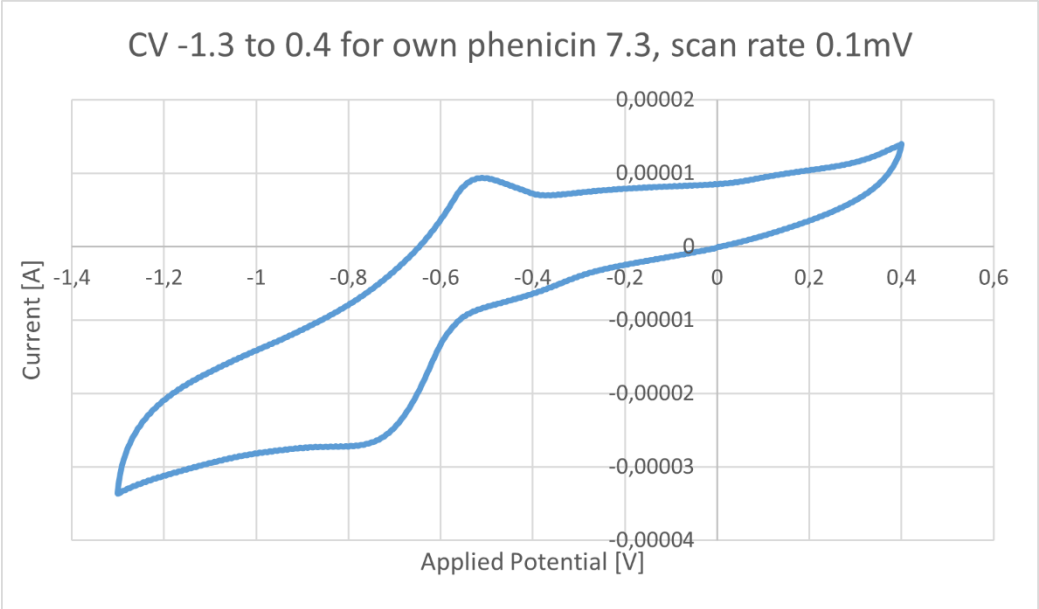


*Figure 13.34: CV curve for batch 7 third tube*

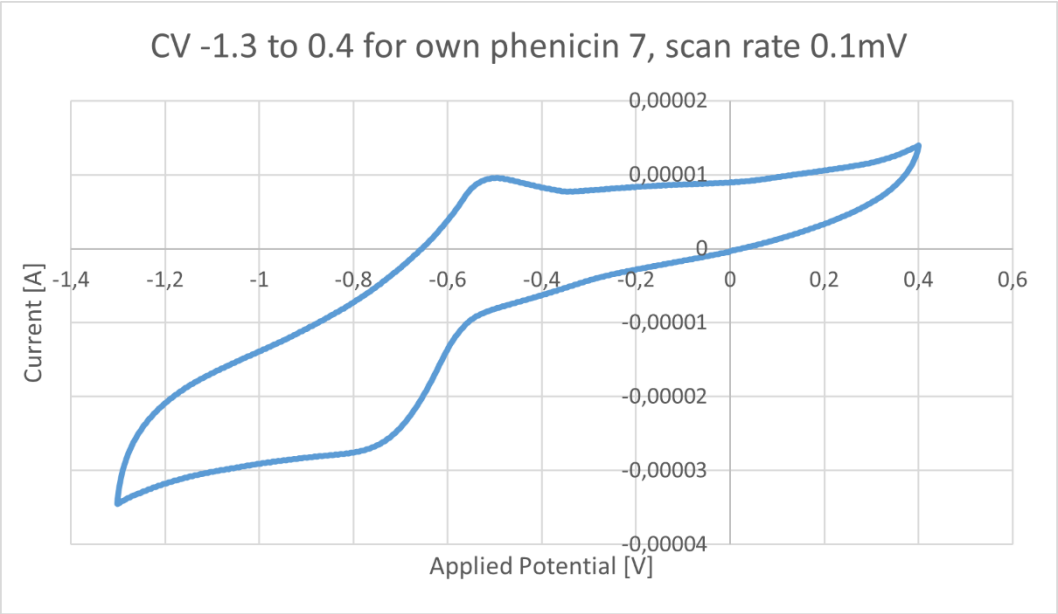


*Figure 13.35: CV curve for batch 7 all tubes together*

# 14. Appendix B – Battery test data for quality check batteries

This appendix shows the remaining data on all the small batteries used for the seven produced phoenicin.

## 14.1. 1st batch quality check battery

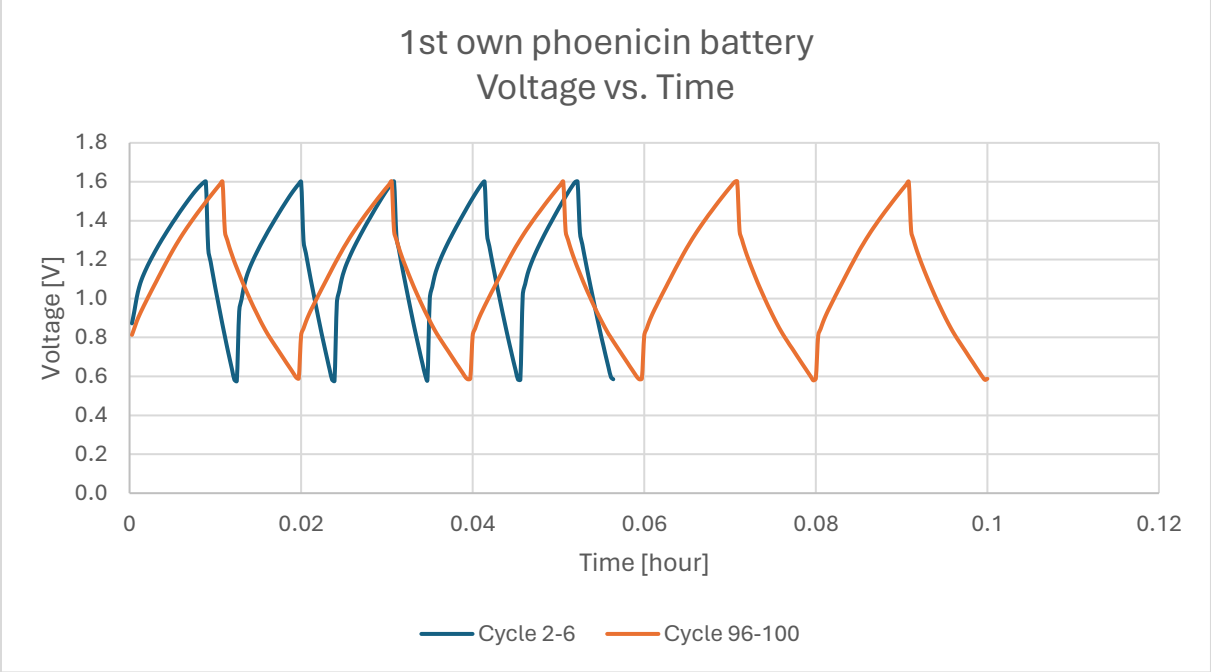


*Figure 14.1: Charge and discharge cycle rate for the 2-6 and 96-100 cycles for the battery running on the 1st own phoenicin*

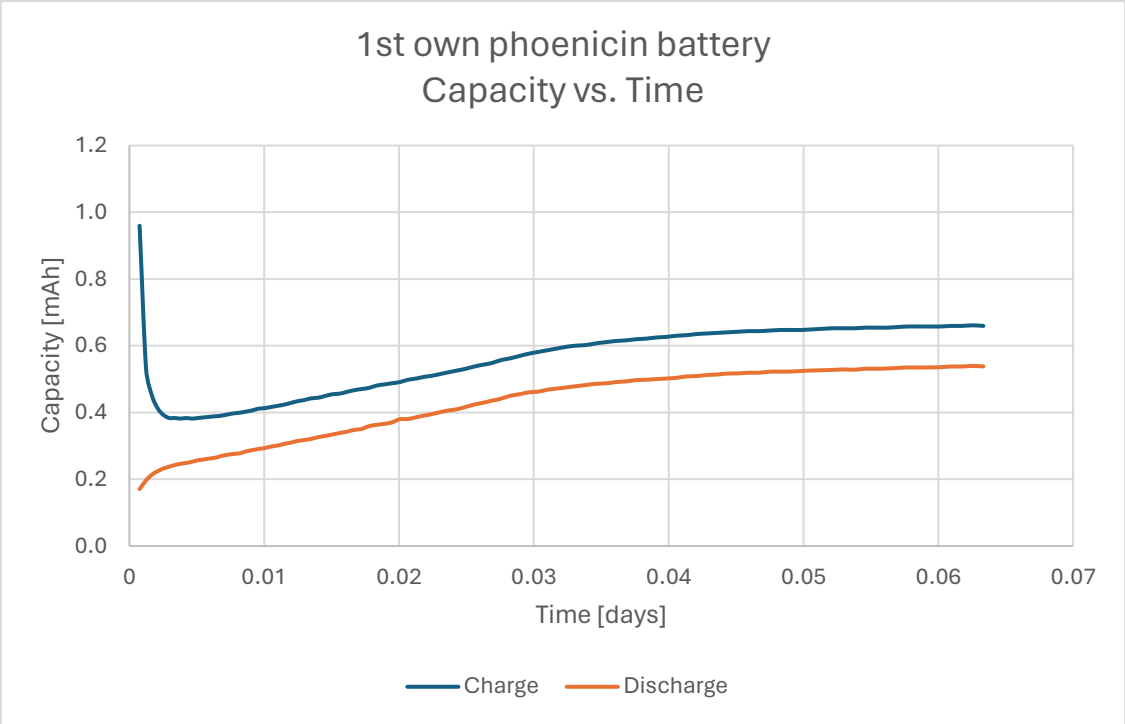


*Figure 14.2: Average capacity per cycle for the battery running on the 1st own phoenicin*

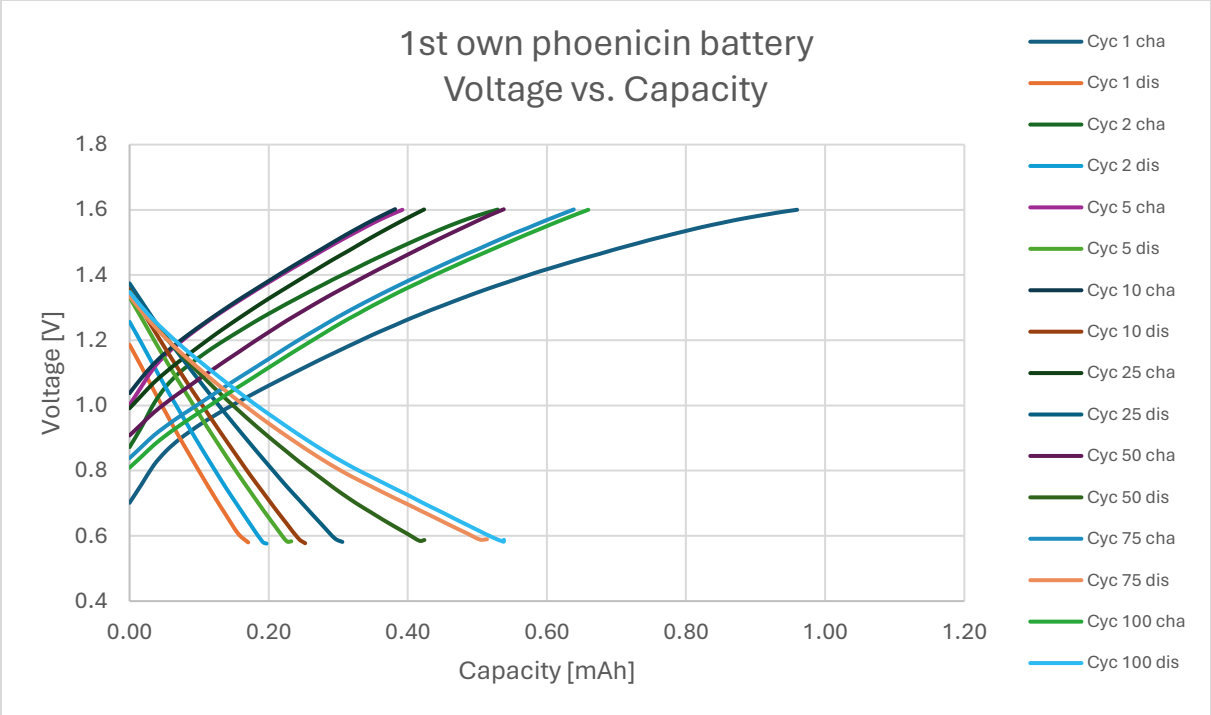


*Figure 14.3: The relation between applied voltage and capacity of the charge and discharge for different cycles for the battery running on the 1st own phoenicin*

## 14.2. 2nd batch quality check battery

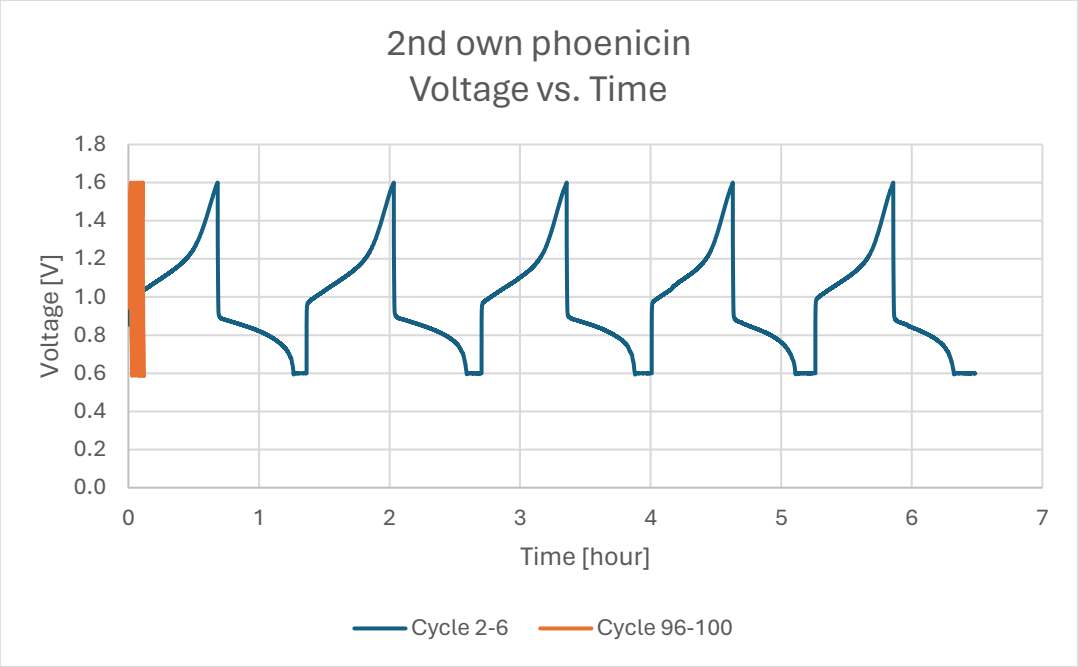


*Figure 14.4: Charge and discharge cycle rate for the 2-6 and 96-100 cycles for the battery running on the 2nd own phoenicin*

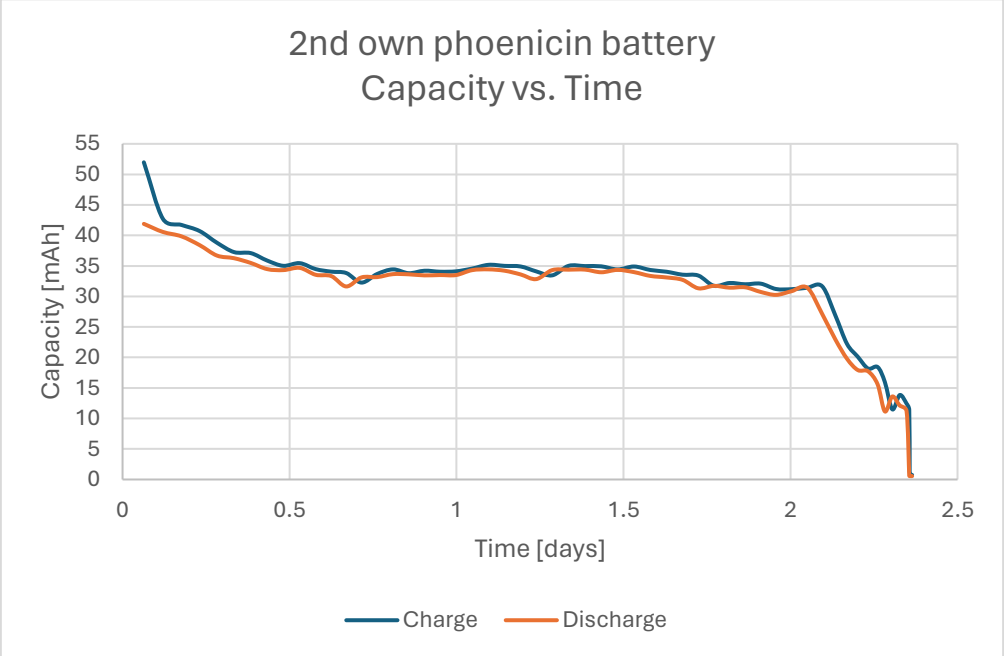


*Figure 14.5. Average capacity per cycle for the battery running on the 2nd own phoenicin*

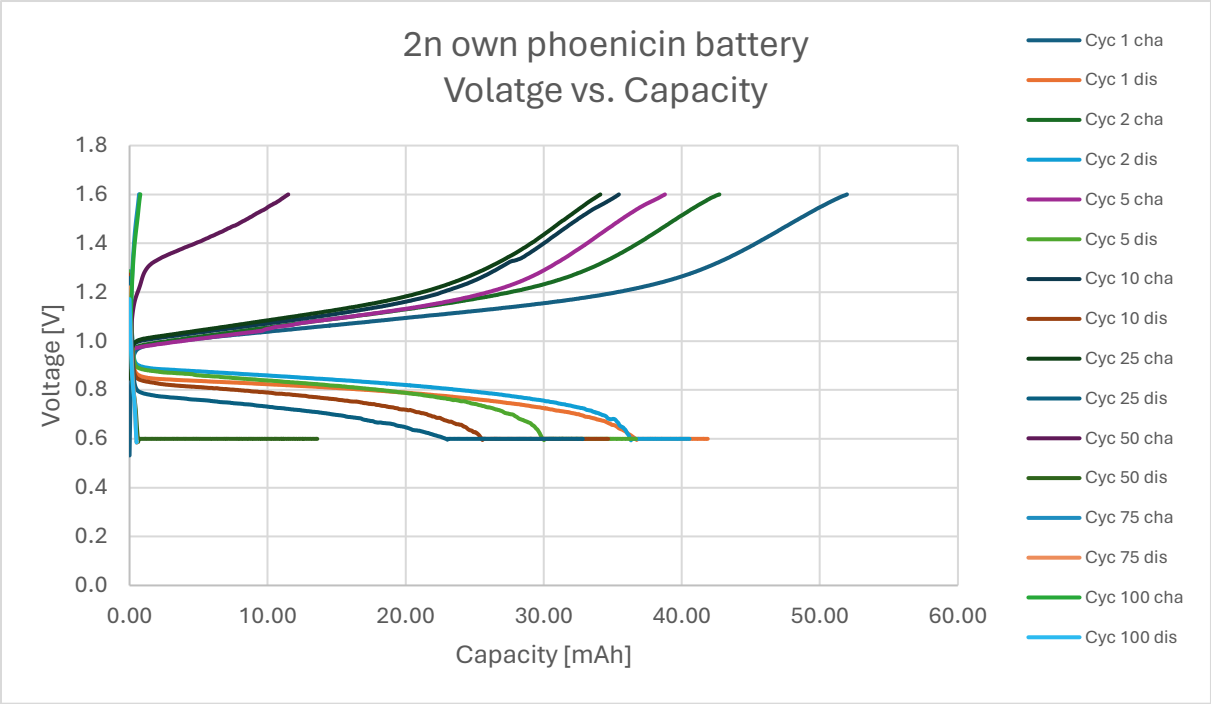


*Figure 14.6: The relation between applied voltage and capacity of the charge and discharge for different cycles for the battery running on the 2nd own phoenicin*

## 14.3. 3rd batch quality check battery

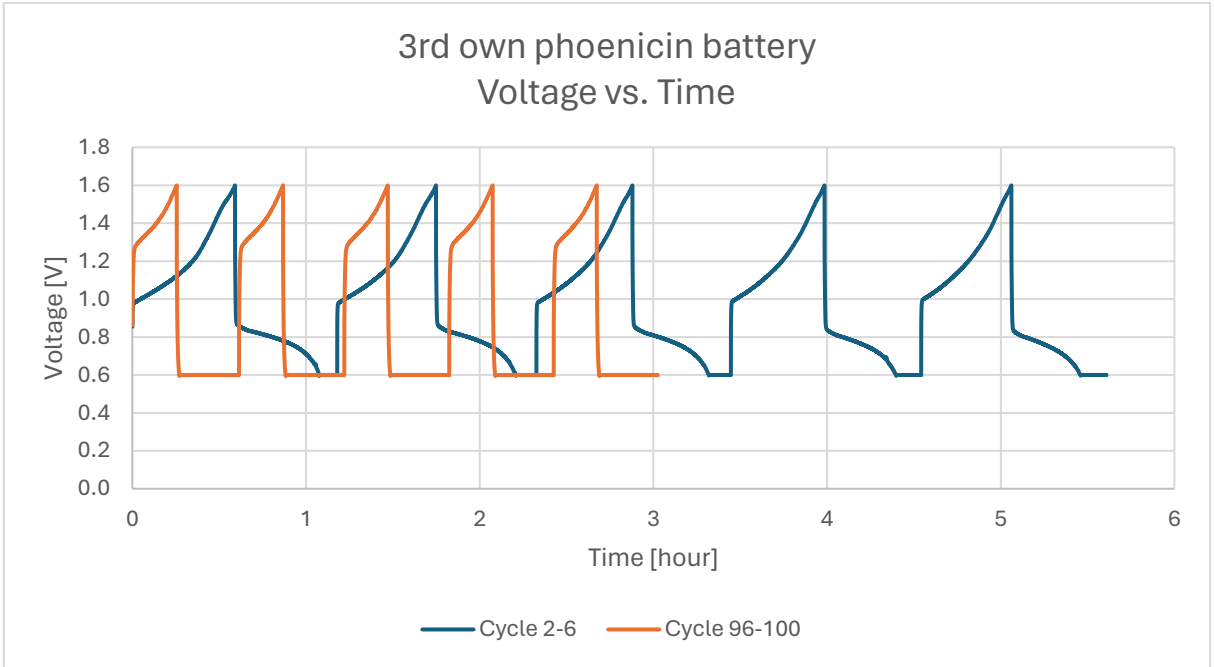


*Figure 14.7: Charge and discharge cycle rate for the 2-6 and 96-100 cycles for the battery running on the 3rd own phoenicin*

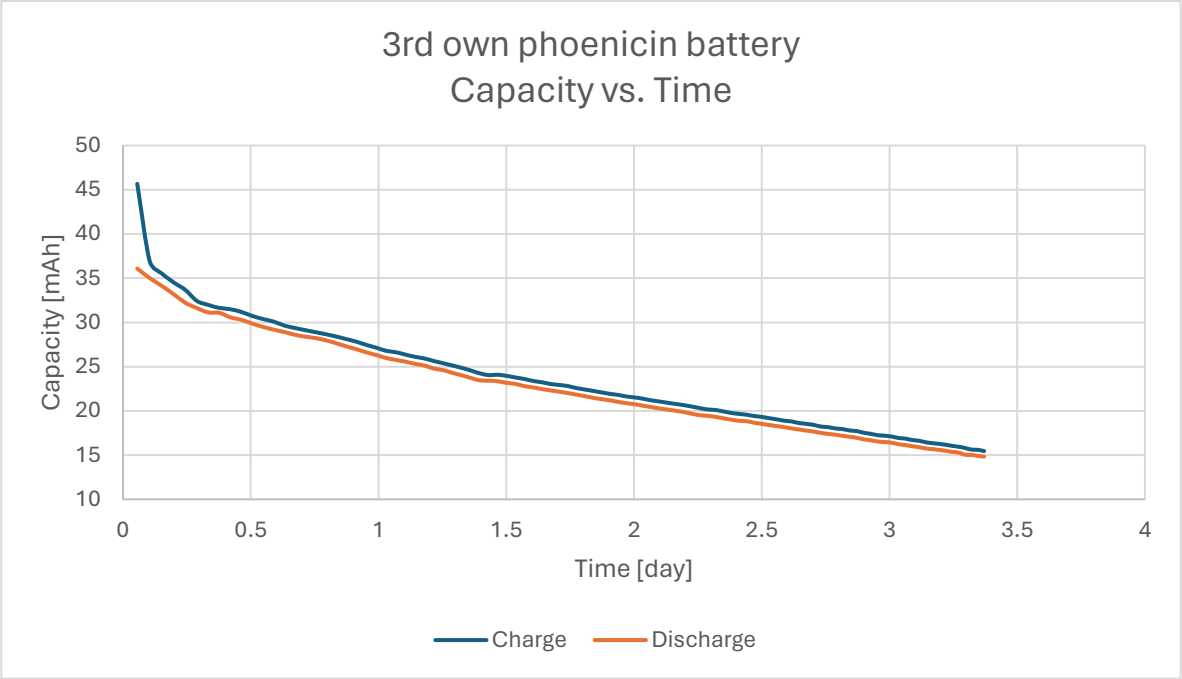


*Figure 14.8. Average capacity per cycle for the battery running on the 3rd own phoenicin*

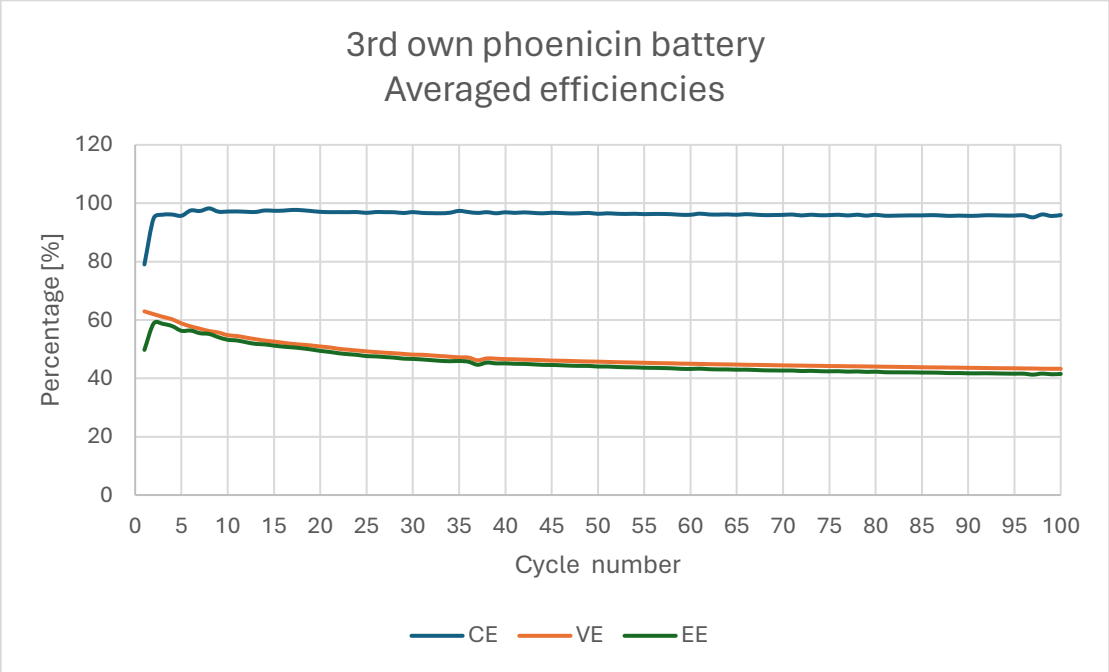


*Figure 14.9: Averaged CE, VE and EE for battery running on the 3rd own phoenicin*

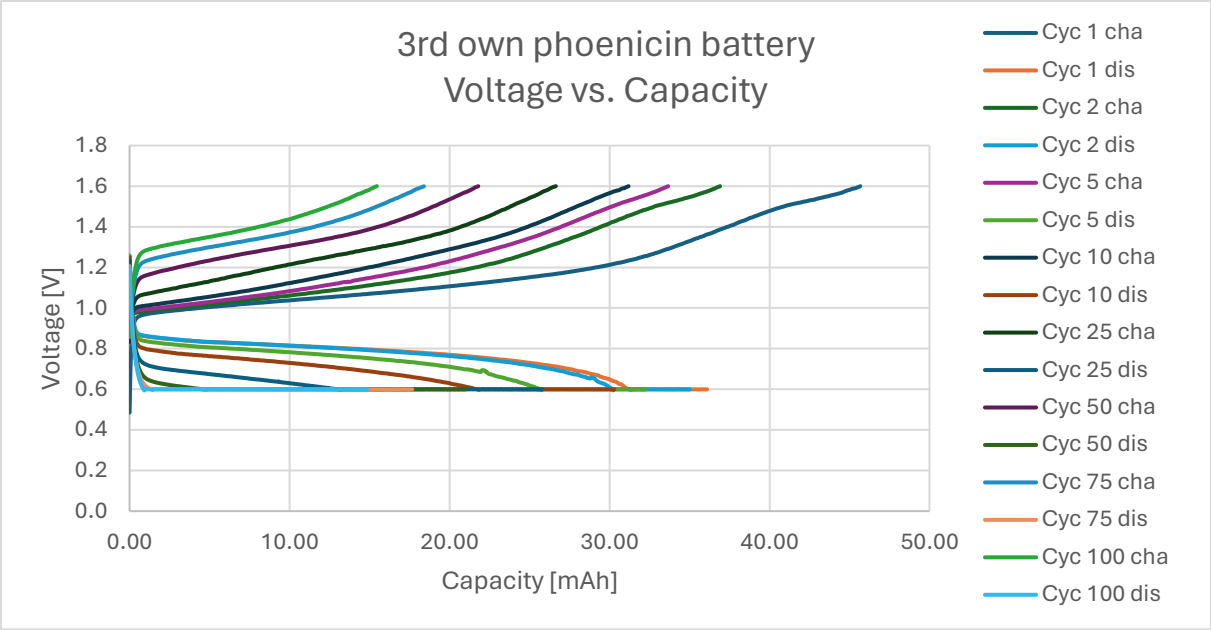


*Figure 14.10: The relation between applied voltage and capacity of the charge and discharge for different cycles for the battery running on the 3rd own phoenicin*

## 14.4. 4th batch quality check battery

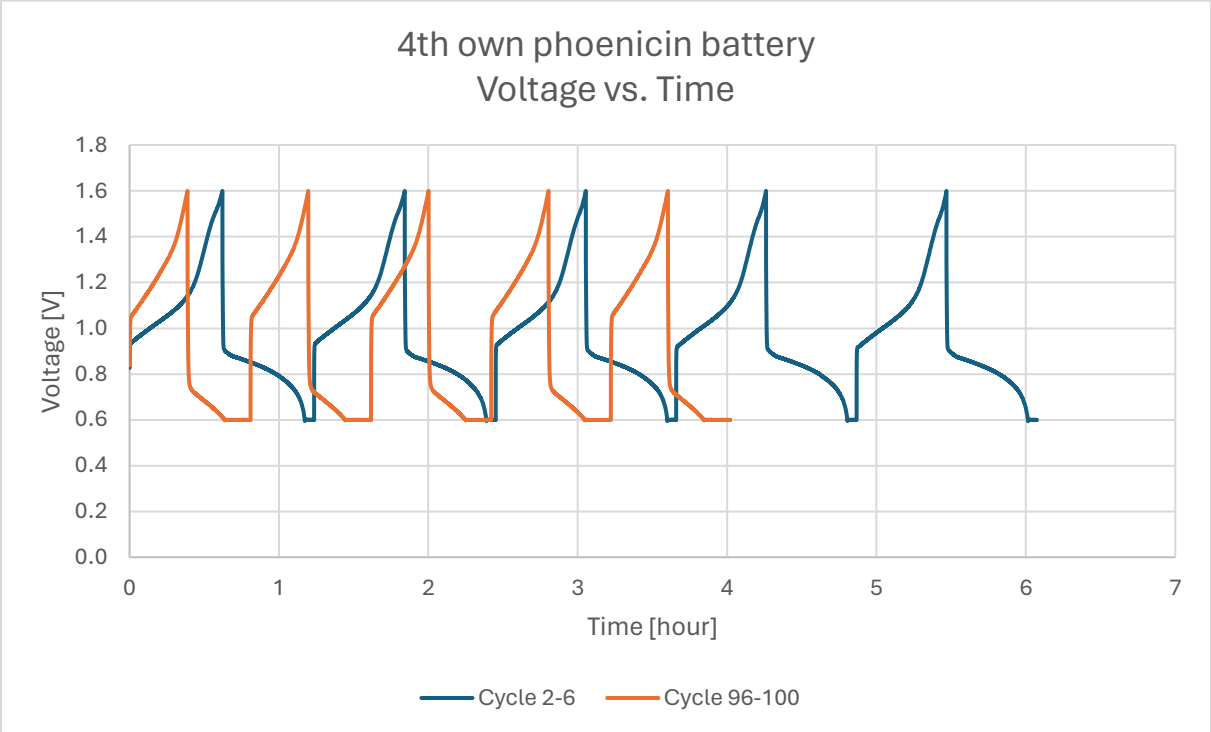


*Figure 14.11: Charge and discharge cycle rate for the 2-6 and 96-100 cycles for the battery running on the 4th own phoenicin*

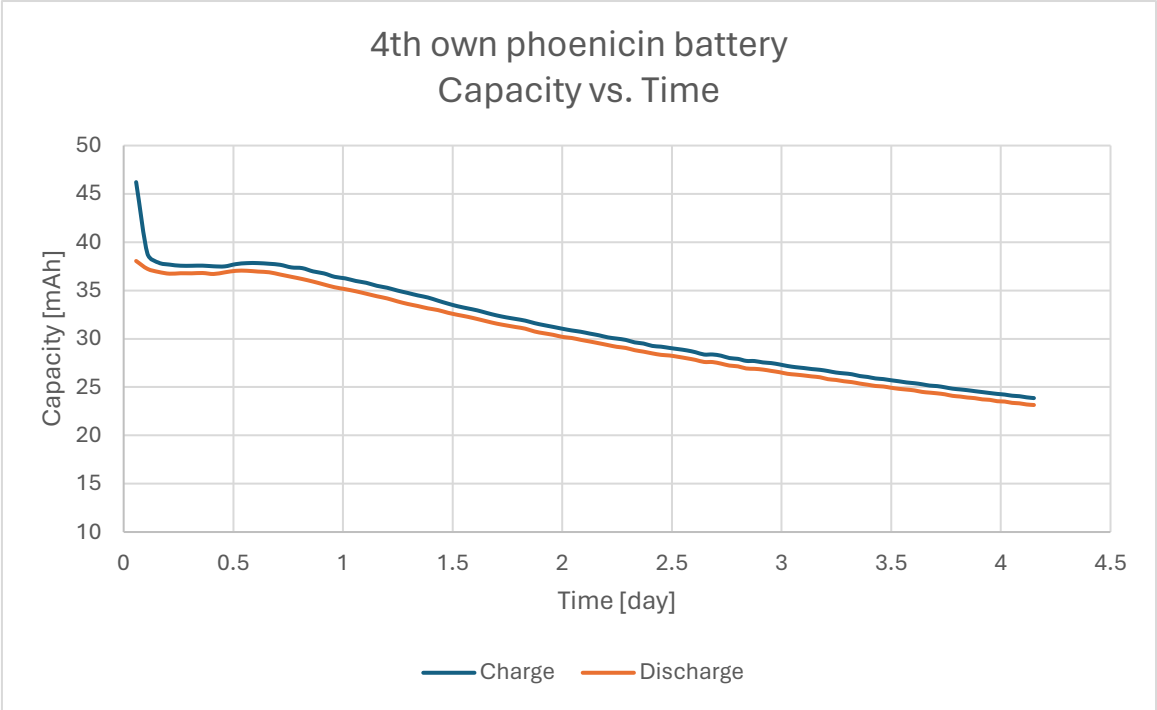


*Figure 14.12: Average capacity per cycle for the battery running on the 4th own phoenicin*

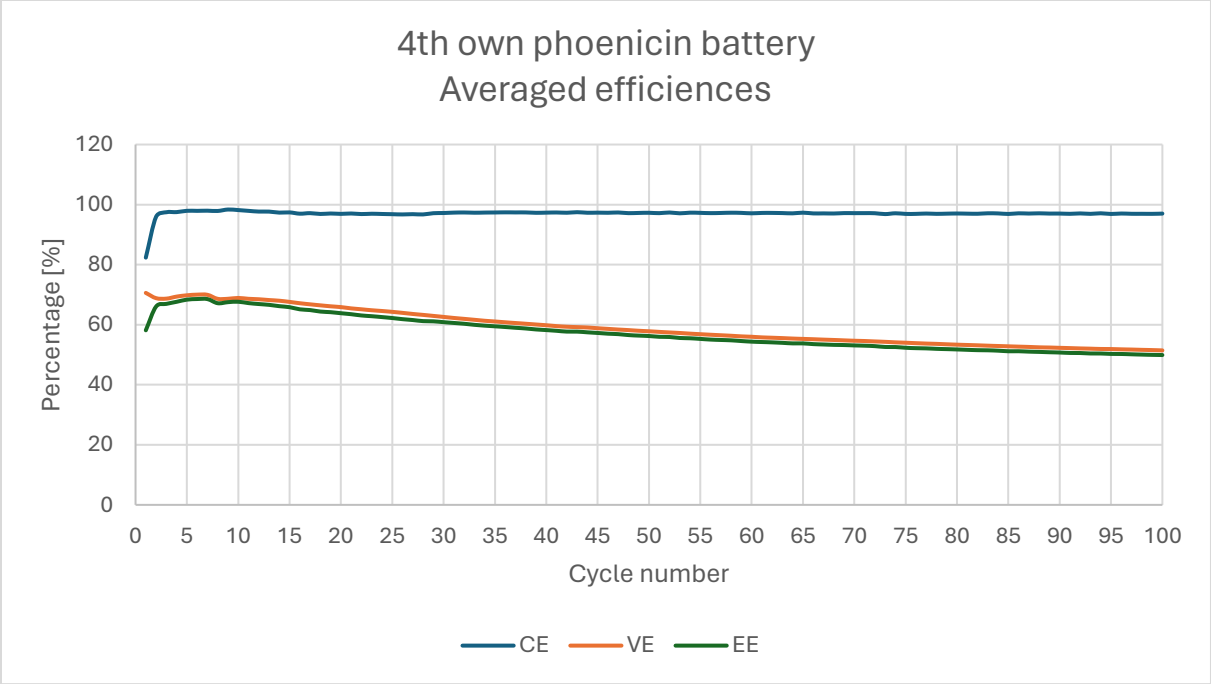


*Figure 14.13: Averaged CE, VE and EE for battery running on the 4th own phoenicin*

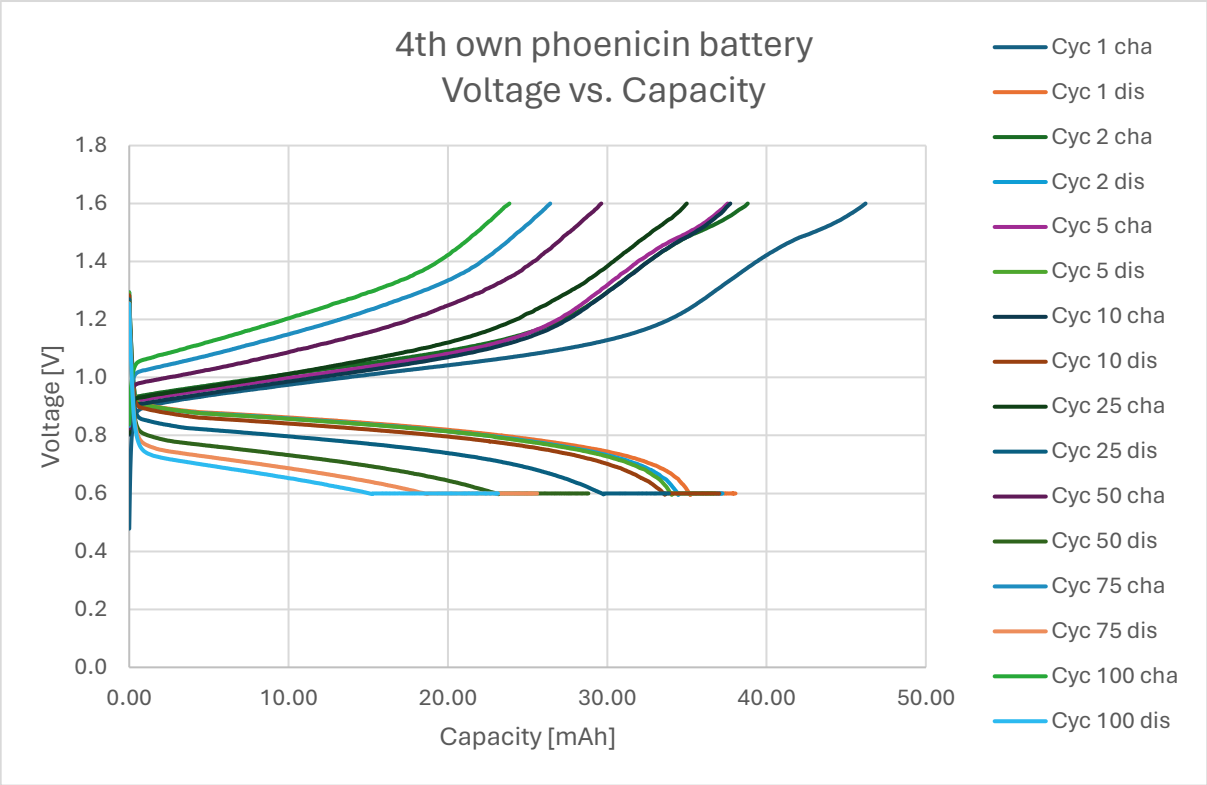


*Figure 14.14: The relation between applied voltage and capacity of the charge and discharge for different cycles for the battery running on the 4th own phoenicin*

## 14.5. 5th batch quality check battery

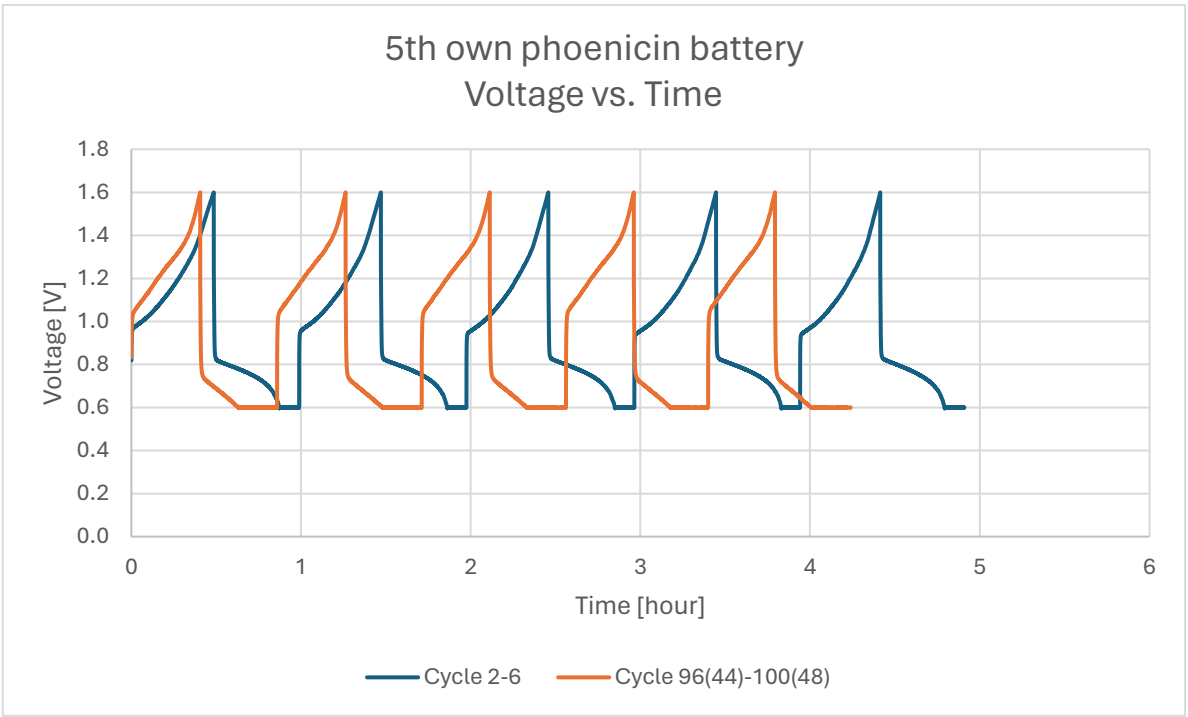


*Figure 14.15: Charge and discharge cycle rate for the 2-6 and 96-100 cycles for the battery running on the 5th own phoenicin*

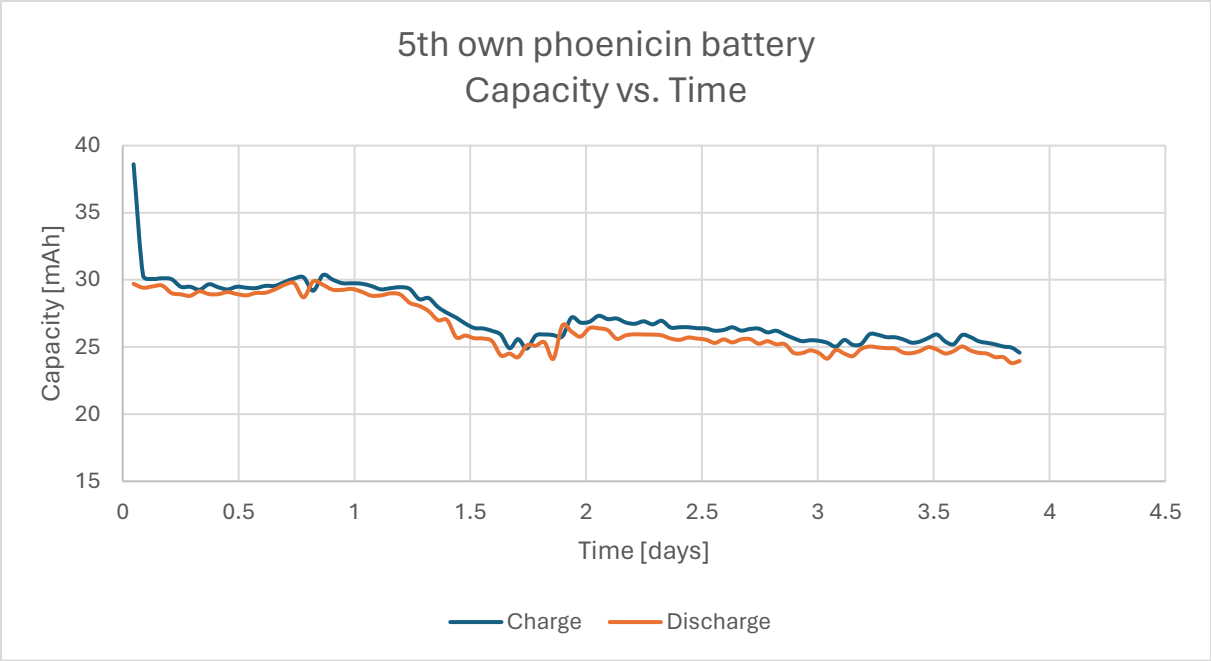


*Figure 14.16: Average capacity per cycle for the battery running on the 5th own phoenicin*

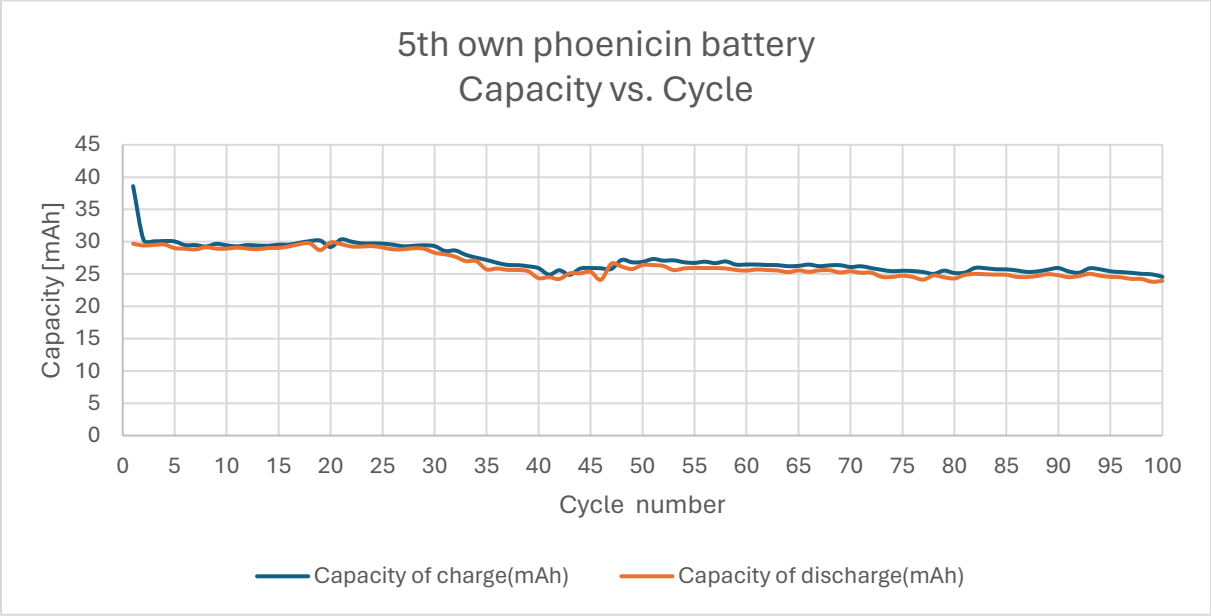


*Figure 14.17: 5th battery charge and discharge capacity for all 100 cycles*

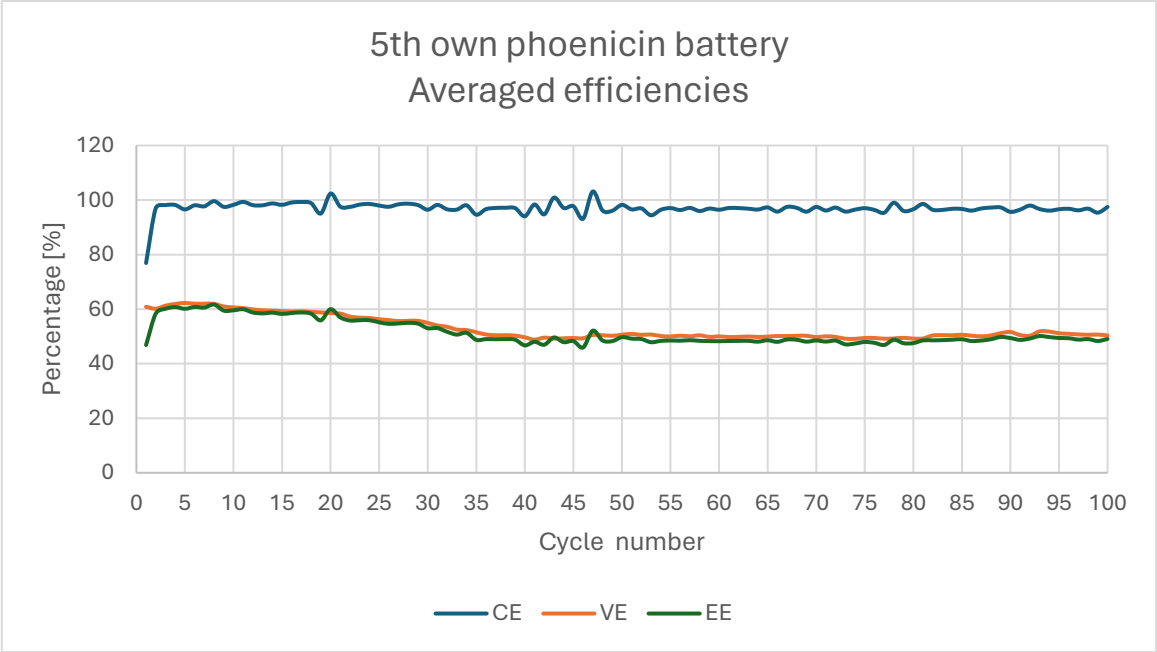


*Figure 14.18: Averaged CE, VE and EE for battery running on the 5th own phoenicin*

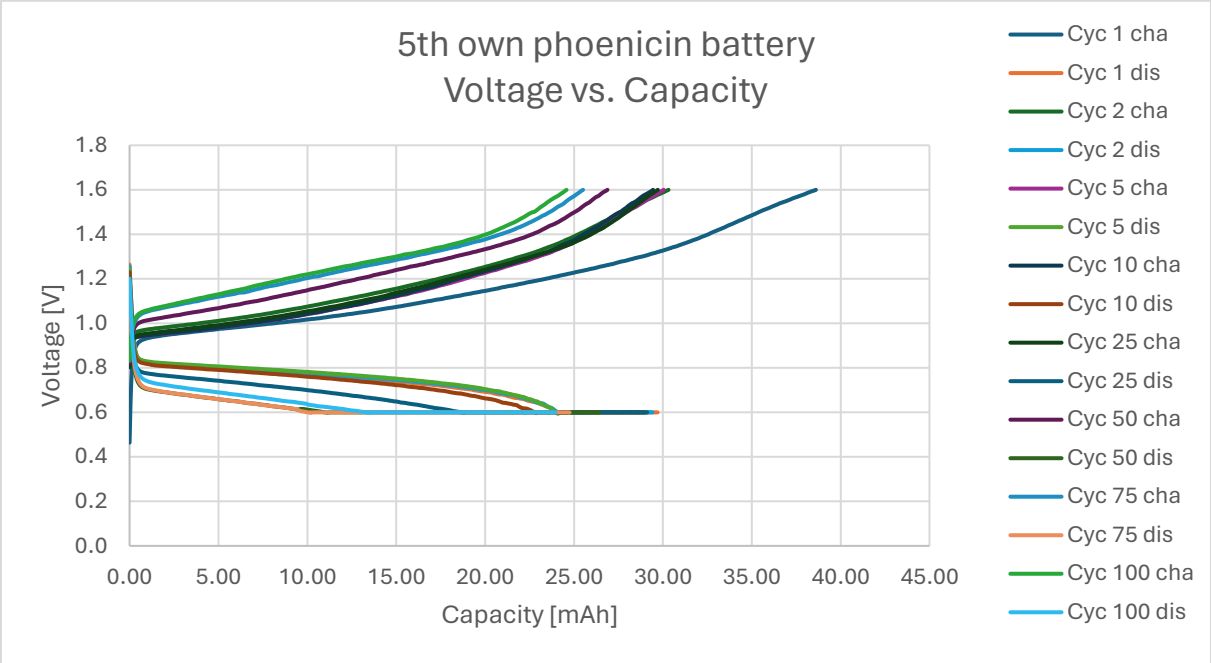


*Figure 14.19:The relation between applied voltage and capacity of the charge and discharge for different cycles for the battery running on the 5th own phoenicin*

## 14.6. 6th batch quality check battery

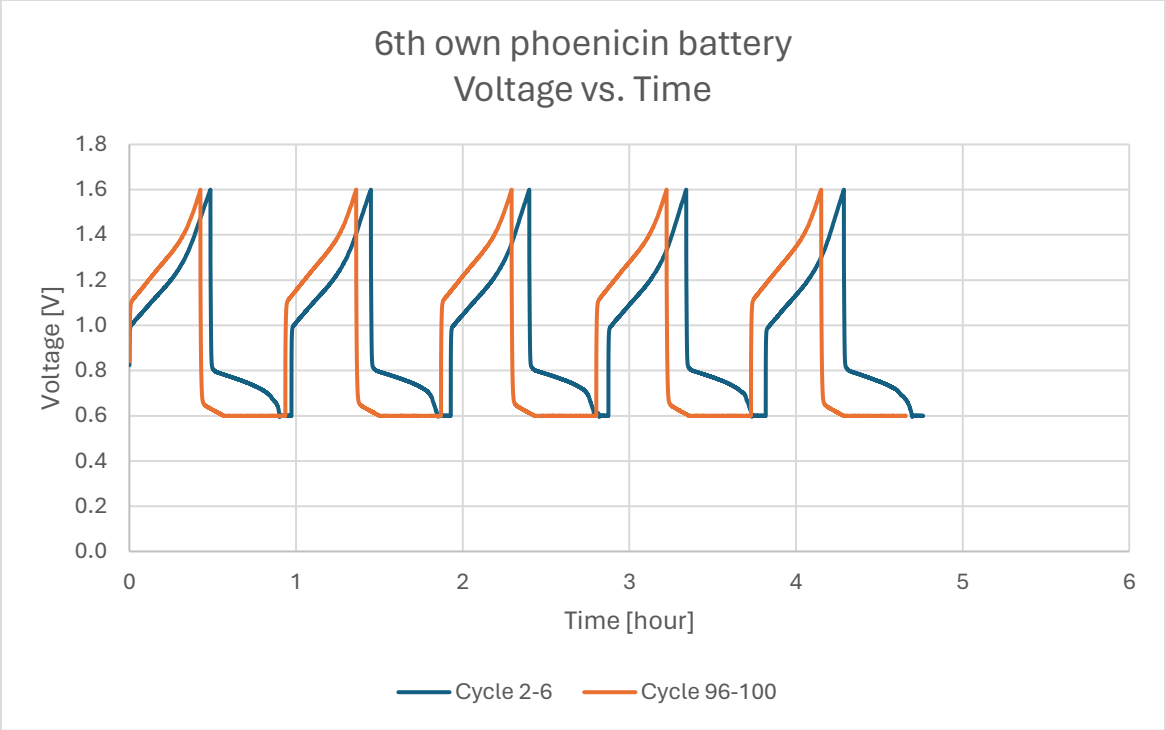


*Figure 14.20: Charge and discharge cycle rate for the 2-6 and 96-100 cycles for the battery running on the 6th own phoenicin*

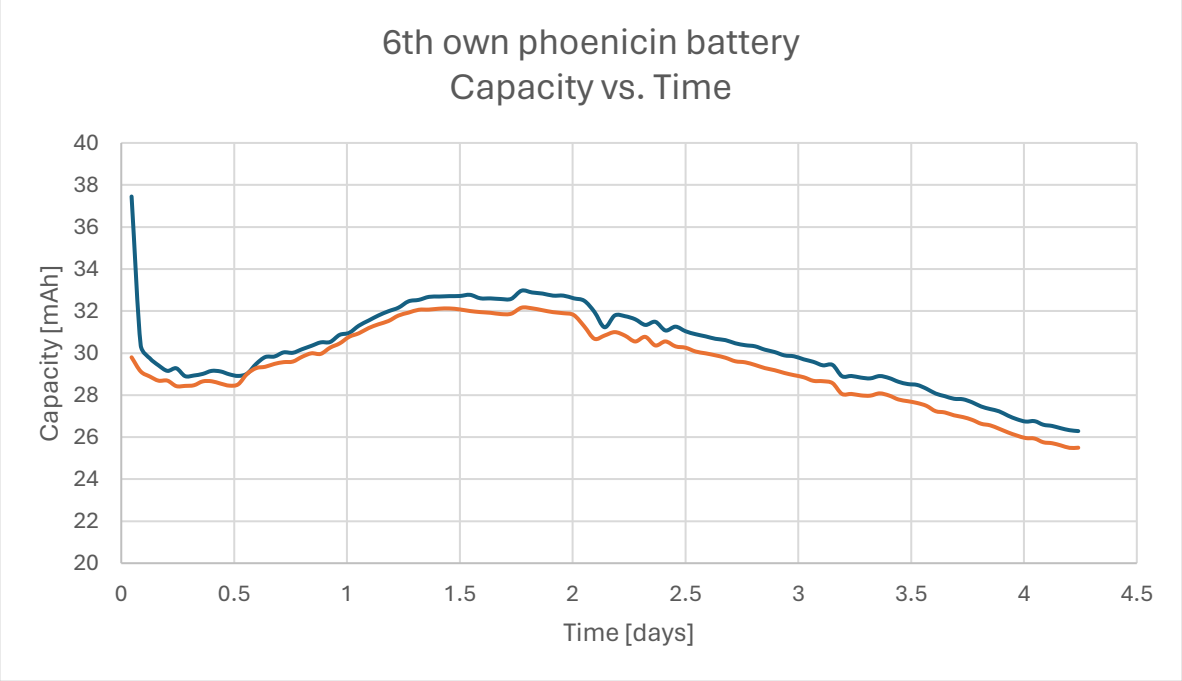


*Figure 14.21: Average capacity per cycle for the battery running on the 6th own phoenicin*

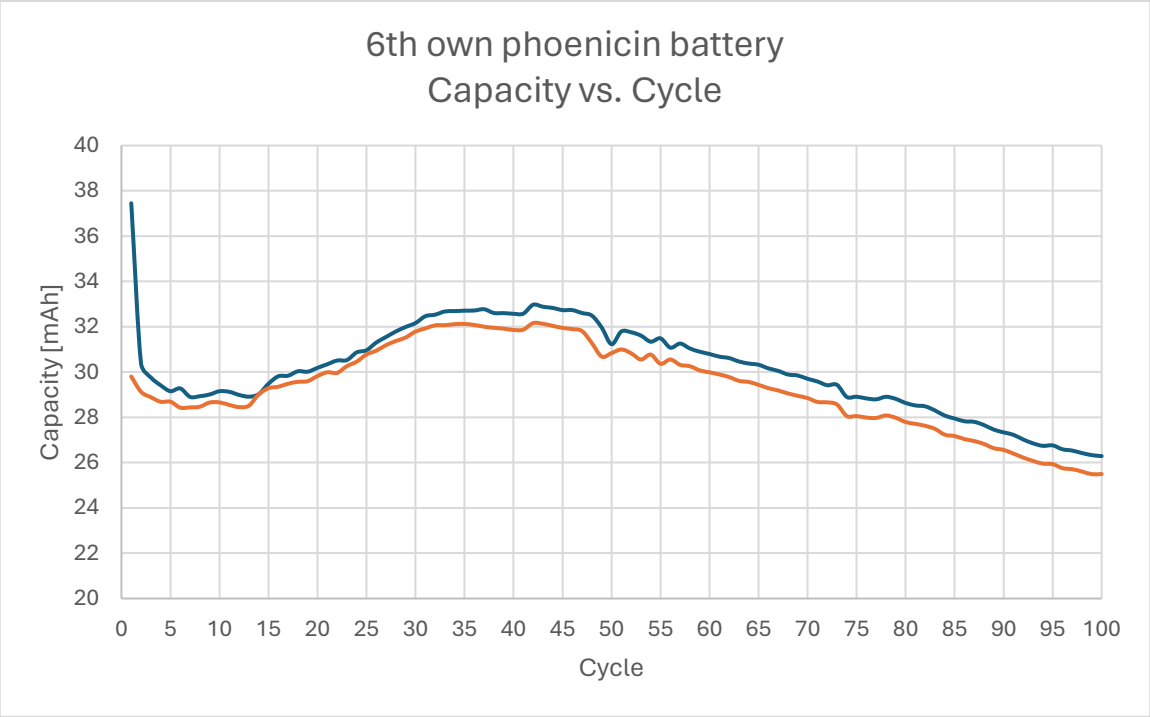


*Figure 14.22: 6th battery charge and discharge capacity for all 100 cycles*

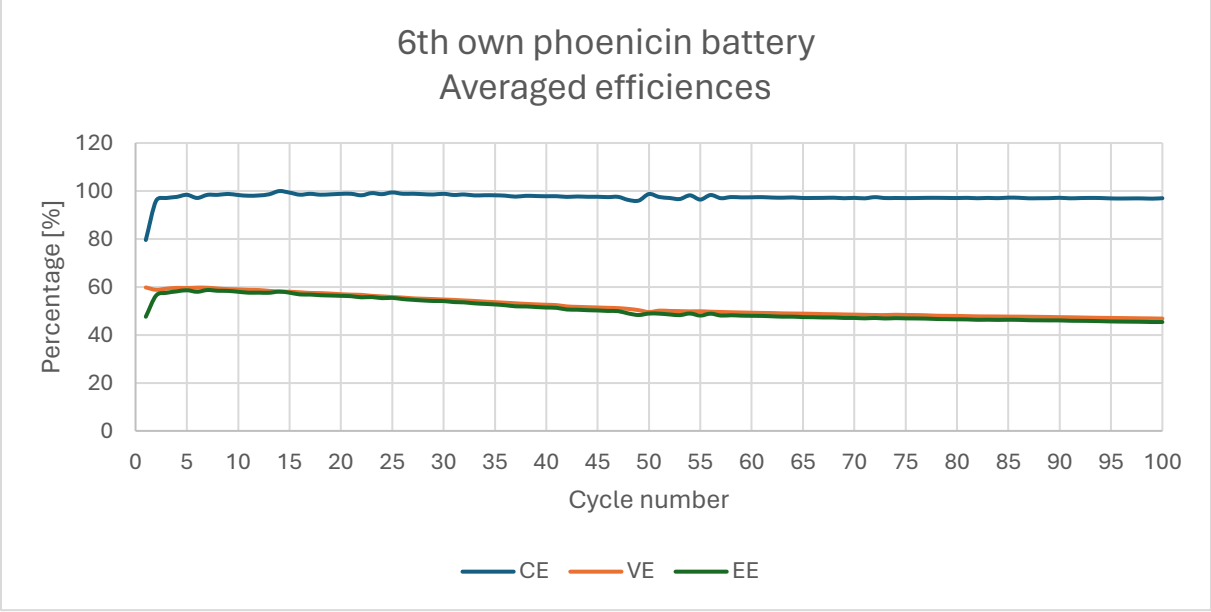


*Figure 14.23: Averaged CE, VE and EE for battery running on the 6th own phoenicin*

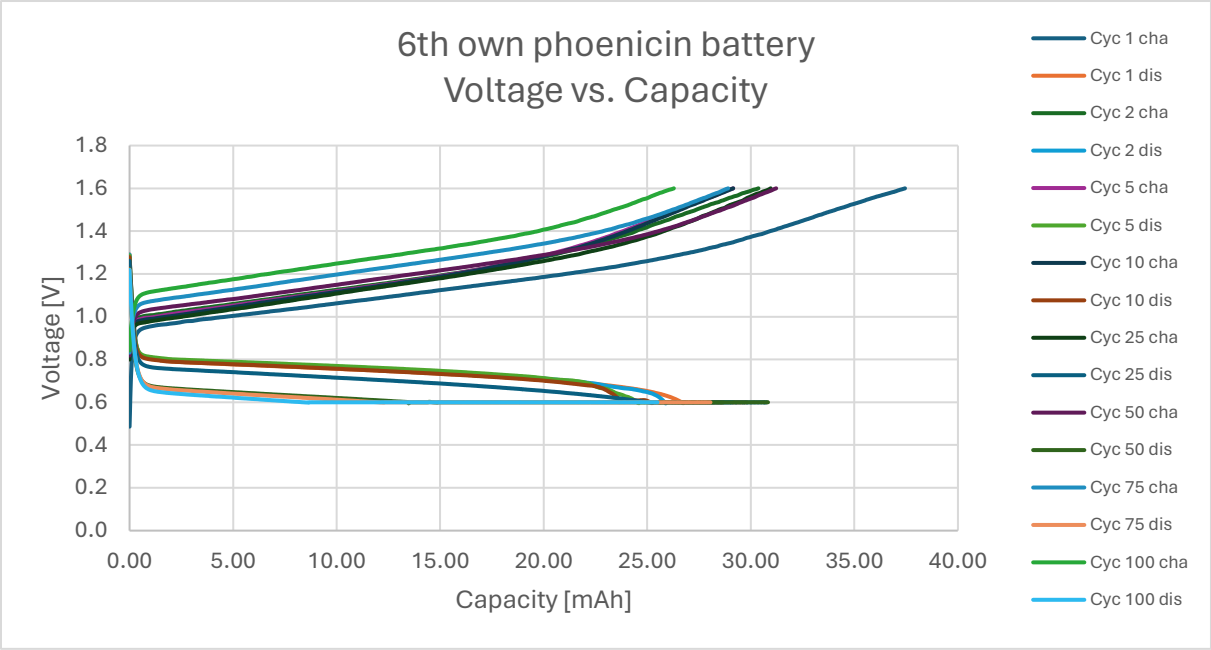


*Figure 14.24: The relation between applied voltage and capacity of the charge and discharge for different cycles for the battery running on the 6th own phoenicin*

## 14.7. 7th batch quality check battery

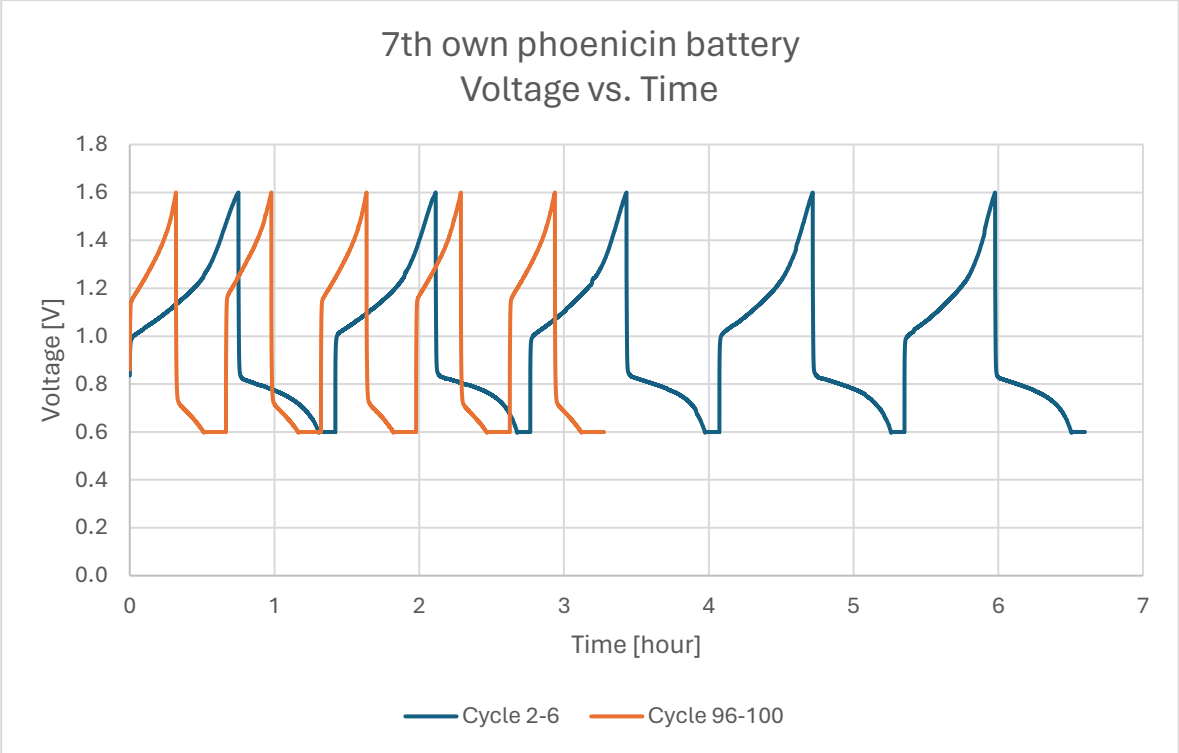


*Figure 14.25: Charge and discharge cycle rate for the 2-6 and 96-100 cycles for the battery running on the 7th own phoenicin*

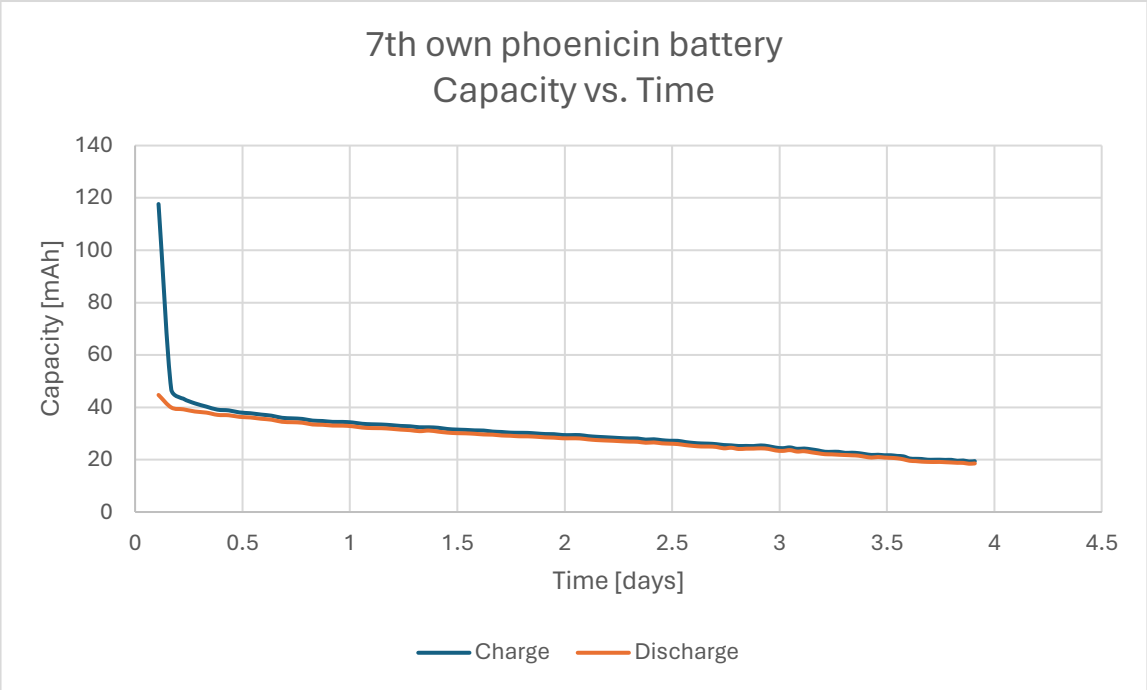


*Figure 14.26: Average capacity per cycle for the battery running on the 7th own phoenicin*

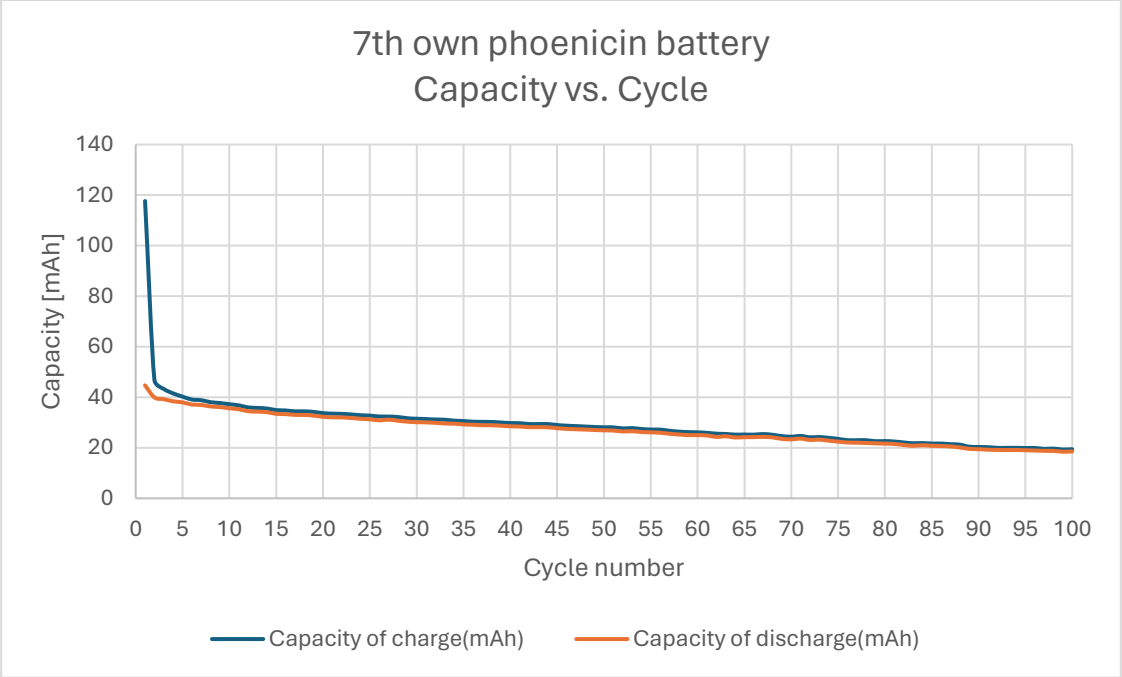


*Figure 14.27: Average capacity per cycle for the battery running on the 7th own phoenicin*

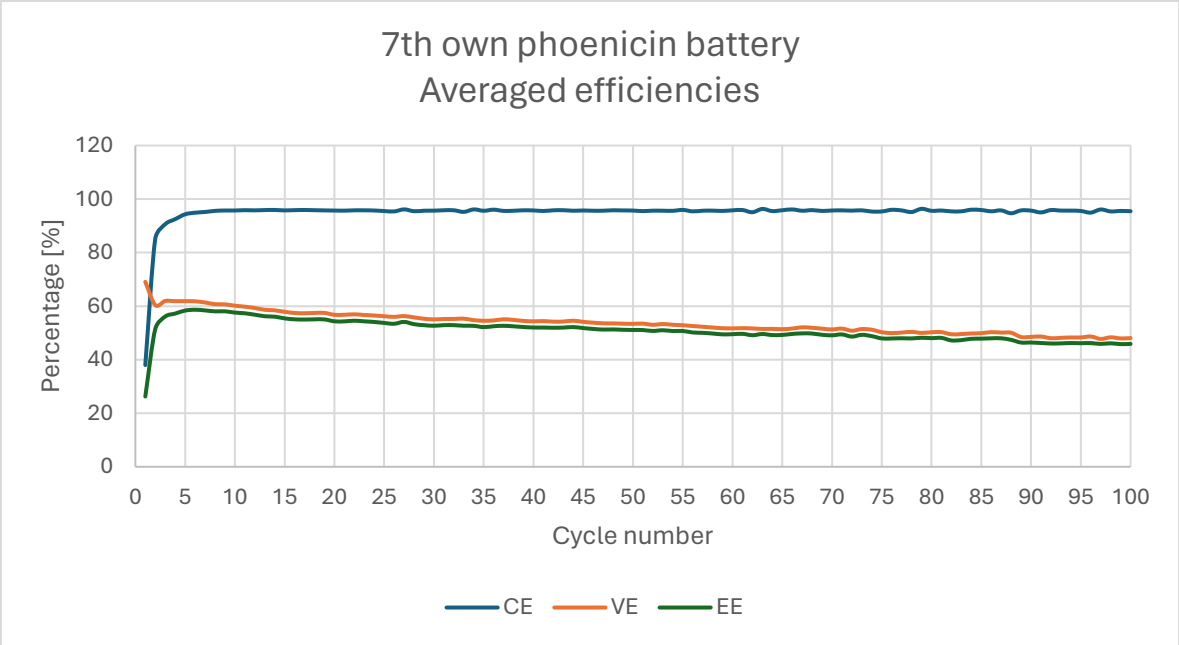


*Figure 14.28: Averaged CE, VE and EE for battery running on the 7th own phoenicin*

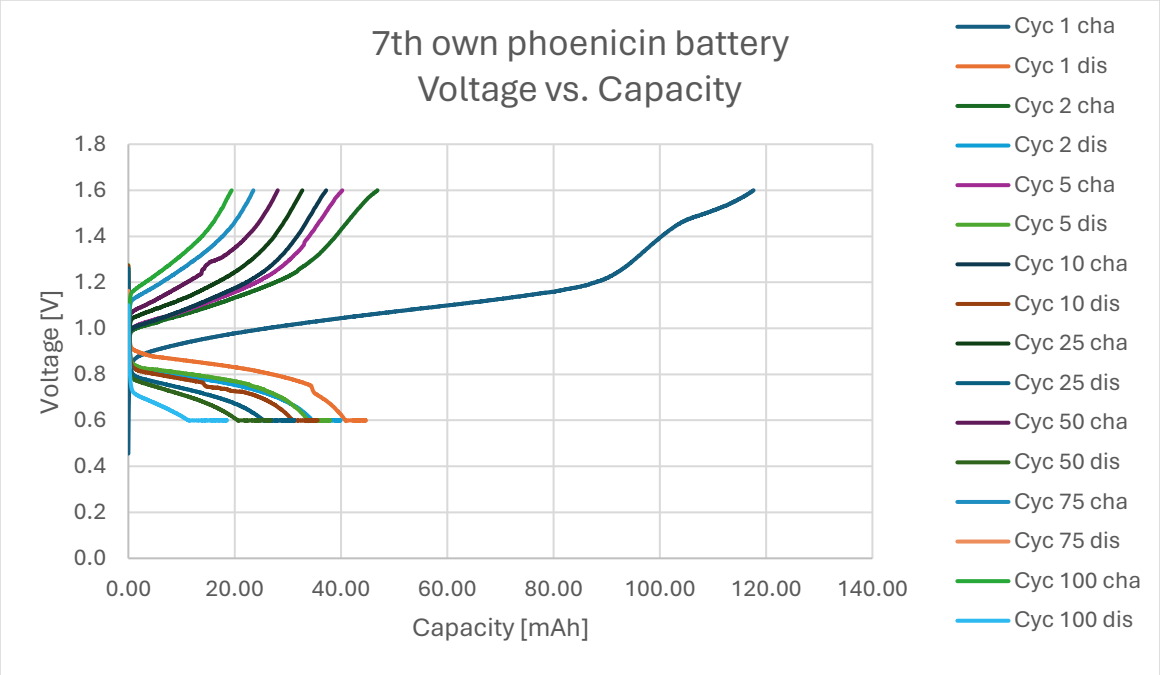


*Figure 14.29: The relation between applied voltage and capacity of the charge and discharge for different cycles for the battery running on the 7th own phoenicin*

# 15. Appendix C – Battery test data for bench-scale batteries

This appendix shows the voltage vs capacity graphs and the charge and discharge vs cycle numbers for each battery running on the five different batches.

## 15.1. 3rd batch bench-scale battery

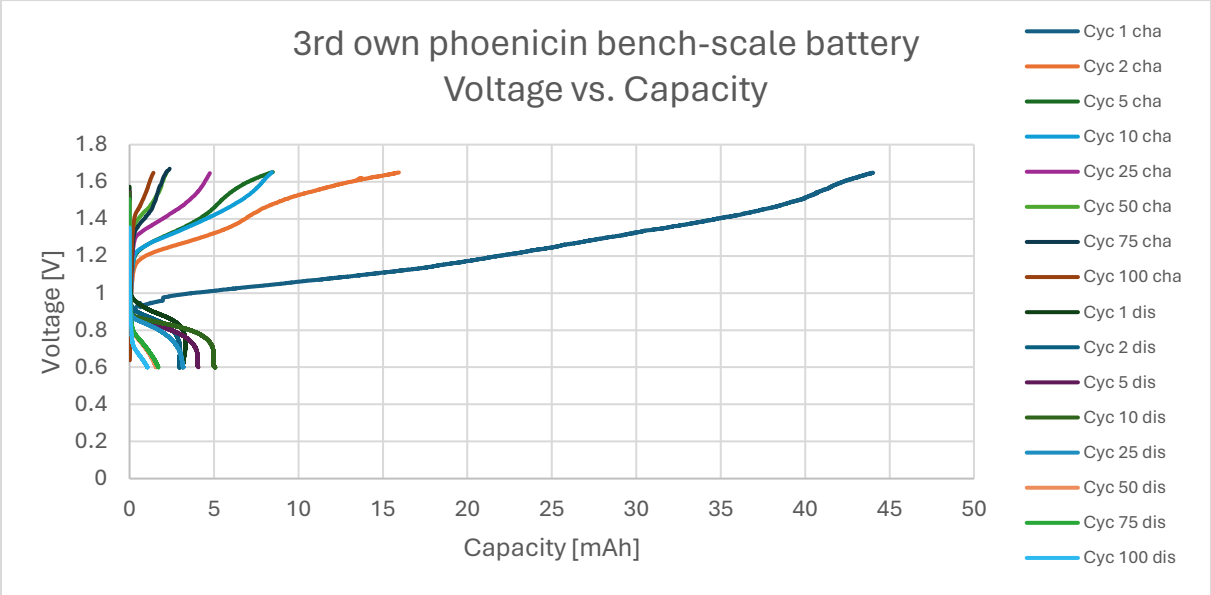


*Figure 15.1: The relation between applied voltage and capacity of the charge and discharge for different cycles for the bench-scale battery running on the 3rd own phoenicin*

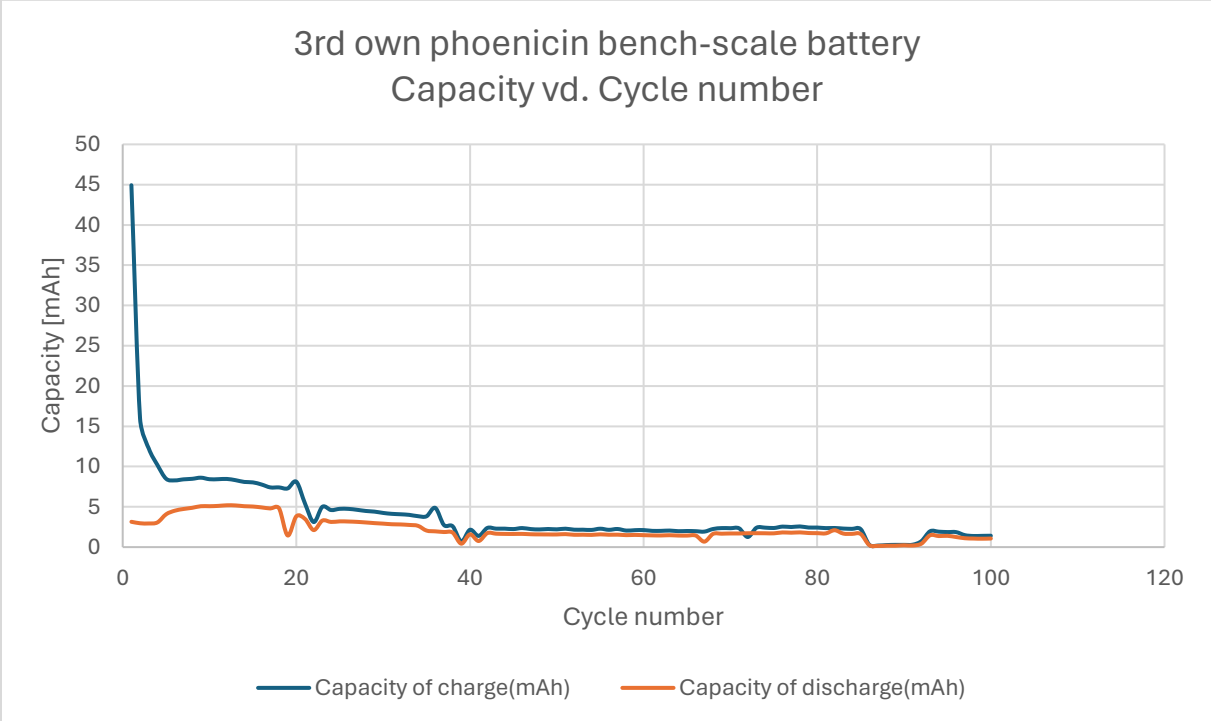


*Figure 15.2: Average capacity per cycle for the battery running on the 3rd own phoenicin*

## 15.2. 4th batch bench-scale battery

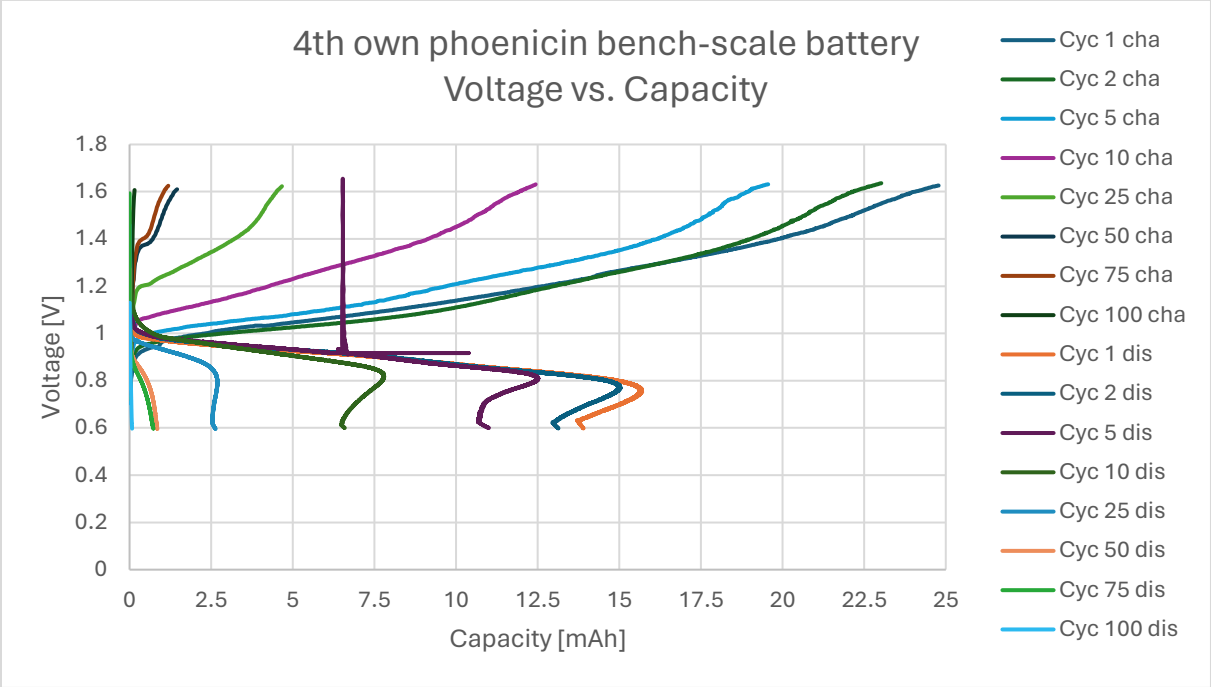


*Figure 15.3: The relation between applied voltage and capacity of the charge and discharge for different cycles for the bench-scale battery running on the 4th own phoenicin*

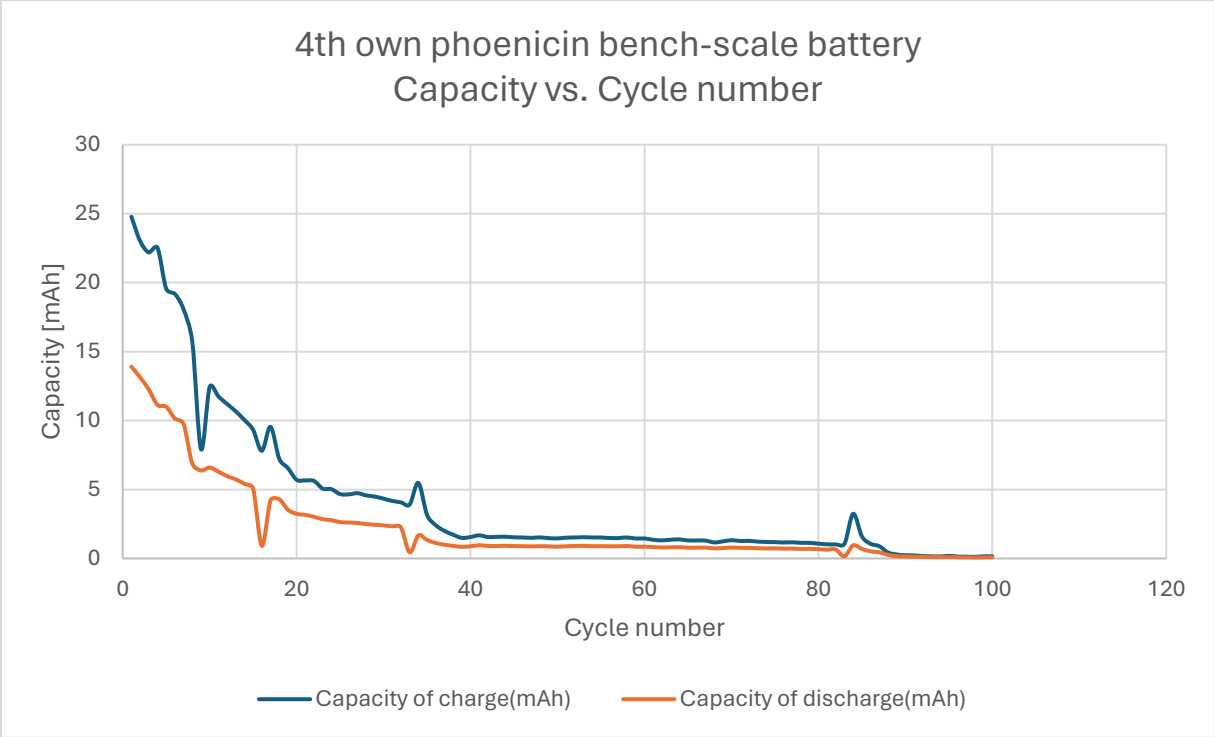


*Figure 15.4: Average capacity per cycle for the battery running on the 4th own phoenicin*

## 15.3. 5th batch bench-scale battery

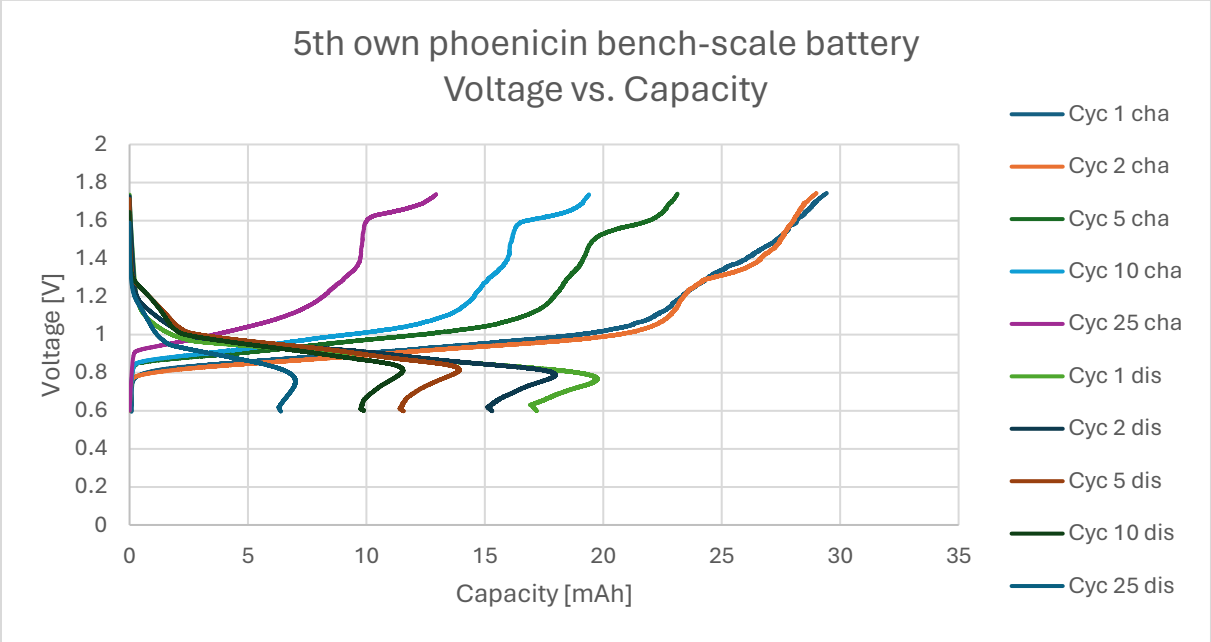


*Figure 15.5: The relation between applied voltage and capacity of the charge and discharge for different cycles for the bench-scale battery running on the 5th own phoenicin*

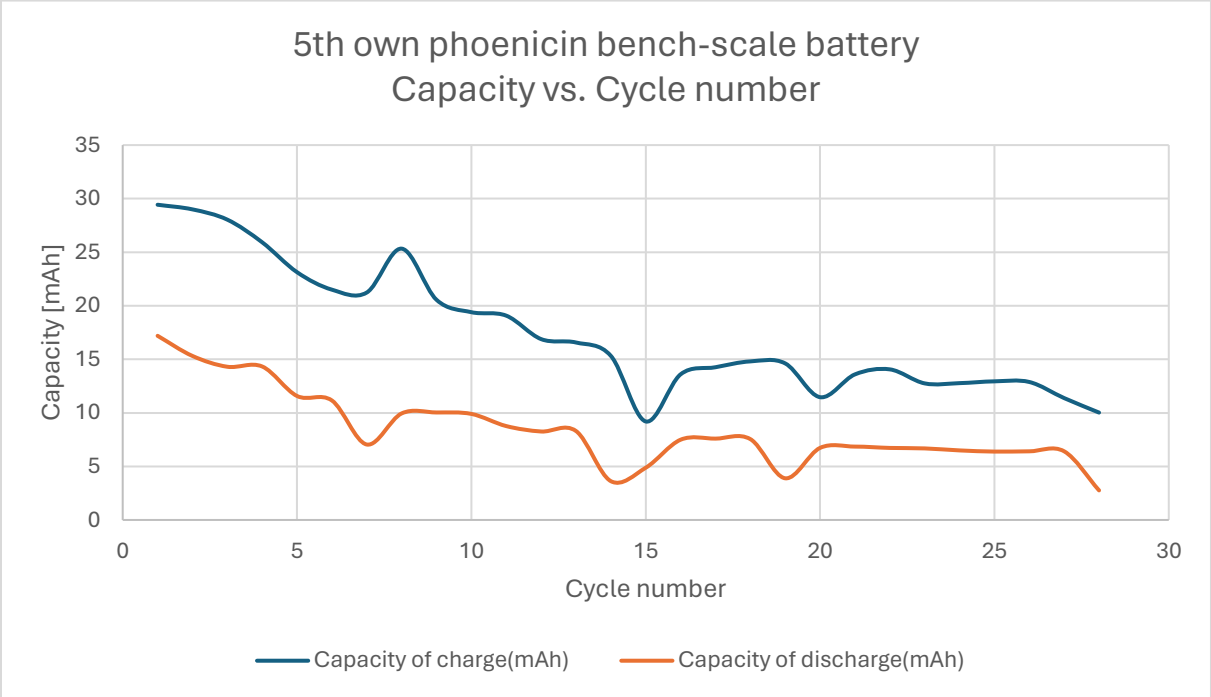


*Figure 15.6: Average capacity per cycle for the battery running on the 5th own phoenicin*

## 15.4. 6th batch bench-scale battery

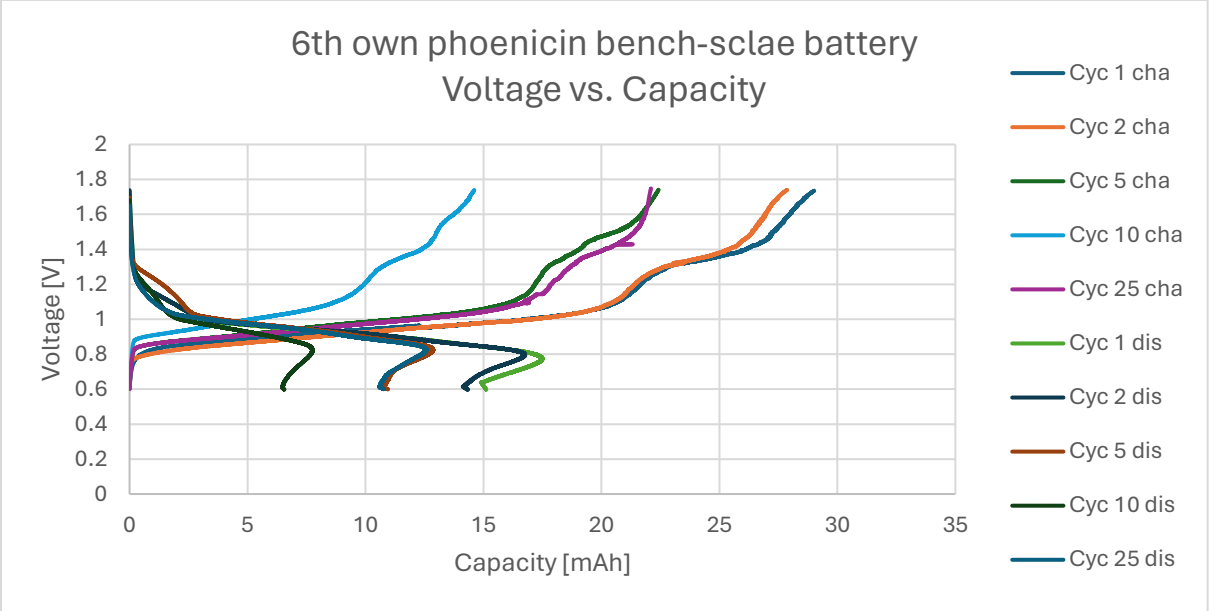


*Figure 15.7: The relation between applied voltage and capacity of the charge and discharge for different cycles for the bench-scale battery running on the 6th own phoenicin*

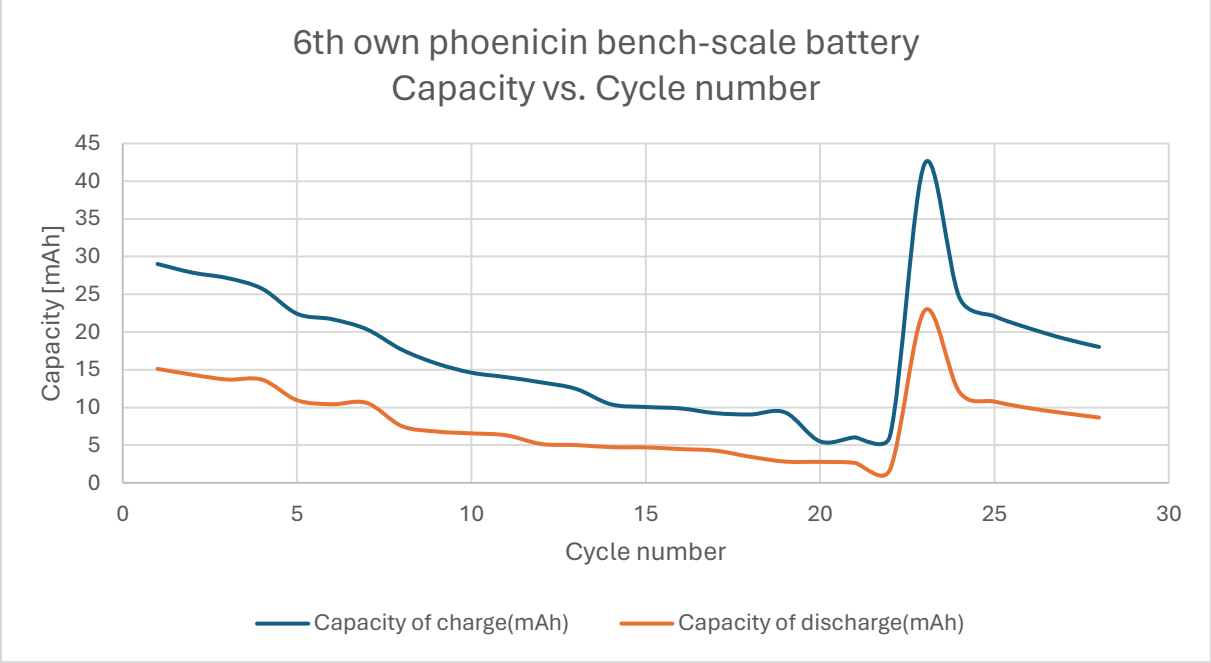


*Figure 15.8: Average capacity per cycle for the battery running on the 6th own phoenicin*

## 15.5. 7th batch bench-scale battery

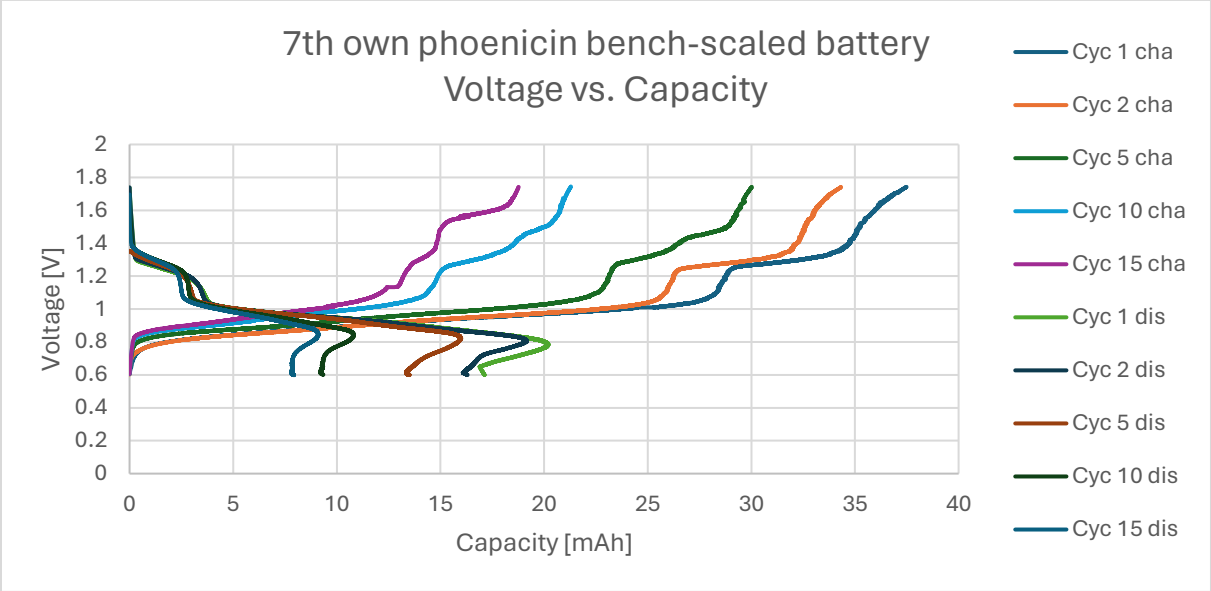


*Figure 15.9: The relation between applied voltage and capacity of the charge and discharge for different cycles for the bench-scale battery running on the 7th own phoenicin*

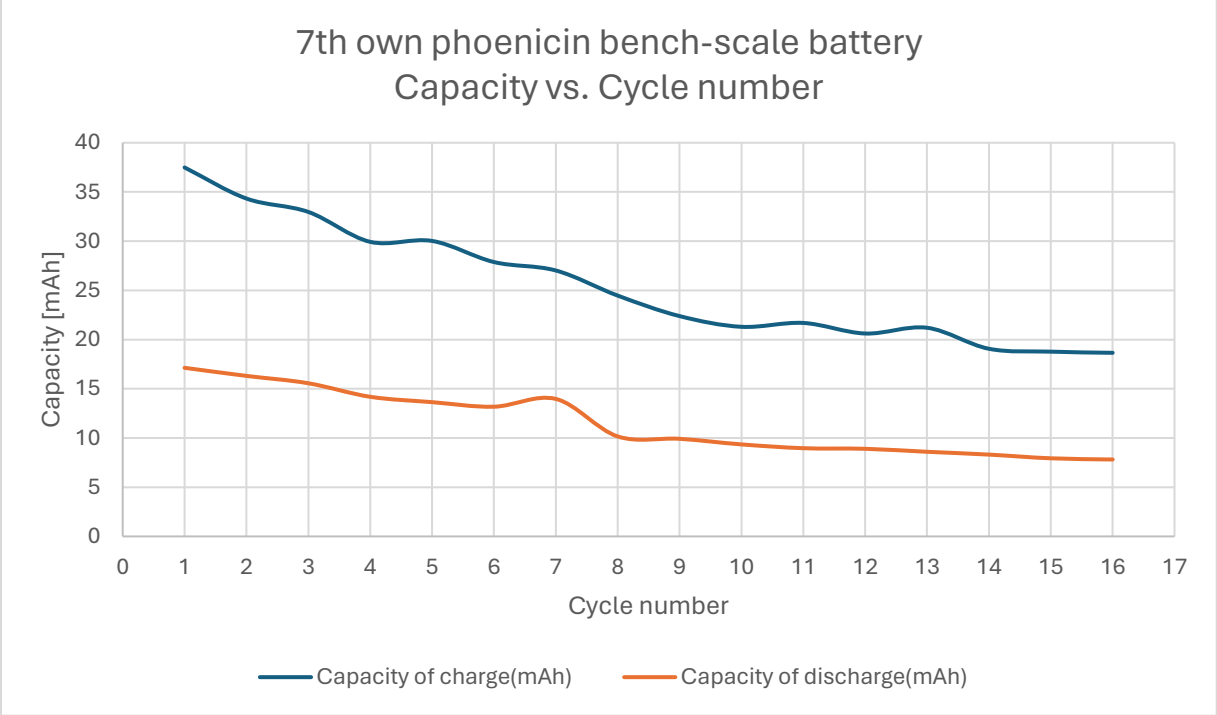


*Figure 15.10: Average capacity per cycle for the battery running on the 7th own phoenicin*

# 16. Appendix D – HPLC chromatograms

In this appendix all chromatograms for the six used batches of self-produced phoenicin are shown.

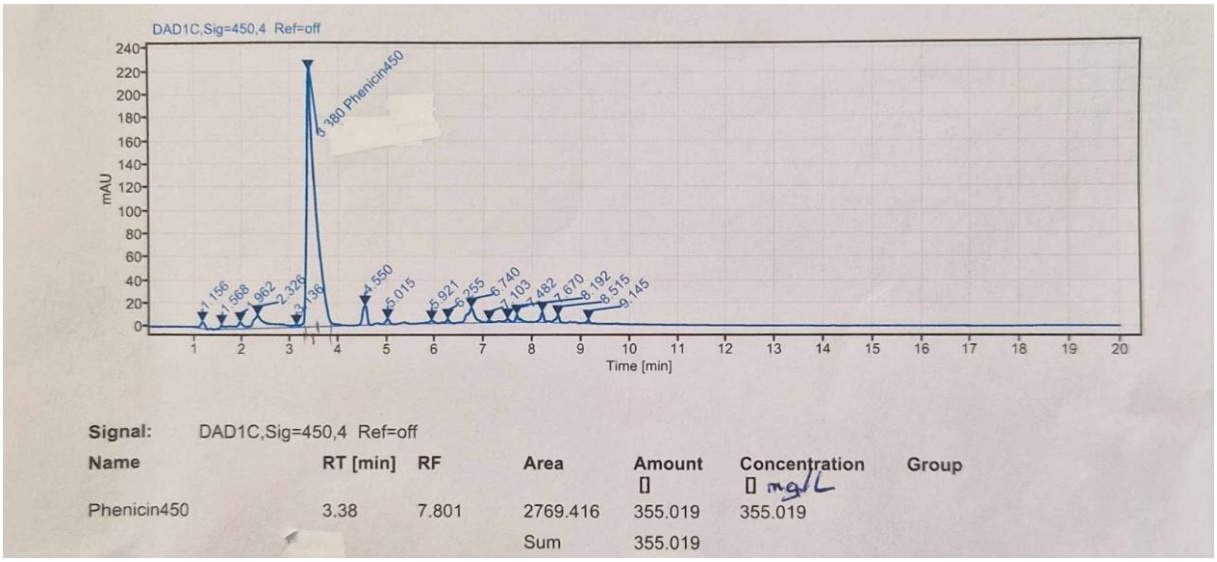


*Figure 16.1: HPLC chromatogram for batch 2*

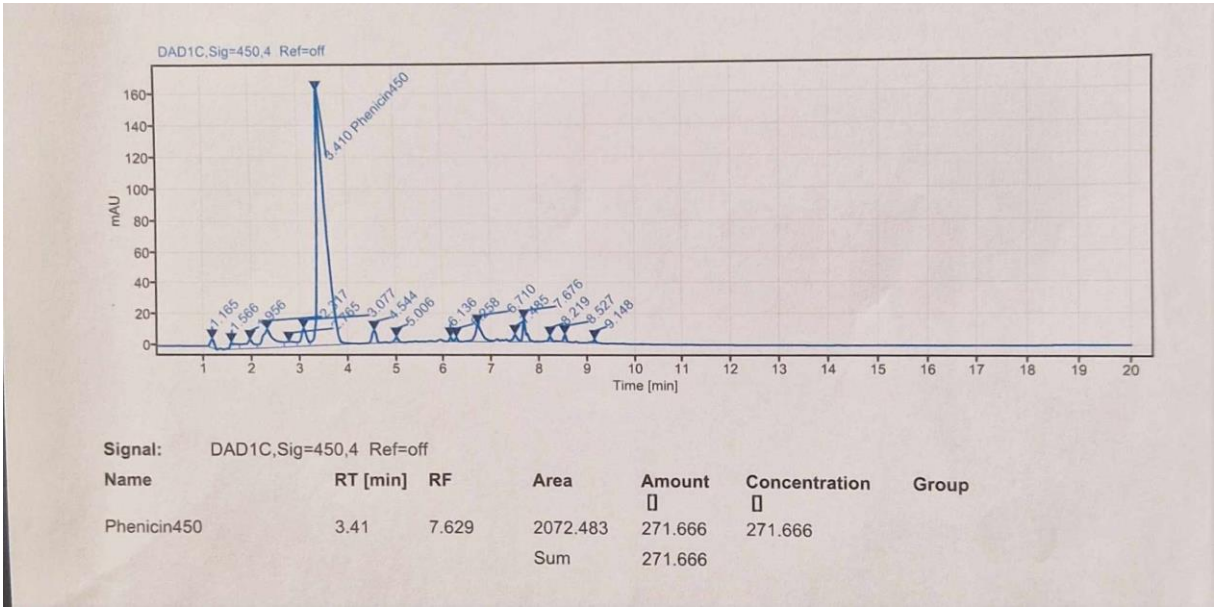


*Figure 16.2: HPLC chromatogram for batch 3*

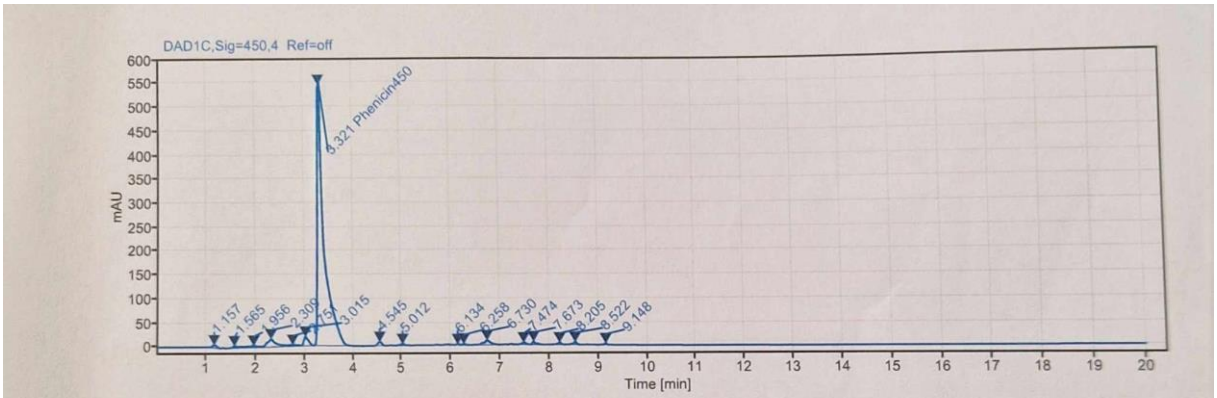


**Signal:** DAD1C,Sig=450,4 Ref=off

| Name | RT [min] | RF | Area | Amount [] | Concentration [] | Group |
|---|---|---|---|---|---|---|
| Phenicin450 | 3.32 | 8.048 | 5117.018 | 635.793 | 635.793 | |
| | | | Sum | 635.793 | | |

*Figure 16.3: HPLC chromatogram for batch 4*

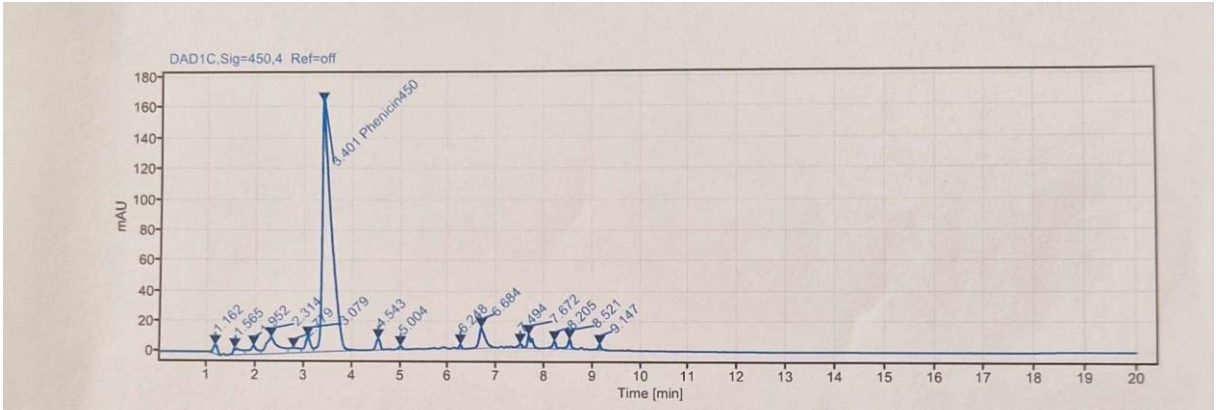


**Signal:** DAD1C,Sig=450,4 Ref=off

| Name | RT [min] | RF | Area | Amount [] | Concentration [] | Group |
|---|---|---|---|---|---|---|
| Phenicin450 | 3.40 | 7.646 | 2127.364 | 278.230 | 278.230 | |
| | | | Sum | 278.230 | | |

*Figure 16.4: HPLC chromatogram for batch 5*

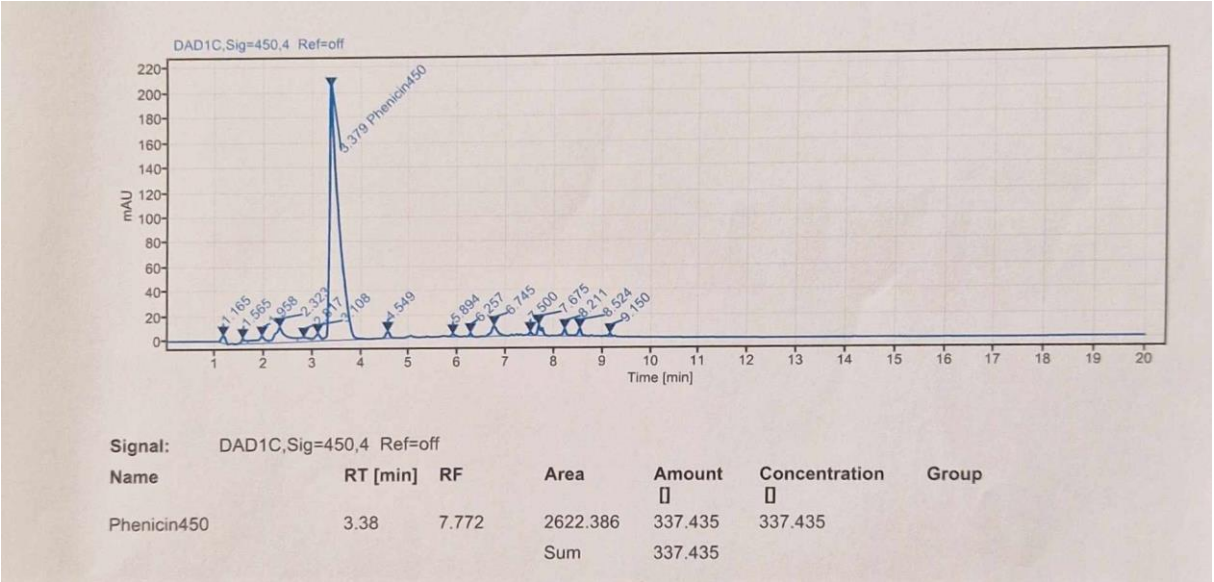


**Signal:** DAD1C,Sig=450,4 Ref=off

| Name | RT [min] | RF | Area | Amount [] | Concentration [] | Group |
|---|---|---|---|---|---|---|
| Phenicin450 | 3.38 | 7.772 | 2622.386 | 337.435 | 337.435 | |
| | | | Sum | 337.435 | | |

*Figure 16.5: HPLC chromatogram for batch 6*

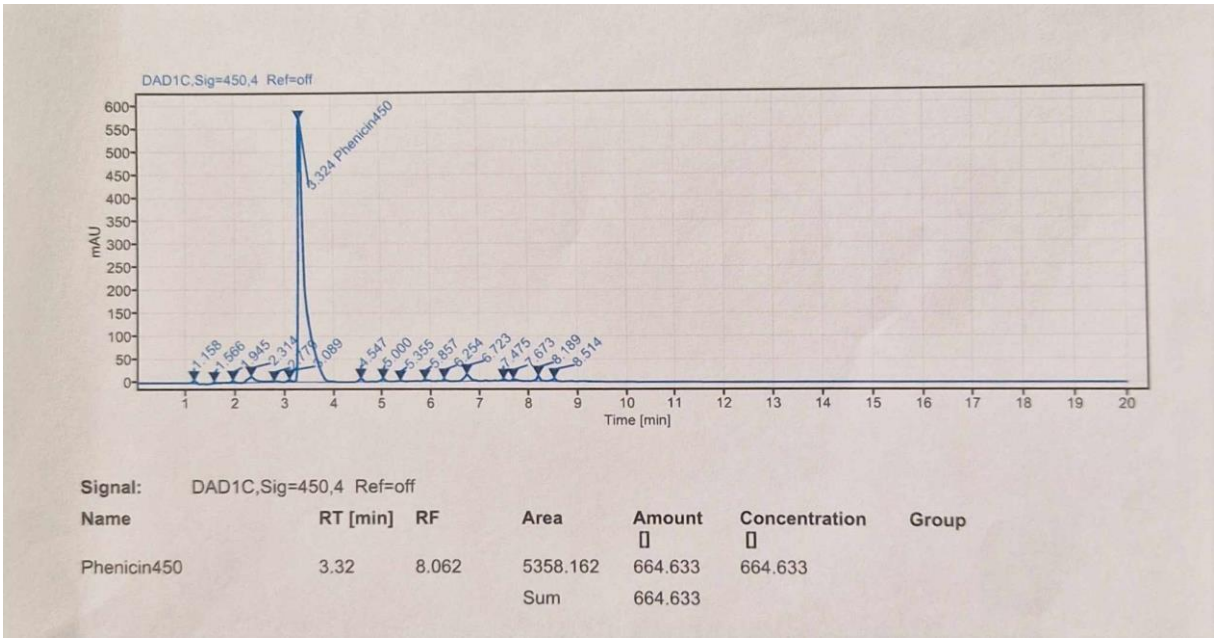


**Signal:** DAD1C,Sig=450,4 Ref=off

| Name | RT [min] | RF | Area | Amount [] | Concentration [] | Group |
|---|---|---|---|---|---|---|
| Phenicin450 | 3.32 | 8.062 | 5358.162 | 664.633 | 664.633 | |
| | | | Sum | 664.633 | | |

*Figure 16.6: HPLC chromatogram for batch 7*